

NASA CR-114658

AVAILABLE TO THE PUBLIC

**HIGH TRANSONIC SPEED
TRANSPORT AIRCRAFT STUDY**

FINAL REPORT

**By Robert M. Kulfan, Frank D. Neumann, James W. Nisbet, Alan R. Mulally, James K. Murakami,
Elias C. Noble, John P. McBarron, James L. Stalter, David W. Gimmestad
and Mark B. Sussman**

(NASA-CR-114658) HIGH TRANSONIC SPEED
TRANSPORT AIRCRAFT STUDY FINAL REPORT,
JUN. 1972-MAY 1973 (BOEING COMMERCIAL
Airplane Co., Seattle) 235 P. HC \$13.25

674-17750

CDCI 010 03/02

JAC:as
31546

Prepared under contract NAS2-7031 by

**BOEING COMMERCIAL AIRPLANE COMPANY
P.O. Box 3707
Seattle, Washington 98124**

for
**Ames Research Center
NATIONAL AERONAUTICS AND SPACE ADMINISTRATION**

1 Report No. NASA CR-114658	2 Government Accession No.	3 Recipient's Catalog No.	
4 Title and Subtitle FINAL REPORT-HIGH TRANSONIC SPEED TRANSPORT AIRCRAFT STUDY		5 Report Date September 1973	
		6 Performing Organization Code	
7 Author(s) R. M. Kulfan, J. P. McBarron, A. R. Mulally, F. D. Neumann, D. W. Gimmestad, J. K. Murakami, J. W. Nisbet, E. C. Noble, J. L. Stalter and Mark B. Sussman		8 Performing Organization Report No.	
9 Performing Organization Name and Address The Boeing Commercial Airplane Company P.O. Box 3707 Seattle, Washington 98124		10 Work Unit No.	
		11 Contract or Grant No. NAS2-7031	
12 Sponsoring Agency Name and Address National Aeronautics and Space Administration Ames Research Center Moffett Field, California 94035		13 Type of Report and Period Covered Final Report June 1972-May 1973	
		14 Sponsoring Agency Code	
15 Supplementary Notes			
16 Abstract <p>An initial design study of high-transonic-speed transport aircraft has been completed. Five different design concepts were developed. These included fixed swept wing, variable-sweep wing, delta wing, double-fuselage yawed-wing, and single-fuselage yawed-wing aircraft. The "boomless" supersonic design objectives of range = 5560 km (3000 nmi), payload = 18 143 kg (40 000 lb), Mach = 1.2, and FAR Part 36 aircraft noise levels were achieved by the single-fuselage yawed-wing configuration with a gross weight of 211 828 kg (467 000 lb). A noise level of 15 EPNdB below FAR Part 36 requirements was obtained with a gross weight increase to 226 796 kg (500 000 lb). The off-design subsonic range capability for this configuration exceeded the Mach 1.2 design range by more than 20%. Although wing aeroelastic divergence was a primary design consideration for the yawed-wing concepts, the graphite-epoxy wings of this study were designed by critical gust and maneuver loads rather than by divergence requirements. The transonic nacelle drag is shown to be very sensitive to the nacelle installation. A six-degree-of-freedom dynamic stability analysis indicated that the control coordination and stability augmentation system would require more development than for a symmetrical airplane but is entirely feasible. A three-phase development plan is recommended to establish the full potential of the yawed-wing concept.</p>			
17 Key Words (Suggested by Author(s)) Aerodynamics, delta wing, flight controls, noise, propulsion, structures, swept wing, transonic transport, variable-sweep wing, weights, yawed wing		18 Distribution Statement	
19 Security Classif. (of this report) Unclassified	20 Security Classif. (of this page) Unclassified	21 No. of Pages	22. Price*

PRECEDING PAGE BLANK NOT FILMED

CONTENTS

	Page
SUMMARY	1
INTRODUCTION	2
SYMBOLS AND ABBREVIATIONS	5
CONFIGURATION DESCRIPTIONS	11
Design Synthesis Procedures	11
Fixed Swept Wing Configuration Model 1-2	14
Variable Sweep Wing Configuration Model 2-2	17
Delta Wing Configuration Model 3-2	17
Double Fuselage Yawed Wing Configuration Model 4-2	17
Single Fuselage Yawed Wing Configuration Model 5-3	21
General Description	21
Configuration Comparisons	27
CONFIGURATION PERFORMANCE	31
Mission Rules and Performance Objectives	31
Configuration Performance	33
Noise Performance Studies	45
Single Fuselage Yawed Wing Configuration Studies	45
Range Capability Versus Gross Weight	45
Range-Speed Sensitivity Study	49
Payload Sensitivity Study	49
Sized Airplane Definition Model 5-3a	49
YAWED WING CONFIGURATION EVOLUTION	57
Configuration Development	57
Initial Configuration Definition	57
Configuration Improvement Studies	63
Bypass Ratio Study	63
Wing Development Studies	73
Yawed Stabilizer	73
Body Cross-Section Study	78
CONFIGURATION ANALYSIS AND METHODS	81
Aerodynamics	81
Aerodynamic Design Approach	81
Aerodynamic Analysis Approach	91
Baseline Configuration Evaluations	91
Low-Speed Capability and High Lift Systems	105

CONTENTS—Concluded

	Page
Nacelle-Airplane Integration Studies	114
Quasi-Elliptical Planform Study	122
Model 5-3 Drag Variation With Mach Number	126
Flight Controls	127
Design Ground Rules	127
Airplane Balance and Empennage Sizing	130
Single Fuselage Yawed Wing Configuration	
Dynamic Stability and Control Characteristics	131
Conceptual Stability Augmentation Arrangement	143
Power Systems and Environmental Considerations	149
Bare Engine Data	149
Propulsion System Candidates	149
Acoustic Considerations	152
Engine Emission Levels	154
Engine Cycle Selection	156
Structures and Materials	162
Configuration Evaluation	162
Materials Selection	164
Yawed Wing Divergence	168
Yawed Wing Analyses	172
Yawed Wing Trade Studies	173
Weight and Balance	180
Weight Analysis Approach	184
Configuration Weight Analysis	184
Balance and Loading	189
Parametric Analysis	189
CONCLUSIONS	195
RECOMMENDATIONS	197
Phase I	197
Phase II	197
Phase III	198
Supporting Technology Development	198
REFERENCES	199
APPENDIX	

HIGH TRANSONIC SPEED TRANSPORT AIRCRAFT STUDY

FINAL REPORT

By Robert M. Kulfan, Frank D. Neumann, James W. Nisbet, Alan R. Mulally, James K. Murakami,
D. W. Gimmestad, Elias C. Noble, John P. McBarron, James L. Stalter, Mark B. Sussman
Boeing Commercial Airplane Company

SUMMARY

An initial design study of transport aircraft having high transonic cruise speed capabilities has been completed. Five different design concepts were configured and compared. These include: (1) aircraft with fixed swept wing, (2) aircraft with variable-sweep wing, (3) aircraft with delta wing, (4) twin-fuselage yawed-wing aircraft and (5) single-fuselage yawed-wing aircraft, as depicted in figure 1. Results of past programs and earlier studies, including the substantial background of the contractor's work on supersonic transport development, were used as important inputs. Additionally, the work done under the NASA-Langley Research Center sponsored contracts, "Study of the Application of Advanced Technologies to Long-Range Transport Aircraft," (NAS1-1071, -1072, and -1073) provided important technology data for aircraft designed to operate in the transonic regime. Further, the aerodynamic development accomplished by NASA's Ames Research Center on the yawed-wing concept provided essential background data for the study.

The design objectives applied to all configurations studied were the following:

Cruise Mach No.:	M = 1.2
Range:	5,560 km (3000 n.mi)
Aircraft noise goal:	15 EPNdB below FAR.36
Passenger Payload:	195 passengers (18,143 kg, 40,000 lb)
Technology level:	Projected for 1985 subject to the undertaking of technology development programs

The results indicated that the "boomless" supersonic mission requirements can be met at FAR 36 noise levels by a delta wing configuration at 226,796 kg (467,000 lb). The noise goal of FAR 36 minus 15 EPNdB can be met with the single body yawed-wing configuration at approximately 226,796 kg (500,000 lb) gross weight. This noise goal cannot be met by the other configurations within the assumed propulsion and jet-noise suppression technology levels. The yawed-wing configuration, because of its superior low speed aerodynamics, has a large advantage in takeoff and landing performance. The variable-sweep and high aspect ratio wing of the yawed-wing configuration provides a 20 percent range improvement for subsonic cruise over its M = 1.2 design range.

The stability and control responses of the yawed-wing airplanes are unique. The results of this study indicate that a flight control system could be developed to give this type of aircraft handling qualities that are similar to those of more conventional aircraft.

The primary structure choice for all of the airplanes was graphite/epoxy honeycomb. The critical structural design conditions for the yawed-wings of this study were gust and maneuver loads rather than aeroelastic divergence.

The yawed-wing aircraft presented unique design and integration problems. Coordinated theoretical-experimental design studies are required to determine if the predicted performance characteristics are indeed achievable. A three-phase development plan has been formulated to establish the full potential of this concept.

Phase I involves analytical studies which follow directly from this contract. Phase II combines wind tunnel and lab test work with further theoretical studies. Phase III carries the development work of Phase I and II to detailed design and flight test of a demonstration vehicle.

INTRODUCTION

This document is the final report of the work accomplished by The Boeing Commercial Airplane Company under contract NAS2-7031, "High Transonic Speed Transport Aircraft Study." for NASA's Ames Research Center. The work began on June 20, 1972 and was completed on May 20, 1973.

As a result of sonic boom from supersonic aircraft flying over populated land masses there is interest in aircraft designed for transonic cruise speeds. This interest has been enhanced by potential improvements in transonic aerodynamic efficiency offered by advances in supercritical flow aerodynamics technology and in design concepts such as yawed-wing aircraft.

There have been two significant design studies applicable to transonic transport aircraft: (1) the NASA Studies of the Application of Advanced Technologies to Long-Range Transport Aircraft (Boeing, General Dynamics, and Lockheed) relative to the Lower transonic regime (up to Mach 1) and (2) the NASA study being reported herein relative to the high transonic regime (up to $M = 1.2$ and beyond). The first study was conducted in 1971 and 1972. The second study has special relevance to boom-free supersonic flight in that the upper speed limit was considered to be that which would avoid sonic boom at ground level.

The objectives of this study were to develop five specific configuration types suitable for cruise in the high transonic regime, make cross-comparisons of each, conduct design trade-off sensitivity studies, and identify critical research areas pertinent to development of high transonic transport aircraft. The five configuration types included: (1) fixed swept wing aircraft, (2) variable-sweep wing aircraft, (3) delta wing aircraft, (4) twin-fuselage yawed-wing aircraft, and (5) single-fuselage yawed-wing aircraft.

In the initial phase of the study, size parameters and technology levels were identified as applicable to all the configurations and a "first cycle" design definition was accomplished for all five configurations. These initial definitions were developed and analyzed in detail to provide the parametric data necessary to determine the optimum wing area and engine match to meet the design objectives. Following this, second cycle designs were completed and reviewed with representatives of the Ames Research Center at the end of approximately 4-1/2 months.

The results at that time identified promising potential for the single-fuselage yawed-wing concept: that would however require more extensive development because of its unique characteristics. The following recommendations were made:

- Concentrate the remainder of the study effort on trade studies to optimize this concept
- Suspend further developmental work on the other concepts
- Forego the comparative performance and economics studies

The study plan was revised to incorporate these recommendations and thereby allow for developing an improved configuration arrangement for this yawed wing concept followed by range, payload, noise and speed sensitivity studies.

This document presents the descriptions and performance characteristics of the configurations that have been synthesized for each of the five concepts. The design evaluation of the single fuselage yawed wing concept is traced. The design and analysis methods are described along with the results of specialized trade studies that provided design guidance.

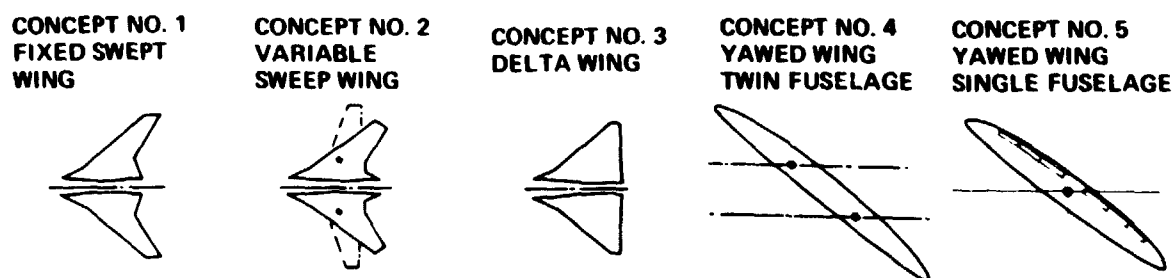


FIGURE 1.—AERODYNAMIC CONCEPTS—MACH 1.2

PRECEDING PAGE BLANK NOT FILMED

SYMBOLS AND ABBREVIATIONS

ALT	altitude
A/P	airplane
APP	approach
AR	aspect ratio
ATA	air transport association
ATT	advanced technology transport
A_{wet}	wetted area
A_y	side acceleration
b, b_w	wing span
b/a	elliptic axes ratio, ratio of semi-major axes
B	body
BPR	bypass ratio of engine
c	basic chord
c'	wing chord including expanded chord of trailing edge flap
C_D	drag coefficient
C_{DF}	friction drag coefficient
C_{DL}, C_{DLIFT}	drag coefficient due to lift (includes the induced drag and wave drag due to lift)
C_{DMISC}	miscellaneous drag coefficient
C_{DTRIM}	trim drag coefficient
C_{DW}	volume wave drag coefficient
C_l	lift coefficient
$C_{LDESIGN}$	wing design lift coefficient

$C_{l\hat{p}}$	rolling moment due roll rate stability derivative -1/rad
C_{Lp}	lift coefficient at which ΔC_{Dp} equals zero
$C_{l\hat{q}}$	rolling moment due to pitch rate stability derivative -1/rad
$C_{l\hat{r}}$	rolling moment due to yaw rate stability derivative -1/rad
CLR	lift coefficient - initial cruise divided by lift coefficient - maximum L/D
$C_{L\alpha}$	lift curve slope
$C_{l\beta}$	rolling moment due to sideslip stability deriv. tive -1/rad
$C_{l\delta_a}$	rolling moment due to aileron deflection stability derivative -1/rad
$C_{l\delta_R}$	rolling moment due to rudder deflection stability derivative -1/rad
C_m	pitching moment coefficient
C_{mC_L}	slope of the pitching moment curve
$C_{m\hat{p}}$	pitching moment due to roll rate stability derivative -1/rad
$C_{m\hat{q}}$	pitching moment due to pitch rate stability derivative -1/rad
$C_{m\hat{r}}$	pitching moment due to yaw rate stability derivative -1/rad
$C_{m\alpha}$	pitching moment due to angle-of-attack stability derivative -1/rad
$C_{m\hat{\alpha}}$	pitching moment due to rate-of-change of angle-of-attack stability derivative -1/rad
$C_{m\delta_a}$	pitching moment due to aileron deflection stability derivative -1/rad
CO	carbon monoxide
\bar{C}_W	mean aerodynamic chord, wing - meters(ft)
$C_{z\hat{q}}$	lift due to pitch rate stability derivative -1/rad
$C_{z\alpha}$	lift due to angle-of-attack stability derivative -1/rad
$C_{z\hat{\alpha}}$	lift due to rate-of-change of angle-of-attack stability derivative -1/rad
$C_{z\beta}$	lift due to sideslip stability derivative -1/rad
$C_{z\delta_e}$	lift due to elevator deflection stability derivative -1/rad

D	diameter
EPNdB	effective perceived noise level
FAR	Federal Aviation Regulations
FT	feet
GWT	gross weight
HC	hydrocarbons
ICAC	initial cruise altitude capability
ka	aerodynamic stiffness
K _E	envelope drag due to lift factor, $C_{D_{LIFT}}/C_L^2$ at the design C_L
k _e	structural stiffness
KT	knots
L	lift, length
LBS	pounds
L/D	lift-to-drag ratio
m _α	bending moment due to a unit wing angle of attack
M	Mach number
M _A	forward wing bending moment
\hat{r}	non-dimensional yaw rate – $\left(\frac{rb}{2V}\right)$
R	yaw rate -rad/sec, rolling moment
S	area
SAS	stability augmentation system
SFC	specific fuel consumption
S _H	horizontal tail area
S.L.	sideline

S_{REF}	wing reference area
S_V	vertical tail area
S_W	wing area
t/c	thickness to chord ratio
T	tail thickness
$(T/C)_{MAX}$	maximum wing thickness/chord ratio
TOFL	takeoff field length
TOGW	takeoff gross weight
T.O. W/CB	takeoff with thrust cutback procedure
T_{SLS}	engine thrust –sea level static
T/W	thrust loading, total rated engine thrust divided by airplane takeoff gross weight
V	true airspeed
W	wing
$(W/B)_{INTERF}$	wing and body mutual wave drag interference
ω_N	dynamic stability undamped natural frequency
W/S	wing loading, airplane gross weight divided by wing area
x/c	fraction of wing chord
X_S	streamwise separation distance
Y	spanwise separation distance
Y/B	fraction of span
Z/C	camber fraction of chord
α	angle-of-attack –rad
$\hat{\alpha}$	nondimensional rate-of-change of angle-of-attack – $(\hat{\alpha} \bar{C}_W / 2V)$
α, α_W	wing angle-of-attack

α_{δ}	flap effectiveness factor—rate of change of angle of attack with flap deflection
α_w	wing twist angle
β	sideslip angle—rad, $M^2 - 1$
δ_a	aileron deflection—rad
$\delta_{CM_{\delta}}$	moment increment due to unit tail deflection
δ_e	elevator deflection
δ_F	flap deflection angle
$\delta_H, \delta_{H_{TAIL}}$	tail deflection angle
δ_R	rudder deflection
δ_s	stabilizer angle—radians
ΔC_{D_i}	additional drag due to lift
ΔC_{D_p}	additional parasite drag coefficient
ΔC_{L_p}	increment in C_{L_p} due to leading edge or trailing edge flap deflection
$\Delta C_{L_{TE}}$	increment in lift due to trailing edge flap deflection
ΔC_L	lift increment due to unit tail deflection
$\frac{\Delta C_{MH}}{\Delta \delta_H}$	tail effectiveness
ΔM	bending moment resulting from roll rate and aileron deflection
ϵ	downwash
λ	taper ratio
Λ	wing sweep angle
$\Lambda_{c/4}$	sweep angle of quarter-chord line

Subscripts

λ	aft flap of double-slotted flap
App	landing approach
f	flap
GE	ground effects
LE	leading edge
MAX	maximum
0	at zero lift
REF	reference
S	stall conditions
TE	trailing edge
TRAP	trapezoid
V_2	takeoff second segment
EFF	effective

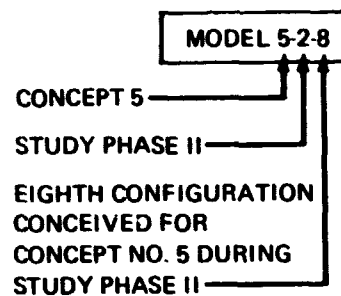
CONFIGURATION DESCRIPTIONS

To provide a basis for the evaluation of advanced technology Mach 1.2 airplane concepts, numerous configurations were considered and developed during the course of this study. The configuration evolution process is depicted in the appendix.

DESIGN SYNTHESIS PROCEDURES

Five basic configuration concepts, identified as concept 1 through 5, were evaluated during the early part of the study. Model numbers were assigned to configuration variations of each concept as a function of the concept, the phase of the study and the variation studied.

For example,



Configurations are referred to by these designations throughout this report.

The design synthesis approach that was used to develop the aircraft configurations in this study is illustrated in figure 2.

The initial step was to define preliminary configuration characteristics that included such general items as:

- Wing planform, size, thickness
- Number of engines, engine cycle and size
- Tail planform, thickness and size
- Estimated maximum takeoff gross weight

These characteristics most often were derived from the results of past related studies or from specially conducted trade studies. These estimated configuration characteristics were used to develop preliminary configuration sketches. These sketches along with supporting aerodynamic design optimization studies, weight and balance analyses, stability and control analyses, and structural layouts provided inputs for developing a detailed configuration layout (step 2).

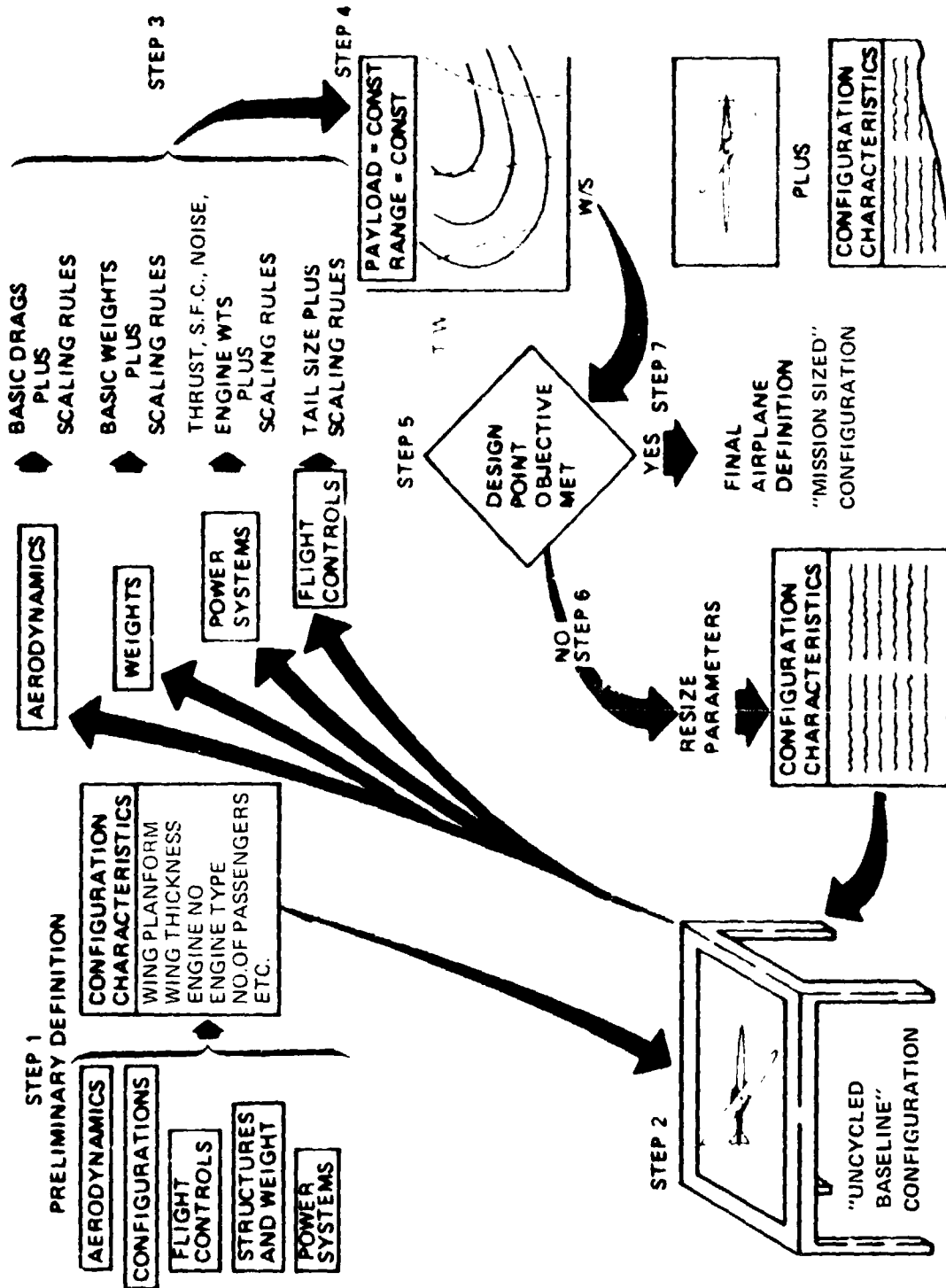


FIGURE 2.--DESIGN SYNTHESIS PROCESS

The detailed design layout defined the “uncycled baseline” configuration. The baseline configuration was then analyzed in depth to determine the basic weight, lift and drag, thrust and noise characteristics. Additional analyses were made to determine the effects of varying engine size, and wing area to establish scaling rules that account for these changes (step 3).

The results of the baseline configuration evaluation along with the scaling rules form the inputs to a parametric performance analysis program that is used to “size” the airplane by determining the minimum gross weight, the wing area, engine size and tail sizes necessary to achieve the mission objective (step 4). This step is discussed in more detail in the performance section of this report.

If the design objectives are not met, or if obvious shortcomings are identified, this process is repeated.

The configuration general arrangements that were developed considered the following requirements and objectives:

- Passenger payload of 18,143 kg (40,000 lb), which is equivalent to 195 passengers and their baggage for domestic operations.
- A 15% first class and 85% tourist class distribution.
- Seat widths of:

	First Class	Tourist
Single	66 cm (26 in.)	56 cm (22 in.)
Double	132 cm (52 in.)	107 cm (42 in.)
Triple	---	160 cm (63 in.)

- Seat pitches of 96 cm (38 in.) and 86 cm (34 in.) in the first class and tourist sections, respectively.
- Passenger service provisions including galleys, lavatories and closets equivalent to current jet transport practice.
- Cabin door design satisfactory to passenger and service ingress and egress and meeting or exceeding the intent of emergency provisions of FAR 25.
- Volume provisions below the passenger cabin floor for containerized and bulk cargo.
- Containerized cargo density of 162 kg/cu meter (10 lb/cu ft).
- A minimum containerized cargo volume of .14 cu meters (5 cu ft) per passenger based on an all-tourist 86.3 cm (34 in.) seat pitch configuration.

- Additional bulk cargo volume of at least 14.1 cu meters (500 cu ft) for all configurations except the single fuselage yawed wing configuration 5-3.
- Passenger cabin doors, cargo doors, and passenger services compatible with current airline ground support equipment.
- Passenger cabin deck heights consistent with current airport passenger loading facilities.

The airplanes were also designed to be compatible with current and projected airport ramp areas, taxiways, and runway facilities. The landing gear designs provided flotation capabilities (fig. 3) for airport facilities projected for the 1980-90 time period.

The characteristics of the final baseline configuration that was developed for each concept (Model 1-2, Model 2-2, Model 3-2, Model 4-2 and Model 5-3) are described below.

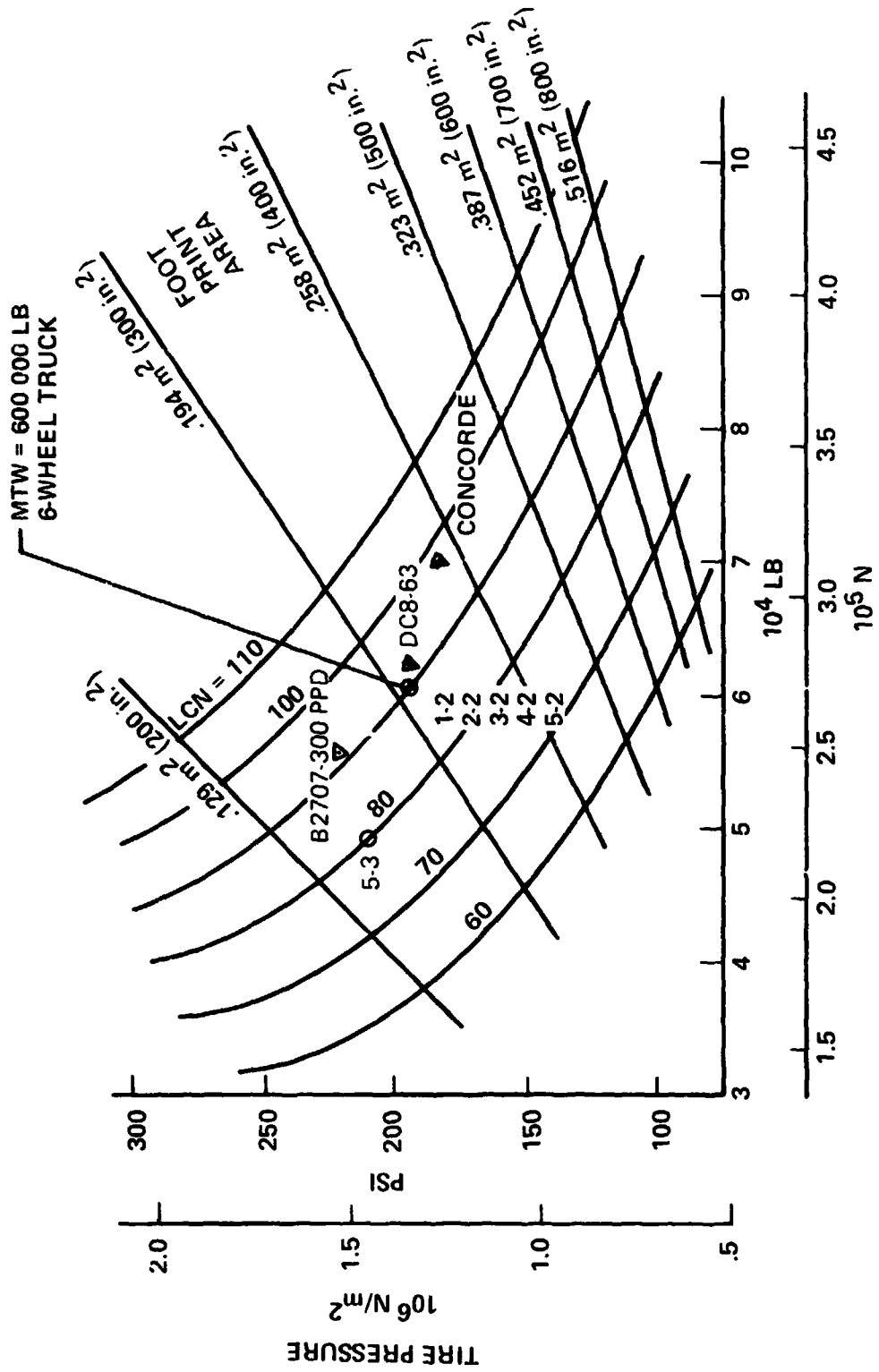
FIXED SWEEP WING CONFIGURATION—MODEL 1-2

The results of previous contractor Transonic and Supersonic Transport studies led to the development of the general arrangement for configuration 1-2 (fig. 4). This arrangement includes four engines mounted in two dual pods under the wing near the trailing edge and outboard of the main landing gears. This allows large span flaps on the outboard wing and good airplane balance characteristics. The passengers are seated in a balanced arrangement fore and aft of the wing. The minimum body cross section is designed for a 4-abreast passenger seating arrangement with a single aisle, plus the underfloor area required for landing gear stowage. The required "area ruling" resulted in a wide fuselage forward and aft of the wing, which locally allowed twin aisles interior arrangements. Provisions were made for containerized cargo in the lower forward fuselage. Bulk cargo could be carried in the lower fuselage aft of the landing gear wheel wells.

The empennage consists of a fin with swept, trapezoidal planform and an all-movable stabilizer that is mounted in the aft fuselage.

The tricycle-type landing gear is arranged to facilitate the required airplane liftoff rotation and to assure nacelle ground clearance during all normal aircraft operating attitudes. The main gear is wing-mounted and is supported by the wing rear spar and a landing gear beam. The gear retracts sideways into the lower fuselage aft of the wing box. The low profile tires are mounted on 6-wheel trucks in order to minimize the airplane frontal area that is required for gear stowage.

Fuel is carried in integral tanks in the outboard wing and in the center wing box. The volume of the wing is limited, however, and additional fuel is carried in body tanks forward of the wing box. More volume is carried in the aft body in a balance/trim fuel tank, forward of the stabilizer carry-through structural box.



(I.C.A.O. AERODROME MANUAL PART 2 PARA 4.1.3)

EQUIVALENT SINGLE WHEEL LOAD

FIGURE 3.--COMPARISON OF AIRPLANE LANDING GEAR FLOTATION CAPABILITIES

$\bar{c} = 10.87 \text{ m}/42.8 \text{ IN}$

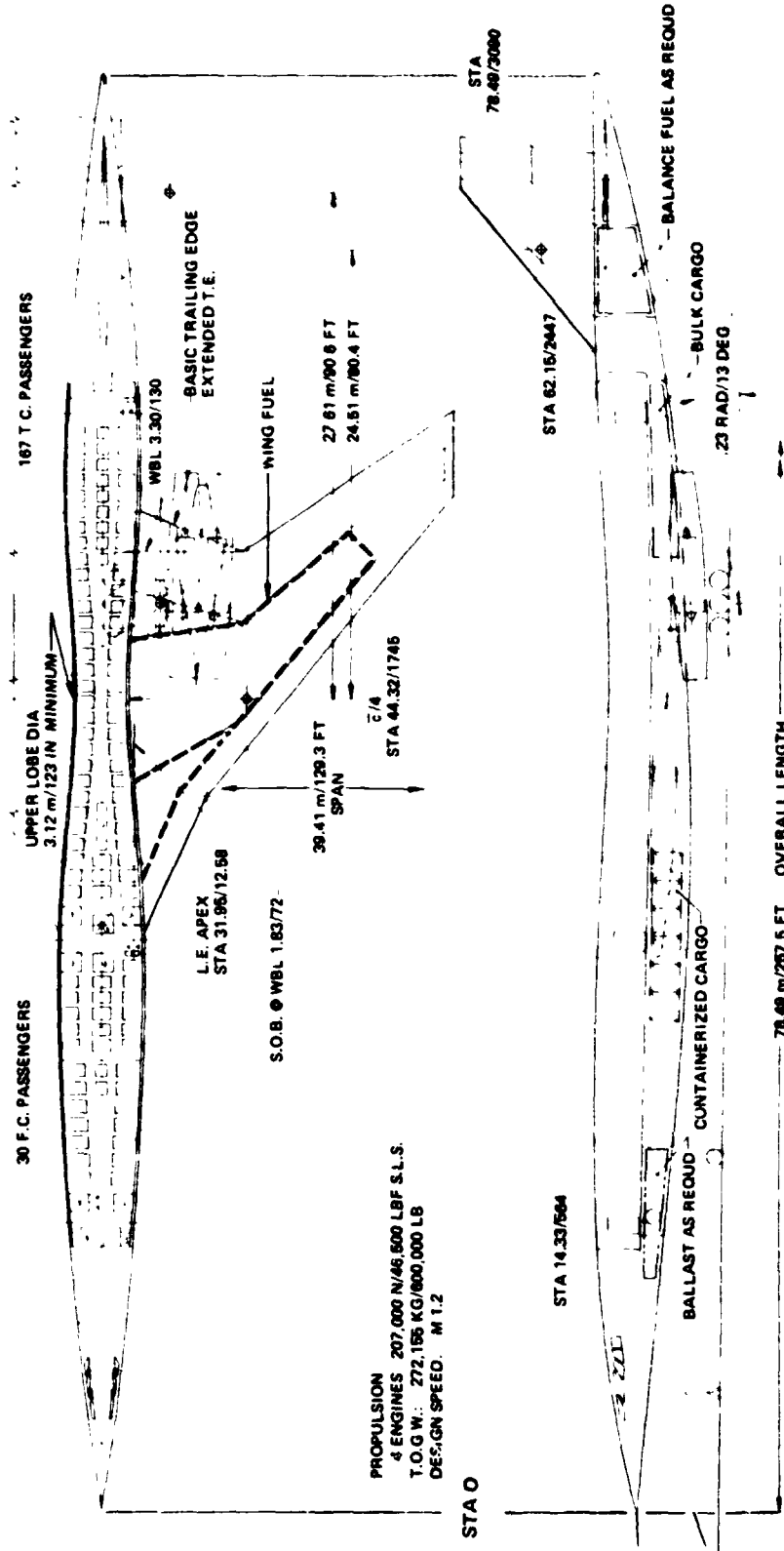


FIGURE 4.—CONCEPT 1 BASELINE CONFIGURATION, MODEL 1-2

A droop nose was used to eliminate the high transonic drag associated with fixed windshields, to eliminate noise and buffet at the pilot station, and to provide good pilot visibility during takeoff, landing and ground maneuvering.

VARIABLE SWEEP WING CONFIGURATION—MODEL 2-2

The overall configuration arrangement, figure 5, is similar to model 1-2, except as described below. The wing has a lower aspect ratio and more sweep in the cruise position. The wing sweep can be varied from .37 rad (21°) to .94 rad (54°).

The engines are mounted in dual pods under the wing near the trailing edge. They are supported by structural members that extend aft from the fixed center wing box and are stabilized by members extending outboard from the fuselage. The main landing gears are located inboard of the engine nacelles. The gears are also supported by structural beams that extend outboard from the fuselage. The inboard wing trailing edge was extended aft in order to fair the gear and nacelle support structure.

Very limited fuel volume is available due to the thin wing combined with the variable sweep design feature. Preliminary results showed that approximately 50% of the total required fuel had to be carried in the fuselage, figure 5.

DELTA WING CONFIGURATION—MODEL 3-2

This arrangement, figure 6, is based on the extensively investigated contractor supersonic transport prototype design. The body length is identical to models 1-2 and 2-2 in order to maintain similar configuration fineness ratios and satisfactory tail arms.

The engines were located well aft of the wing aerodynamic center, as compared to models 1-2 and 2-2. The wing is also located further aft on the body for airplane balance. As a result the fuselage area distribution is less symmetric forward and aft of the wing, with a larger volume ahead of the wing. Although the same minimum fuselage cross section was used, all passengers can be accommodated in the wide fuselage forward of the wing rear spar. The passenger cabin length was, therefore, reduced by approximately 6.1 m (20 ft). The aircraft was balanced with full payload. Water ballast is carried for some off-design operation at low passenger load factors. A small amount of the total fuel is carried in body fuel tanks.

The other configuration characteristics are similar to those of model 1-2.

DOUBLE FUSELAGE YAWED WING CONFIGURATION—MODEL 4-2

The general arrangement and the geometry of the wing and the two fuselages on this configuration, figure 7, was developed from recent NASA-Ames studies. The distance between the two fuselages is equivalent to 30% of the wing span. A four-engine arrangement was chosen with a separate empennage on each fuselage.

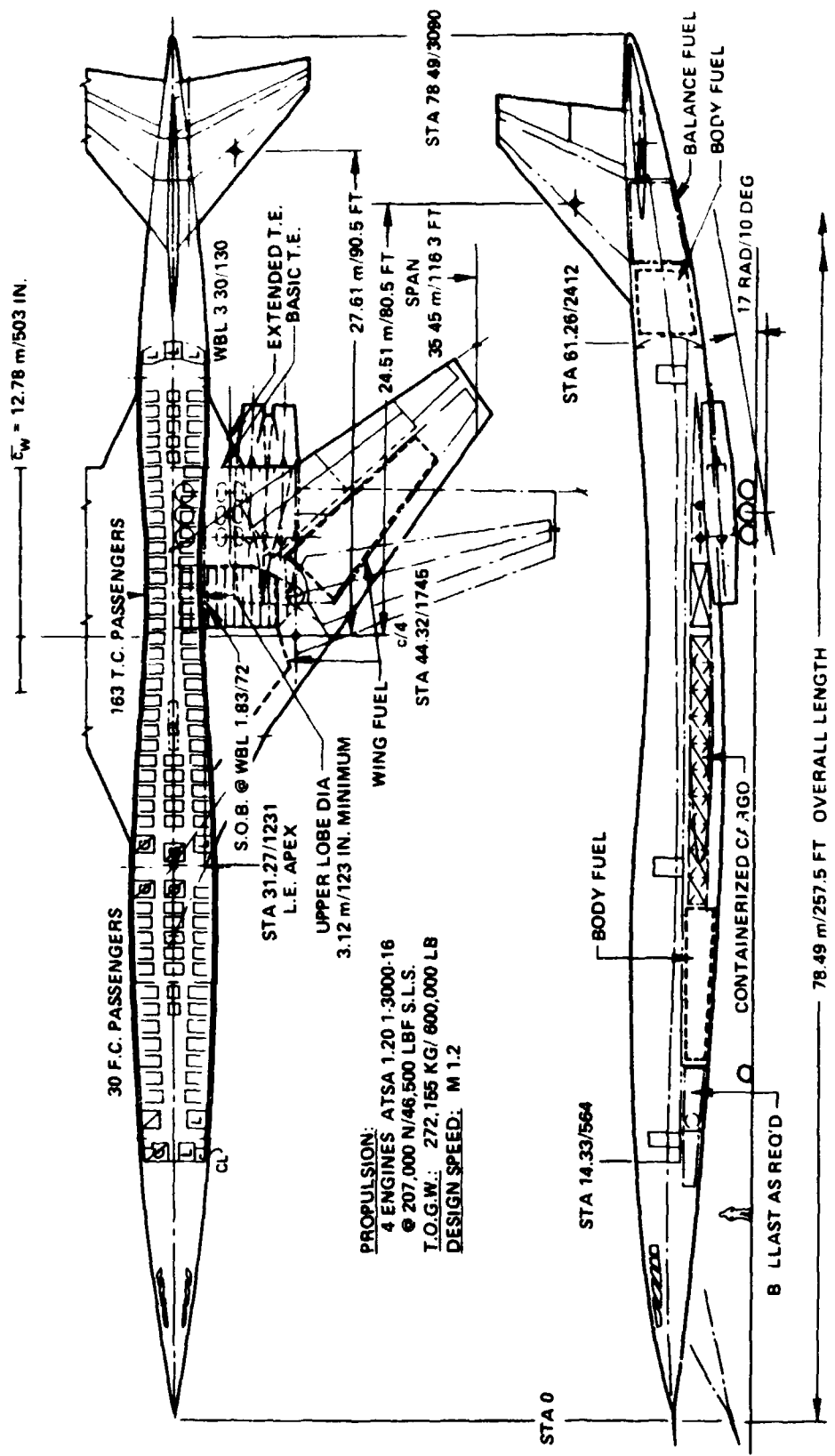


FIGURE 5.—CONCEPT 2 BASELINE CONFIGURATION, MODEL 2-2

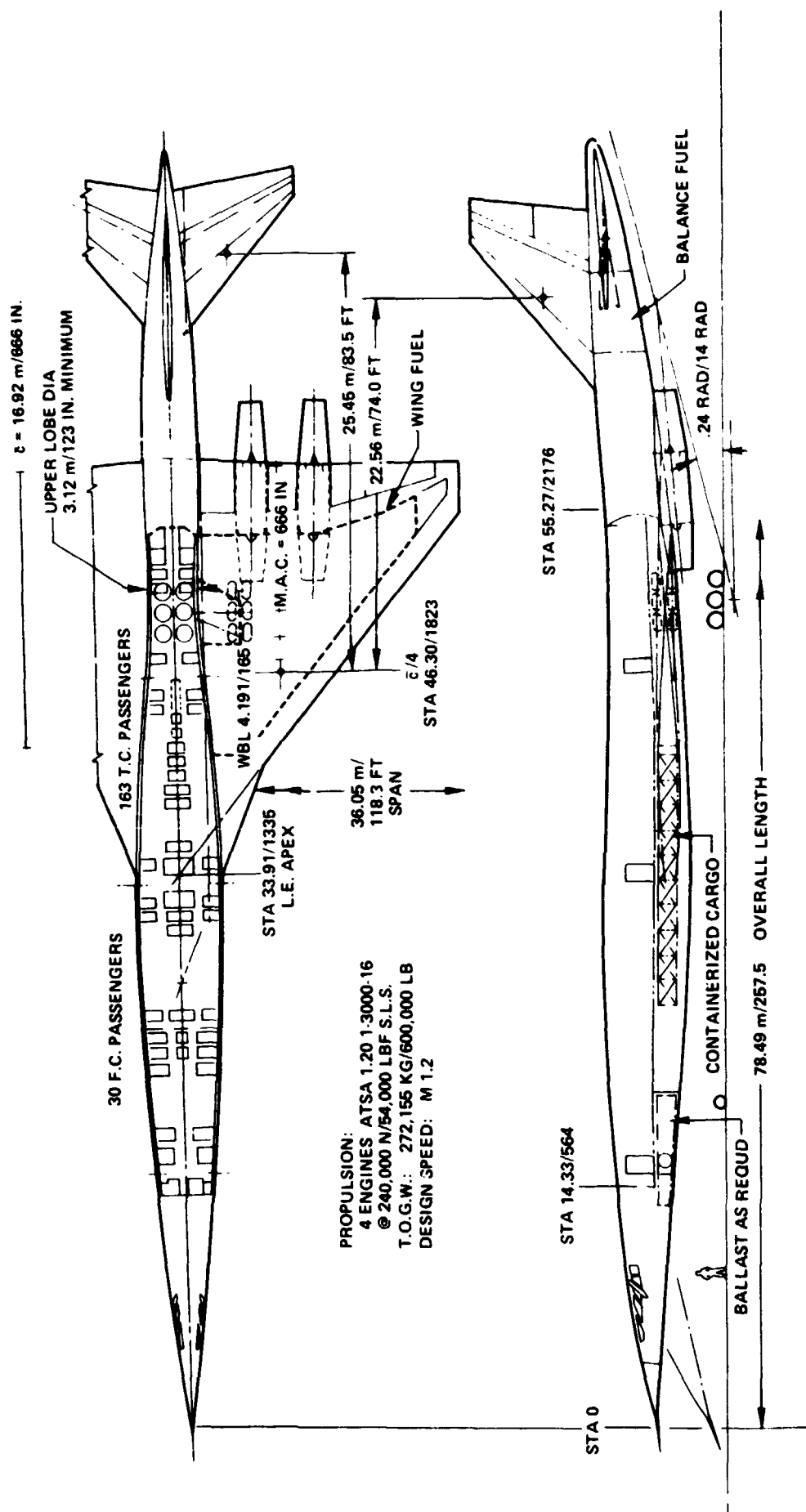


FIGURE 6.—CONCEPT 3 BASELINE CONFIGURATION, MODEL 3-2

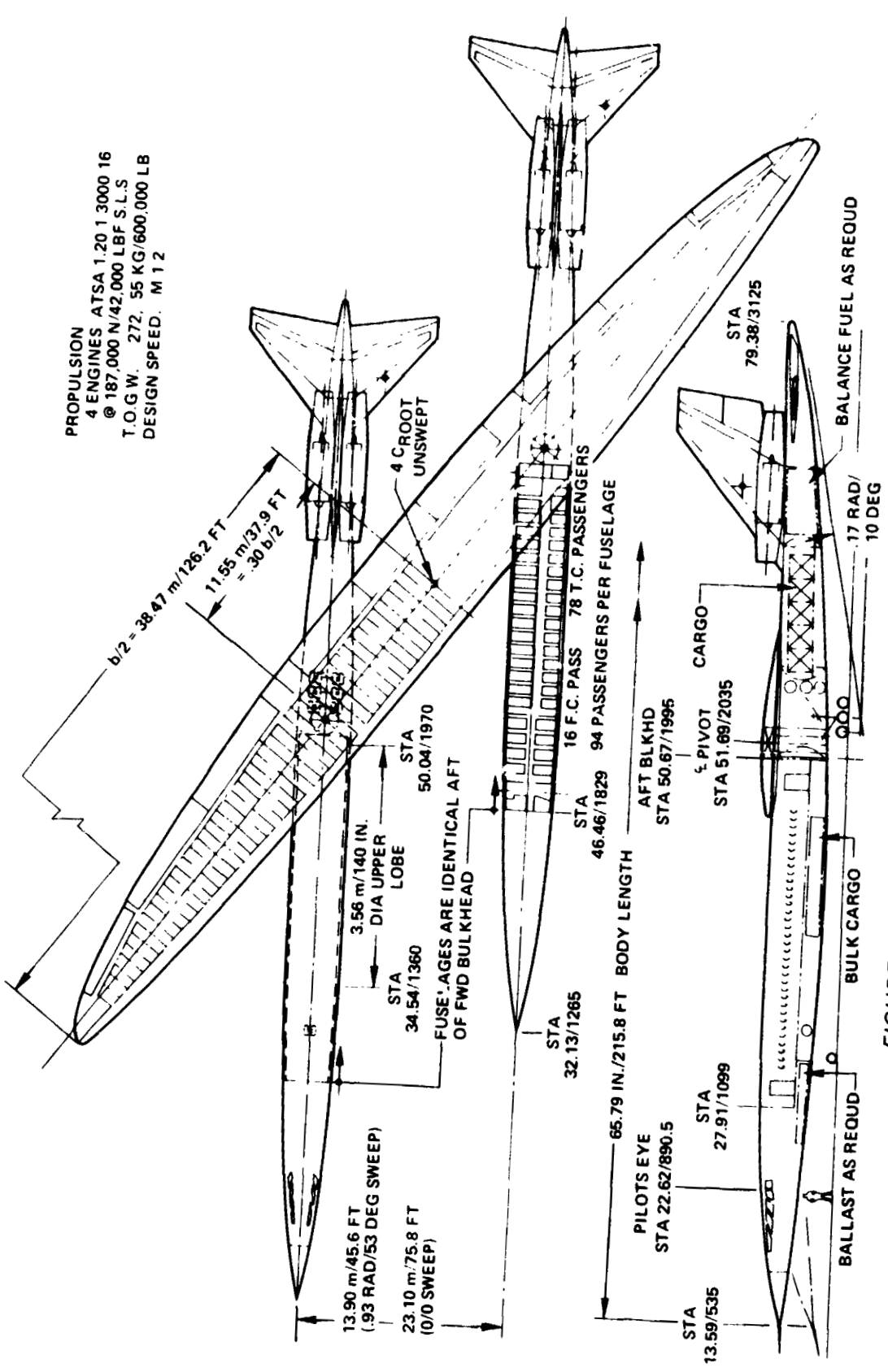


FIGURE 7.—CONCEPT 4 BASELINE CONFIGURATION, MODEL 4.2

The area distribution of each fuselage was carefully developed in the presence of the respective part of the yawed wing. It was found possible to design both fuselages to be identical. All passengers are accommodated in the fuselages forward of the wing pivots in a four-abreast first class, five-abreast tourist class seating layout. This arrangement had the passenger cabin ahead of an unpressurized section of the fuselage which facilitated the structural integration of wing pivot and landing gear. A section of the fuselage aft of the landing gear was used for cargo, baggage, and body fuel, followed by a compartment for a trim fuel tank. The flight crew compartment was located in the leading fuselage. The engines were mounted symmetrically on each side of the two vertical tails immediately above the body. This allows a balanced engine support scheme with a common thrust reverser for each dual engine installation. The all-moveable stabilizers were located on the fuselages below and aft of the engine nozzles to reduce downward jet noise propagation.

The landing gear system consists of main and nose gears, mounted in each body. The main gear was located to allow conventional liftoff rotation of the aircraft. It is mounted in the fuselage aft of the wing pivot support structure and retracts rearward into the fuselage ahead of the pressurized cargo baggage compartment. The main gear carried a six-wheeled truck with horizontal stabilization during retraction to minimize drag and was size limited by body diameter.

The nose gears are conventional with steering capability and retract aft into the body.

Most of the mission fuel is carried in integral wing tanks with the remainder being carried in a mid-fuselage tank plus the aft body balance/trim fuel tank.

SINGLE FUSELAGE YAWED WING CONFIGURATION—MODEL 5-3

The evolution of this configuration is illustrated in the appendix. This configuration shown in figure 8 represents the single fuselage, yawed wing airplane with the lowest gross weight that was developed during this contract for the design mission. The extensive configuration evolution process that led to this configuration is described in more detail further on in this report. Table 1 summarizes some of the unique characteristics, demands or requirements present on a yawed wing design and the resulting unique configuration design features that were incorporated on Model 5-3.

General Description

Fuselage

The diameter of the circular fuselage varies from 356 cm to 406 cm (140 to 160 inches) over the length of the passenger cabin. The seating arrangement is 4-, 5-, or 6-abreast with a single aisle. Baggage is carried in 707-size containers on the lower deck. The configuration offers a very high degree of payload flexibility since the passenger cabin is not obstructed by other airframe/engine components. The passenger appeal should be very high because of good visibility and low cabin noise due to the aft engine installation. The cab is provided with a movable visor for improved flight crew visibility at low speeds. The full droop nose feature was not necessary since the unswept wing of high aspect ratio will not need large nose-up attitudes during takeoff and landing approach.

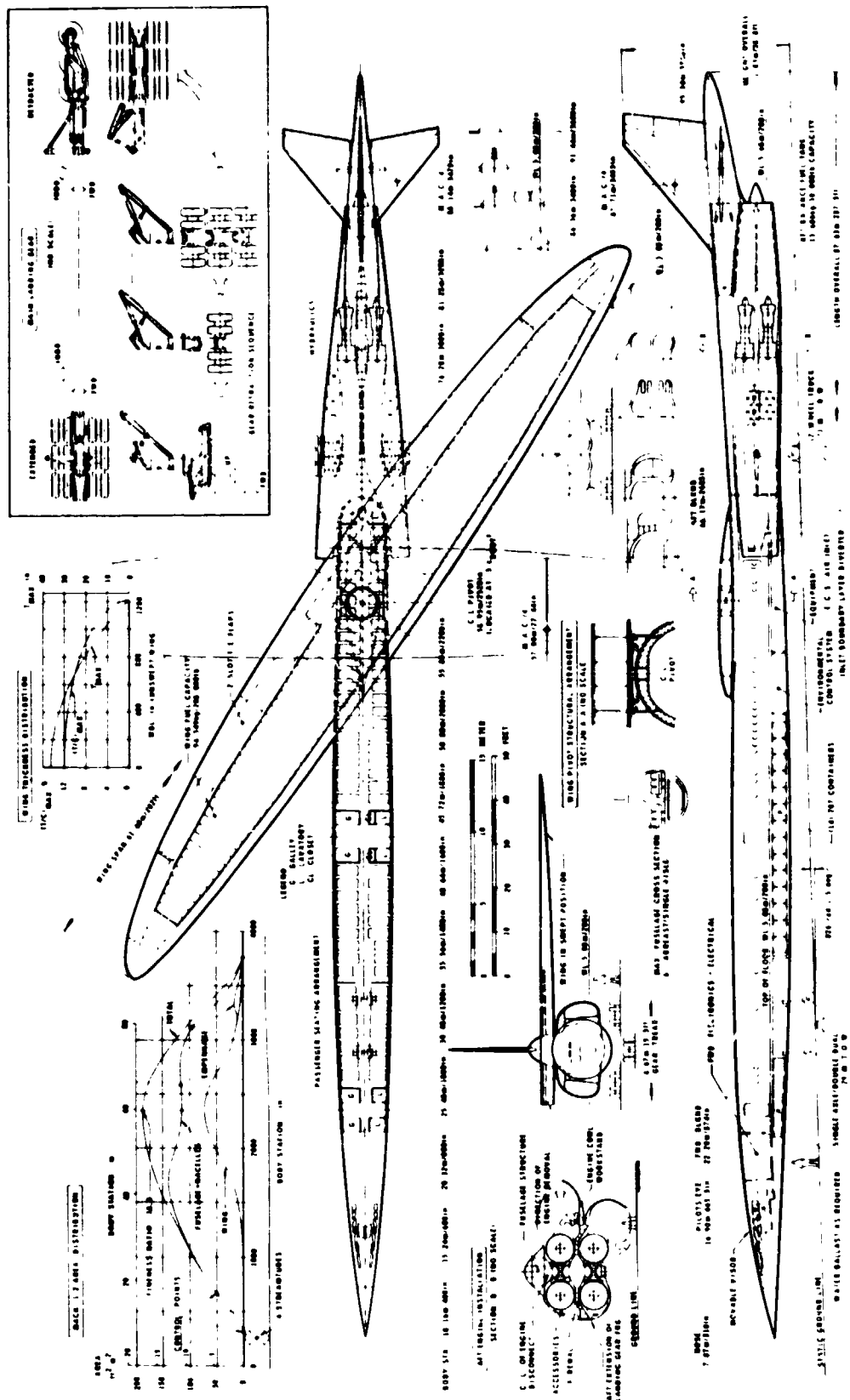


FIGURE 8.—CONCEPT 5 SINGLE FUSELAGE, YAWED WING (8:1 ELLIPSE), MODEL 5-3

TABLE 1.—DESIGN REQUIREMENTS VS CONFIGURATION FEATURES,
MODEL 5-3, YAWED WING—SINGLE FUSELAGE

DESIGN REQUIREMENT OR CHARACTERISTIC	RESULTING CONFIGURATION FEATURE
<ul style="list-style-type: none"> ● PIVOTING WING 	<ul style="list-style-type: none"> — BODY-MOUNTED ENGINES — BODY-MOUNTED LANDING GEAR WITH NARROW TREAD — HIGH WING ARRANGEMENT — USEABLE FUSELAGE CROSS SECTION REDUCED BELOW PIVOT
<ul style="list-style-type: none"> ● POWER PLANT INSTALLATION WITH LOW DRAG 	<ul style="list-style-type: none"> — 4 ENGINES INTEGRATED IN AFT FUSELAGE
<ul style="list-style-type: none"> ● LANDING GEAR ARRANGEMENT THAT DOES NOT COMPROMISE CONFIGURATION FINENESS RATIO 	<ul style="list-style-type: none"> — BICYCLE-TYPE LANDING GEAR AFT OF PASSENGER CABIN — LONG-DUCT ENGINE INLETS — NEAR-LEVEL ATTITUDE OF AIRCRAFT DURING TAKEOFF AND LANDING — TWIN STRUT NOSE GEAR, LARGE NUMBER OF GEARS
<ul style="list-style-type: none"> ● WING-BODY ARRANGEMENT WITH LOW DRAG AND EASE OF CONFIGURATION 	<ul style="list-style-type: none"> — HIGH WING ARRANGEMENT
<ul style="list-style-type: none"> ● WING-BODY INTEGRATION STRUCTURALLY EFFICIENT 	<ul style="list-style-type: none"> — HIGH WING ARRANGEMENT — WING SUPPORT BEARINGS LOCATED OUTSIDE OF PRESSURIZED FUSELAGE
<ul style="list-style-type: none"> ● WING PLANFORM WITH OPTIMUM WEIGHT/DRAG TRADE 	<ul style="list-style-type: none"> — 8:1 ELLIPSE
<ul style="list-style-type: none"> ● FUSELAGE LENGTH WITH OPTIMUM WAVE DRAG/WEIGHT TRADE 	<ul style="list-style-type: none"> — LARGE FUSELAGE FINENESS RATIO (ZZ:1) — MINI-PIVOT ARRANGEMENT WITH 4 ABREAST BELOW PIVOT — AFT FUSELAGE EXTENSION FOR EMPENNAGE SUPPORT
<ul style="list-style-type: none"> ● AIRCRAFT BALANCE 	<ul style="list-style-type: none"> — AFT-MOUNTED ENGINE BALANCED BY FORWARD PAYLOAD AND/OR FORWARD BALLAST
<ul style="list-style-type: none"> ● PASSENGER SAFETY, LOW CABIN NOISE 	<ul style="list-style-type: none"> — AFT-MOUNTED ENGINES
<ul style="list-style-type: none"> ● LOW DRAG COCKPIT 	<ul style="list-style-type: none"> — MOVEABLE VISOR NOSE

Wing Pivot

A preliminary wing pivot design is shown in figure 9. The bearing rings for the pivot of the yawed wing are approximately 2.1 m (7 ft) in diameter. The rings are located between the top of the fuselage and the wing underside. They are fastened to the wing and the body without interrupting the carry-through structure of either. The thickness of the circular fuselage frames below the pivot is twice that of regular frames in order to react bending loads introduced by the wing.

Duct/Propulsion Installation

Figure 8 shows a preliminary design for the integration of inlet, engines and nozzles with the aft fuselage. The two D-shaped inlet faces are separated from the sides of the fuselage to capture undisturbed freestream air. Following the straight diffuser section the inlet ducts are bent towards the aircraft centerline and the duct shape gradually changes into 4 circular sections. After an S-bend the ducts are led straight aft past the landing gear bay. The volume required for support and stowage of the landing gear is created in the shadow of the S-bend. The structure around and between the inlet ducts forms the primary structure in that region of the fuselage. Over the entire length of the engine bay the fuselage structure has a cruciform shape which is jointed on top to the empennage boom, figure 10. The 4 engines are supported from the side and have large cowl doors hinged for engine access and removal. Structure for the engine nozzles is integrated with the empennage boom. Space for engine accessories is provided by the aft fairing of the landing gear.

Main Landing Gear

The main landing gear truck geometry represents a scaled version of the contractor SST Model 2707-300, 6-wheel, 12-tire truck. The main gear is shown in figure 11. The gear retracts aft into the fairing behind the intake ducts and goes through three retraction cycles to get there. The sequences are chosen to minimize drag. After takeoff, when the gear is fully extended, the truck is rotated about the shock strut 90° and relocked to complete the first cycle. The truck is then rotated vertically about the center wheel axle against the shock strut and is held there by the truck rotation actuators completing the second cycle. The whole gear is rotated about the upper trunnion to complete the third cycle thus completing retraction. The reverse sequence is initiated for gear extension. The down lock jury strut also serves as an uplock. This arrangement has only a partial free fall capability and is completely dependent on hydraulic power sequencing for the three cycle operation.

The location of the Main Gear is dependent on the space available behind the intake ducts and is forced much further aft than is conventional causing a higher proportion of gear load to be placed on the nose gear. There is an advantage here because wheel brakes can be included in the nose gear wheels. Takeoff rotation and high angle landing flare is not required for this configuration. Because of the small gear tread and the large turnover moments of this high-wing aircraft, stability during ground maneuvers is an area that requires more detailed investigations.

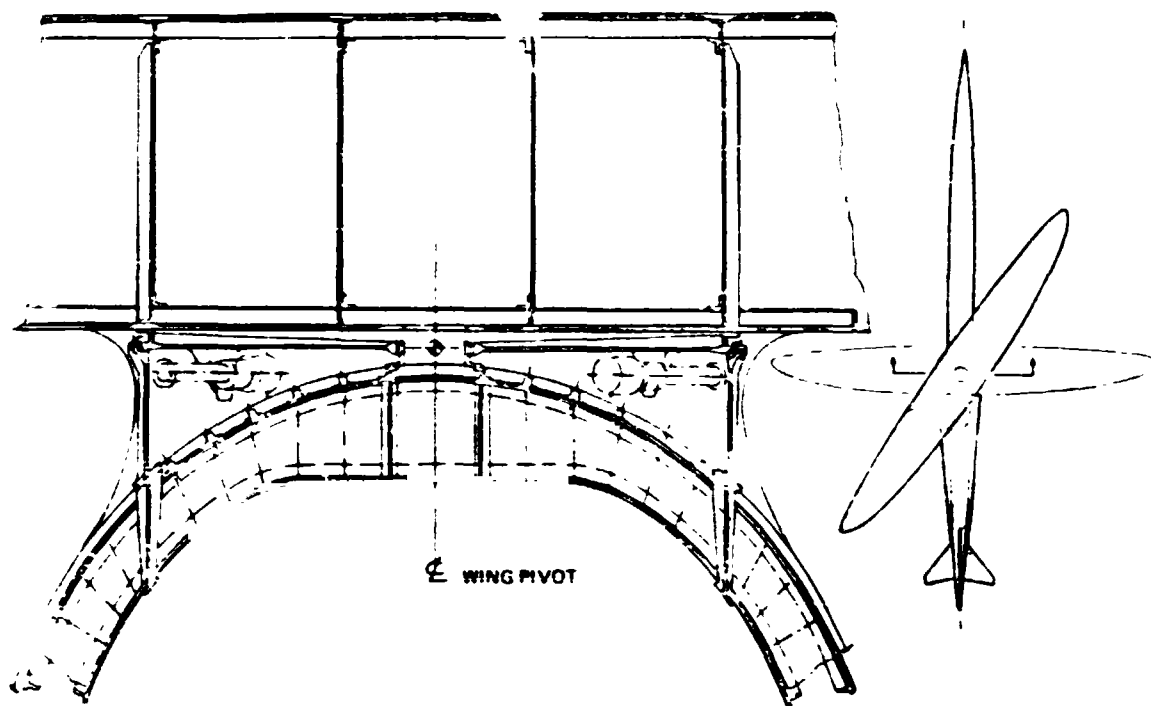


FIGURE 9.—YAWED WING PIVOT STRUCTURAL ARRANGEMENT

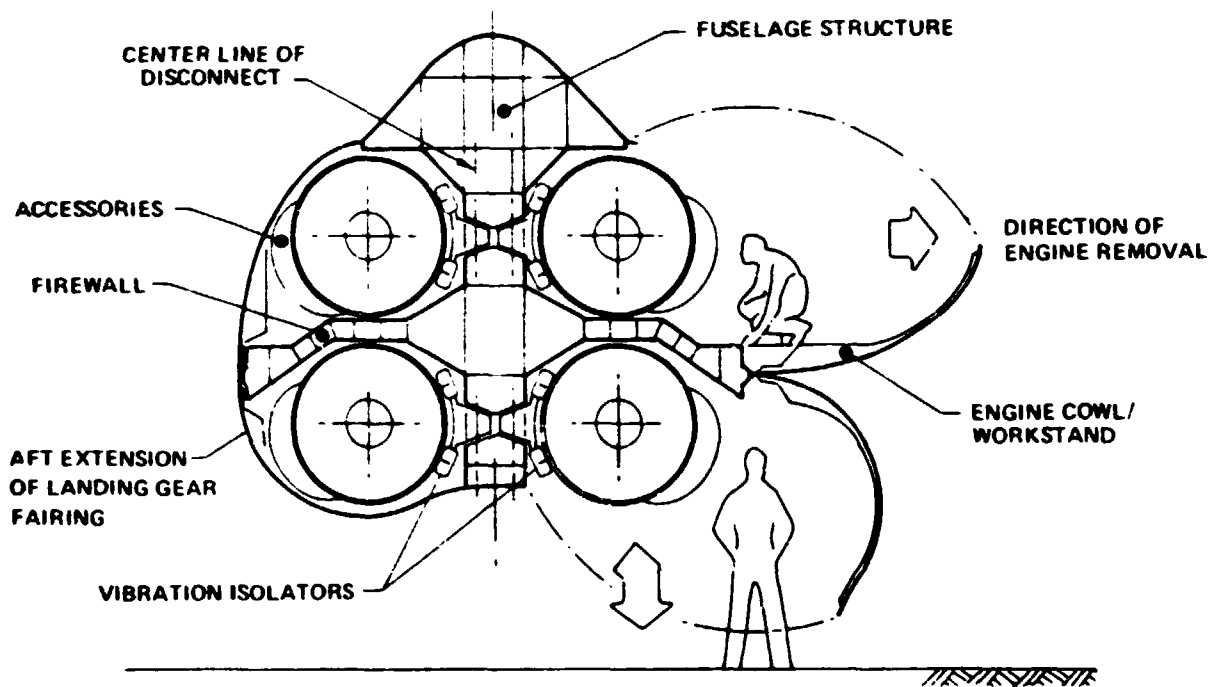


FIGURE 10.—AFT ENGINE INSTALLATION, MODEL 5-3

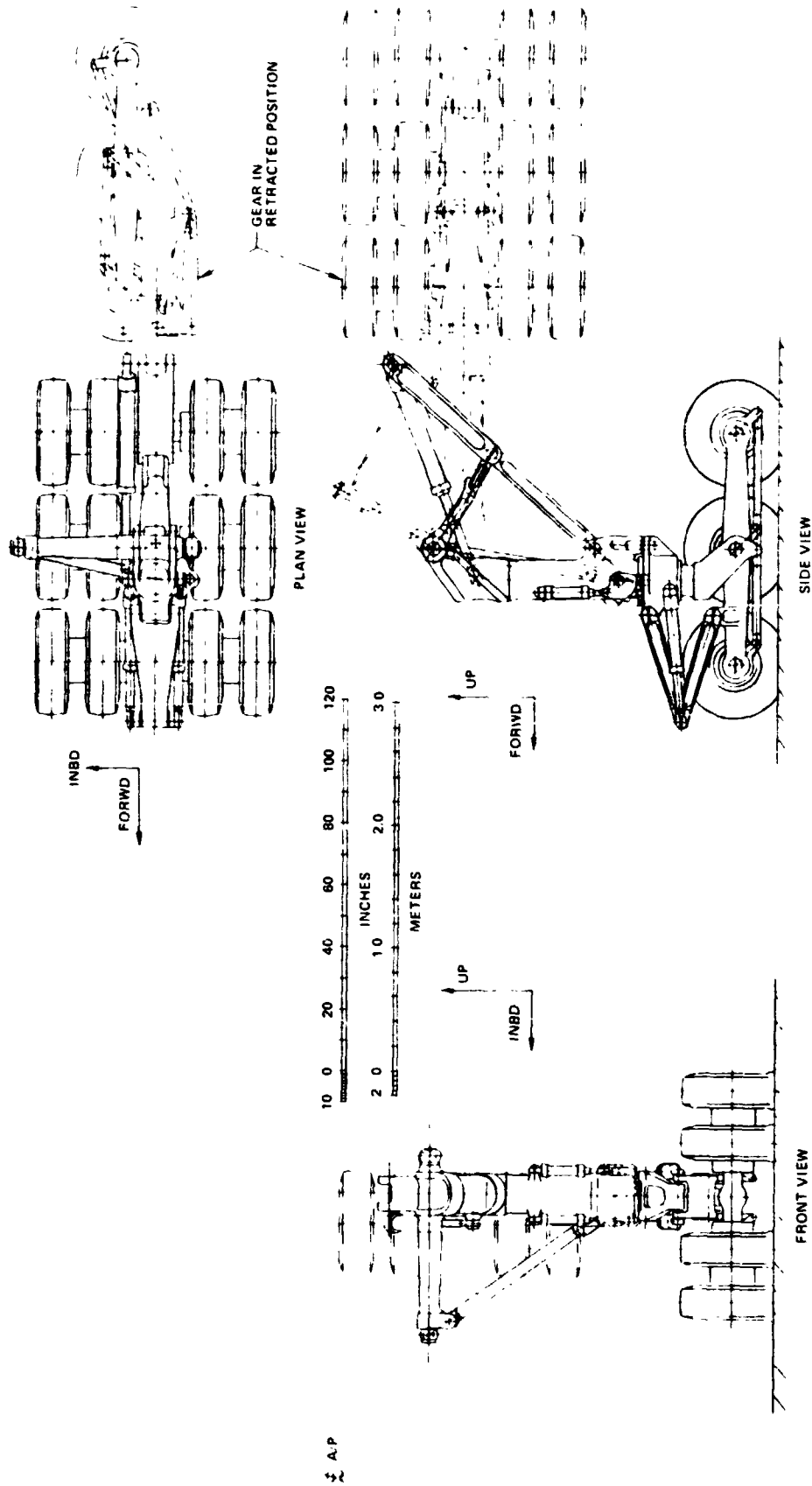


FIGURE 11.—MAIN LANDING GEAR, MODEL 5-3

Nose Gear

The nose landing gear supports approximately 30% of the aircraft weight. Since the available section for gear stowage is very limited below the passenger floor, two tandem nose gears have been incorporated. Each gear has a single axle with four wheels. All tires on the aircraft are the same size. The nose gear arrangement is shown in figure 12.

The outer cylinder of the shock strut is the only component that is not common to both the forward and aft nose gear units. Landing at reduced sink rate will be possible with either unit retracted in the event one gear hangs-up in flight. A conventional steering unit is included in each unit.

Empennage

The general arrangement of the empennage is shown in figure 8. The stabilizer is all movable and is spindle-mounted near the rear spar of the vertical tail.

Aircraft Systems

Volume and access is provided for all of the required systems. The locations are shown in figure 8. The systems have been located to enhance the balance of the airplane.

Fuel System

The wing fuel capacity is sufficient for the design mission requirements. Fuel is carried in integral tanks as shown in figure 8. A dry bay is provided around the wing pivot. An aft balance/trim tank is provided in the empennage boom ahead of the stabilizer.

CONFIGURATION COMPARISONS

Configuration weights are compared in figure 13. The initial baseline configurations were developed for a gross weight of 272,155 kg (600,000 lb). Model 5-3 which underwent a much longer period of development was configured with a maximum gross weight of 226,796 kg (500,000 lb). The solid lines are the operational empty weights for the mission sized airplanes.

The distribution of wing fuel and body fuel for the 5 baseline configurations are compared in figure 14. The single-fuselage yawed-wing configuration provides sufficient fuel volume for the 5560 km (3000 nmi) mission. Some of the fuel for the twin-fuselage yawed-wing configuration must be carried in body fuel tanks. The wings on concepts 1 and 2 provide only very limited fuel capacity. Approximately 131 cu meter (4000 cu ft) of the fuselage volume would be used for fuel tanks on the variable-sweep wing airplane, model 2-2.

The methods and results of "sizing" these baseline configurations to achieve the design mission objectives are discussed in the performance section that follows.

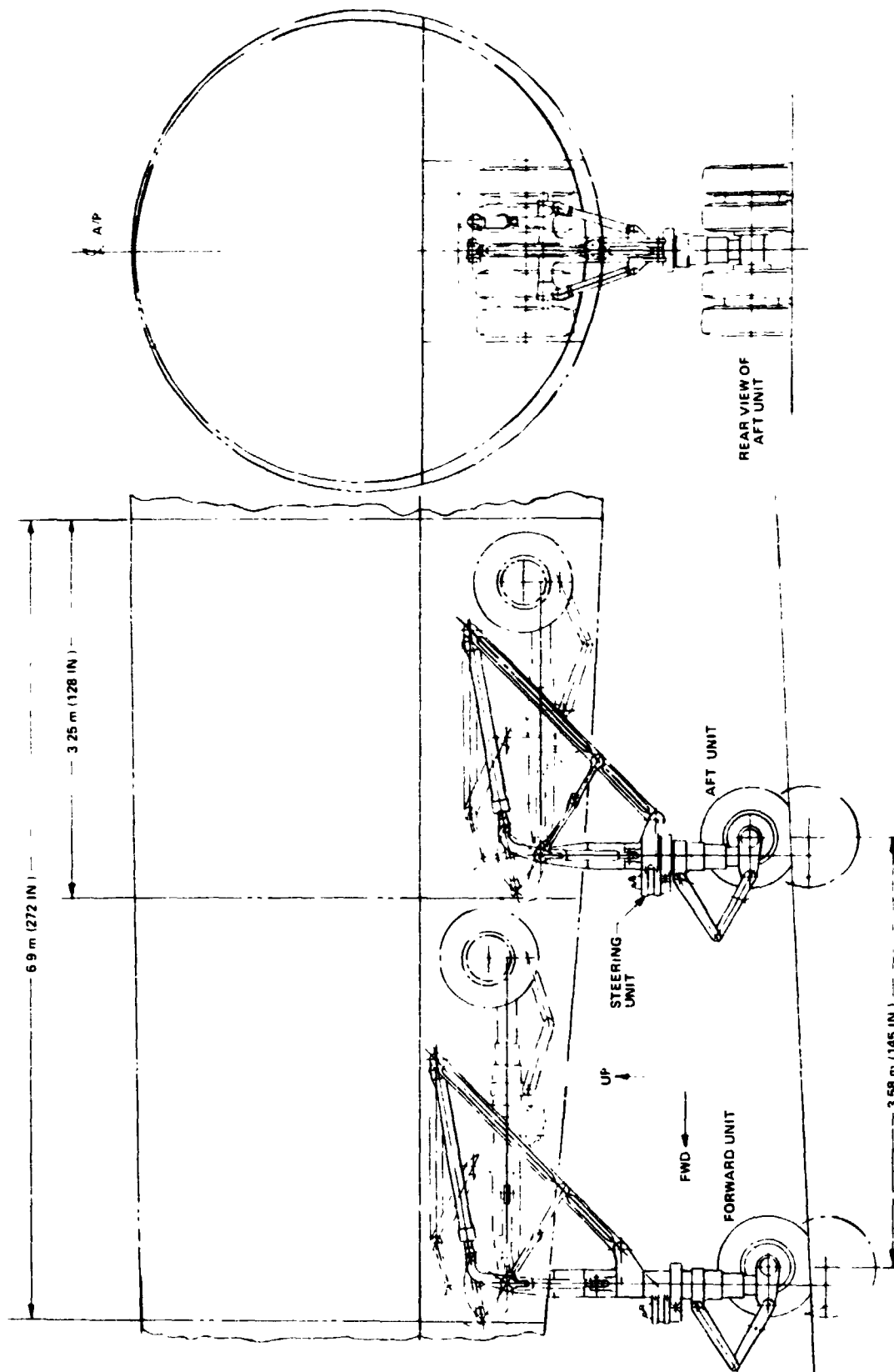


FIGURE 12.—NOSE LANDING GEAR, MODEL 53

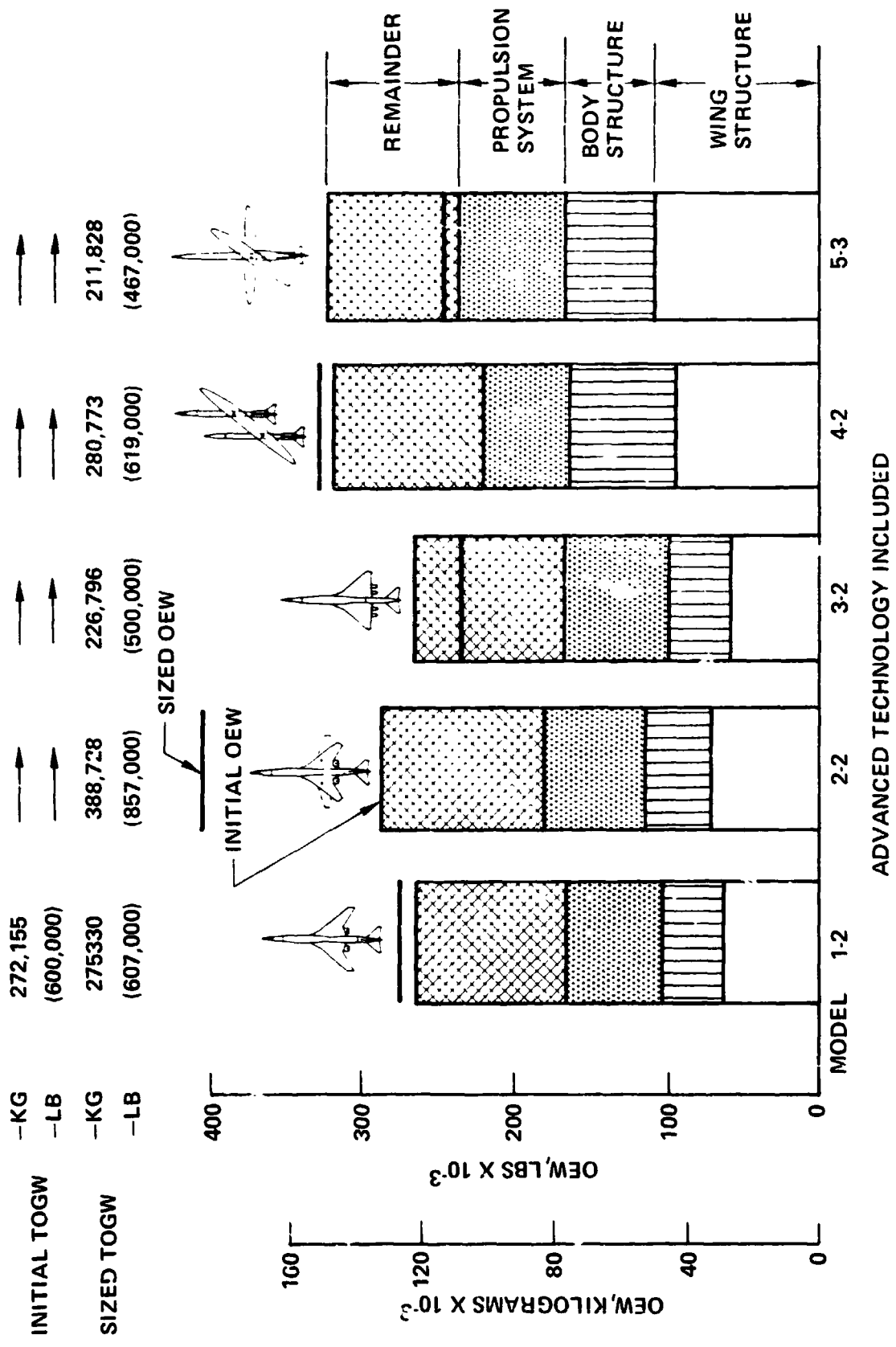


FIGURE 13.—BASE CONFIGURATION WEIGHTS COMPARISON

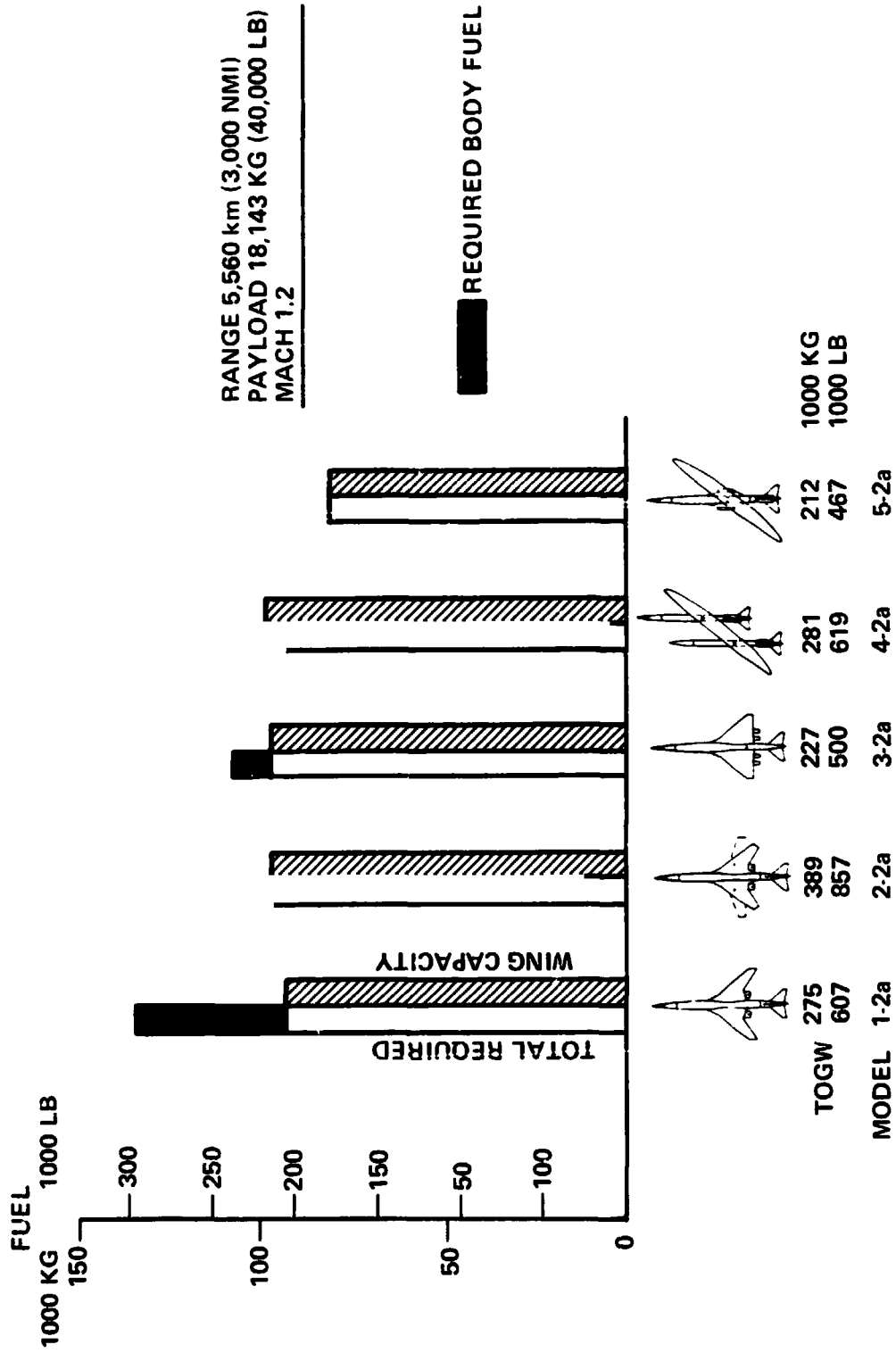


FIGURE 14.—FUEL VOLUME COMPARISON, SIZED AIRPLANE

CONFIGURATION PERFORMANCE

The following tasks were required to evaluate the performance of each airplane configuration:

- Assess the performance of the configuration as represented by its three-view drawing.
- Determine, by parametric scaling, the airplane size required to meet the mission objectives.
- Evaluate the detailed performance characteristics of the selected sized airplane.
- Determine the impact of the noise goals on the sized airplane takeoff gross weight.

These tasks were completed for the fixed-swept wing configuration 1-2, the variable-sweep wing configuration 2-2, the delta wing configuration 3-2, the twin-fuselage yawed wing configuration 4-2, and the single fuselage yawed wing configuration 5-3.

The sized airplane configuration for Model 5-3a has been used as a baseline for additional studies that included:

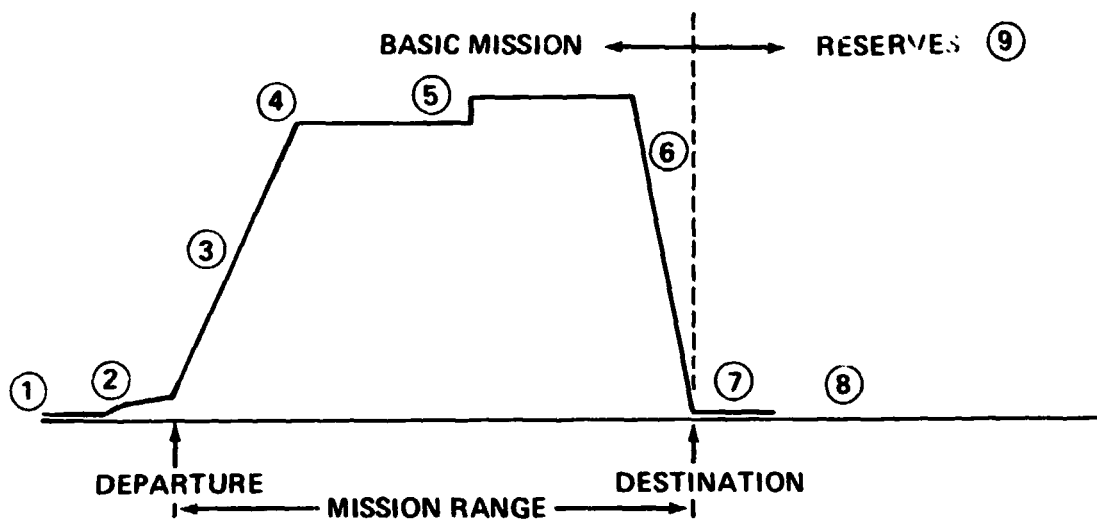
- Flap angle study to examine the trade between noise and field length
- Range capability versus gross weight
- Design payload sensitivity study
- The range capability for off design cruise speed (Mach .9 to 1.35)

In addition performance studies were made to identify the optimum yawed wing aspect ratio and to aid in the development of an efficient aerodynamic configuration. The critical sensitivity of all the configuration concepts to engine bypass ratio and to nacelle installed drag was identified.

MISSION RULES AND PERFORMANCE OBJECTIVES

The flight profile and mission rules used in the sizing process (fig. 15) were consistent with those used in the NASA advanced transport technology study. The allowances shown in this figure were used for the climb, descent and reserves in lieu of detailed evaluations. A step cruise was used for the design domestic range.

The following performance objectives and constraints have been used to size the airplane configurations.



- | | | |
|---|------------------------|--|
| ① | TAXI OUT | <ul style="list-style-type: none"> • NINE MINUTES TAXI THRUST |
| ② | TAKEOFF | <ul style="list-style-type: none"> • FIELD LENGTH PERFORMANCE PER FAR PART 25
305m / 32° C (1000 FT / 90 F) • ONE MINUTE TAKEOFF THRUST • TAKEOFF AND SIDELINE NOISE CALC. PER FAR
PART 36 CONDITIONS |
| ③ | ENROUTE CLIMB | <ul style="list-style-type: none"> • Δ RANGE = 272 Km (147 NMI) $\Delta W_F = .034$ TOGW |
| ④ | INITIAL CRUISE
ALT. | <ul style="list-style-type: none"> • DETERMINES BY LEVEL FLIGHT, MAX, CRUISE
THRUST, CRUISE MACH |
| ⑤ | CRUISE | <ul style="list-style-type: none"> • 1219m (4000 FT) STEP ALT. CRUISE |
| ⑥ | DESCENT | <ul style="list-style-type: none"> • $\Delta R = 306$ Km (165 NMI) $\Delta W_F = 726$ KG (1600 LB) |
| ⑦ | LANDING | <ul style="list-style-type: none"> • FIELD LENGTH PERFORMANCE PER FAR PART 25
305m (1000 FT) • APPROACH NOISE CALC. PER FAR PART 36
CONDITIONS |
| ⑧ | TAXI IN | <ul style="list-style-type: none"> • FIVE MINUTES TAXI THRUST |
| ⑨ | RESERVES | <ul style="list-style-type: none"> • .075 TOGW |

FIGURE 15.—FLIGHT PROFILE AND MISSION RULES

- Objectives

Payload:	18,143 kg (40,000 lb)
Range:	5,560 km (3,000 nmi)
Cruise Mach:	1.2

- Constraints

Minimum cruise altitude:	11,887 m (39,000 ft)
Field length:	3,505 m (11,500 ft) maximum
Landing approach speed:	333.4 km/hr (180 kt) maximum

- Noise goal 15 EPNdB below FAR Part 36

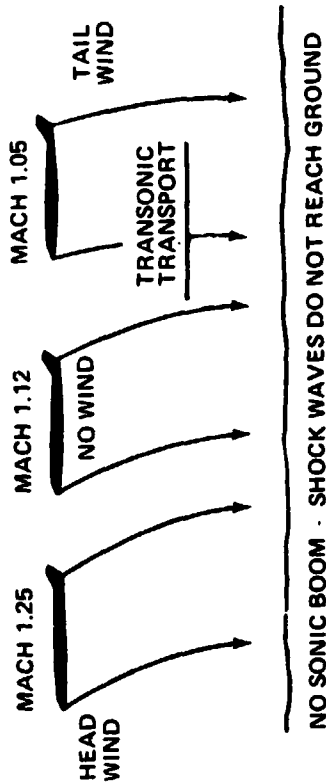
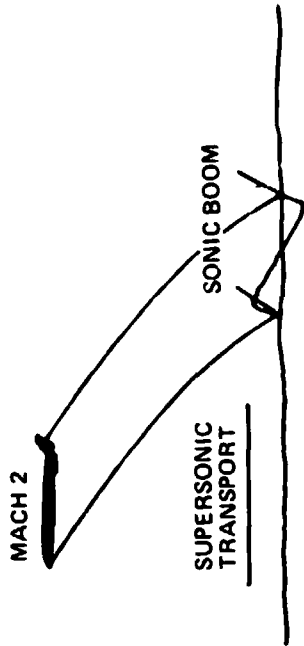
The range and payload objectives were selected for compatibility with the ATT study (ref. 1). The Mach number was selected to achieve boom-free supersonic flight. This requires that the airplane ground speed be less than the local speed of sound propagation on the ground. Depending upon flight direction, season, and airplane altitude, cruise Mach numbers in the range of 1.05 to 1.25 are allowed (fig. 16 from ref. 2) for east to west and west to east transcontinental U.S. flights. A Mach 1.2 cruise speed has been selected since the required engine thrust to balance drag is the largest at a high boom free cruise speed. This thrust level would then permit cruise at lower Mach numbers.

The minimum cruise altitude constraint was set by the selected maximum structural design equivalent air speed of 180 m/s (350 kts) (see page 162). The field length and landing approach speed were selected as maximum allowable upper limits.

The noise goal was a specified study objective. In order to assess the impact of this design objective on each of the configuration concepts, performance calculations were made with different sets of propulsion data representing three levels of sound suppression. The results then clearly identify the gross weight penalty to achieve a specific noise level. The engine design characteristics are defined in the Power System section of this report.

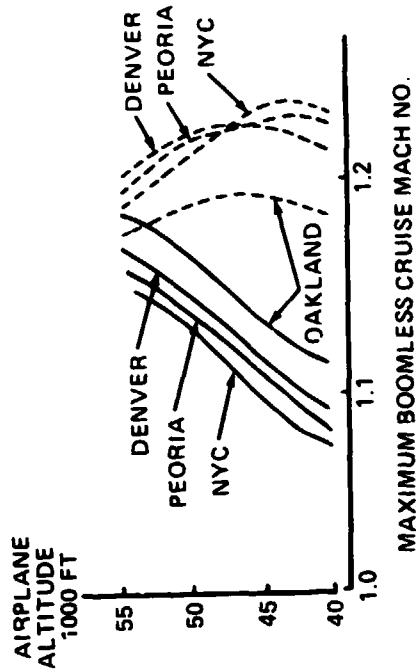
CONFIGURATION PERFORMANCE

The procedure that has been used to size the airplane configurations is illustrated in steps 3 and 4 in the design synthesis chart of figure 2. The detailed design layout of each configuration was evaluated to provide detailed basepoint thrust, weight, aerodynamic, noise and flight controls data. In addition, scaling rules were derived by further analyses to account for changes in wing size, engine size and gross weight variations in the resizing cycle.



REFERENCE 2.0

JULY



JANUARY

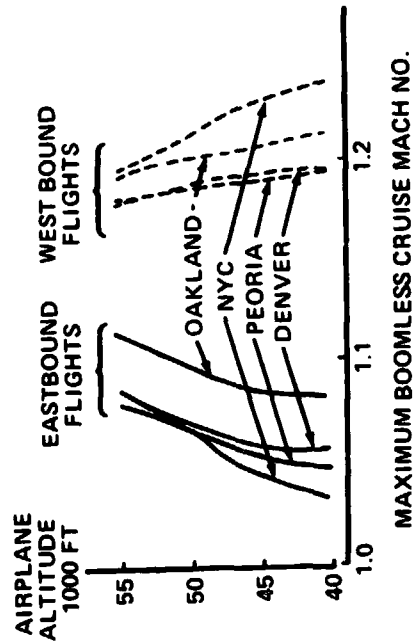


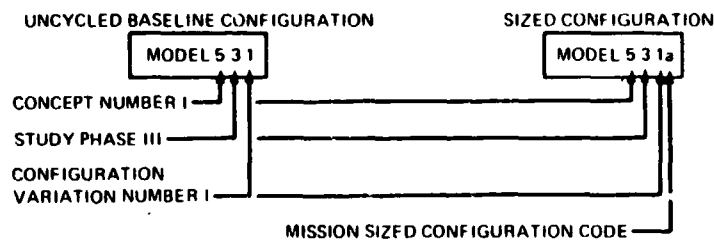
FIGURE 16.—AVOIDING SONIC BOOM

A parametric performance analyses described in references 3 and 4 were used to determine the combination of aircraft characteristics that result in airplanes that meet the range/payload objectives. A grid of various combinations of thrust to weight ratios, (T/W), and wing loadings, (W/S), were selected to construct the design selection chart. For each combination of T/W and W/S, a takeoff gross weight was determined that balanced the operational empty weight, OEW, calculated for the component weights with the OEW required by the mission. The mission required OEW was equal to the takeoff gross weight minus the payload, fuel and reserves.

The mission analyses determined the cruise range, initial cruise altitude capability (thrust and drag balance), and fuel required along the flight profile including reserves. Engine performance was corrected for engine bleed requirements and installation losses. Takeoff field length was calculated from generalized empirical performance curves. Flap settings that minimize field length were determined. Approach speed was calculated for the landing weight (OEW plus payload plus reserves) using the landing flap stall lift coefficient and a 30% speed margin. Based on the payload and range objectives, the engine thrust size and wing area were selected from design selection charts. The size selection was based on minimizing takeoff gross weight (TOGW) while satisfying the performance objectives and constraints.

The airplanes derived from the “unscaled baseline” configurations by this procedure are referred to as “mission sized” configuration or as “sized” configurations. These sized configurations are distinguished from the parent uncycled baseline configuration by the addition of a small letter after the parent configuration designator.

Example:



This small letter also designates the design mission objectives as shown in table 2.

TABLE 2.—SIZED CONFIGURATION DESIGNATION CODE

LETTER CODE	MACH NUMBER	RANGE	PAYLOAD	NOISE OBJECTIVES
a	1.2	5560 Km (3000 NMI)	18,143 KG (40,000 LB)	FAR 36
b				FAR 36 5 EPNdB
c				FAR 36 15 EPNdB
d			13,608 KG (30,000 LB)	FAR 36
e			22 680 KG (50,000 LB)	

Typical design selection charts are shown in figures 17, 18, and 19 for the fixed-swept wing, delta wing, and single fuselage yawed wing configurations. These design charts show parametrically the effect of thrust/weight ratio (T/W), wing loading (W/S), minimum TOGW (EYE), TOGW, initial cruise altitude capability (ICAC), takeoff field length (TOFL), approach speed (V_{APP}), and ratio of initial cruise lift coefficient to the lift coefficient for maximum lift to drag ratio (CLR). All configurations were constrained by the 11,887 m (39,000 ft) initial cruise altitude requirement. The delta wing configuration was also constrained by the takeoff field length objective not to exceed 3505 m (11,500 ft). The minimum gross weight represented by the "eye" shown on the parametric design chart does not meet the performance constraints. The effects of the design constraints are shown in figure 20.

The performance characteristics of the sized configuration for the five concepts are summarized in table 3. The corresponding design characteristics are shown in table 4. The single fuselage yawed wing configuration (5-3a) has the lowest: takeoff gross weight, wing area, engine thrust size, approach speed, and FAR Part 36 noise levels. This configuration has the highest cruise lift/drag ratio, L/D. This required a smaller engine with a correspondingly lower fuel consumption.

The fixed swept wing configuration 1-2a and the variable sweep wing configuration 2-2a were appreciably heavier. The primary cause was the high installed nacelle drag associated with the double pod arrangements. The pivoting wing structural weight of configuration 2-2a provided an additional detrimental effect.

The delta wing configuration 3-2a has the lightest structural weight. The landing and takeoff speeds and field lengths exceed those of the other configurations. This is the result of the low aspect ratio of the delta wing.

The double-fuselage yawed wing configuration, 4-2a, has excellent low speed performance but is quite heavy. This configuration could probably be improved with a lower aspect ratio wing and a favorable nacelle arrangement.

Figure 21 contains a gross weight comparison of all of the configurations.

A flap angle study on the 5-3a configuration was made to identify the field length versus noise trade, figure 22. At the maximum flap setting, the takeoff speed, and field lengths were the lowest. This setting was used in the parametric charts for the airplane sizing. By reducing the flap angle the L/D's were increased at the expense of higher liftoff speeds and longer field lengths. The higher L/D increased the climb gradient and altitude over the 6.48 km (3.5 nmi) FAR Part 36 takeoff noise station. This combined with a lower engine power setting after cutback reduced the noise level approximately 5 EPNdB. The higher L/D at approach with lower flap angle reduced the required engine thrust to maintain the 0.052 rad (3°) glide slope over the 1.85 km (1 nmi) FAR Part 36 approach noise station. A noise reduction of approximately 2 EPNdB results. However, the approach speed and landing field length were increased.

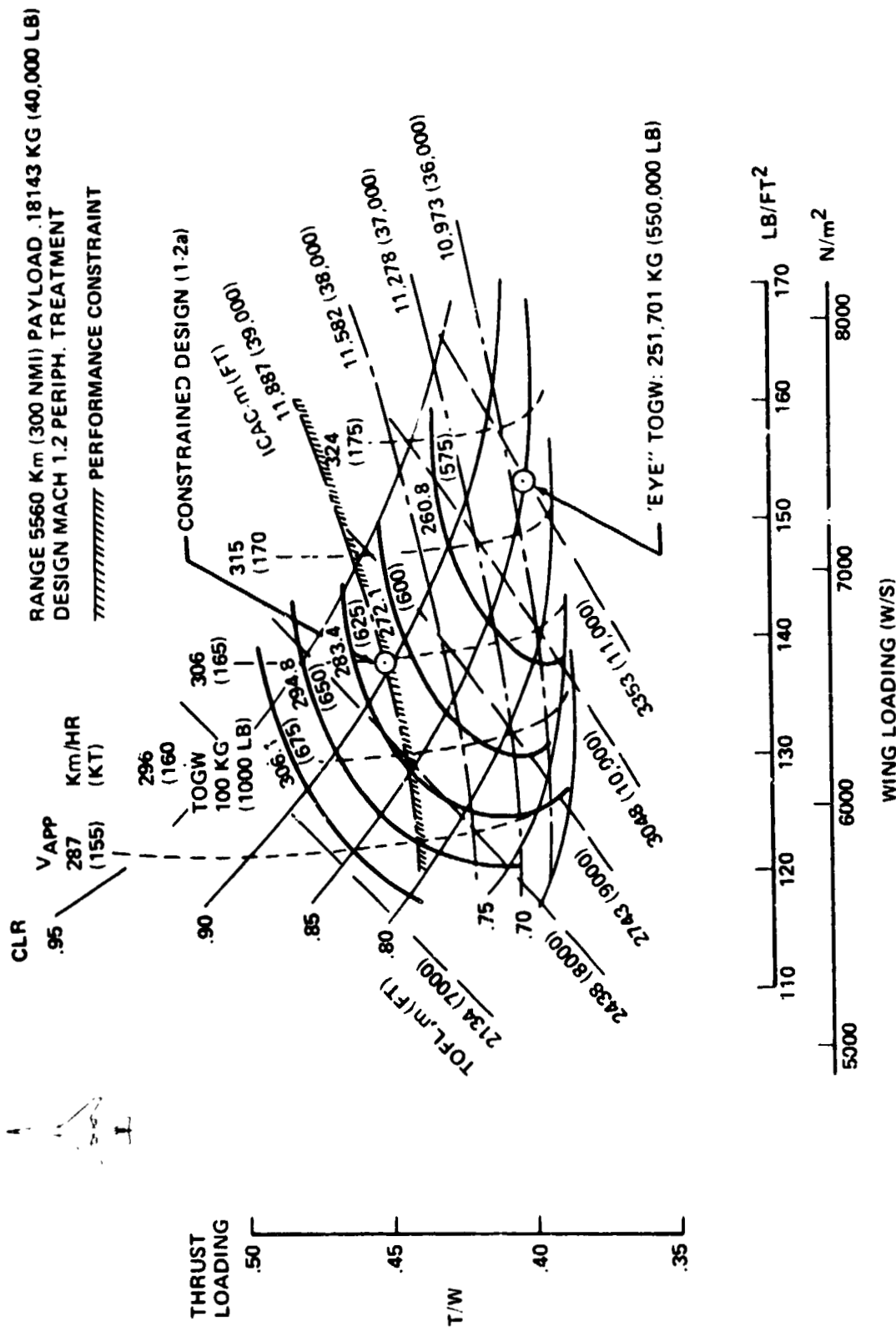


FIGURE 17.-1.2 FIXED ARROW WING CONFIGURATION DESIGN SELECTION CHART

RANGE 5560 m (3000 NMI) PAYLOAD = 18,143 KG
 (40,000 LB)
 DESIGN MACH 1.2 PERIPHERAL TREATMENT

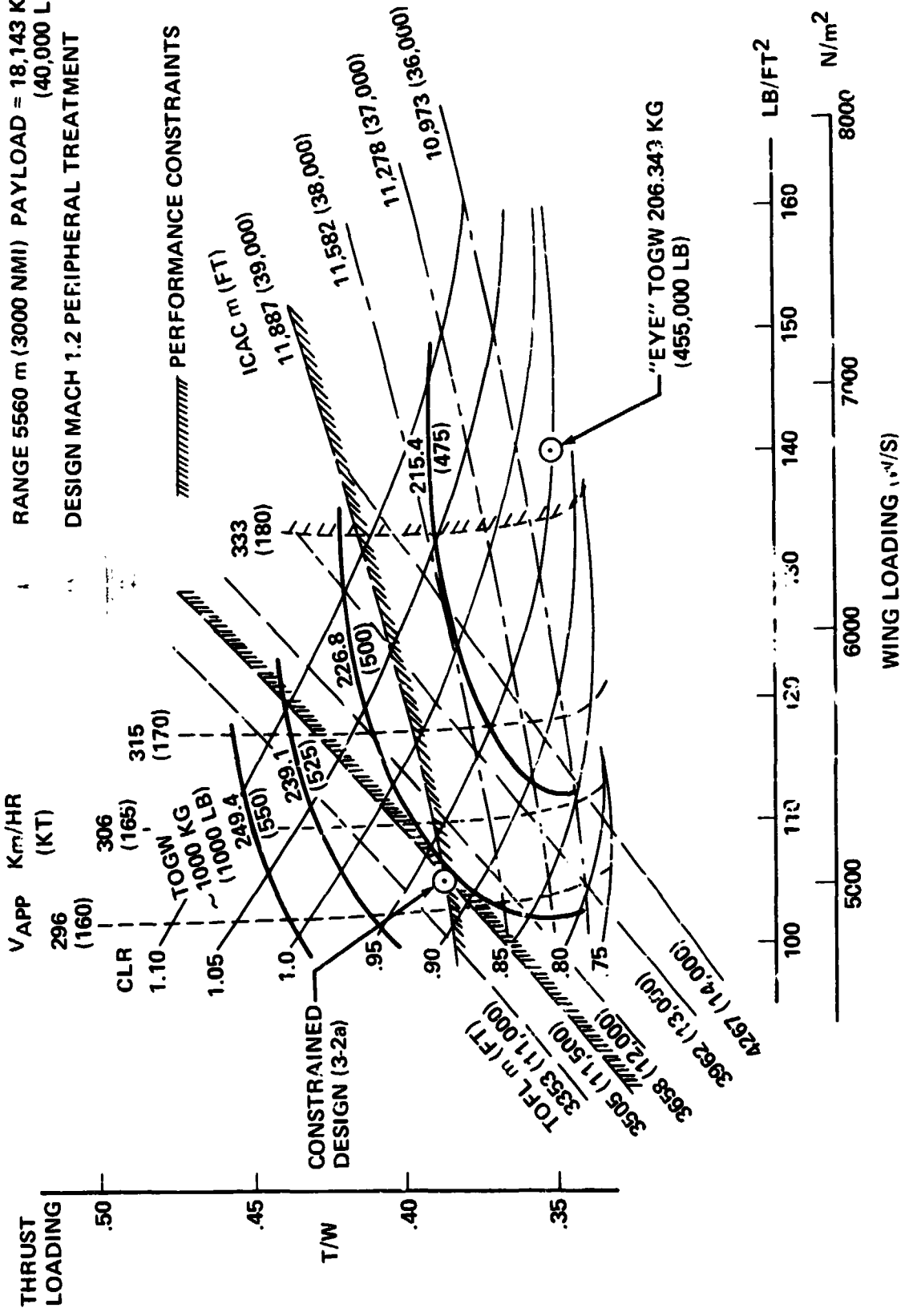


FIGURE 18.-3-2 FIXED DELTA WING CONFIGURATION DESIGN SELECTION CHART

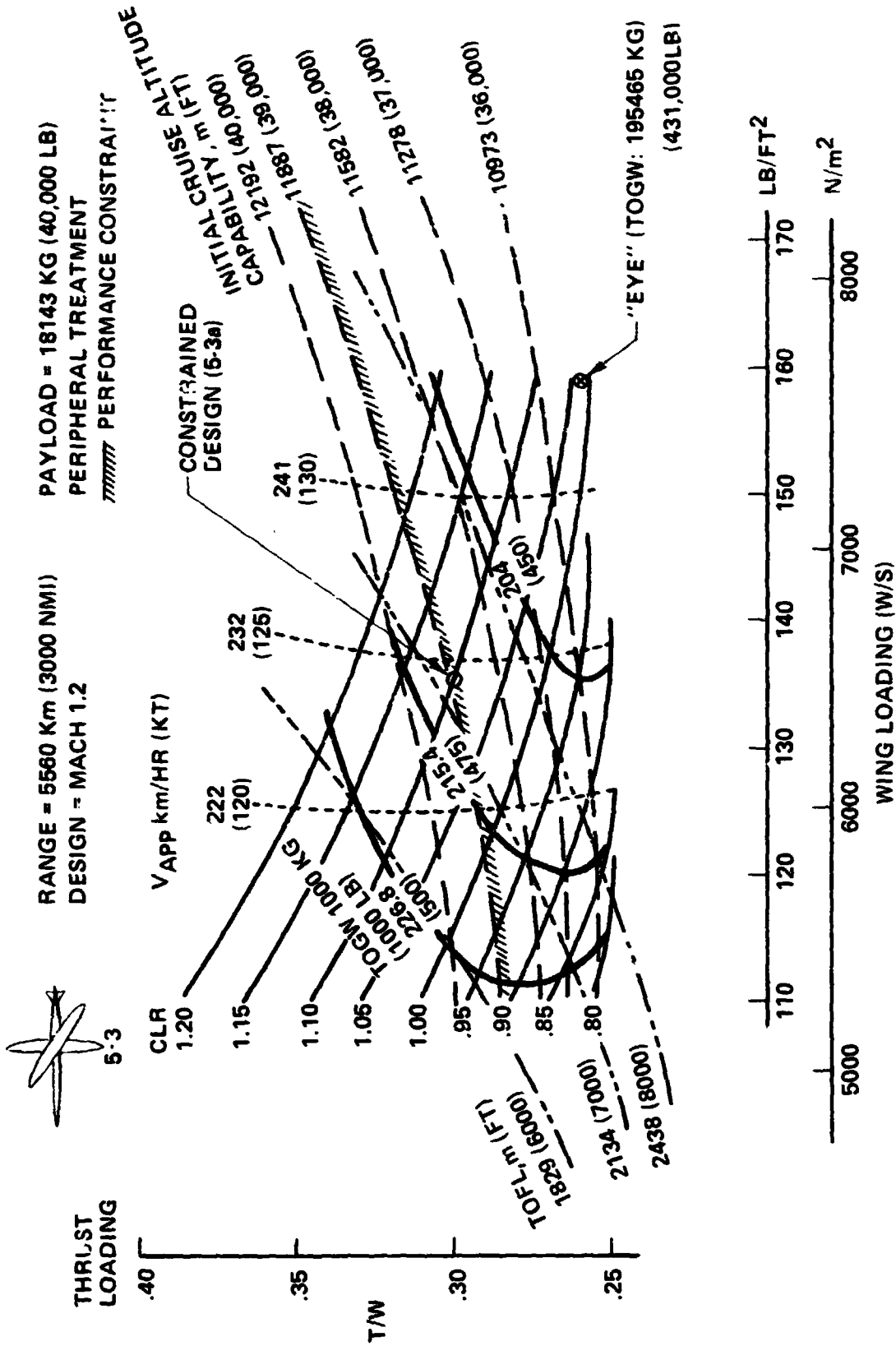


FIGURE 19 - MODEL 5-3 SINGLE BOD, YAWED WING CONFIGURATION DESIGN SELECTION CHART

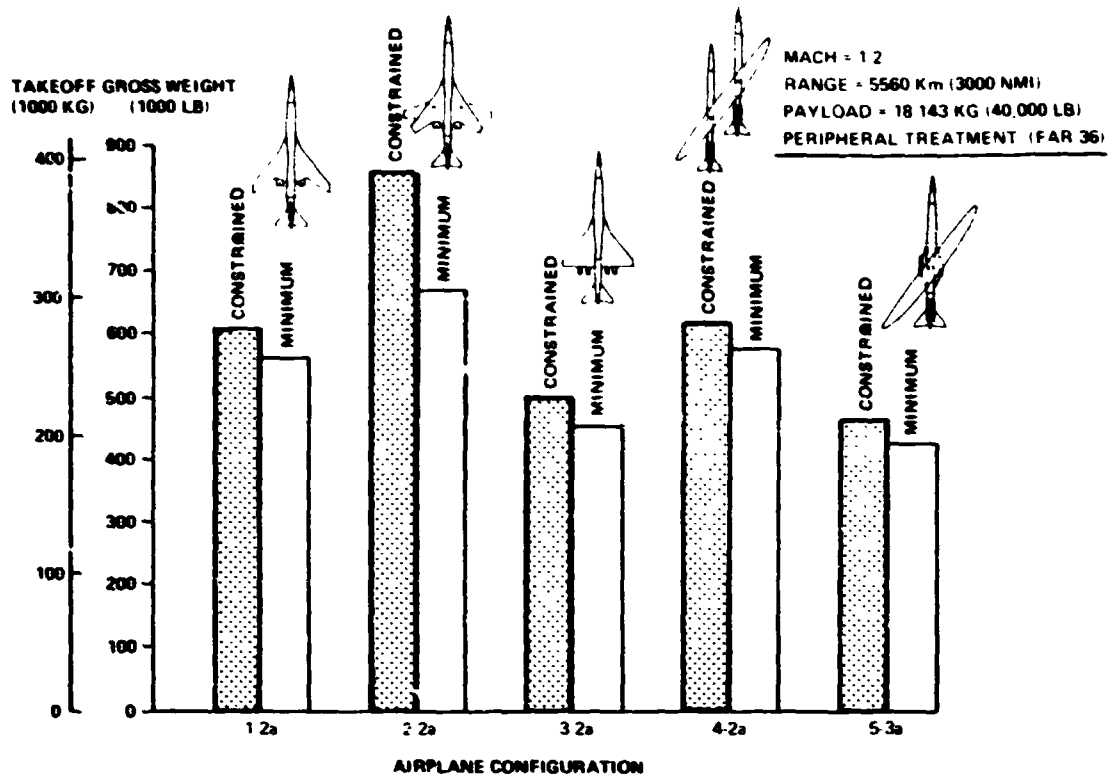


FIGURE 20.—CONSTRAINED VERSUS MINIMUM GROSS WEIGHT COMPARISON

TABLE 3.-AIRCRAFT CHARACTERISTICS AND PERFORMANCE

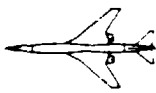
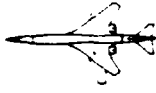
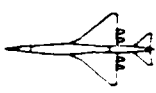


<p>MACH 1.2 PAYLOAD = 18 143 KG (40 000 LB) RANGE = 5560 Km (3000 NMI) INITIAL CRUISE ALTITUDE = 11 887 m (39 000 FT) TAKEOFF FIELD LENGTH 3505 m (11 500 FT) PERIPHERAL NOISE TREATMENT</p>						
AIRPLANE CONFIGURATION		1-2a	2-2a	3-2a	4-2a	5-3a
TAKEOFF GROSS WEIGHT	KG (LBS)	275283 (607000)	388283 (857000)	226786 (500000)	280726 (617000)	211828 (467000)
OPERATING EMPTY WEIGHT	KG (LBS)	122626 (270600)	180726 (398500)	103855 (229000)	146804 (322600)	113832 (251000)
WING AREA	m ² (FT ²)	433.8 (4670)	612.2 (6590)	436.6 (4700)	442.2 (4760)	319.6 (3440)
ENGINE THRUST RATING	N (LBS)	284241 (63900)	406123 (91300)	216184 (48600)	226859 (51000)	156113 (35100)
NUMBER OF ENGINES / BYPASS RATIO		4/1	4/1	4/1	4/1	4/1
THRUST LOADING (T/W)		0.42	0.43	0.39	0.33	0.30
WING LOADING (W/S)	N/m ² (LB/FT ²)	6224 (130)	6224 (130)	5075 (106)	6224 (130)	6512 (136)
L/D CRUISE		8.1	8.1	8.9	10.6	12.3
TAKEOFF FIELD LENGTH: MAX FLAPS	m(FT)	2438 (8000)	1554 (5100)	3505 (11500)	2225 (7300)	2179 (7150)
REDUCED FLAPS	m(FT)	3353 (11000)	2286 (7500)	3505 (11500)	3078 (10100)	2947 (9670)
L/D COMMUNITY: REDUCED FLAPS		8.8	9.2	6.3	22	6.9
APPROACH SPEED: REDUCED FLAPS	Km/HR/KT	333 (180)	296 (160)	317 (171)	261 (141)	254.5 (137.4)
COMMUNITY NOISE: Δ EPNdB FROM FAR PART 36						
• TAKEOFF WITH THRUST CUTBACK AT NOISE STATION		-6.0	-10.2	+1.8	-15.0	-0.4
• SIDELINE		+3.0	+3.5	+3.4	+3.1	+2.0
• APPROACH		-0.7	-1.9	-0.5	-2.8	-2.0
• TRADED		+1.0	+1.5	+1.4	+1.1	0.

TABLE 4. - MACH 1.2 SIZED TRANSPORT CONFIGURATION DESIGN BASELINE CHARACTERISTICS

ITEM	CONFIGURATION CONCEPT				
	1-2a	2-2a	3-2a	4-2a	5-3a
MODEL NUMBER	197	193	193	188	190
PASSENGERS (18%/85% MIX)	5560 (3000)	5560 (3000)	5560 (3000)	5560 (3000)	5560 (3000)
RANGE KM (NM)	14.6	15.0	14.0	14.7	18.5
CONFIGURATION FINENESS RATIO, 1/g ₀	1.2	1.2	1.2	1.2	1.2
DESIGN MACH NUMBER					
WEIGHT	275 300 (607 000)	388 300 (867 000)	226 786 (500 000)	260 700 (581 000)	211 828 (467 000)
FUSELAGE					
BODY LENGTH, m (FT)	78.49 (257.5)	46.91 (153.9)	40.94 (134.3)	66.79 (219.0)	87.83 (288.5)
CABIN LENGTH, m (FT)	47.83 (156.9)	3.12/4.88 (123/192)	3.12/5.38 (123/212)	22.78 (74.7)	43.97 (144.3)
MIN/MAX DIAMETER (TC) (M/M) (IN./IN.)	3.12/4.88 (123/192)	4/6	4/7	3.56/3.56 (140/140)	3.56/4.06 (140/160)
MIN/MAX AHEAD SEATING (TC)	4/6	1/2	1/2	1/1	4/6
MIN/MAX NO. OF AISLES (TC)	1/2			1/1	1/1
WING					
AREA, m ² (FT ²)	934 (4870)	612 (6690)	437 (4700)	442 (4760)	319.6 (3440)
ASPECT RATIO	3.96	3.06 (SWEPT)	2.81	12.8 (UNYAWED)	10.2 (UNYAWED)
LE SWEEP RAD (DEG)	0.87 (50)	0.94 (54)	0.90 (51)	0.92 (53)	0.96 (55)
THICKNESS RATIO, ROOT/TIP, %/%	4.87/2.5	4.17/2.5	3.67/3.0	10.0/0	12.0/0
TAPER RATIO	0.30	0.285	0.127	10.1 ELLIPSE	8.1 ELLIPSE
WING C/A LOCATION ON BODY % BODY LENGTH	56.5	56.5	59	56	56
EMPELLAGE					
HORIZONTAL TAIL AREA, m ² (FT ²)	50.8 (547)	110.8 (1183)	34.7 (373)	67.7 (729) x 2	27.4 (295)
ASPECT RATIO	2.6	2.6	2.6	2.6	2.6
LE SWEEP RAD (DEG)	0.87 (50)	0.87 (50)	0.87 (50)	0.87 (50)	0.87 (50)
THICKNESS RATIO, ROOT/TIP, %/%	4.0/4.0	4.0/4.0	4.0/4.0	4.0/4.0	4.0/4.0
TAPER RATIO	0.2	0.2	0.2	0.2	0.2
VERTICAL TAIL AREA, m ² (FT ²)	36.7 (390)	73.2 (788)	37 (398)	86.7 (933) x 2	26.5 (275)
ASPECT RATIO	1.11	1.11	1.11	1.11	1.11
LE SWEEP RAD (DEG)	0.87 (50)	0.87 (50)	0.87 (50)	0.87 (50)	0.87 (50)
THICKNESS RATIO, ROOT/TIP, %/%	3.57/3.5	3.57/3.5	3.57/3.5	3.57/3.5	3.57/3.5
TAPER RATIO	0.264	0.264	0.264	0.264	0.264
PROPULSION					
TYPE/BNR	ATSA 1.20 1.3000-16/1	ATSA 1.20 1.3000-16/1	ATSA 1.20 1.3000-16/1	ATSA 1.20 1.3000-16/1	ATSA 1.20 1.3000-16/1
NUMBER OF ENGINES/LOCATION	4/UNDERWING	4/UNDERWING	4/UNDERWING	4/TAIL	4/TAIL BODY
STATIC THRUST/ENGINE, SL/90 F. N(LBF)	284 241 (63 900)	408 122 (91 300)	216 (48 600)	228 666 (51 000)	166 133 (36 100)

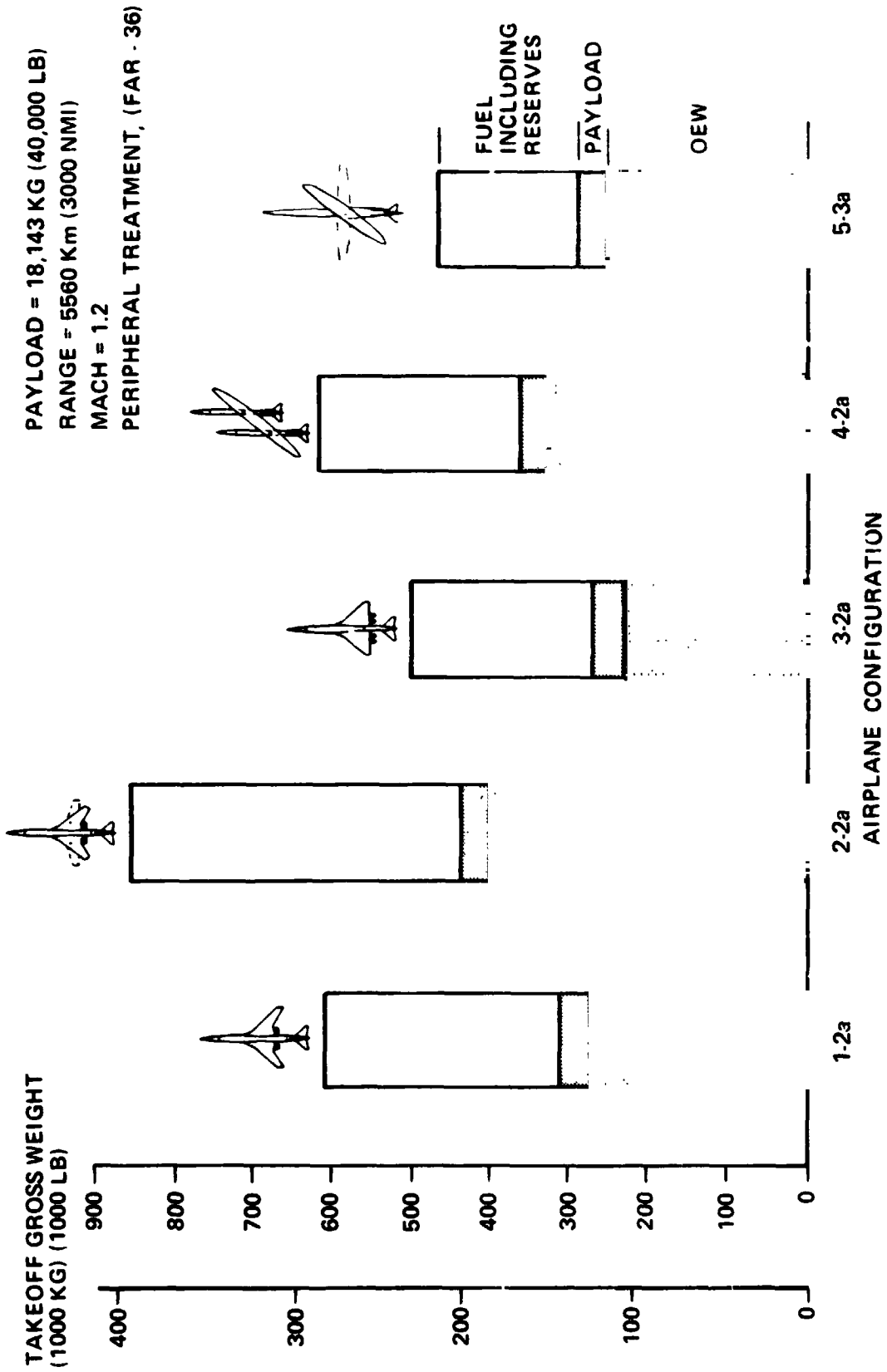


FIGURE 21. —SIZED AIRPLANES GROSS WEIGHT SUMMARY

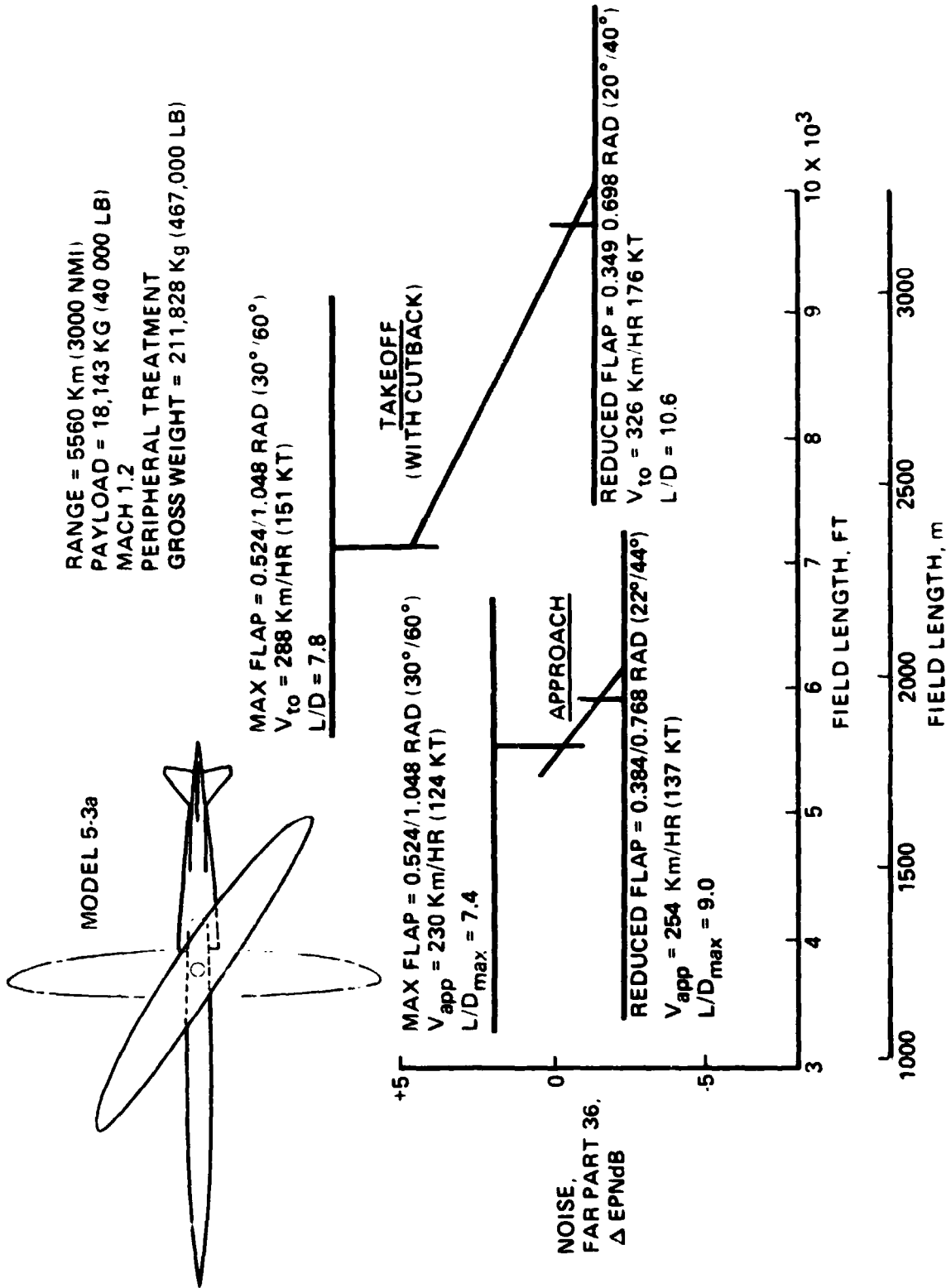


FIGURE 22. -NOISE VERSUS FIELD LENGTH

NOISE PERFORMANCE STUDIES

Three levels of engine nacelle noise treatment have been assessed on the study configurations to determine the TOGW penalty versus noise reduction. The minimum noise treatment level consisted of acoustically lined walls of the engine nacelle (peripheral) and provided the lightest TOGW. The traded noise level calculated from FAR Part 36 was used as a single noise level comparison criteria.

The impact on TOGW of achieving lower noise levels, with engine nacelle noise treatment, is shown in figure 23. The TOGW increase was due to weight being added for acoustical treatment and engine performance losses due to the acoustic treatment.

The yawed wing configurations were the only configurations found to be capable of achieving relatively easily the noise goal of FAR 36 15 EPNdB. The single fuselage yawed wing configuration achieved this objective with a gross weight slightly in excess of 227,000 kg (500,000 lb). As shown in table 3, the yawed wing configuration had a large advantage in takeoff and landing performance over the fixed swept and delta wing configurations.

Constant traded noise levels for model 5-3a as shown on the design selection chart, figure 24, indicate that the constrained design was close to the minimum noise. At the baseline wing loading of 6512 N/m (136 psf), FAR noise levels versus thrust loading are shown on figure 25a. A decrease in thrust loading from the baseline caused the maximum noise level to become takeoff/cutback dominant compared to sideline noise. Thrust loading of .25 to .30 caused rapid changes in takeoff/cutback noise level. FAR Part 36 traded noise versus TOGW, figure 25b, showed similar trends to the traded noise versus T/W of figure 25a.

At the baseline thrust loading of .3, FAR noise levels versus wing loading are shown on figure 26a. Sideline noise was dominant at most wing loadings. The resulting noise versus TOGW, figure 26b, shows little sensitivity to wing loading because sideline noise is primarily affected by thrust for a given engine cycle and noise treatment.

SINGLE FUSELAGE YAWED WING CONFIGURATION STUDIES

Range Capability Versus Gross Weight

The range capability of configuration 5-3a was evaluated with a wing area = 319.6 m (3440 ft), sized engine thrust (TSLs) of 156,113 N (35,100 lb), a payload of 18,141 kg (40,000 lb), and a cruise Mach number of 1.2, figure 27. The range was affected by: changes to the baseline fuel weight, cruise altitude, cruise L/D, and engine SFC. The 11,887 m (39,000 ft) minimum cruise altitude constraint was not satisfied at ranges greater than 5560 km (3000 nmi). At ranges exceeding the design range, increasing airplane gross weight resulted in a lower altitude capability, lower L/D, increased fuel consumption, and a range limit of 7408 km (4000 nmi).

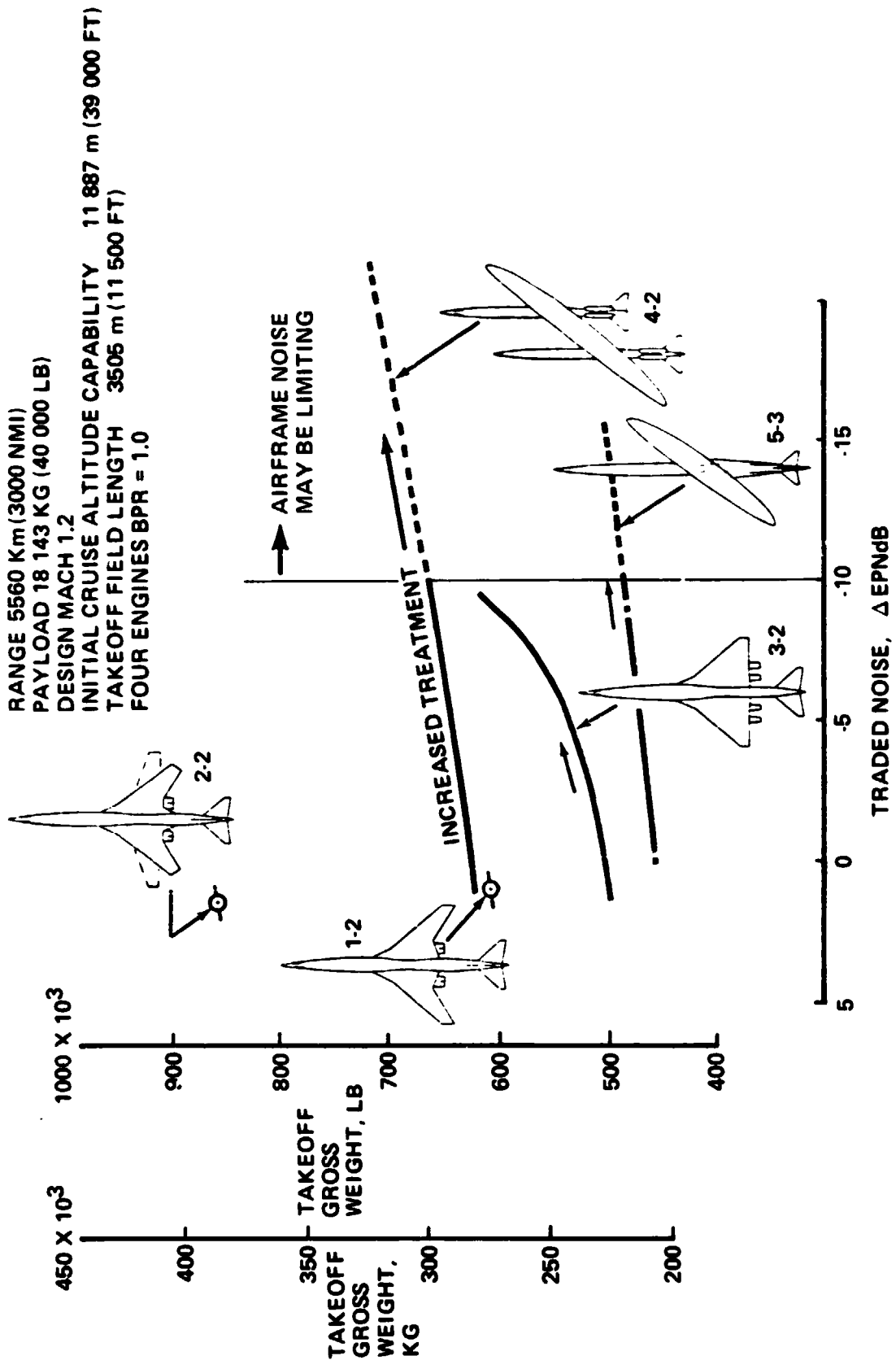


FIGURE 23.—IMPACT OF NOISE TREATMENT ON SIZED AIRPLANE TAKEOFF GROSS WEIGHT

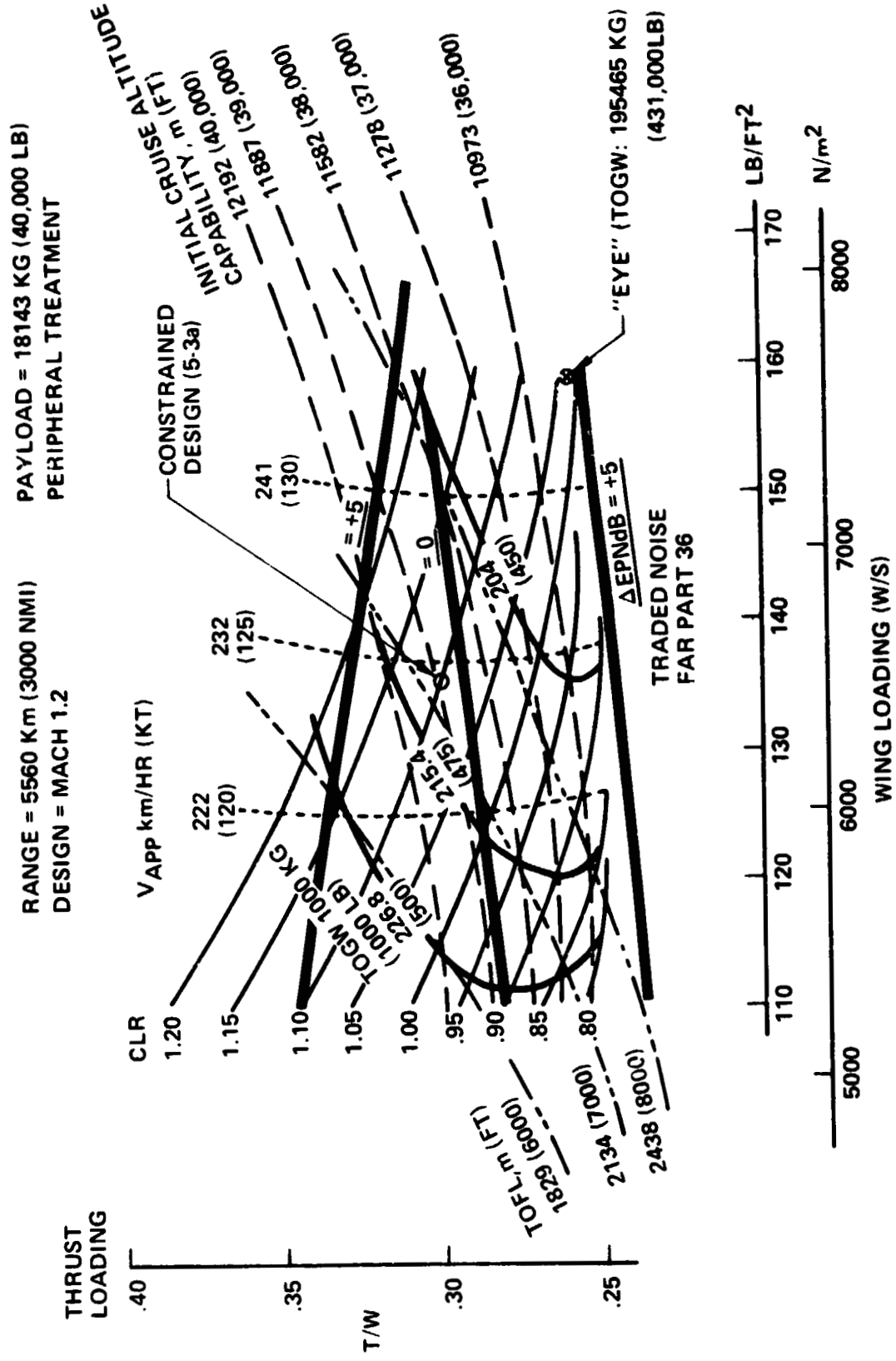


FIGURE 24.—MODEL 5-3 DESIGN SELECTION CHART

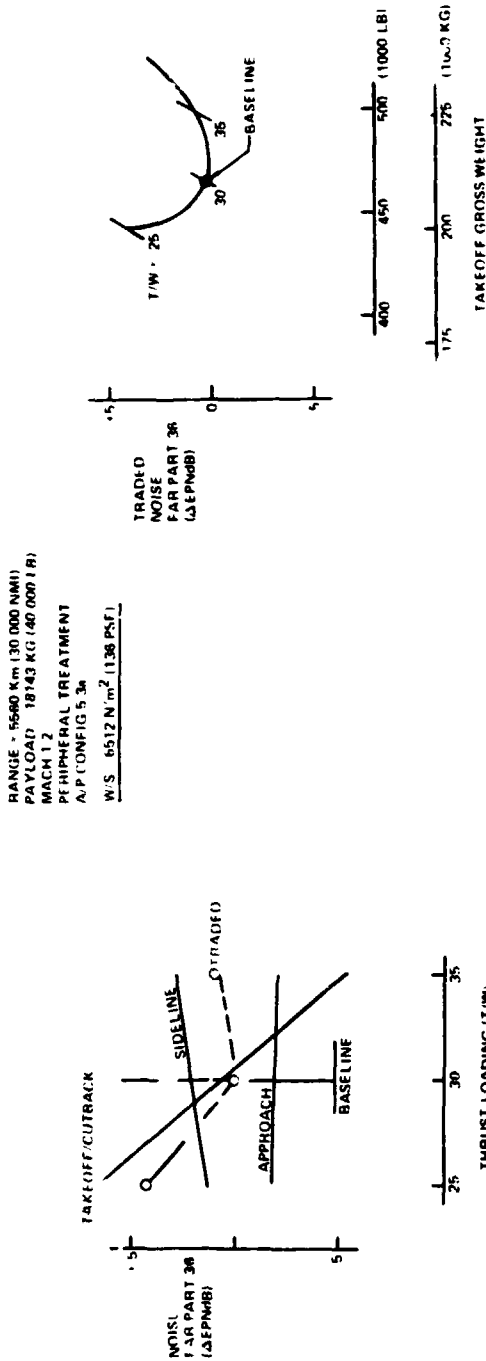


FIGURE 25.—EFFECT OF THRUST/WEIGHT ON COMMUNITY NOISE

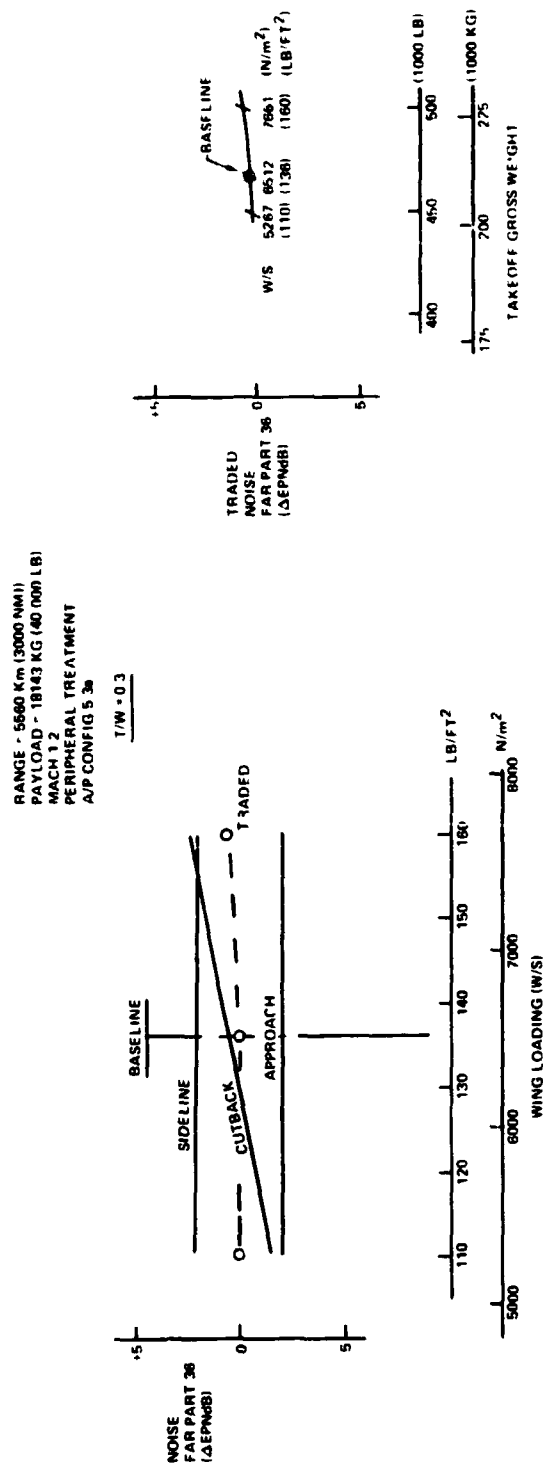


FIGURE 26.—EFFECT OF WING LOADING ON COMMUNITY NOISE

Range-Speed Sensitivity Study

The 5-3a configuration, which was designed for a cruise Mach number of 1.2 and sized for a range of 5560 km (3000 nmi), was evaluated to determine its range capability at cruise Mach numbers of 0.9, 1.05, 1.35. The results, as shown in figure 28, indicated that this configuration could achieve the design range of 5560 km (3000 nmi) for the complete “boomless” speed regime up to Mach 1.2. At Mach numbers above Mach 1.2 the cruise thrust cannot balance the aerodynamic drag at altitudes that satisfy the structural speed placard. The subsonic range capability is more than 20% greater than the M = 1.2 design range.

Payload Sensitivity Study

Two additional payloads, 13,605 kg (30,000 lb) and 22,675 kg (50,000 lb) were evaluated and compared to the baseline configuration, 18,141 kg (40,000 lb) payload. The weight, drag, and tail size changes due to the body length variations were accounted for in each of these configurations.

The results of this study are shown in figure 29. TOGW increased as the payload increased. However, the ratio of payload to TOGW (payload fraction) shows an improvement with increasing payload. The sized airplanes for each of the different payloads had equal wing loading and the OEW/TOGW was nearly constant. The equal wing loadings resulted in increasing wing area with payload. The friction and wave drag changes associated with the required body length changes were found to be self-canceling. However, the increased wing area, as shown in figure 30, increased the lift/drag ratio. As a result, the fuel/TOGW requirements were less. This produced the improvement in payload/TOGW ratio with payload size.

Sized Airplane Definition—Model 5-3a

A number of trade and development studies were conducted with mission sized configurations derived from the parent uncycled baseline configuration 5-3. These include:

- Range capability study
- Design payload study
- Impact of noise on TOGW
- Wing aspect ratio study

The first three studies have been discussed in this section of the report. The wing aspect ratio study is discussed in the yawed wing configuration evolution section.

Figure 31 identifies the particular configurations used in each of these studies.

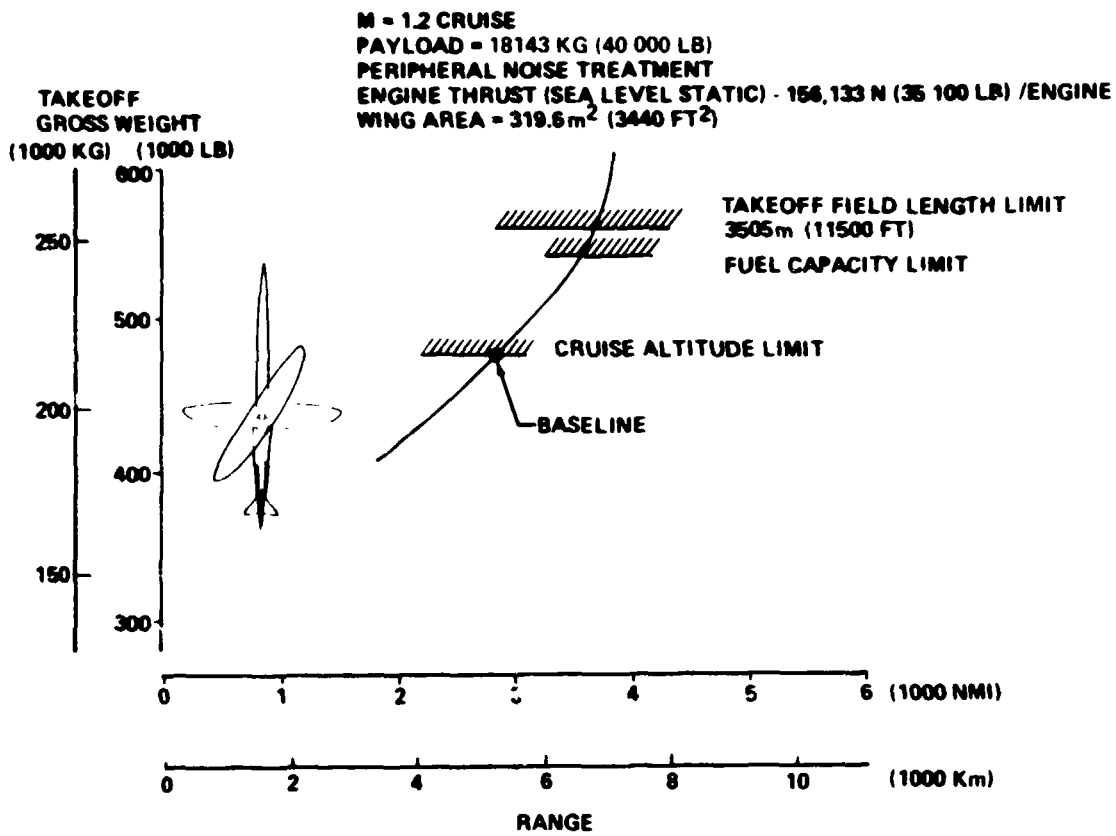


FIGURE 27.—MODEL 5-3A RANGE CAPABILITY STUDY

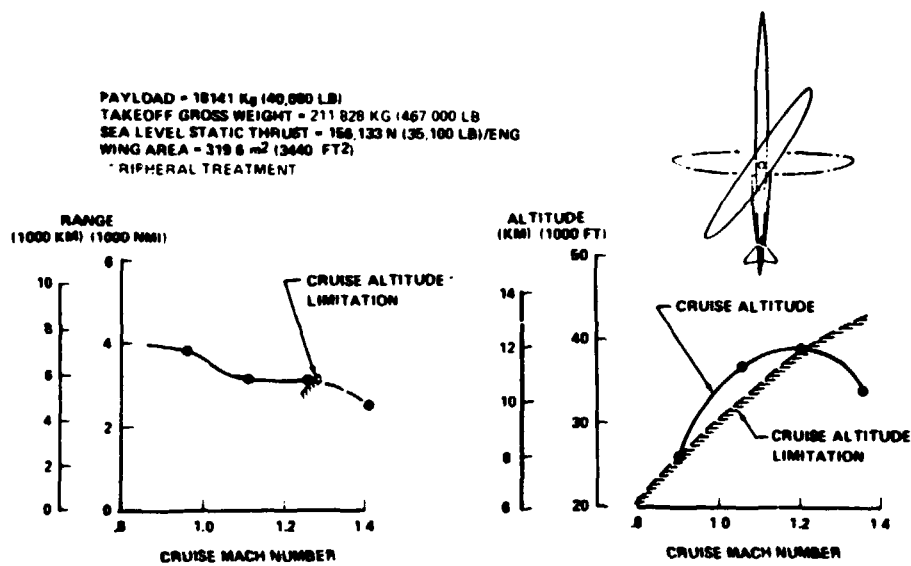


FIGURE 28.—MODEL 5-3 RANGE VS SPEED

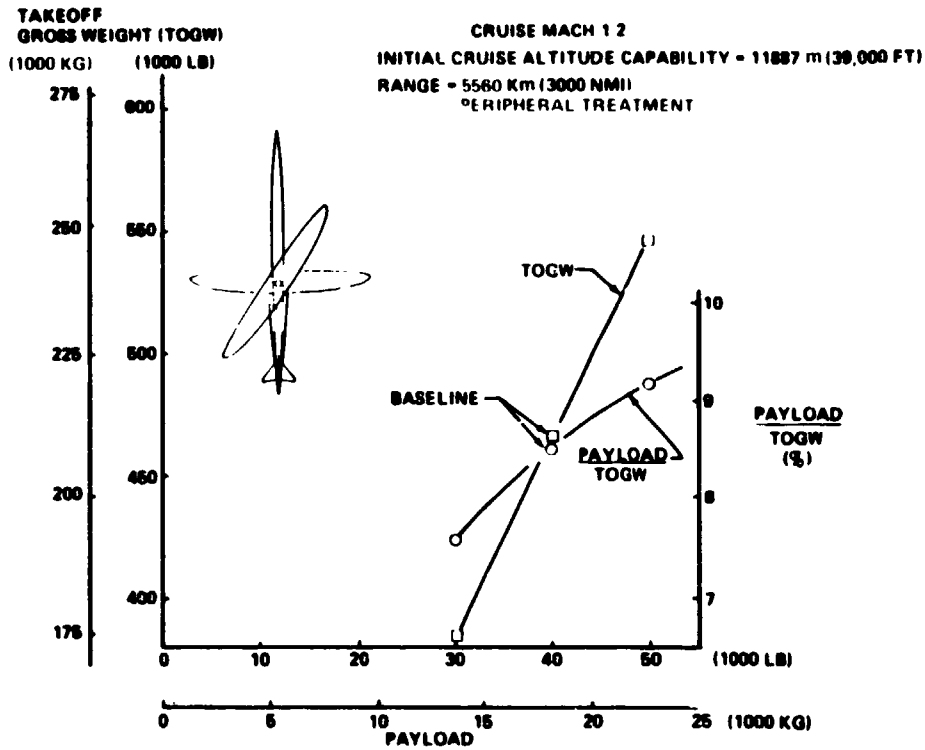


FIGURE 29.—MODEL 5-3A PAYLOAD STUDY

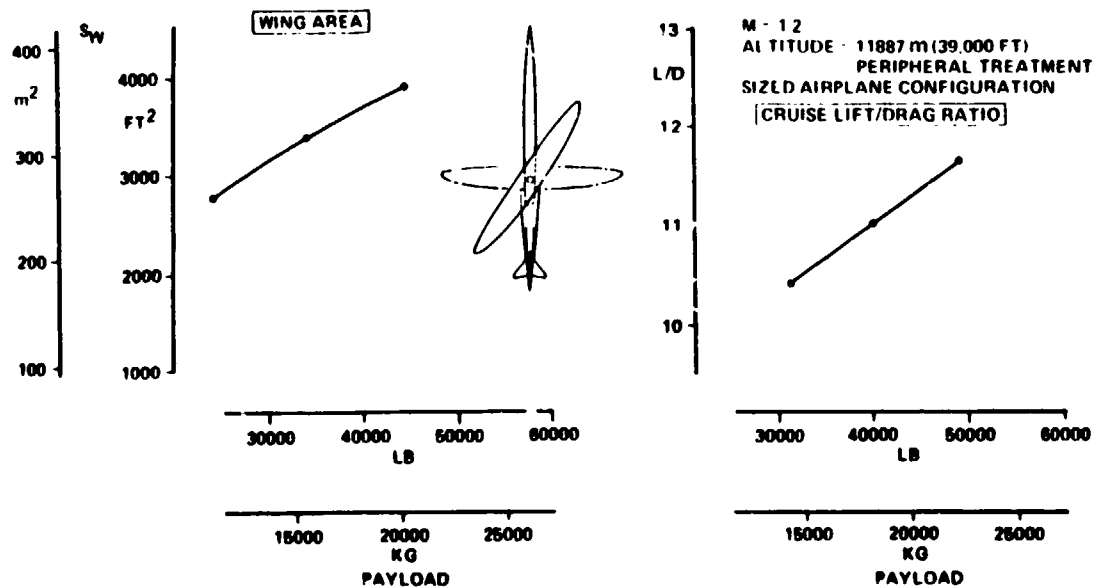


FIGURE 30.—MODEL 5-3A WING AREA AND CRUISE L/D VARIATION WITH PAYLOAD

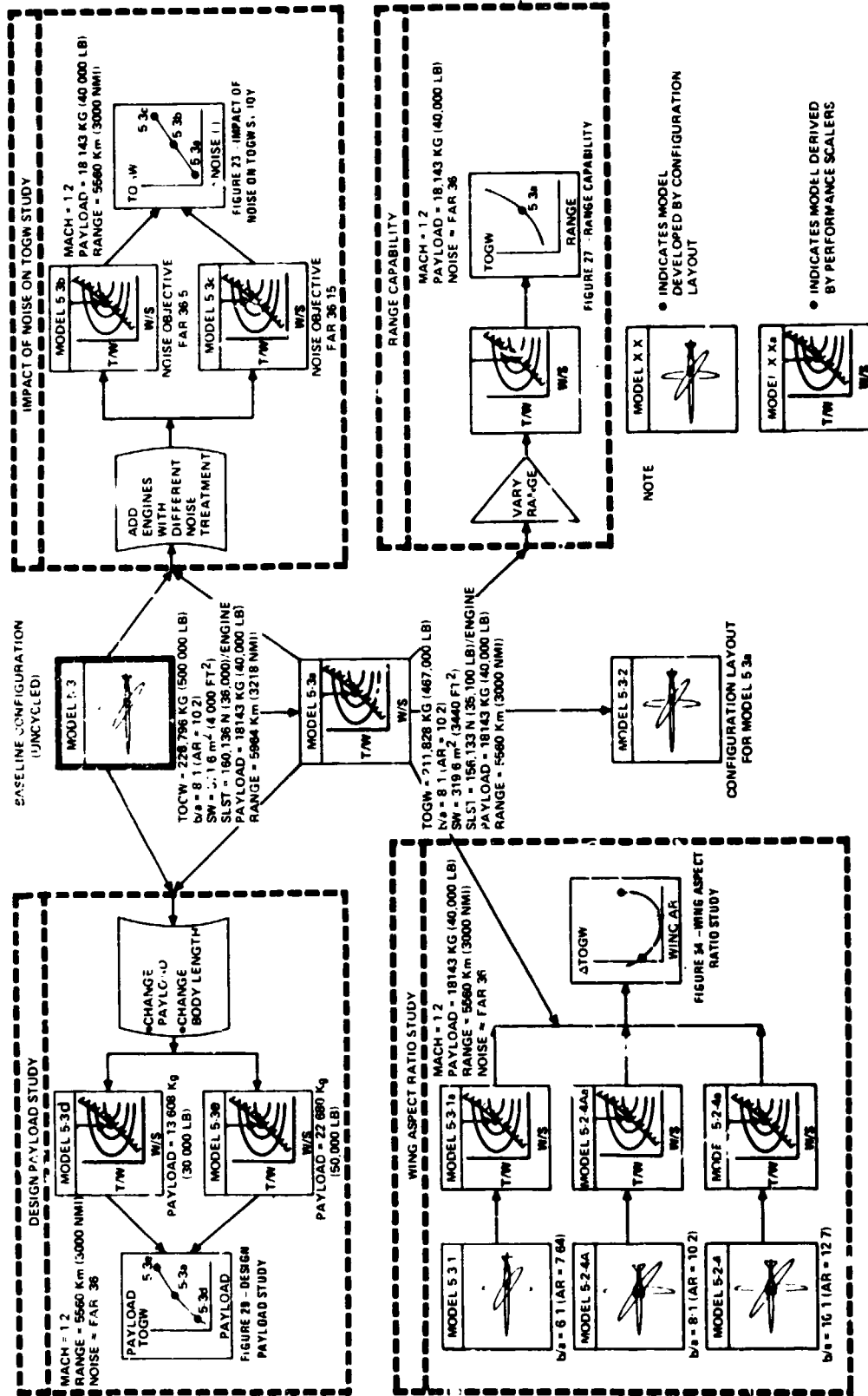


FIGURE 31.—MODEL 5-3 STUDY AND DEVELOPMENT FAMILY

Model 5-3a is the primary sized configuration derived from model 5-3 that has been used in each of these development and trade studies. The configuration drawing on figure 32, the drag summary on table 5, and the weight statement on table 6, illustrate the characteristics of model 5-3a derived from the mission scalars.

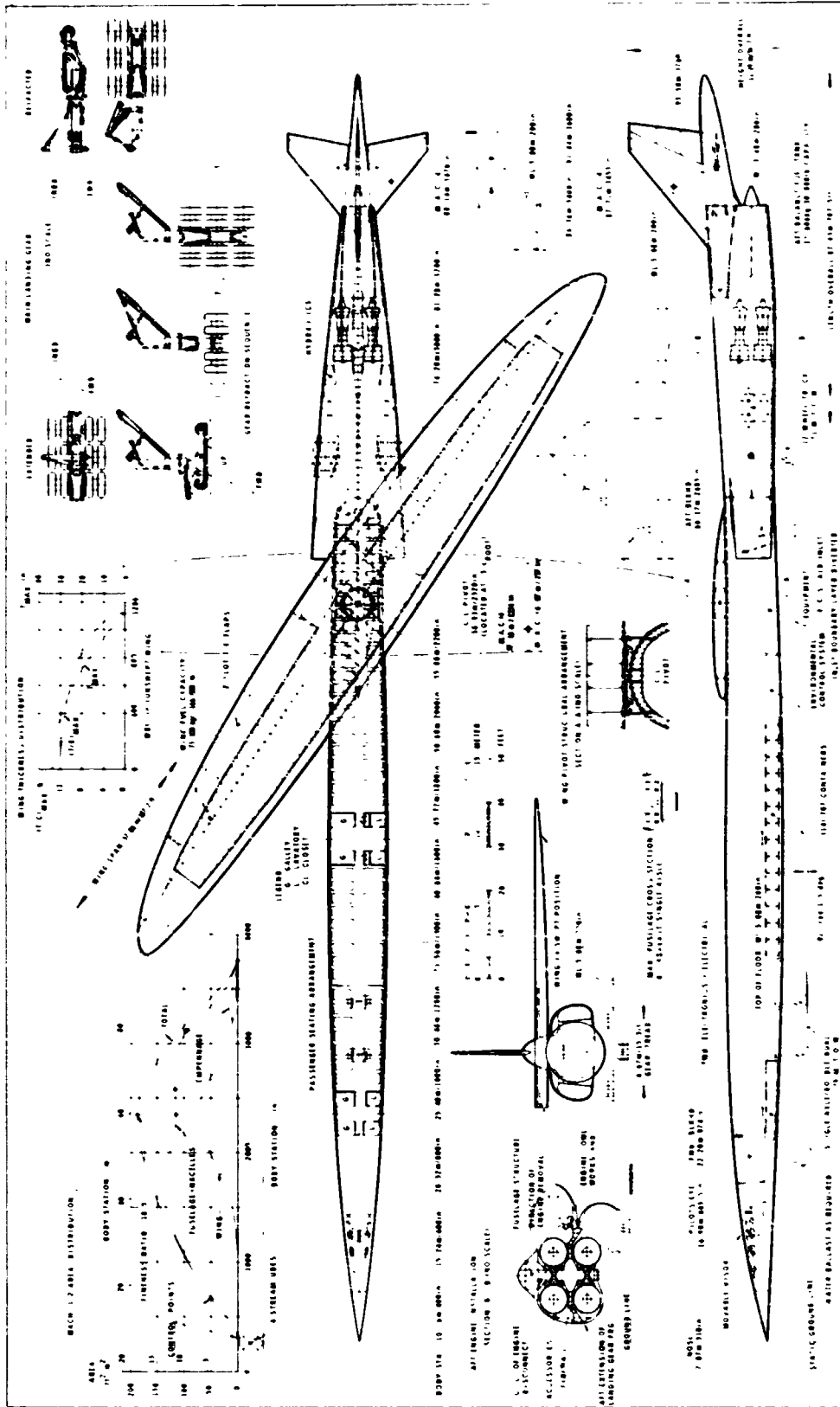
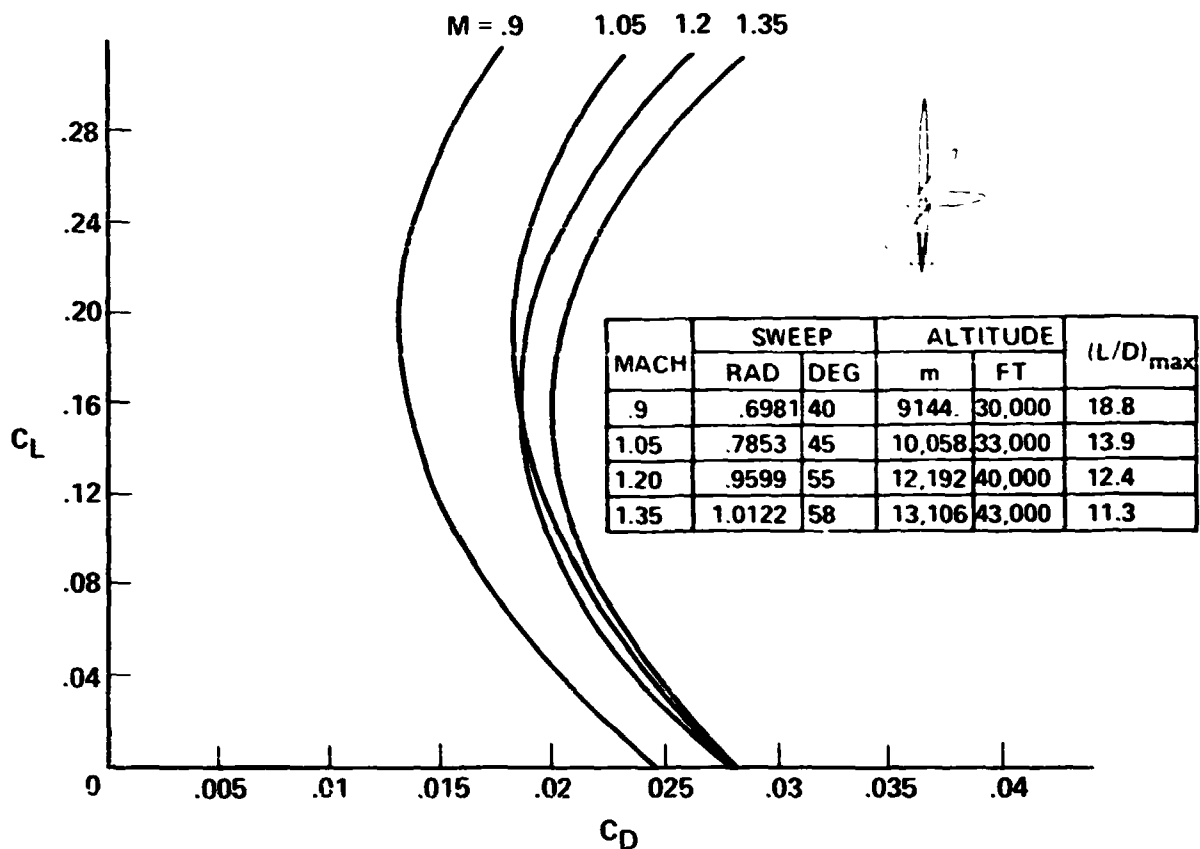


FIGURE 32.—CONCEPT 5 RESIZED CONFIGURATION (5-3a), MODEL 5-3-2

TABLE 5.-SCALED CRUISE DRAG SUMMARY, MODEL 5-3A



M = 1.2
 ALTITUDE = 12192.0 m (40,000 FT)

COMPONENT	A _{WET} /S	REF. LENGTH		C _{DF}	C _{DW}	COMMENT
		m	(FT)			
BODY	2.442	87.78	(288)	.00359	.00150	"NO ENGINE" BODY
(W · B) _{INTERF.}					-.00005	"NO ENGINE" WING + BODY
WING	1.946	9.61	(31.5)	.00379	.00163	S _{REF} = 319.6 m ² (3440 FT ²)
NACELLES + (W · N) _{INTERF.}	306	87.78	(288)	.00045	-.00015	ALL WAVE DRAG RELATIVE TO "NO ENGINE" AIRPLANE
HORIZONTAL TAIL	171	3.24	(10.64)	.00038	.00050	S _H = 27.4 m ² (295 FT ²)
VERTICAL TAIL	163	4.81	(15.79)	.00034	.00037	S _V = 25.5 m ² (275 FT ²)
MISCELLANEOUS					.00076	ROUGHNESS AND PROTUBERANCES
						THRUST SLST = 156,133 N (35,100 LB) ENGINE
						SIZED AIRPLANE
TOTALS	5.028			.00855	.00456	

TABLE 6.--UNCYCLED AND SIZED AIRPLANE WEIGHT COMPARISON MODEL 5.3

FUNCTIONAL GROUP	UNCYCLED AIRPLANE (5-3)		MISSION SIZED AIRPLANE (5-3a)	
	KG	LB	KG	LB
WING	35,830	79,000	30,120	66,400
HORIZONTAL TAIL	1,640	3,620	1,210	2,680
VERTICAL TAIL	860	1,900	670	1,490
BODY	26,040	57,400	26,000	57,310
MAIN LANDING GEAR	6,920	15,250	6,730	14,830
NOSE LANDING GEAR	2,090	4,600	2,030	4,480
NACELLE AND STRUT	11,310	24,930	9,950	21,930
TOTAL STRUCTURE	84,690	186,700	76,710	169,120
ENGINE	8,890	19,600	7,120	15,700
ENGINE ACCESSORIES, ENGINE CONTROLS, STARTING SYSTEM	650	1,430	650	1,430
FUEL SYSTEM	2,460	5,430	2,460	5,430
TOTAL PROPULSION GROUP	12,000	26,460	10,230	22,560
ACCESSORY DRIVE SYSTEM	490	1,080	490	1,080
INSTRUMENTS	480	1,050	480	1,050
SURFACE CONTROLS	3,030	6,690	2,980	6,570
HYDRAULICS	1,970	4,330	1,940	4,270
PNEUMATICS	660	1,450	660	1,450
ELECTRICAL	1,810	3,980	1,810	3,980
ELECTRONICS	1,390	3,070	1,390	3,070
FLIGHT PROVISIONS	430	950	430	950
PASSENGER ACCOMODATIONS	5,570	12,280	5,570	12,280
CARGO HANDLING	750	1,660	750	1,660
EMERGENCY EQUIPMENT	340	740	340	740
AIR CONDITIONING	1,810	4,000	1,810	4,000
INSULATION	1,330	2,930	1,330	2,930
AUXILIARY POWER UNIT	610	1,350	610	1,350
WATER BALLAST SYSTEM	110	250	110	250
TOTAL FIXED EQUIPMENT	20,780	45,810	20,700	45,630
EXERIOR PAINT + CUSTOMER OPTIONS	1,230	2,700	1,230	2,700
MANUFACTOR'S EMPTY WEIGHT	118,700	261,670	108,900	240,010
STANDARD + OPERATIONAL ITEMS	5,140	11,330	5,140	11,330
OPERATIONAL EMPTY WEIGHT	123,840	273,000	114,040	251,340
MAXIMUM TAKEOFF WEIGHT	226,796	500,000	211,828	467,000

NOTE: THE WEIGHT DATA FOR THE MISSION SIZED CONFIGURATION, 5-3a, WERE DERIVED FROM THE UNCYCLED BASELINE CONFIGURATION, 5-3, BY THE WEIGHT SCALES USED IN THE DESIGN SELECTION PROGRAM. DETAILED WEIGHT AND BALANCE ANALYSES WERE NOT PERFORMED ON THIS PARTICULAR CONFIGURATION.

YAWED WING CONFIGURATION EVOLUTION

The design and analysis experience that had been accumulated during the SST prototype program and past transonic-supersonic system studies provided a broad data base to develop the delta, fixed swept-wing, and variable-sweep configurations. The integration of all the aircraft components into an integrated design proved to be quite straightforward for the twin-fuselage yawed wing configuration. Extensive conceptual design and analyses efforts were, however, necessary to evolve the single fuselage yawed wing configuration, 5-3.

The evolution process summarized in the appendix is discussed in this section along with a review of supporting configuration development trade studies.

CONFIGURATION DEVELOPMENT

The major difficulty in developing the single fuselage yawed wing configuration proved to be the integration of the landing gear and engines with the pivoting wing mounted on the slender fuselage. The more than 30 conceptual arrangements necessary to develop the initial single-fuselage configuration far exceeded the number of arrangements required to develop the other aircraft concepts (table 7). Some of these early concepts are illustrated in figures 33 through 38.






Initial Configuration Definition

A high wing configuration with four engines was selected for more extensive development. The wing planform selected corresponded to the quasi-elliptical wing of the wind tunnel model tested at NASA Ames (ref. 5). This wing had an equivalent elliptical axes ratio of 10:1 which corresponds to an unswept aspect ratio of 12.7. The characteristics of this planform are described in the aerodynamics section of this report.

Qualitative high-wing versus low-wing design investigations indicated that a location of the pivoting wing high on the fuselage allowed a greater degree of flexibility for developing an integrated configuration than a low wing arrangement. Preliminary NASA wind tunnel data had indicated that the high wing installation has less drag. The relative merits of the high-wing versus low-wing arrangements are summarized in table 8.

Integrating the landing gear with the airframe requires different design approaches for high-wing and low-wing aircraft. On concepts 1-2, 2-2, and 3-2 where the wing is mounted low on the fuselage, the center of gravity, cg, is also located low in the fuselage. In order to provide the aircraft with sufficient stability when maneuvering on the ground a minimum angle of 1.05 rad (60°) is required between the center of gravity and the contact points of the wheels on the ground. This determines the minimum gear tread. Because of the high wing location for model 5, the center of gravity is located considerably higher in the fuselage and a much larger landing gear tread is required (fig. 39). A high-wing does not provide a satisfactory support for the landing gear. Supporting struts extending from the lower fuselage were therefore added. The struts were designed to also support two engines

TABLE 7.—CONFIGURATIONS LEADING TO INITIAL ARRANGEMENTS

AERODYNAMIC CONCEPT	ENGINE LOCATION			WING LOCATION			EMPENNAGE			LDG. GEAR	CONFIGURATIONS
	2 ENG.	3 ENG.	4 ENG.	LOW	HIGH	TANDEM	LOW	HIGH	YAWED		
 ①	-	1	1	1	-	-	1	-	-	1	2
 ②	-	1	2	1	-	-	1	1	-	2	3
 ③	-	-	3	1	-	-	1	-	-	2	3
 ④	-	-	4	-	1	2	1	-	1	3	5
 ⑤	4	9	16	5	9	1	5	1	4	6	32
GRAND TOTAL											45

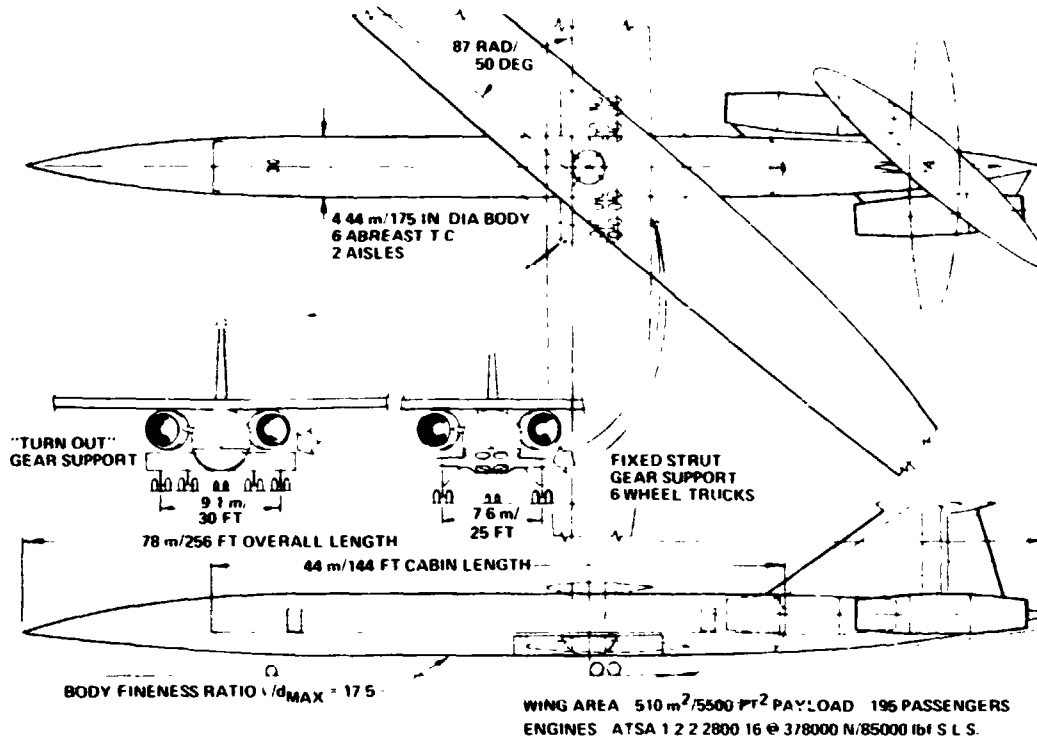


FIGURE 33.-MODEL 5-01 CONFIGURATION

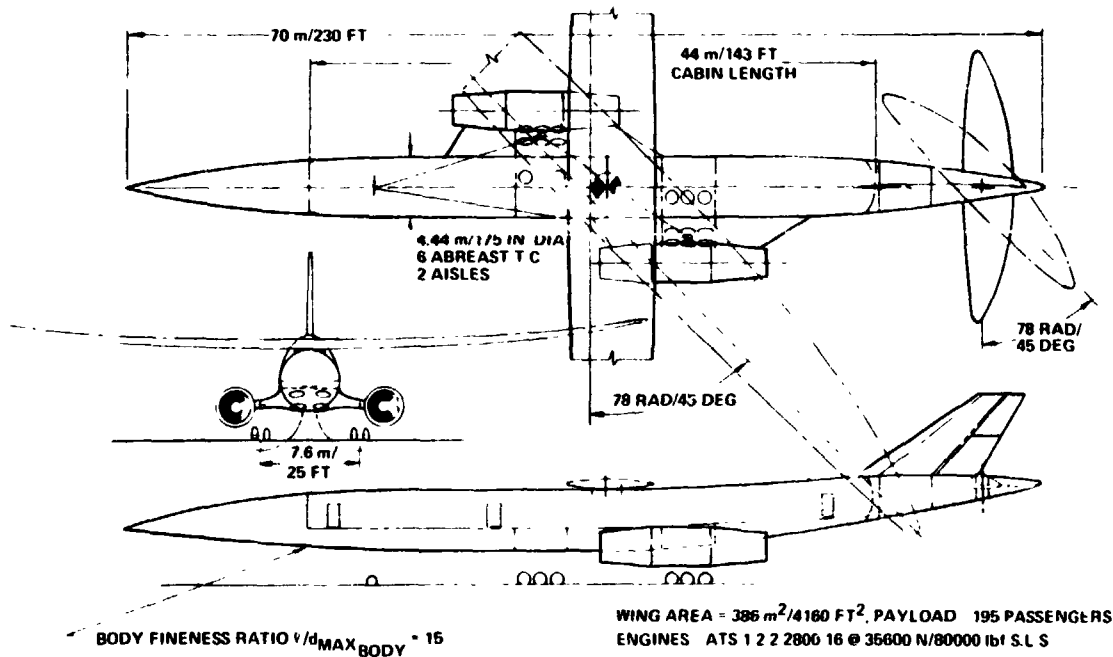


FIGURE 34.-MODEL 5-02 CONFIGURATION

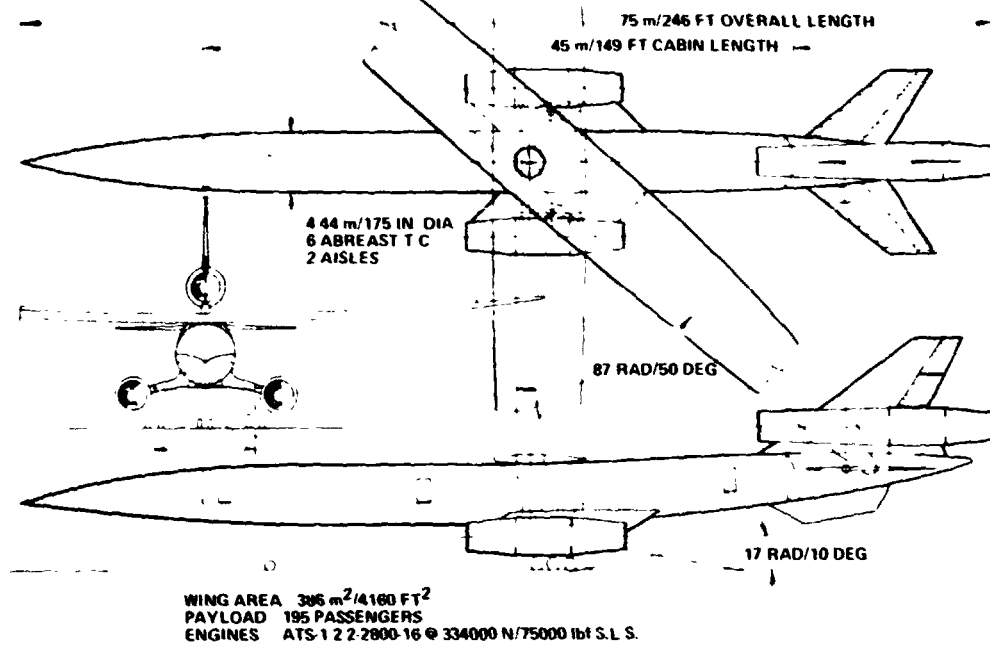


FIGURE 35.—MODEL 5-04 CONFIGURATION

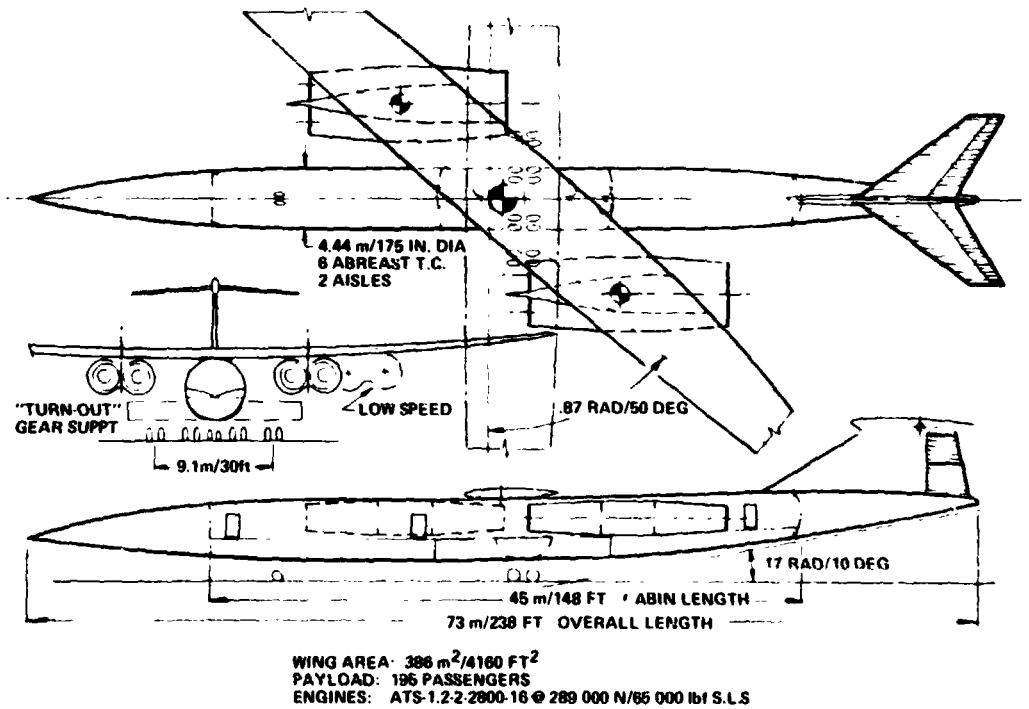


FIGURE 36.—MODEL 5-06 CONFIGURATION

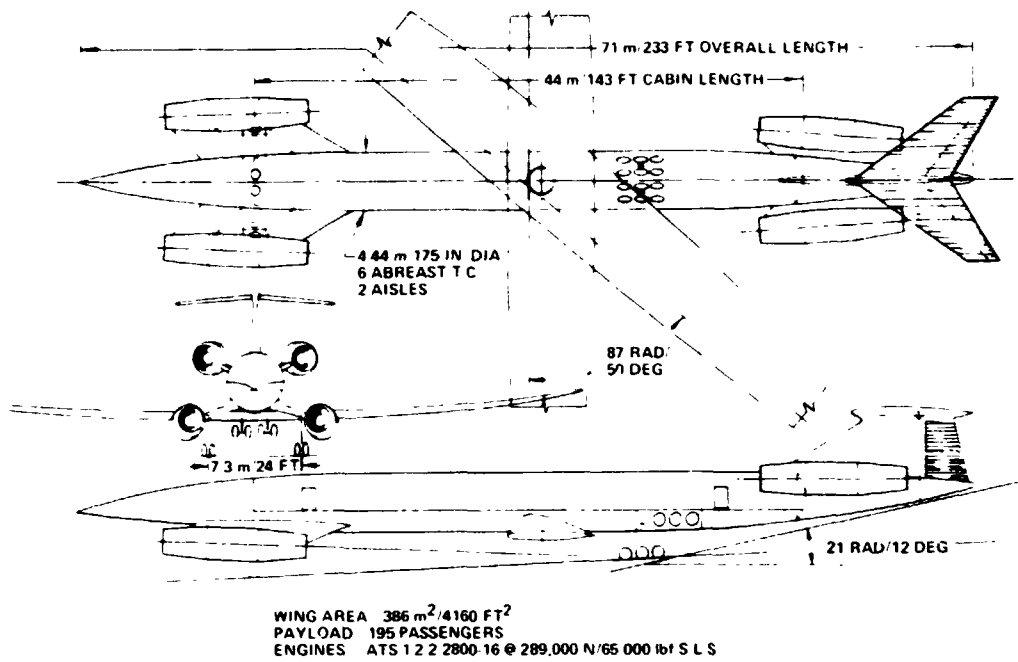


FIGURE 37.—MODEL 5-07 CONFIGURATION

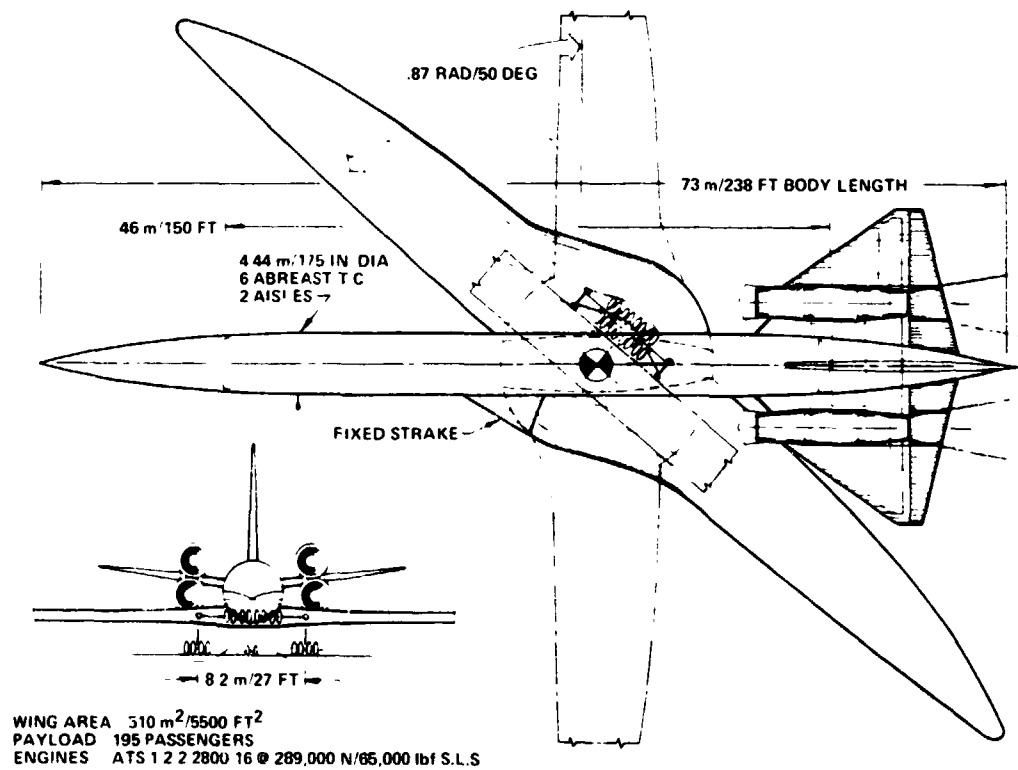


FIGURE 38.—MODEL 5-010 CONFIGURATION

TABLE 8.—LOW-WING VS HIGH-WING COMPARISON

DESIGN ITEM	WING LOCATION	
	HIGH WING	LOW WING
WING-MOUNTED MAIN GEAR	-	+*
A/P GROUND MANEUVERING	-	+
OUTRIGGER GEAR	-	+
PASSENGER SAFETY	-	+
CONFIGURATION INTEGRATION	+	-
FUSELAGE ACCESSIBILITY	+	-
WING/BODY FAIRING	+	-
TAKEOFF ROTATION	+	-
AERODYNAMIC DRAG	+	-

*+ INDICATES FAVORED WING LOCATION

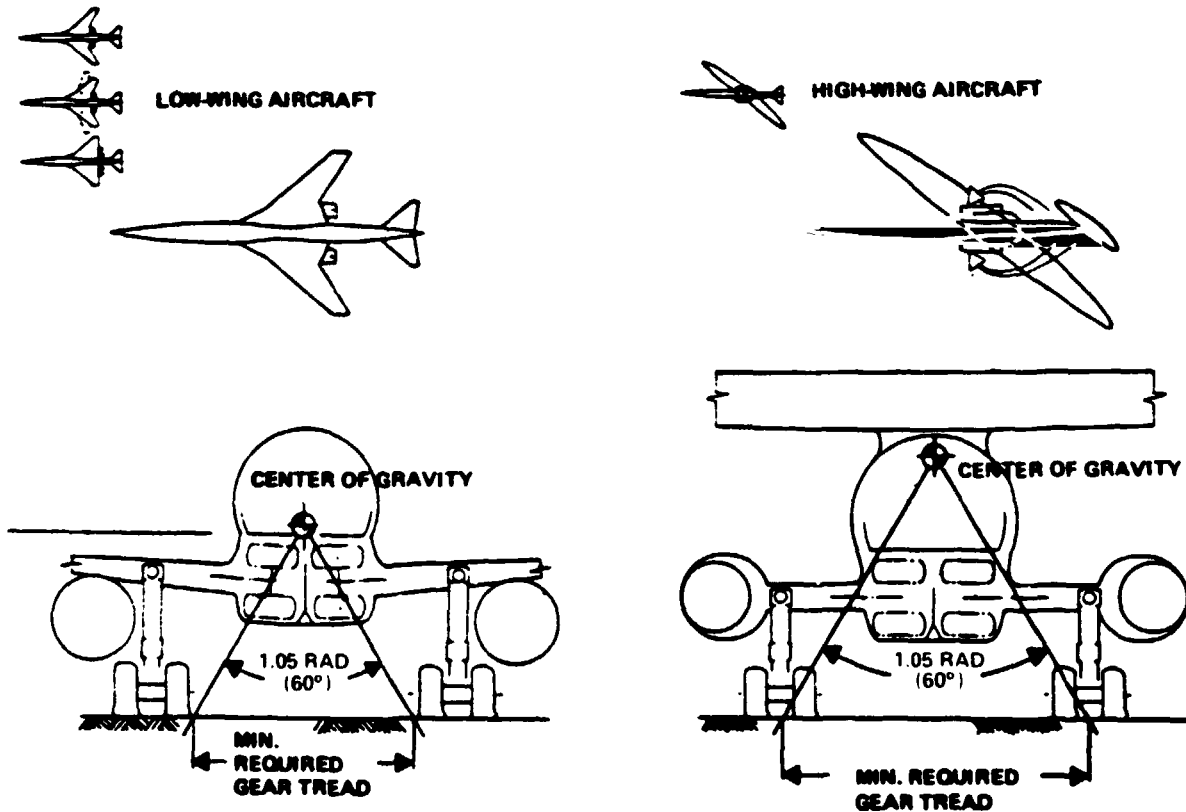


FIGURE 39.—LANDING GEAR INTEGRATION

and thereby fulfill a dual function. A full front view of the single fuselage, yawed wing configuration is shown in figure 40. The landing gear is stowed below the cabin floor. In order to avoid interference between engine efflux and the all flying stabilizer, the second set of nacelles were mounted on each side of the vertical tail. The configuration that evolved from these considerations is shown in figure 41.

A detailed drag evaluation of this configuration identified high wave drag associated with the installation of the two rear engines. This design was modified by replacing the tail mounted engines by a single center engine with S-duct inlet, figure 42. This was the initial single fuselage yawed wing configuration analyzed in depth for comparative evaluation with the other concepts.

Configuration Improvement Studies

Results of the initial detailed configuration evaluations are shown in figure 43. The unit wing weight of the single fuselage yawed wing configuration was significantly higher than that of the conventional planform configurations. In addition, the wave drag for this configuration was higher than had been anticipated.

Further configuration development efforts were, therefore, directed at designing an aerodynamically improved arrangement with a reduced wing weight. The method employed was first to reduce the wing unswept aspect ratio from 12.7 to 10.2 and then to increase overall configuration slenderness ratio by reducing the body cross-sectional area, increasing the body length and moving the engines and landing gear away from the concentrated area near the wing-body pivot station. Configurations that were developed to achieve these objectives are shown in figures 44 through 49.

Based on the qualitative assessments shown in tables 9, 10, and 11, and weight versus drag evaluations summarized in table 12, the aft-integrated engine arrangement, 5-2-8A, was selected for detailed development and definition. This led to configuration, model 5-3, which incorporated a wing with an elliptic axes ratio of 8:1 (aspect ratio = 10.2). Subsequent studies have indicated that this is nearly the optimum elliptic axes ratio for this configuration. The detailed characteristics of this configuration are discussed in the configuration description section.

The results of the reduced span and configuration improvement efforts as summarized in figure 50 provided a significant reduction in the size of the airplane required to achieve the design mission objectives.

BYPASS RATIO STUDY

The sensitivity of the single fuselage yawed wing configuration to engine bypass ratio was investigated on the three-engine arrangement 5-2-4 (fig. 42). The bypass ratio 1 engines were replaced with bypass ratio 4 engines. The redesigned configuration with the bypass ratio 4 engines is shown in figure 51. The configuration was resized to achieve the design mission.

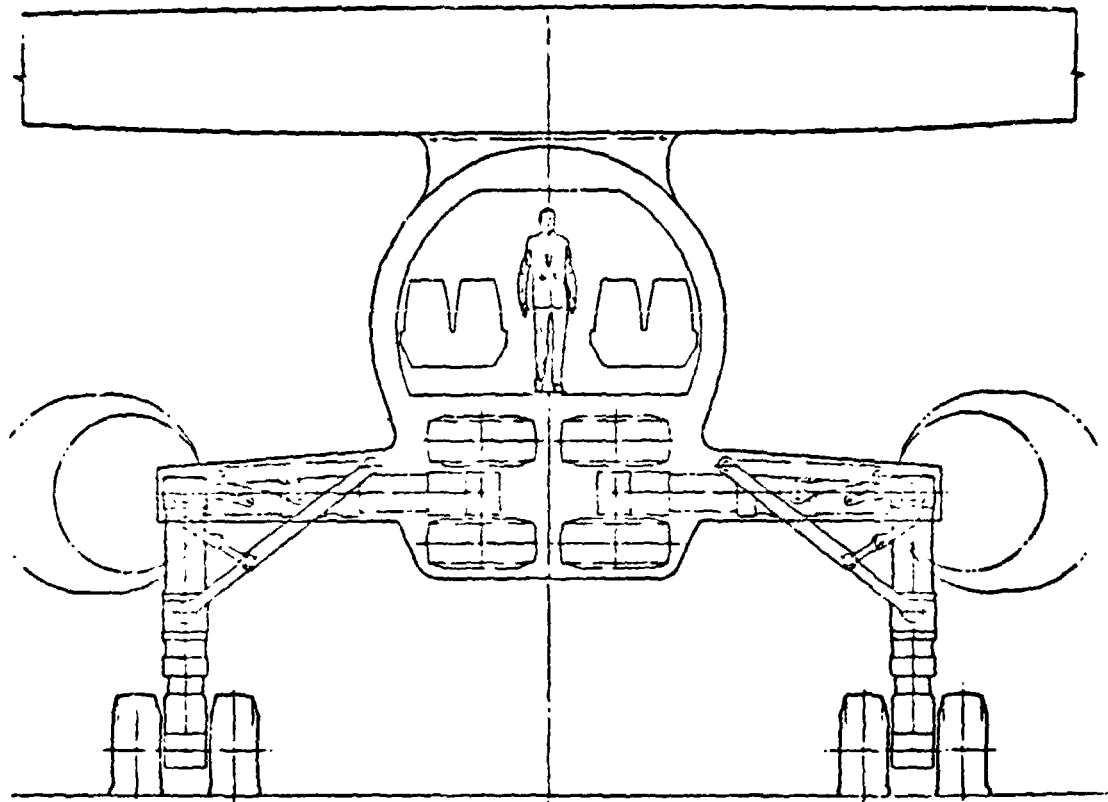


FIGURE 40.—CONCEPT 5 BASIC CROSS SECTION

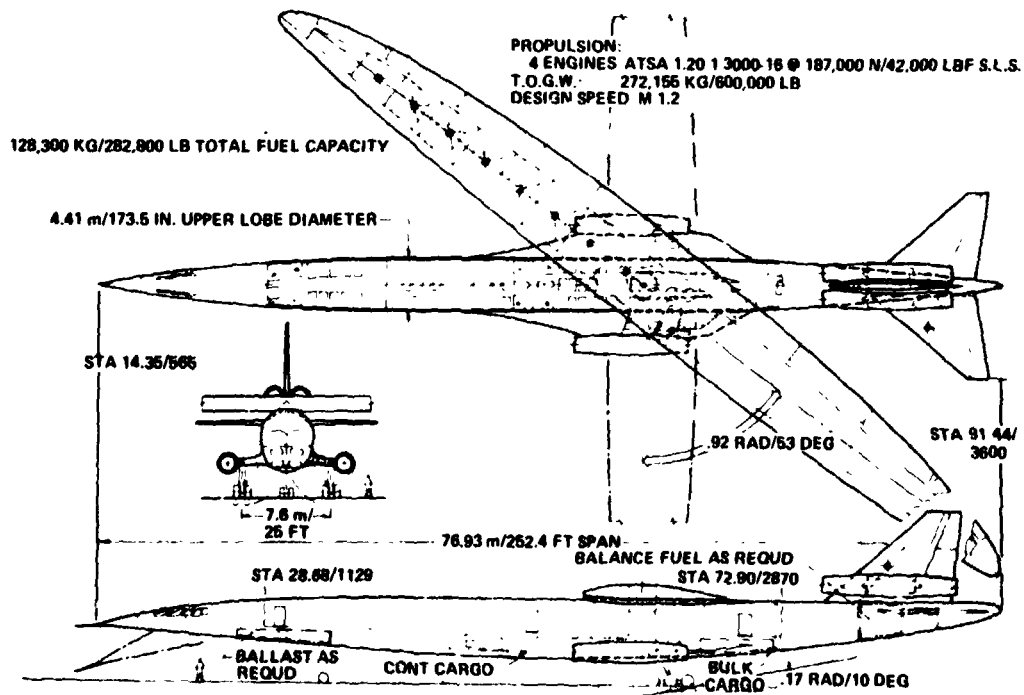


FIGURE 41.—GENERAL ARRANGEMENT, MODEL 5-2

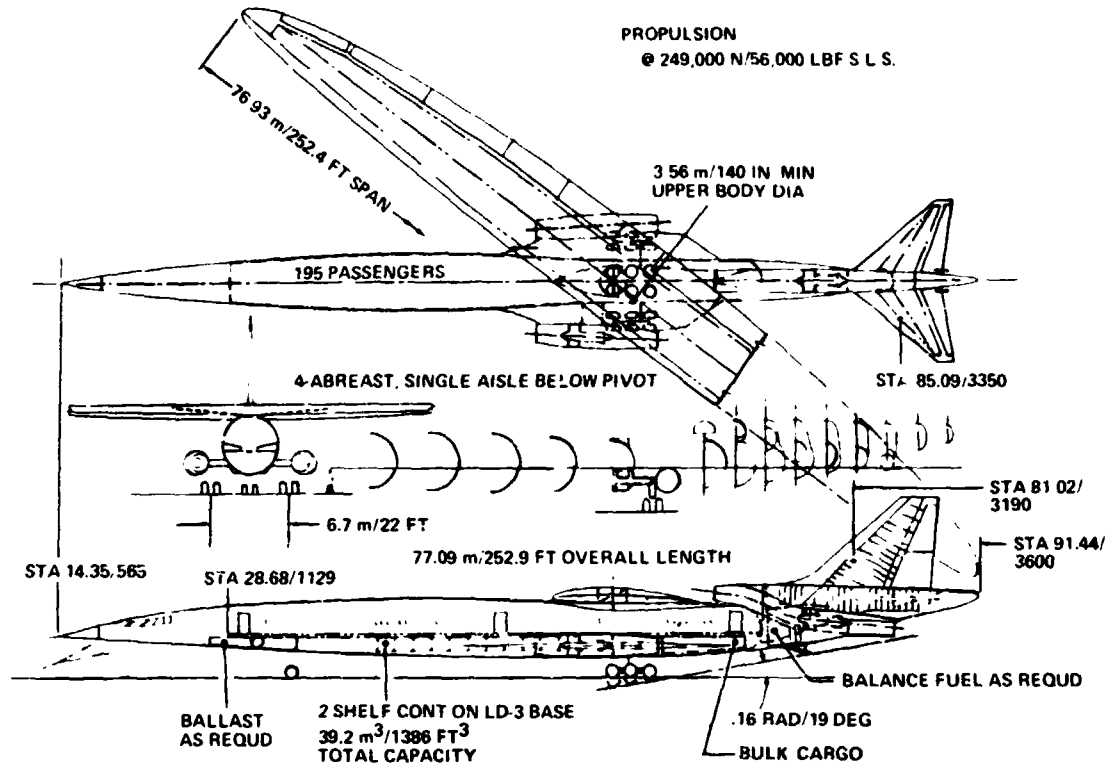


FIGURE 42.—GENERAL ARRANGEMENT, MODEL 5-2-4

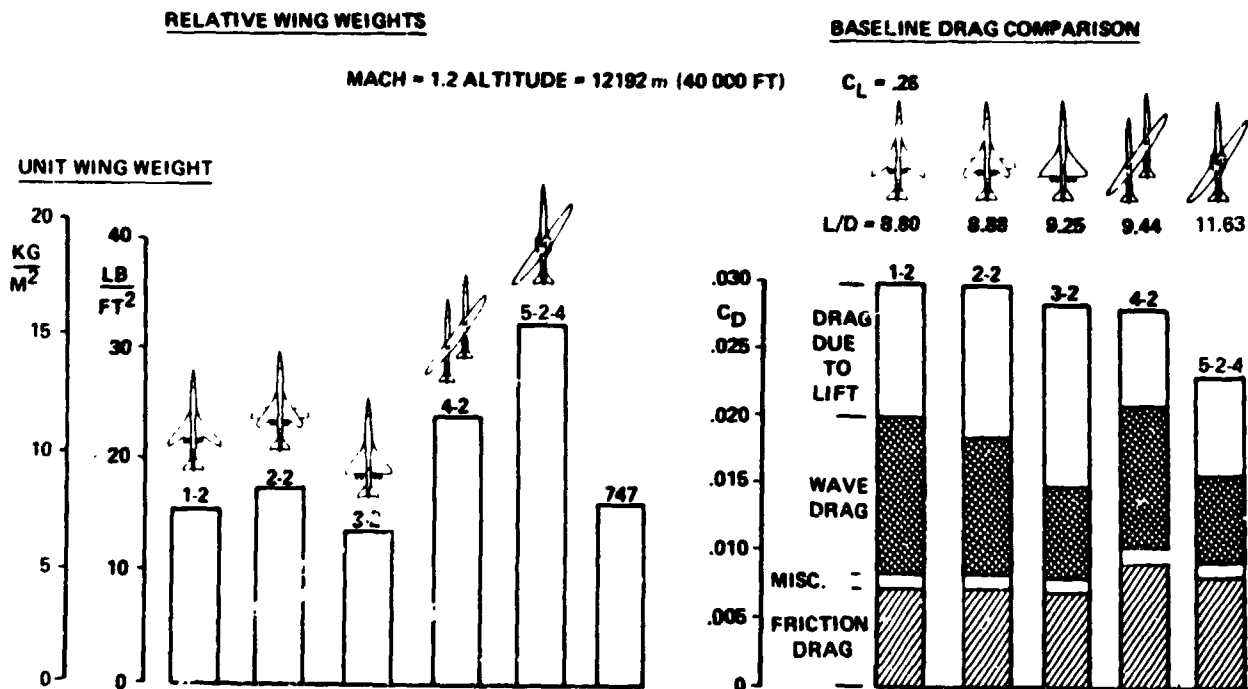


FIGURE 43.—INITIAL UNSIZED CONFIGURATION EVALUATIONS

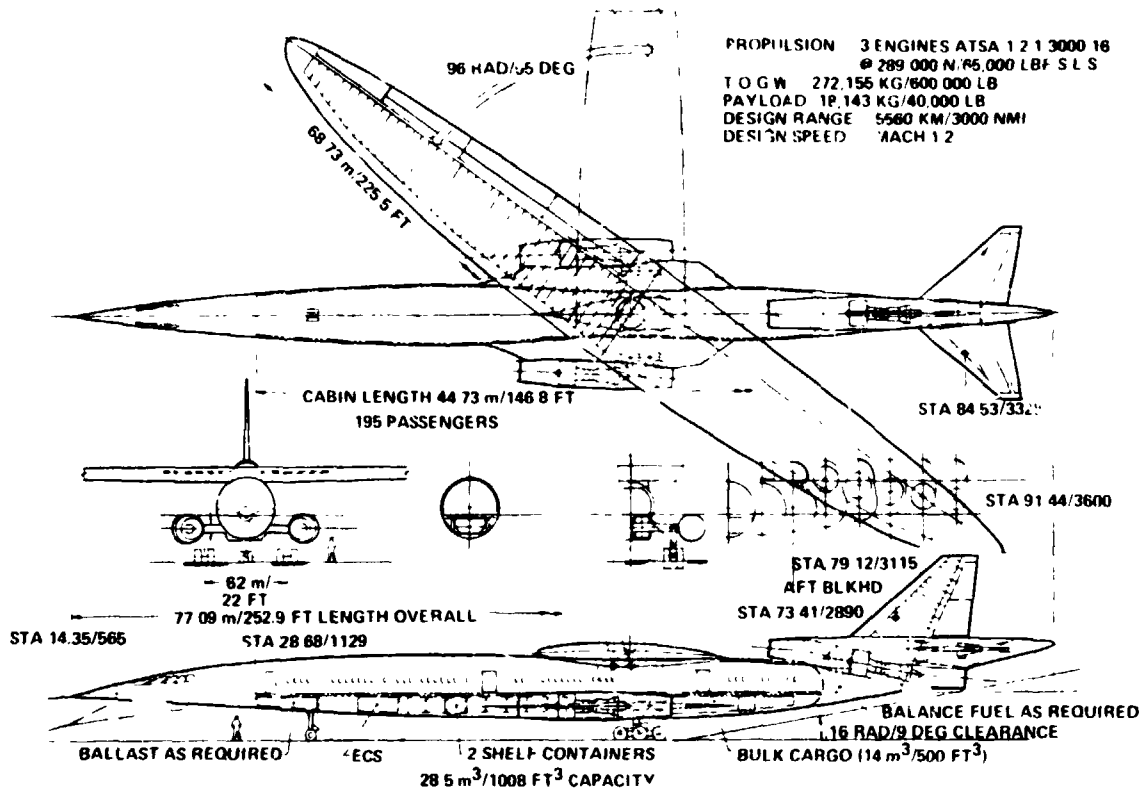


FIGURE 44.—GENERAL ARRANGEMENT, MODEL 5-2-4A

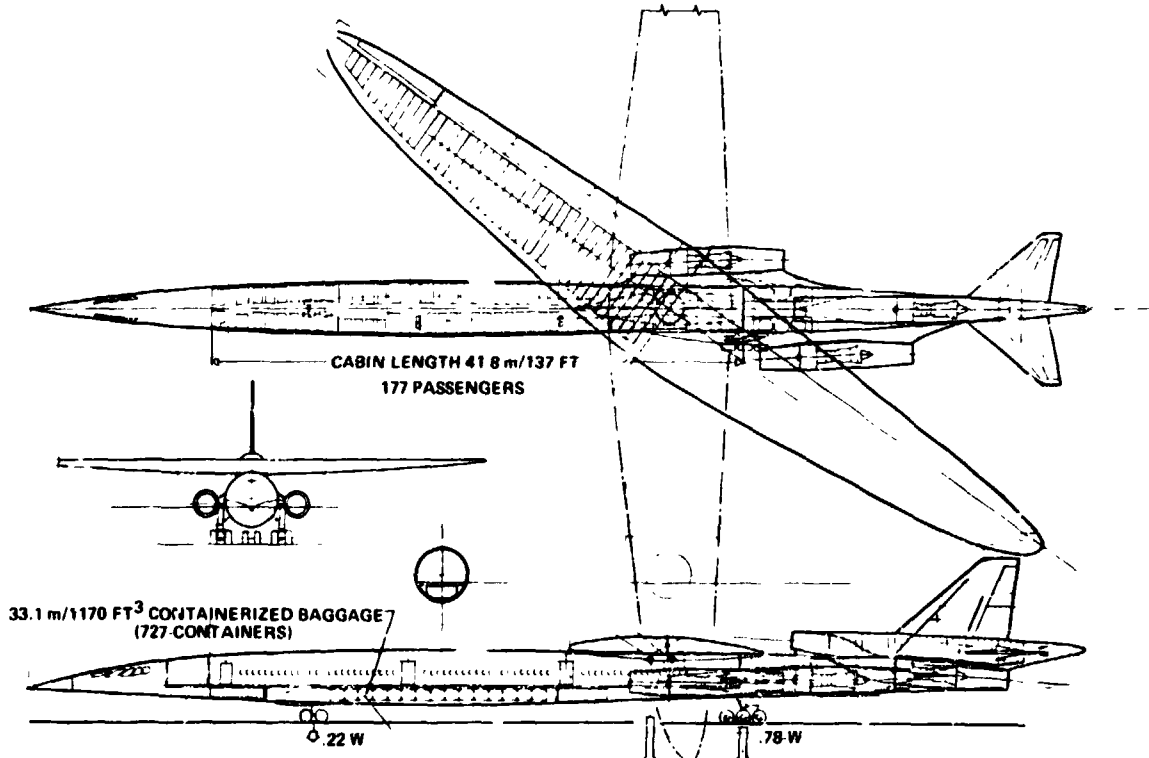


FIGURE 45.—GENERAL ARRANGEMENT, MODEL 5-2-5

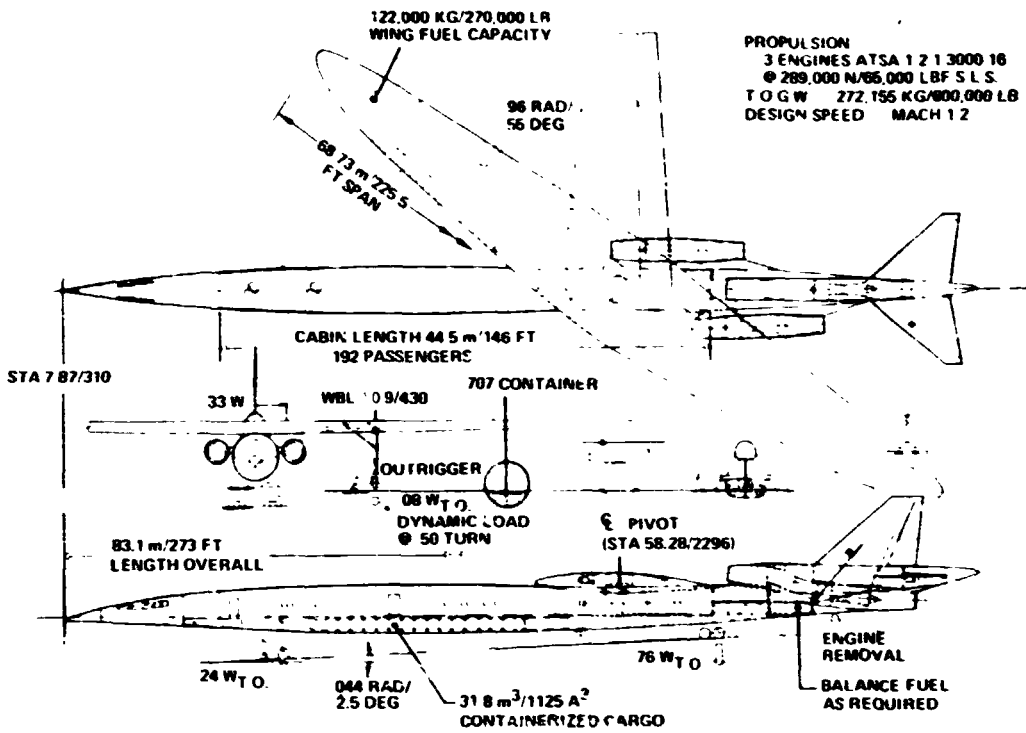


FIGURE 46.—GENERAL ARRANGEMENT, MODEL 5-2-6

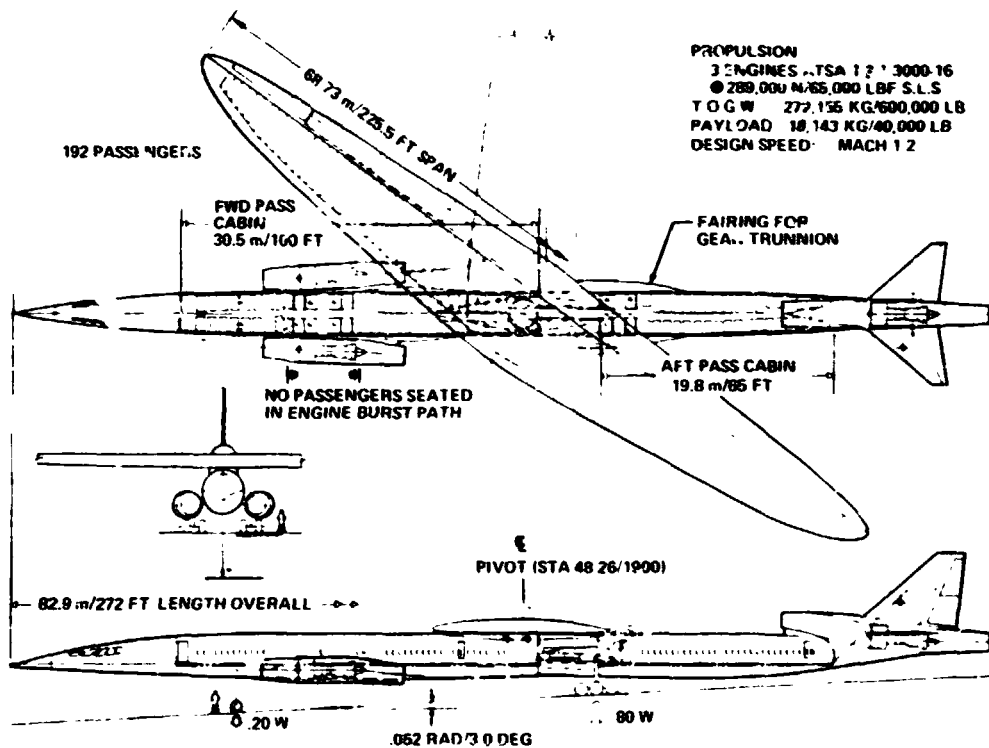


FIGURE 47.—GENERAL ARRANGEMENT, MODEL 5-2-7A

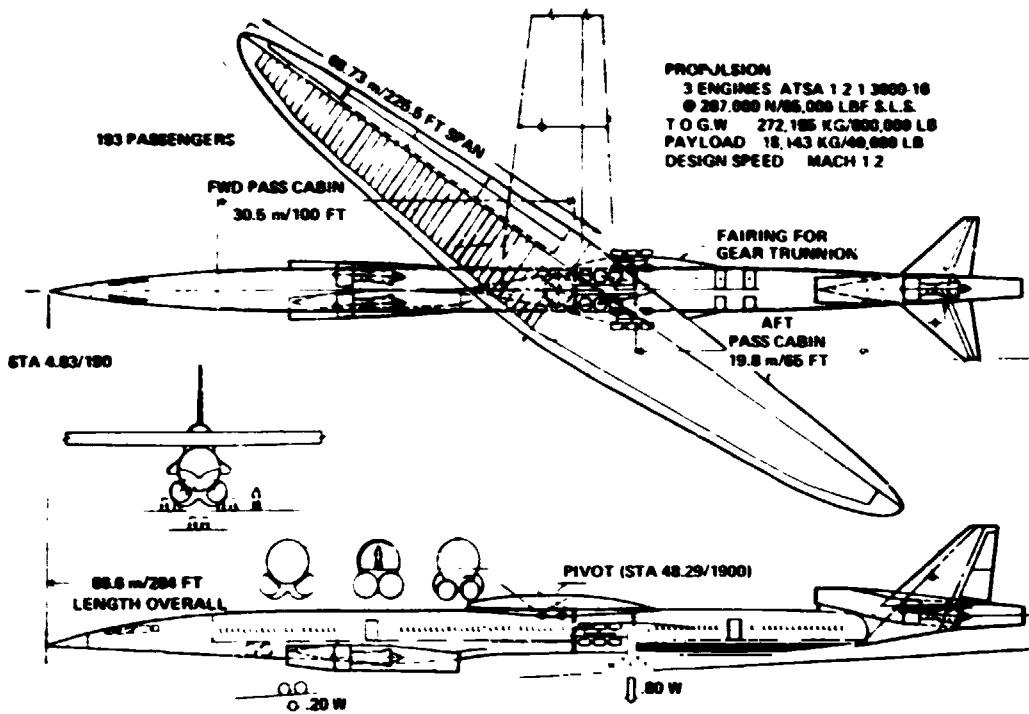


FIGURE 48.—GENERAL ARRANGEMENT, MODEL 5-2-7B

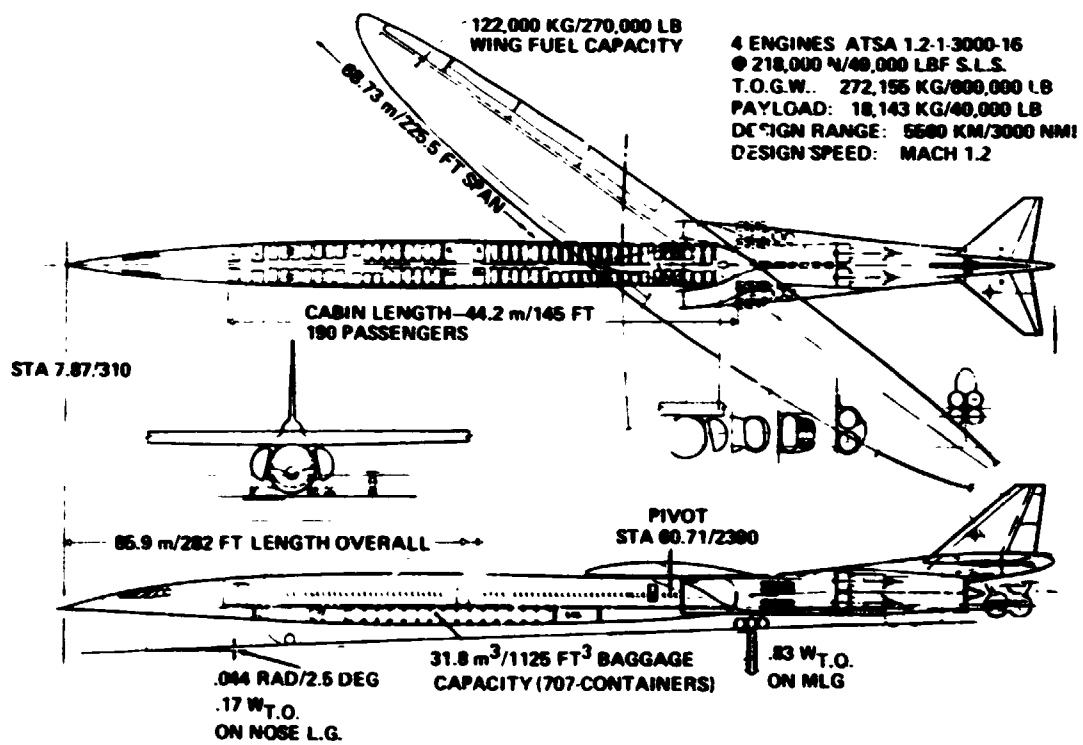
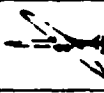
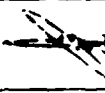



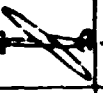






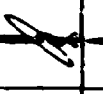
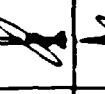
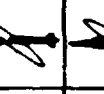
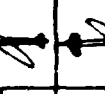



FIGURE 49.—GENERAL ARRANGEMENT, MODEL 5-2-8A

TABLE 9.-CONFIGURATION ASSESSMENT

CRITERIA	YAWED WING, SINGLE FUSELAGE CONFIGURATIONS							
								
	B-24A	B-25	B-26	B-27	B-27A	B-27B	B-28	B-28A
DESIGN INTEGRATION	○	●	●	●	●	●	●	●
TECHNICAL RISK	●	●	●	●	●	●	●	●
AIRFRAME GROWTH POTENTIAL	●	●	●	○	○	○	●	●
LANDING GEAR COMPLEXITY	○	●	●	●	●	●	●	●
EMPENNAGE INTEGRATION AND CONTROL	○	○	○	○	●	●	●	●
OPERATIONAL C.G. RANGE	●	●	●	○	○	○	●	●
PAYLOAD FLEXIBILITY	○	●	●	●	●	●	○	○
PASSENGER APPEAL	●	●	●	●	●	●	○	○
PASSENGER CABIN ACCESSIBILITY	○	●	●	●	●	●	○	○
CARGO VOLUME AND ACCESSIBILITY	○	●	○	●	●	●	●	●
AIRPLANE GROUND MANEUVER STABILITY	●	●	○	●	●	●	●	●
TOTAL PASSENGERS	185	177	182	185	192	182	180	180

LEGEND ○ GOOD
 ○ AVERAGE
 ● POOR

TABLE 10.-PROPULSION-NOISE ASSESSMENT

CRITERIA	MACH 1.2 TRANSPORT CONFIGURATIONS								
									
	5-24	5-24A	5-25	5-26	5-27	5-27A	5-27B	5-28	5-28A
INLET/INLET FLOW FIELD SUITABILITY	●	●	●	●	○	○	●	●	●
THRUST REVERSER DESIGN FLEXIBILITY	●	●	●	●	○	○	○	○	●
INLET FOREIGN OBJECT DAMAGE HAZARD	●	●	●	●	○	○	○	●	○
ENGINE ACCESSIBILITY	●	●	●	●	●	●	●	●	●
INSTALLATION EFFICIENCY (POTENTIAL THRUST/SFC LOSSES)	○	○	○	○	●	●	●	●	●
JET IMPINGEMENT	○	○	○	○	●	●	●	○	○
RISK OF MULTI ENGINE FAILURE	●	●	●	●	●	●	●	●	●
PASSENGER INTERIOR NOISE COMFORT	●	●	●	●	●	●	●	○	○
PASSENGER HAZARD DUE TO ENGINE FAILURE	●	●	●	●	●	●	●	○	○

LEGEND
 ○ GOOD | SATISFACTORY ●
 ○ AVERAGE | MARGINAL ●
 ● POOR

TABLE 11.--FLIGHT CONTROLS ASSESSMENT

CRITERIA	MACH 1.2 TRANSPORT CONFIGURATIONS								
	524	524A	525	526	527	527A	527B	528	528A
LANDING APPROACH TRIM AND FLARE CAPABILITY	○	○	⊙*	⊙*	⊙*	⊙*	⊙*	⊙	⊙*
LONGITUDINAL STABILITY	○	○	○*	○*	⊙*	⊙*	○*	●	⊙*
LONGITUDINAL CONTROL	○	○	○*	○*	⊙*	⊙*	○*	●*	○*
PITCH-UP (MODERATED)	⊙	⊙	●	●	⊙	⊙	⊙	●	●
DEEP STALL (HIGH M)	⊙	⊙	●	●	⊙	⊙	⊙	●	●
JET IMPINGEMENT ON THE HORIZONTAL TAIL	⊙	○	⊙	⊙	○	○	○	○	⊙
TAKE-OFF ROTATION, HORIZONTAL TAIL SLICK-DOWN	○	○	NDC	NDC	NDC	NDC	NDC	NDC	NDC
DIRECTIONAL STABILITY	○	⊙*	⊙*	⊙*	○*	○*	○*	⊙*	⊙*
ENGINE-OUT CONTROL	○	⊙*	⊙*	⊙*	○*	○*	○*	⊙*	⊙*
UNSYMMETRICAL SIDEWASH CHARACTERISTICS	NDC	NDC	●	●	NDC	NDC	NDC	NDC	NDC

LEGEND
 ○ ADEQUATE TAIL SIZE
 ⊙ POTENTIAL PROBLEM

LEGEND
 ○ ADEQUATE TAIL SIZE | S...ACTORY ⊙ (WITH SMALL MODIFICATION)
 ⊙ POTENTIAL PROBLEM | MARGINAL ●
 ● PROBABLE PROBLEM |
 * LARGER TAIL SIZE REQUIRED (15-20%)
 NDC NOT A DESIGN CONSTRAINT OR CONSIDERATION

TABLE 12.—CONFIGURATION COMPARISON

MCR = 1.2
 ALTITUDE = 12192 m (40,000 FT)
 (CL) CR = 0.25

CONFIGURATION	Δ(OEW) EQUIV. DRAG		Δ OEW		Δ OEW NET EQUIV.		Δ(TOGW) NET	
	KG	(LB)	KG	(LB)	KG	(LB)	KG	(LB)
5-2-4 (10:1)	5896.7	(-13,000)	11884.12	(26,200)	5987.42	(13,200)	19413.75	(42,800)
5-2-4A	BASE		BASE		BASE		BASE	
5-2-5	-2721.55	(-6,000)	5715.26	(12,600)	2993.71	(6,600)	11974.84	(26,400)
5-2-5 (NON-STAGGER)	-3628.74	(-8,000)	5715.26	(12,600)	2086.52	(4,600)	8346.1	(18,400)
5-2-6	-1814.37	(-4,000)	7212.12	(15,900)	5397.75	(11,900)	21591	(47,600)
5-2-7A	-15875.73	(-35,000)	7275.62	(16,040)	-8600.11	(-18,960)	-34400.45	(-75,840)
5-2-7B	-16329.33	(-36,000)	7711.07	(17,000)	-8618.26	(-19,000)	-34473	(-76,000)
5-2-8A**	-18597.29	(-41,000)	8495.79	(18,730)	-10101.5	(-22,270)	-40406	(-89,080)**

SENSITIVITY RELATIONS:

$$\Delta C_D = .0001 \approx \Delta OEW = 454 \text{ KG (1000 LB)} \approx \Delta TOGW = 1814 \text{ KG (4000 LB)}$$

**DOES NOT INCLUDE THRUST AND SFC LOSSES = W/O SPLITTER $\frac{\text{THRUST}}{\text{THRUST}} = -2.7\%$
 WITH SPLITTER $\frac{\text{SFC}}{\text{SFC}} = .95\%$

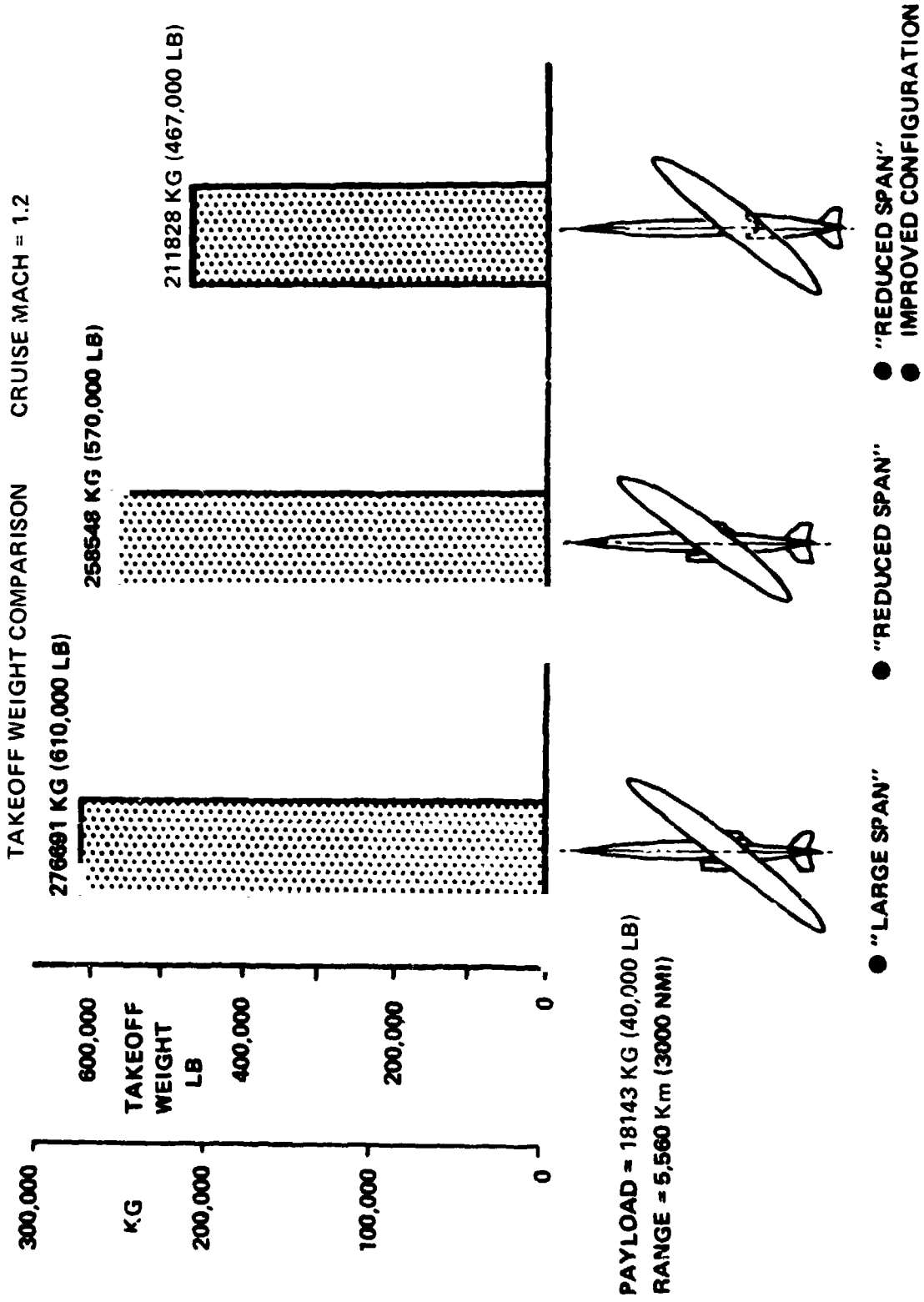


FIGURE 50.-IMPROVED CONFIGURATION RESULTS

The results of this study are shown in figure 52. The bypass ratio 4 configuration is significantly heavier than the bypass ratio 1 configuration having the same type of acoustic treatment.

Increasing the acoustic treatment on the bypass ratio 1 engine by addition of a jet suppressor indicates that even at equal noise levels the bypass ratio 1 configuration is a much lighter arrangement. The higher bypass ratio configuration suffers from the weight penalty associated with the rapid growth in engine size required to produce the same thrust at the cruise altitude as for a lower bypass ratio engine.

WING DEVELOPMENT STUDIES

A weight versus drag trade study was made to determine the optimum wing thickness/chord ratio for 8:1 and 6:1 for elliptic axes ratio wing planforms. The 8:1 elliptic axes ratio wing with a maximum unswept thickness/chord ratio of 12% was selected as the reference configuration. The variations of wing weight, OEW, and drag, C_D , with thickness ratio are shown in figure 53. These variations in weight and drag were combined and equated to equivalent takeoff weight changes, TOGW, by sensitivities derived for the single body yawed wing configuration 5-2-4.

These results show that the thickness/chord ratio of 12% is close to the optimum thickness/chord ratio for the 6:1 wing. The unconstrained optimum thickness/chord ratio for the 8:1 wing exceeds 12%. Because the increased possibility of buffet and flow separation for thick wings, the wing maximum thickness has been limited to 12% in this study.

During the configuration development studies on the single fuselage yawed wing configuration, the effect of reducing the wing elliptic axes ratio from 10:1 to 8:1 was investigated on the three-engine configuration 5-2-4. The elliptic axes ratio effect was further investigated on the aft integrated engine configuration 5-3 by reducing the elliptic axes ratio from 8:1 to 6:1. The combined results of these studies are shown in figure 54. The wing aspect ratio has a profound influence on the design takeoff gross weight. Furthermore, the elliptic axes ratio 8:1 wing (aspect ratio = 10.2) is very nearly optimum for the single body yawed wing configuration.

YAWED STABILIZER

The single fuselage yawed wing configuration developed in this system study incorporated a conventional swept planform horizontal stabilizer because of design simplicity. One of the possible arrangements for utilizing an oblique horizontal tail investigated for the three-engine configuration, 5-2-4, is shown in figure 55. The tail is located above the fuselage with the supporting structure inside the fuselage. The leading edge is aft of the vertical tail rear spar. In this way, neither the stabilizer nor the elevator will interfere with the body and fin during all modes of operation. Spanwise cutouts in the elevator are not likely to be required. Support of the stabilizer in the body will result in a

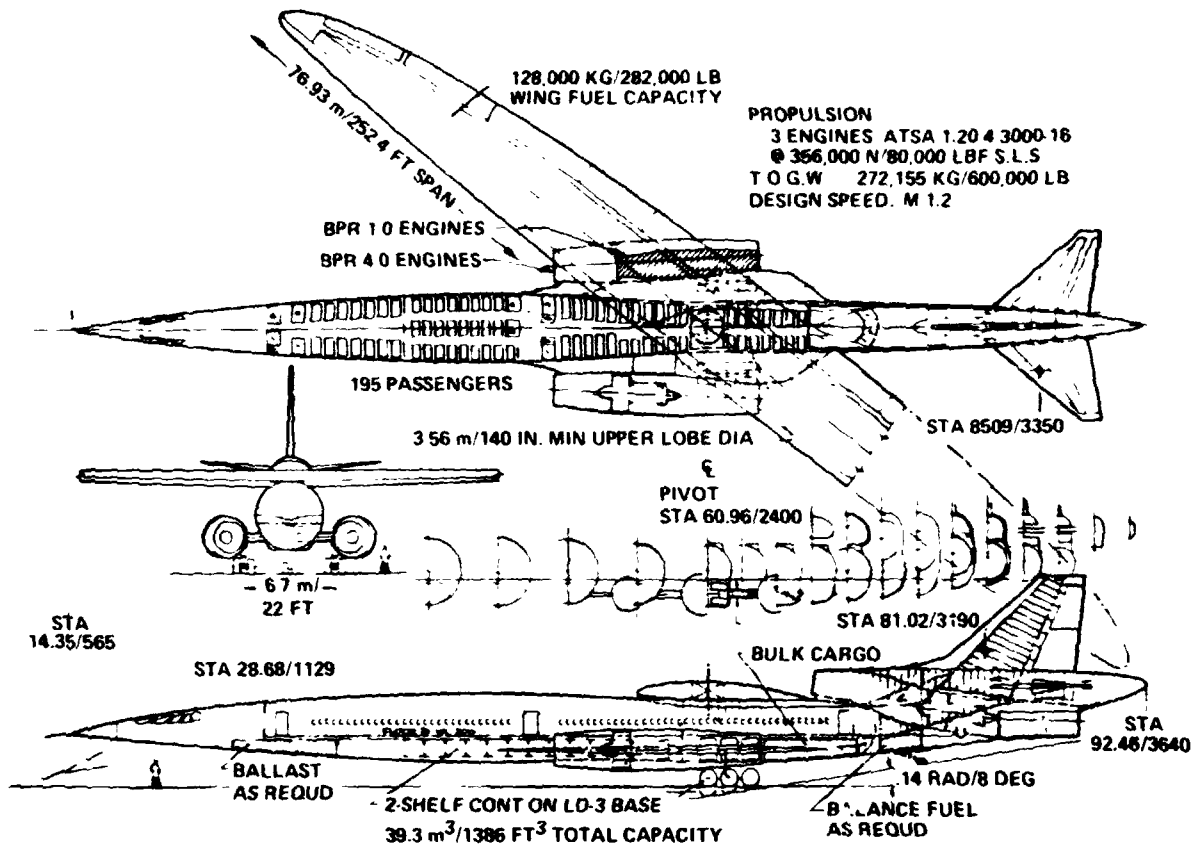


FIGURE 51.—GENERAL ARRANGEMENT, MODEL 5-2-3

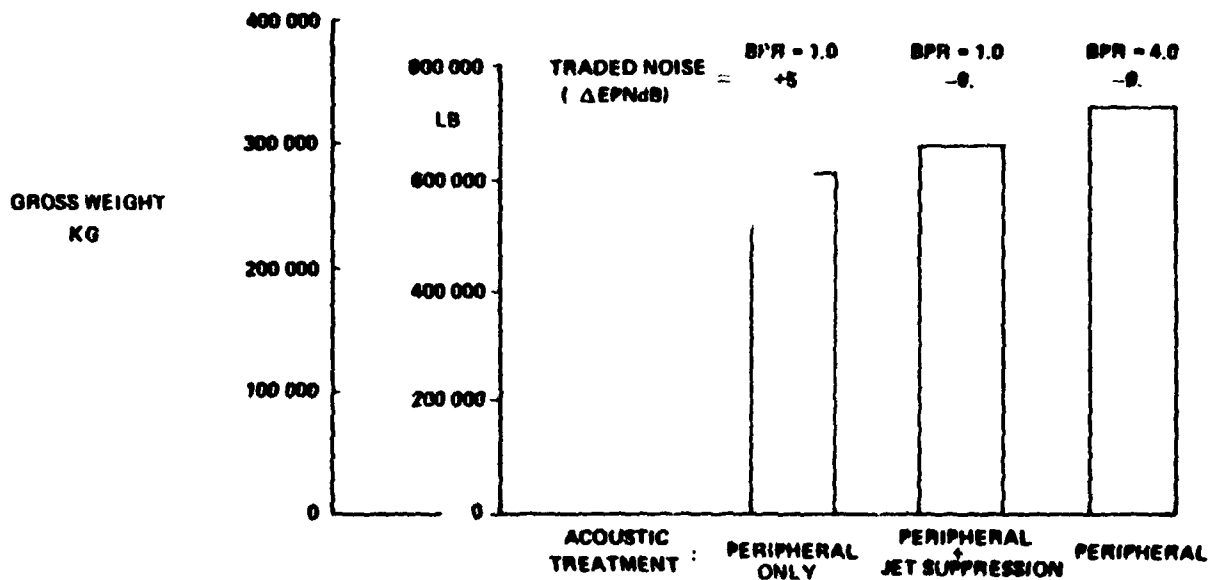


FIGURE 52.—BYPASS RATIO STUDY RESULTS

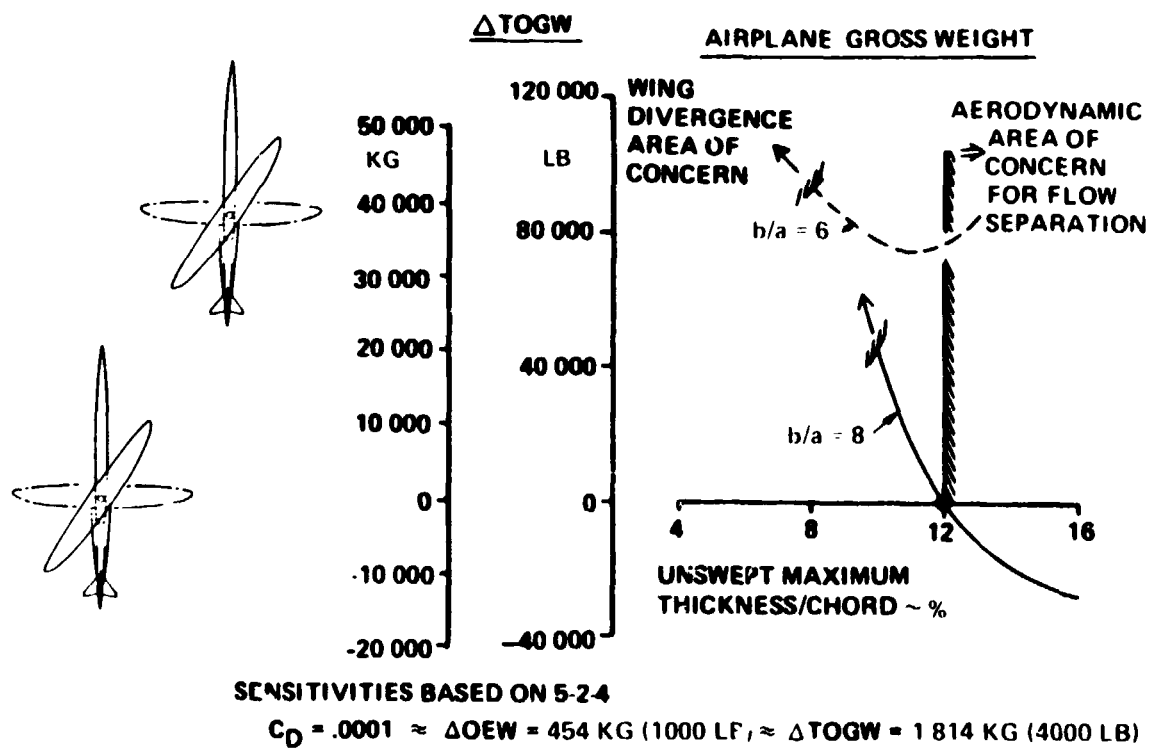
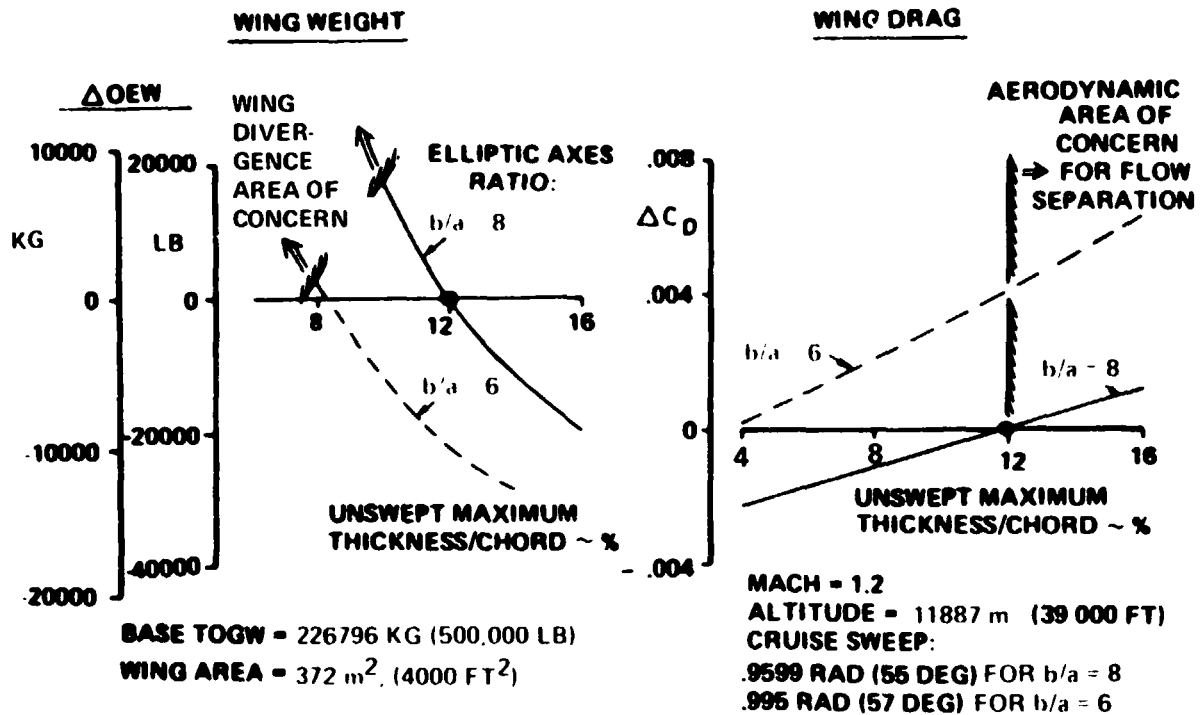


FIGURE 53.—YAWED WING THICKNESS STUDY RESULTS

PAYLOAD = 18143 KG (40 000 LB)

RANGE = 5560 Km (3000 NMI)

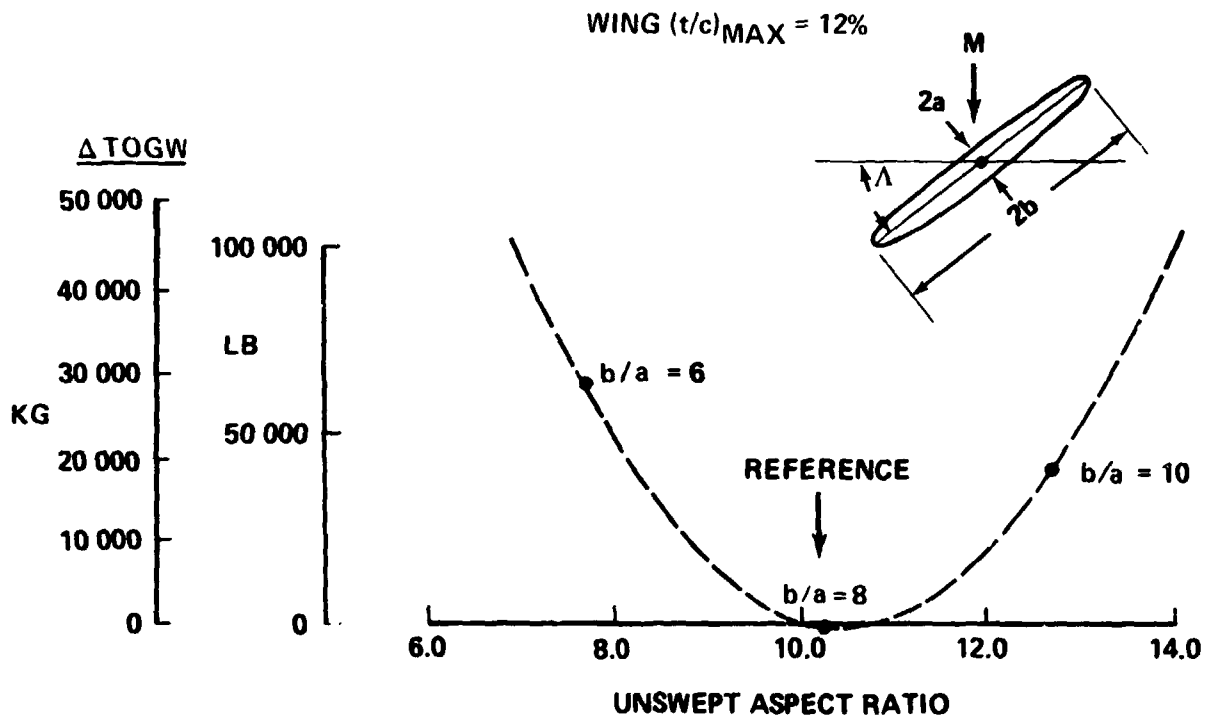
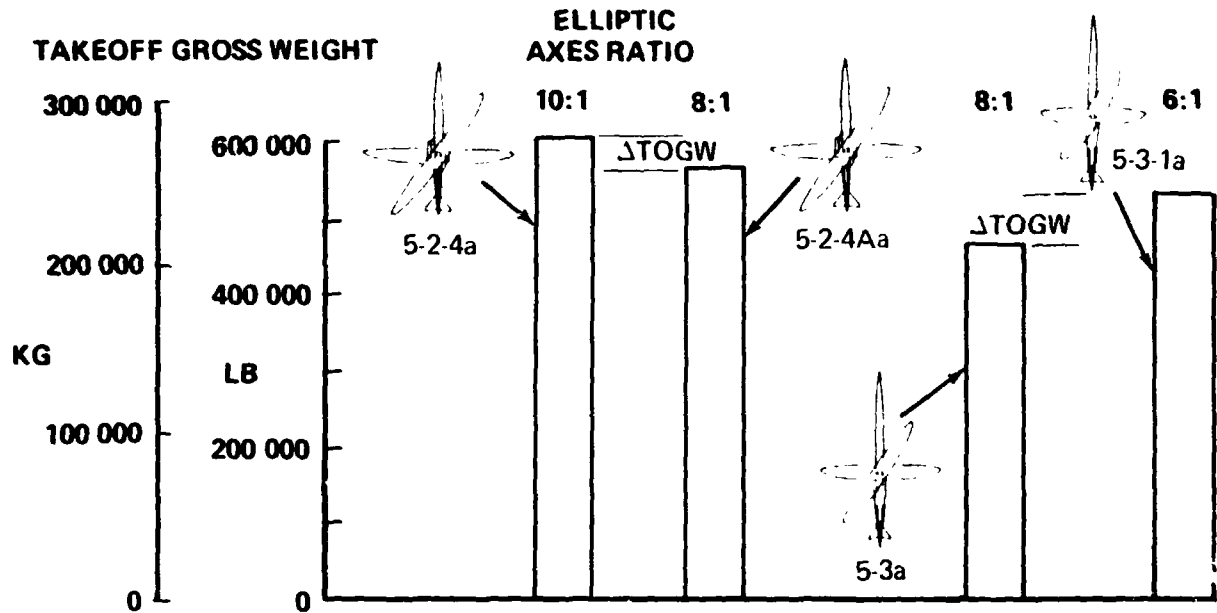


FIGURE 54.—WING ASPECT RATIO STUDY RESULTS

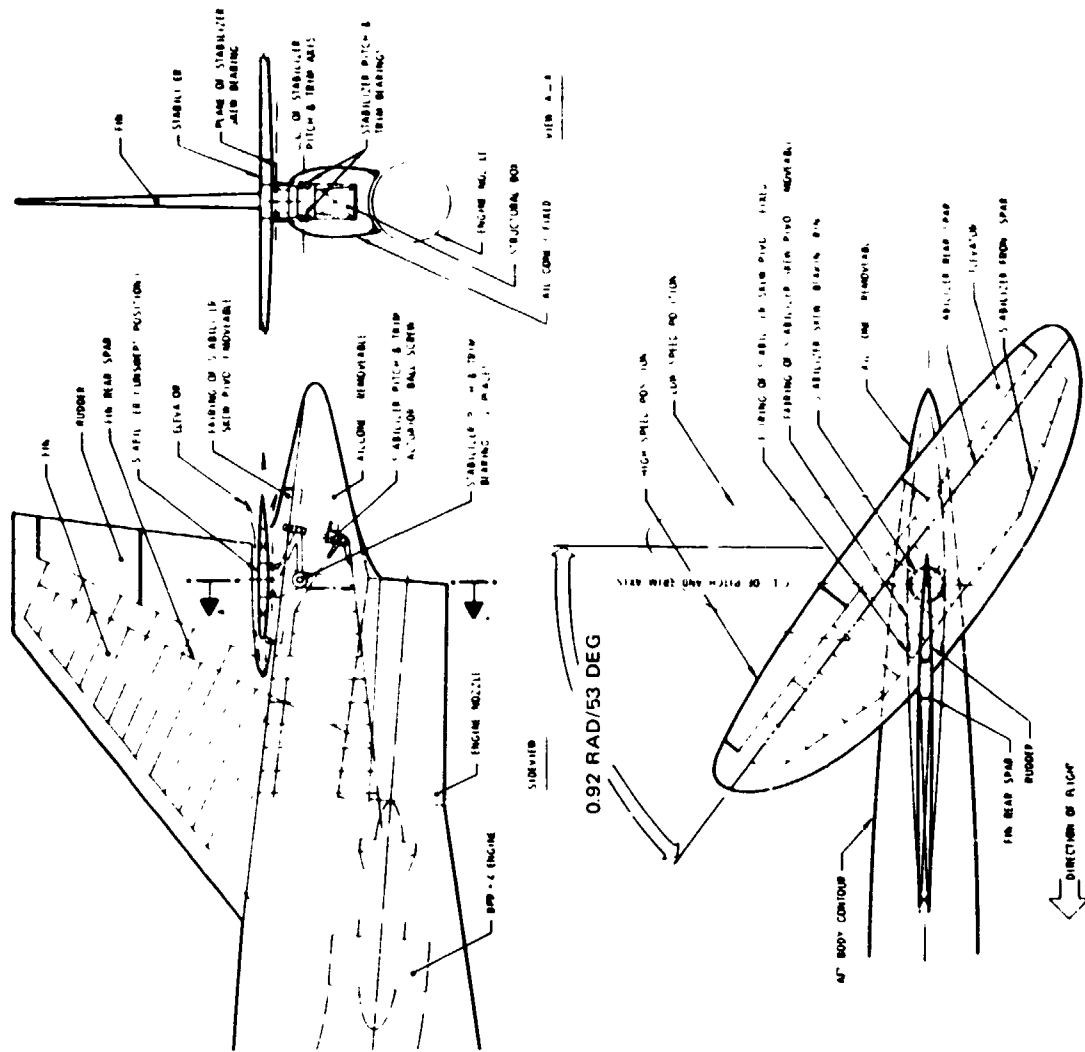


FIGURE 55.—YAWED STABILIZER

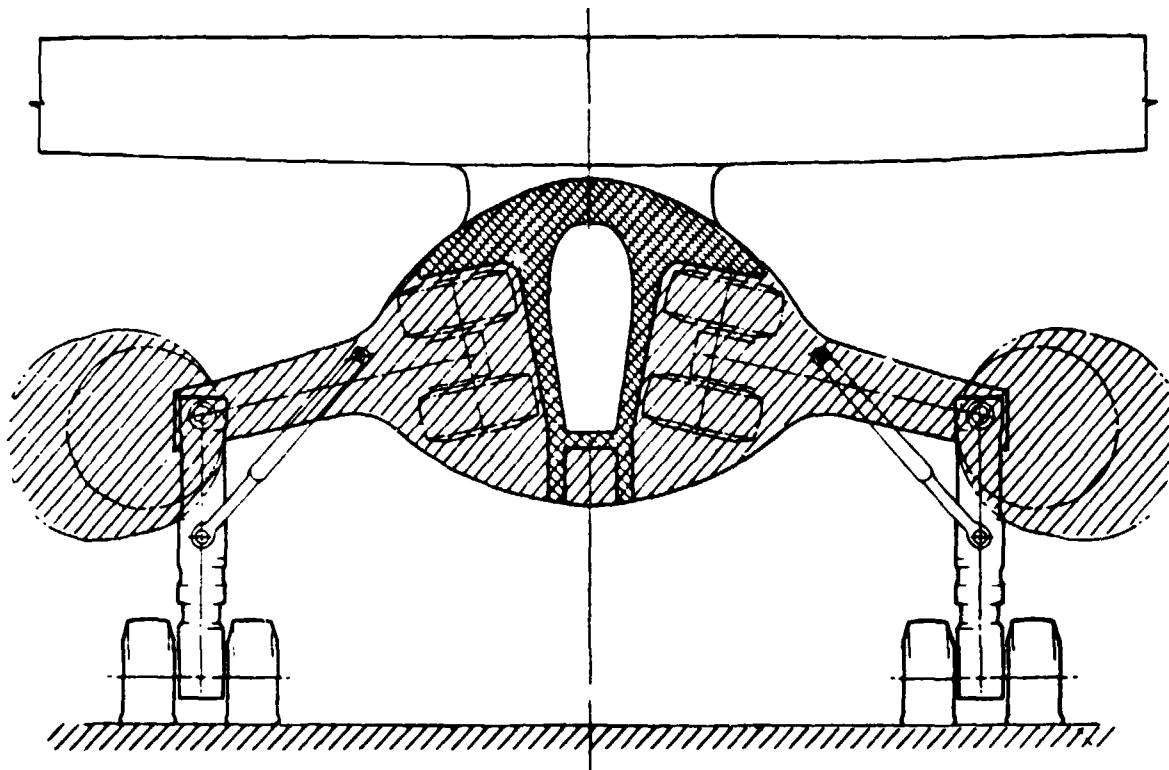
short and efficient structural load path. The use of a yawed stabilizer could offer potential performance benefits by a reduction in the aerodynamic drag, and a possible reduction in the required tail size. This would require a detailed study with supporting wind tunnel data.

BODY CROSS-SECTION STUDY

The minimization of body cross-sectional area is aerodynamically important on transonic and supersonic configurations. A blended strut-body arrangement was examined as a possible approach to reduce the body area on the three-engine configuration 5-2-4 (fig. 56).

The passenger cabin for this arrangement was locally interrupted for gear storage. The forward and aft passenger compartments were connected by a narrow corridor. The reduction in fuselage depth eliminated the underfloor cargo compartment. Fuselage length was therefore added for storage of passenger baggage on the upper floor. Further lengthening of the fuselage was necessary in order to make up for the passenger floor area that was lost for landing gear storage.

The modification reduced the fuselage cross-sectional area by more than 2.78 m^2 (30 ft^2). This combined with the increase in length reduced the supersonic wave drag of the fuselage substantially. The structural design of the fuselage however, would be compromised considerably. The effect on passenger appeal of a partially windowless fuselage would have to be examined. The results of this study are summarized in figure 56.



CROSS SECTION COMPARISON

OLD (FUSELAGE + STRUTS)	16.0 m ² (172 FT ²)
NEW (FUSELAGE + STRUTS)	12.5 m ² (135 FT ²)
Δ AREA	-3.5 m ² (-37 FT ²)
Δℓ BODY	+7.6 m (25 FT)
Δ C _D WAVE	-.0012
	15-20 % OF C _D WAVE _{TOTAL}

CONCERNS

- FUSELAGE STIFFNESS (+ WEIGHT)
- WING PIVOT SUPPORT (+ WEIGHT)
- NONCIRCULAR PRESSURE SHELL (+ WEIGHT)
- ADDED BODY LENGTH (+ WEIGHT)
- STRUCTURAL INTEGRATION (ENGINE & LANDING GEAR) (+ WEIGHT)
- LOSS OF WINDOWS, SERVICES (PASSENGER APPEAL)

FIGURE 56.—BODY CROSS-SECTION STUDY

REMAINING PAGE BLANK NOT FILMED

CONFIGURATION ANALYSIS AND METHODS

This section contains a description of the design and analysis methods that have been used in the study. The technology levels assumed in the development of the configurations are identified. The results of specialized studies that impact the development of the configurations have also been included.

AERODYNAMICS

The aerodynamics tasks included the following:

- Aerodynamic design integration of the five basic concepts for efficient flight.
- Development of the aerodynamic characteristics of the configurations by specialized tradeoff studies.
- Integration of a compatible high lift system for each concept.
- Evaluations of the aerodynamic characteristics of all concepts to provide the necessary resizing data for the performance calculations. These included both flaps up cruise configurations as well as the flaps down takeoff and landing evaluations.

The theoretical methods used in the aerodynamic design and analyses studies were modified to permit application to the yawed wing configurations.

Aerodynamic design characteristics were developed for each of the airplane concepts. The high speed cruise and the low speed landing and takeoff aerodynamic data were calculated for the study configurations. Low speed aerodynamic calculations were also made for the single fuselage yawed wing configuration to compare the takeoff and landing performance with and without rotation.

Parametric and off-design aerodynamic data were developed for the airplane sizing, trade, and sensitivity studies.

Aerodynamic studies were also undertaken to obtain a better understanding of wing-nacelle interference and body-nacelle interference at transonic speeds.

Aerodynamic Design Approach

The aerodynamic design approach was to design for minimum cruise drag within practical design constraints. These practical constraints which impact such things as wing thickness distribution, wing aspect ratio, airfoil shapes, and nacelle location are necessary to provide a balance between aerodynamic, structural, and configuration arrangement requirements. The aerodynamic characteristics for all of the concepts were developed by similar procedures as summarized in table 13.

TABLE 13.—DESIGN SELECTION PROCEDURE

<p>WING</p> <p>PLANFORM</p> <p>THICKNESS</p> <p>CAMBER & TWIST</p>	<p>EXPLOIT AERODYNAMIC BENEFITS WITHIN STRUCTURAL CONSTRAINTS</p> <p>WEIGHT VS DRAG TRADE STUDIES</p> <p>DEVELOPED BY LINEAR THEORY</p>
<p>BODY</p> <p>AREA DISTRIBUTION</p>	<p>AREA RULED TO MINIMIZE CRUISE DRAG</p>
<p>NACELLES</p> <p>SHAPE</p> <p>LOCATIONS</p>	<p>DICTATED BY ENGINE SIZE, AERODYNAMIC, WEIGHT CONSIDERATIONS AND CONFIGURATION ARRANGEMENT</p> <p>CONFIGURATION ARRANGEMENT AND AERODYNAMIC CONSIDERATIONS</p>
<p>TAILS</p> <p>PLANFORM</p> <p>THICKNESS</p>	<p>SET BY FLIGHT CONTROL REQUIREMENTS</p> <p>WEIGHT VS DRAG TRADE STUDIES</p>

Wing Definition

A realistically optimized wing planform requires a delicate balance between the often conflicting demands imposed by aerodynamic, control, configuration, and weight considerations. Previous contractor transonic/supersonic aerodynamic/weight trade studies were reviewed to aid in the selection of the wing planform and thickness characteristics for the fixed swept wing, variable sweep wing, and delta wing configurations.

The B2707-300 SST wing planform and thickness distribution were used for the delta wing configuration (model 3-2). Previous aerodynamic studies had shown that this was close to the optimum transonic planform for a low aspect ratio delta wing.

The outboard leading edge sweep for the variable sweep planform of model 2-2 is .96 rad (55°). This is close to the optimum sweep for a moderate aspect ratio planform. The outboard leading edge sweep for the fixed wing of model 1-2 is .87 rad (50°). This is less than the optimum sweep but provides a greater aspect ratio (more span) for the low speed conditions. Both the variable sweep wing and fixed swept wing have supersonic trailing edges to reduce the structural span lengths. The inboard trailing edges were extended in the streamwise direction on both planforms out to approximately 40% semispan. This provides additional wing depth and volume without increasing the thickness/chord ratios which influence the wing wave drag. Increasing the inboard leading edge sweep is aerodynamically beneficial for the fixed wing and variable sweep wing configuration. This leading edge "strake" helps the configuration arrangements by providing additional depth for the front portion of the landing gear box. Leading edge strakes, however, can produce severe wing pitch up. A review of B2707-300 SST wind tunnel data established that a strake comparable with the B2707-300 strake would be acceptable. The spanwise thickness distributions were derived from the results of previous trade studies.

The yawed wing planform that has been studied and tested at NASA-Ames (ref. 5) was initially selected for the yawed wing concepts. The elliptic axes ratio of the planform was subsequently reduced from 10:1 to 8:1 as a result of detailed weight vs drag trade studies. Since the design objective for all of the wings was to minimize cruise drag, a study was made to determine the optimum cruise sweep angle. An aerodynamic parametric analysis and optimization program that combines the analytic wave drag and drag-due-to-lift for a yawed elliptic (refs. 5, 6, and 7), and the skin friction method of reference 8 was used to calculate the isolated wing lift/drag ratios. The design cruise sweep angle was selected as the angle for maximum isolated-wing lift/drag ratio. Typical results are shown in figure 57. The sweep angle which maximizes the wing lift/drag ratio depends primarily on the elliptic axes ratio and wing thickness and provides a normal Mach number that is below the critical Mach number of current technology airfoil designs. As the design Mach number is increased, the optimum wing sweep increases to maintain approximately the same normal Mach number.

An elliptic spanwise variation of thickness was selected for the yawed wing. This is the thickness variation for minimum wave drag (ref. 6). The maximum unswept thickness to chord ratio was limited to 12% to allow the wing to achieve its design potential without encountering flow separation. The selected spanwise variation of thickness, as shown in figure 58, has significantly less wave drag than the type of thickness distribution that has

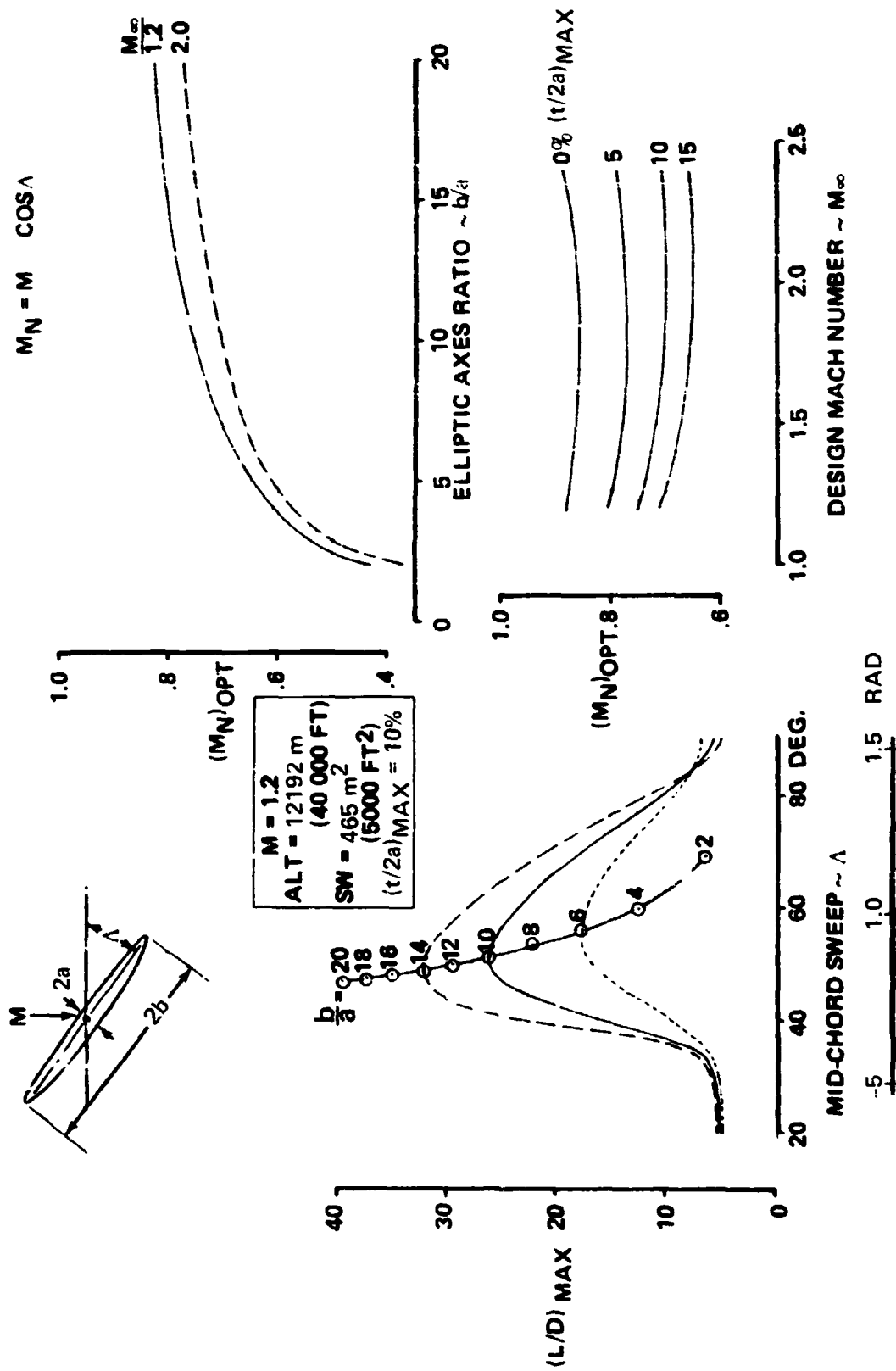


FIGURE 57.—YAWED WING CRUISE SWEEP SELECTION

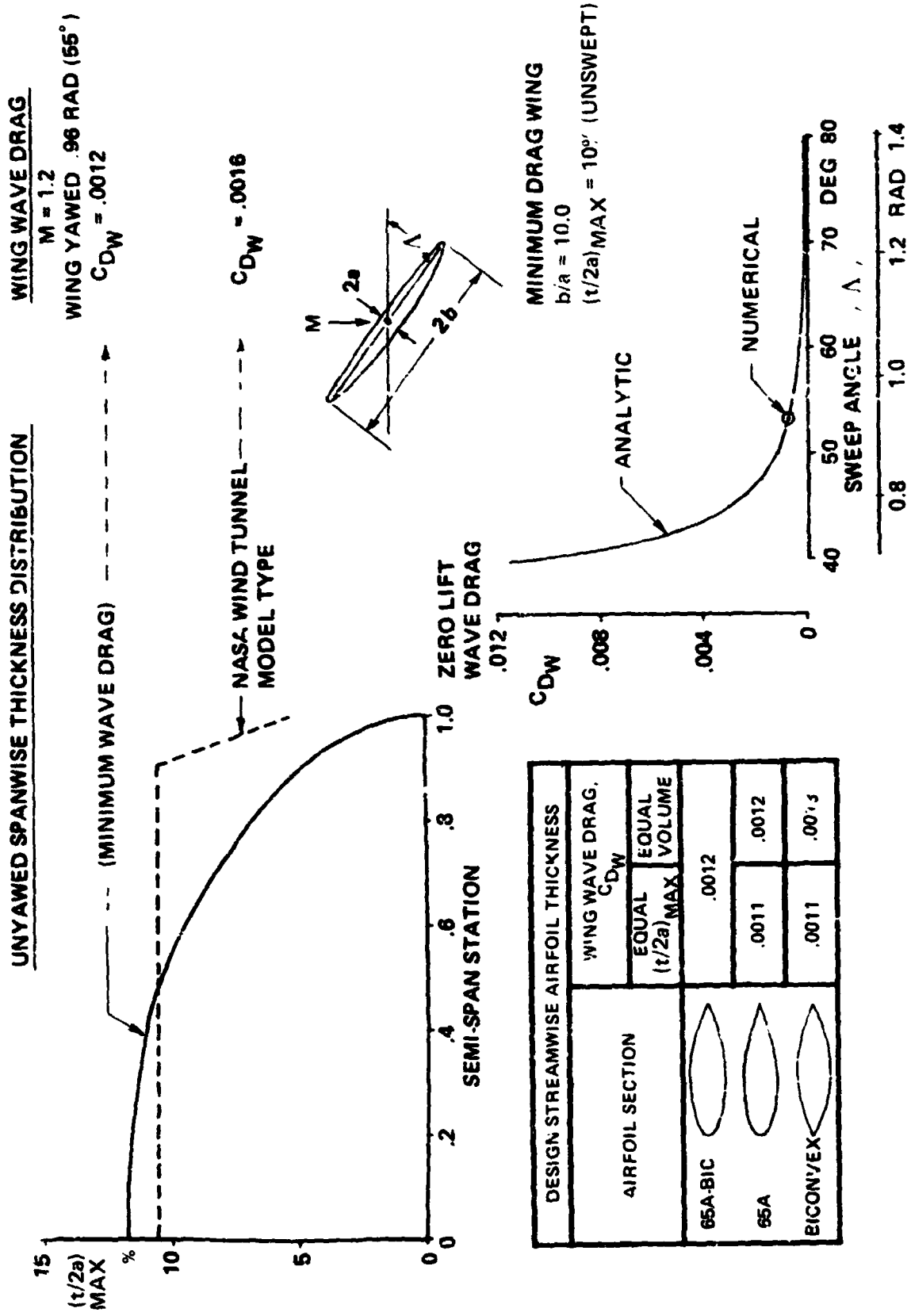


FIGURE 58. — YAWED WING AIRFOIL AND THICKNESS DISTRIBUTION

been used on the earlier NASA wind tunnel models. An airfoil shape was selected to provide the necessary spar depths with a generous leading edge radius. This same airfoil was used for all of the planforms.

The camber and twist distributions for all configurations were developed by the five-step procedure shown in figure 57 using linear aerodynamic theory.

The twist distributions for the conventional planforms, as shown in figure 60, have severe variations in the area of the body, near the strake junction and near the tip region. Modifications in the twist distributions were necessary to remove these discontinuities introduced by the linearized theory. As a result of the modifications, these planforms cannot achieve the theoretical minimum drag due to lift.

The smooth design camber and twist distribution for the yawed wing should be able to achieve nearly the minimum drag due to lift. The main area of concern is the possibility of trailing edge separation induced by the pressure gradients near the trailing edge.

The numerical calculation procedure for the yawed wing was checked by comparisons with the exact theory minimum drag due to lift (ref. 7). An example of this comparison is shown in the upper right corner of figure 60.

Body Design

The bodies for all of the configurations were area ruled to minimize the volume wave drag by the use of the transfer rule described in references 9 and 10. The nacelles on the low-wing conventional planform configurations were shielded from the body pressure field by the wing. The bodies for these configurations were therefore area ruled only in the presence of the wing and tails (fig. 61).

The nacelles on the yawed wing configurations are strongly influenced by the body pressure field. The body area ruling for these configurations considered the wing, tails, and nacelles. The automated numerical procedures used for area ruling the conventional planform is shown in figure 62. This numerical procedure was adapted for the yawed wing applications as shown in figure 63. The wing area distribution was calculated as one-half the sum of the area distributions of an equivalent swept forward wing and an equivalent aft swept wing. The wing area distribution was then converted to an equivalent-area center nacelle and then input with the other airplane components into the standard program.

Nacelle Considerations

The nacelle shape, size, location, and operating conditions all influence the nacelle interference with the other configuration components. The nature of the aerodynamic interference is strongly affected by the aircraft configuration arrangement characteristics. The dominant interference effect is between the nacelles and the wing on the delta wing, fixed wing, and variable sweep configurations. The dominant interference effect is between the nacelles and body on the yawed-wing configurations.

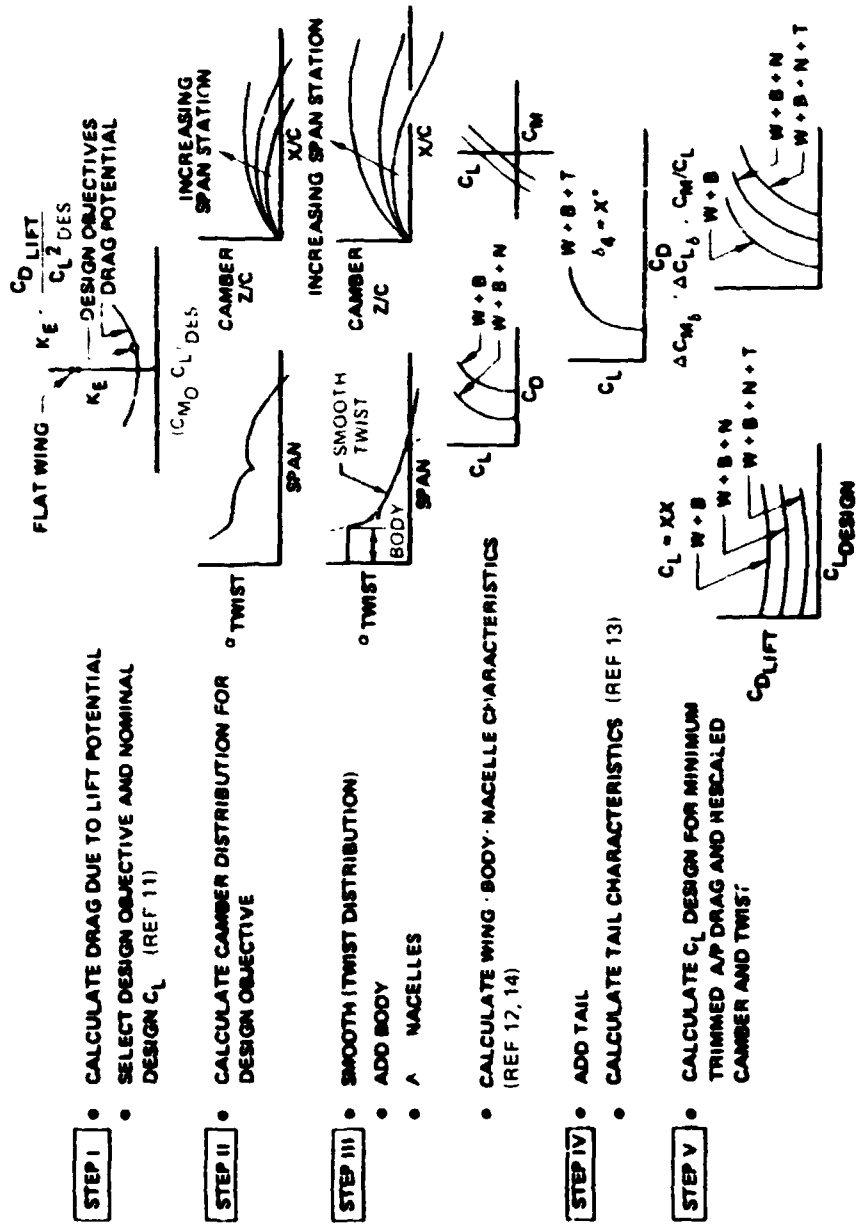


FIGURE 59.—CAMBER AND TWIST DESIGN AND ANALYSIS PROCEDURE

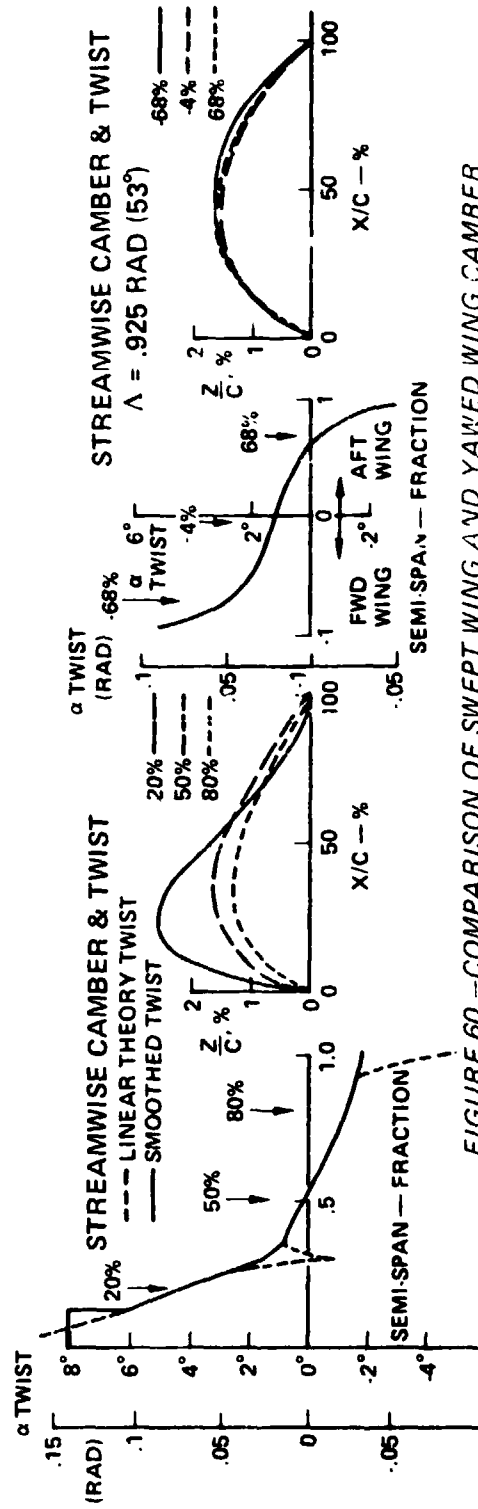
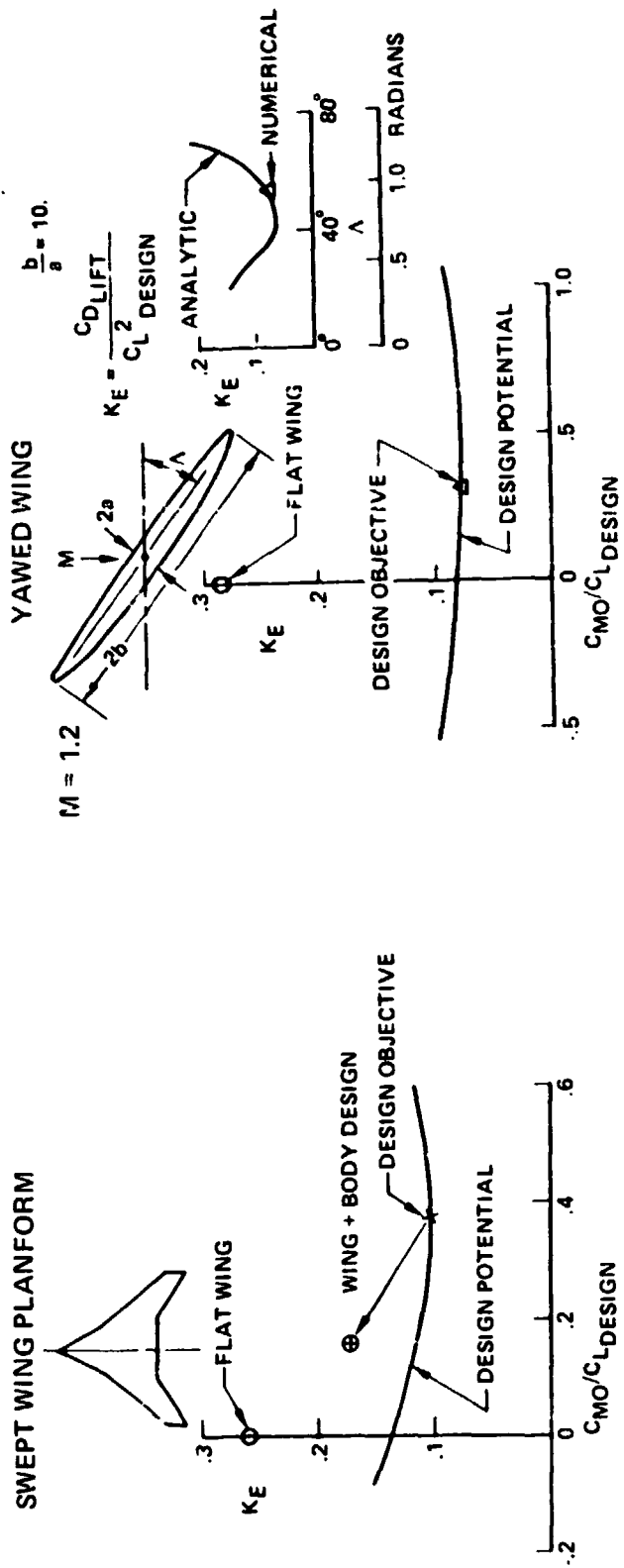


FIGURE 60.—COMPARISON OF SWEPT WING AND YAWED WING CAMBER AND TWIST DISTRIBUTIONS

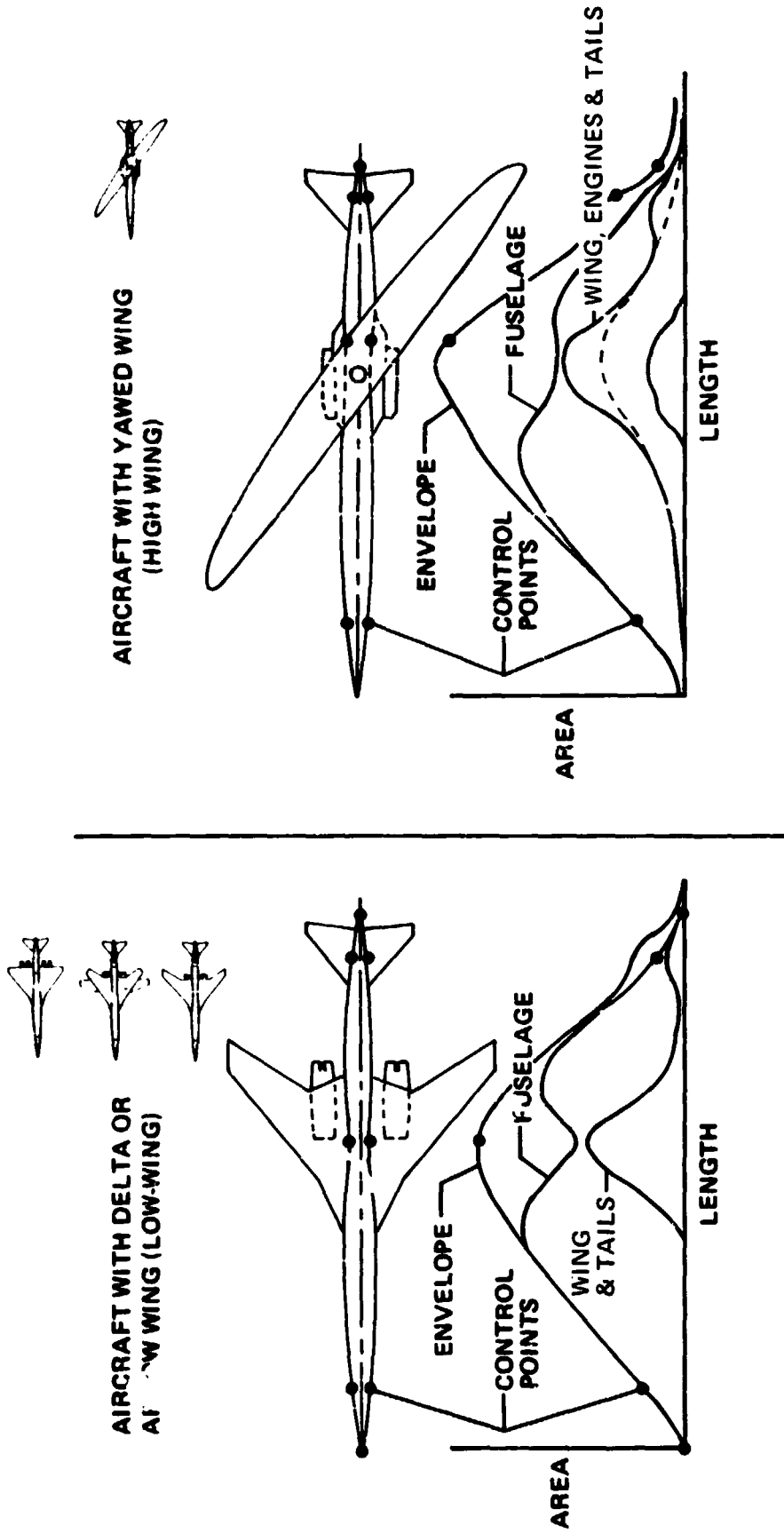


FIGURE 61.—AREA DISTRIBUTION DEVELOPMENT (MACH 1.2)

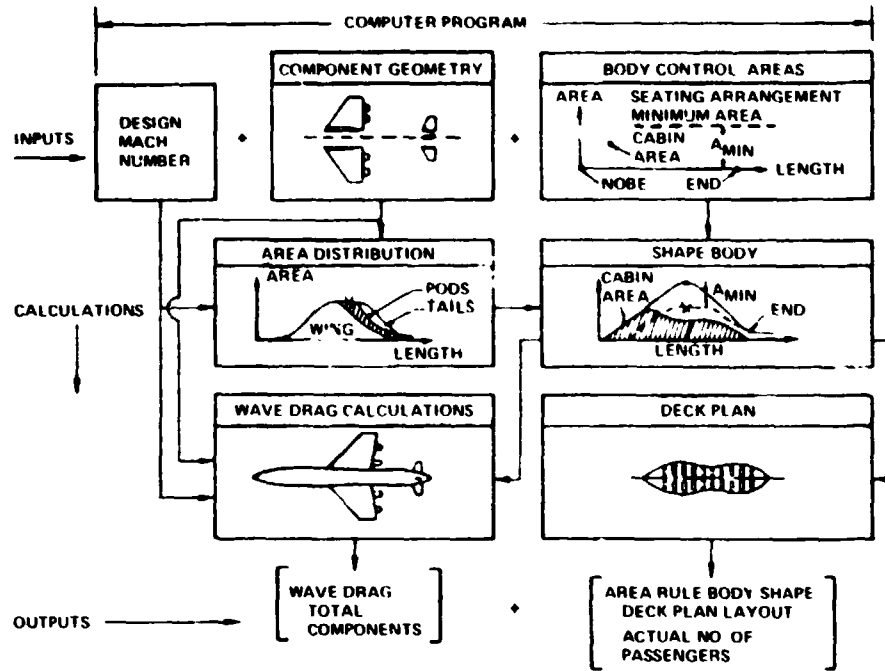


FIGURE 62.—CONVENTIONAL PLANFORM AREA RULE PROCEDURE

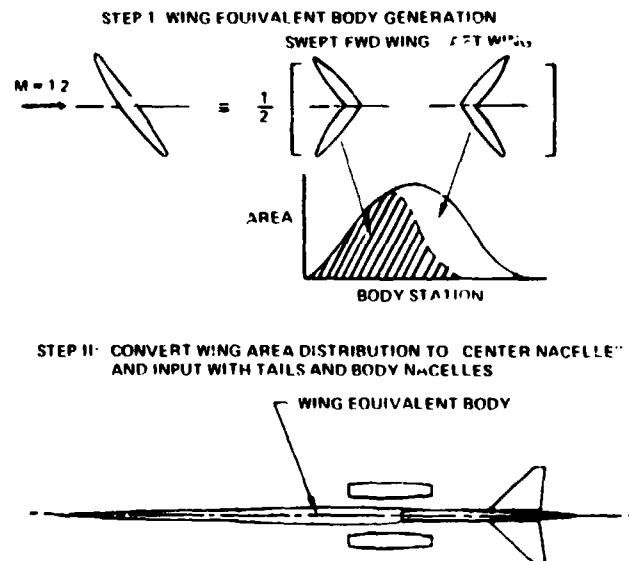


FIGURE 63.—YAWED WING CONFIGURATION AREA RULE PROCEDURE

The analyses of the early baseline configurations indicated that the nacelle installed drag was a major drag item on all of the configurations. Studies were therefore initiated to gain a better understanding of transonic installed nacelle drag. The results of these studies are discussed in the nacelle-airplane integration studies section (page 114).

The linear aerodynamic theory numerical methods (refs. 9, 10, 11, 14, and 15) that have been used for the aerodynamic design of the study configurations are summarized in table 14.

Figures 64, 65, and 66 illustrate the aerodynamic configuration definitions for the fixed wing, delta wing, and single-fuselage yawed wing configurations.

Aerodynamic Analysis Approach

The drag calculation methods (refs. 8 and 12 through 15) that have been used for all of the configurations are summarized in table 15. These methods which were used in the contractor SST development studies have been well substantiated for conventional aircraft configurations by numerous test vs theory comparisons such as those of figure 67. Although the theories are equally applicable for configurations without lateral symmetry, modifications to the numerical methods were necessary for the yawed wing analyses.

The trim drag for any configuration depends on a number of things that include the required tail trim angle, the wing drag due to lift, the downwash in the region of the tail, and the lift coefficient. The required tail angle is determined by the required moment to be trimmed, the tail trimming effectiveness, the center of gravity location, and the elastics of the airplane.

The minimum theoretical trim drag as shown in figure 68 has been used throughout this study for all airplanes. This was necessary since the pitching moment characteristics and the tail trim capability must be determined by test data, and a detailed aeroelastic analysis. This is an area where further study is necessary to develop the trim drag characteristics of each configuration.

Baseline Configuration Evaluations

The cruise drag polars, wetted areas, and component drags for each of the five uncycled baseline configuration concepts are shown in tables 16 through 20. A similar cruise drag description for the mission sized configuration 5-3a as developed by the drag scalars is shown in the performance section (table 5).

A cruise drag comparison of the various uncycled baseline configurations is shown in figure 69. The friction drag is nearly identical for all configurations. The double body configuration friction drag increase is the result of the increased wetted area of the two bodies. The effect of the higher aspect ratio in reducing the drag due to lift is quite evident for the yawed wing configurations. A major difference in drag for the configurations was found to be the wave drag due to volume.

TABLE 14.—AERODYNAMIC DESIGN METHODS

Aerodynamic design item	Method	Reference
Camber and twist distribution	Middleton-Carlson Mach box	11
Body contouring	Transfer rule	9 10
Nacelle design and location <ul style="list-style-type: none"> ● Thickness interference ● Lift interference 	<ul style="list-style-type: none"> ● Area rule program ● Modified Middleton-Carlson 	15 14

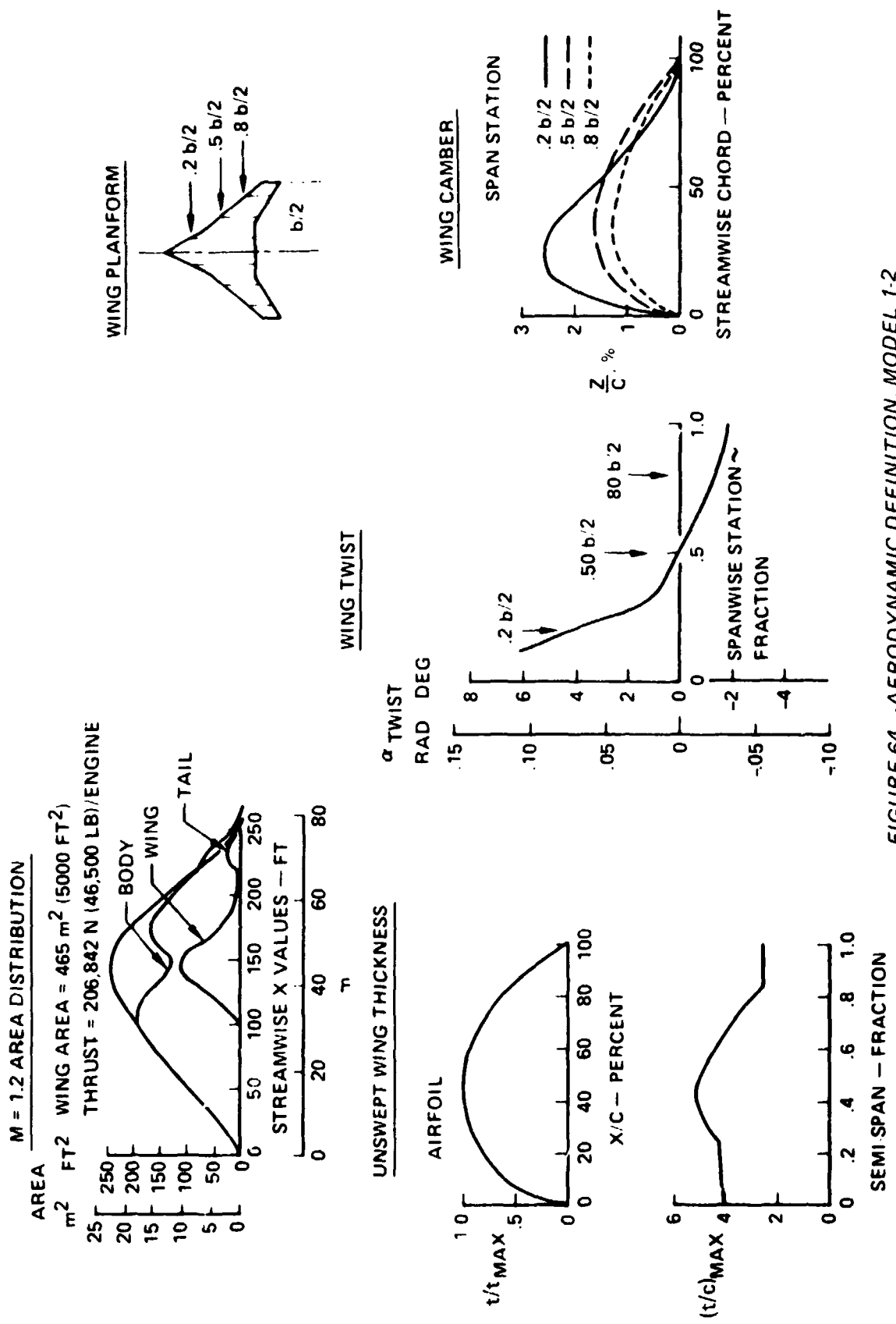


FIGURE 64.—AERODYNAMIC DEFINITION, MODEL 1-2

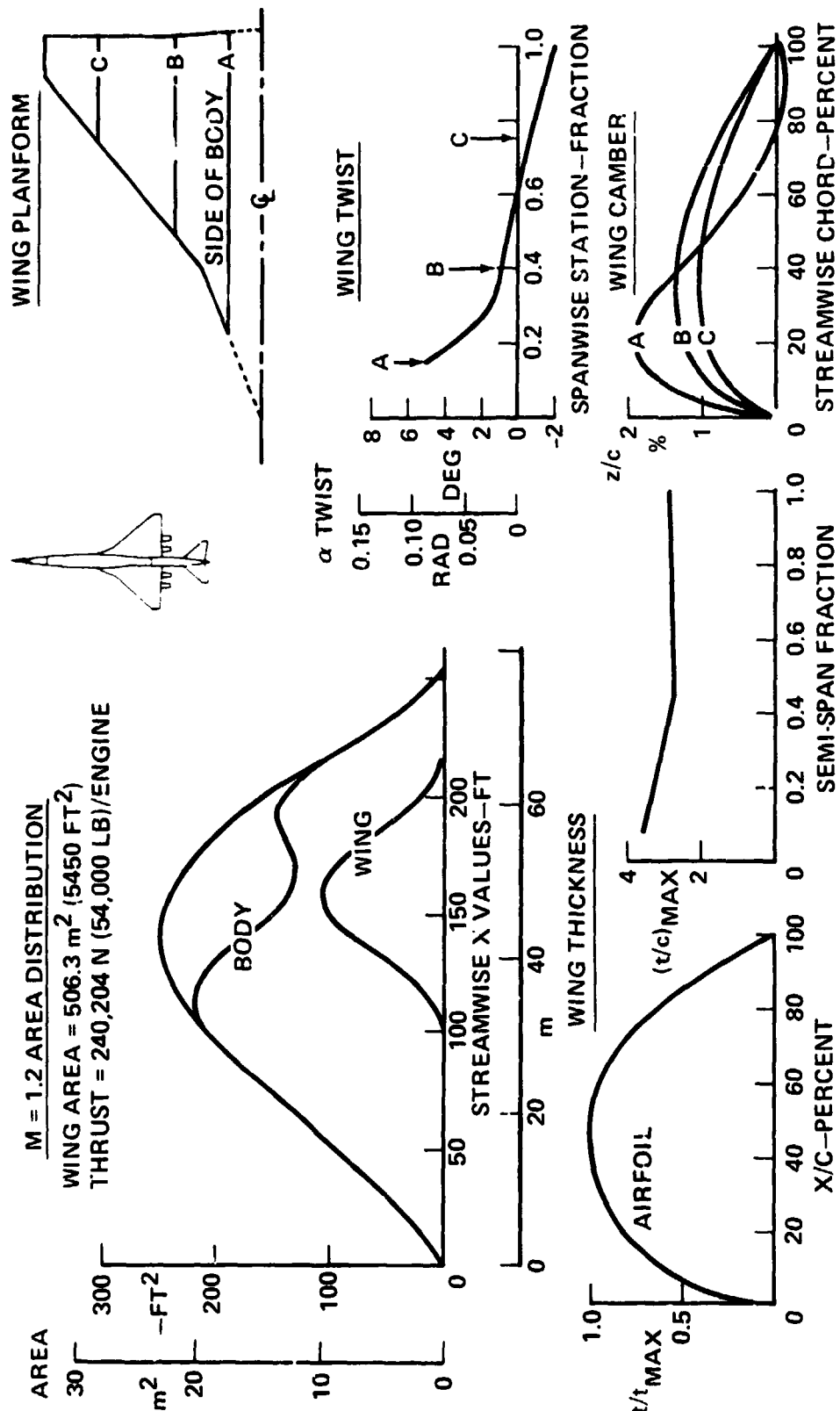


FIGURE 65.--AERODYNAMIC DEFINITION, MODEL 3-2

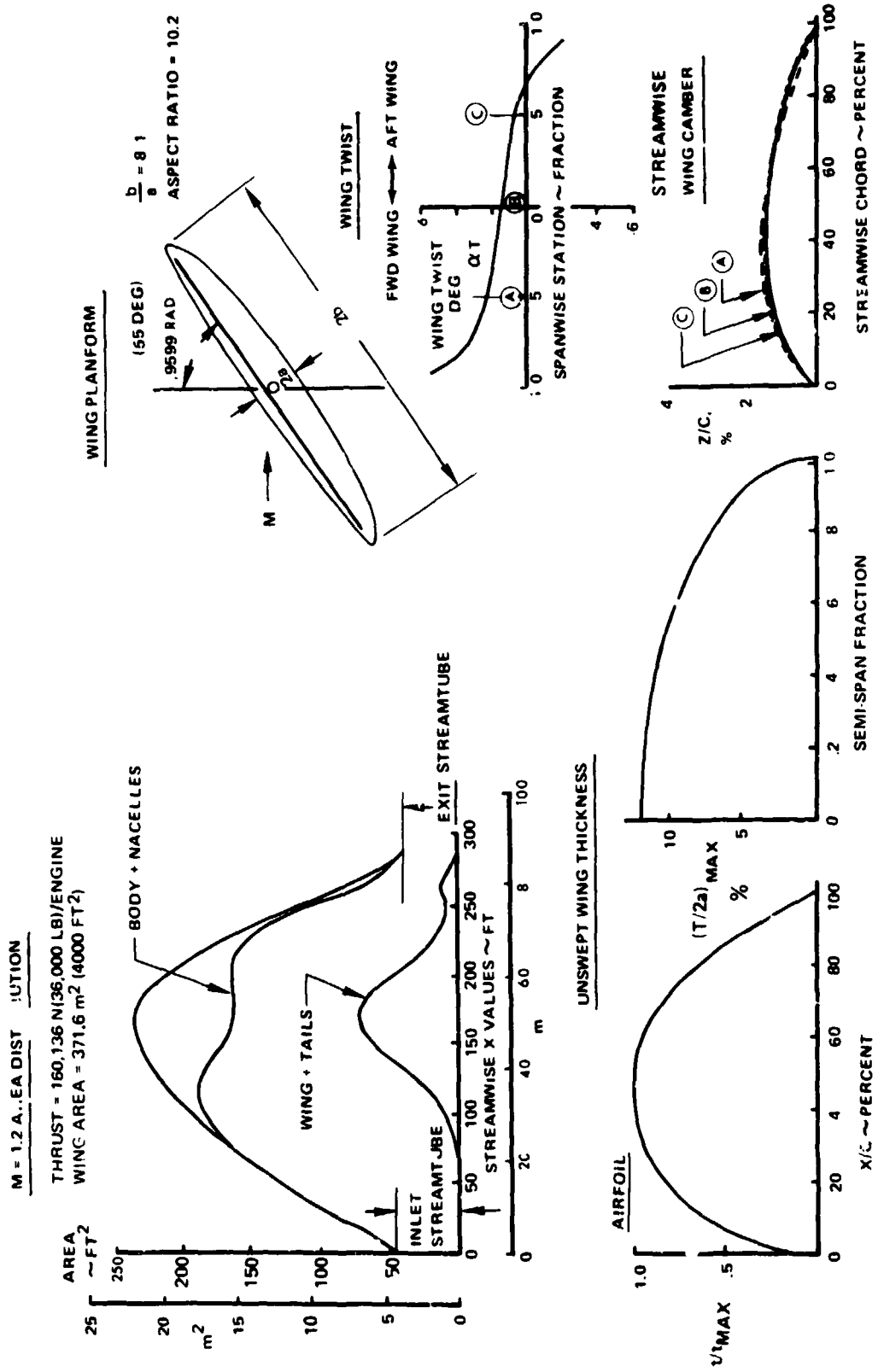
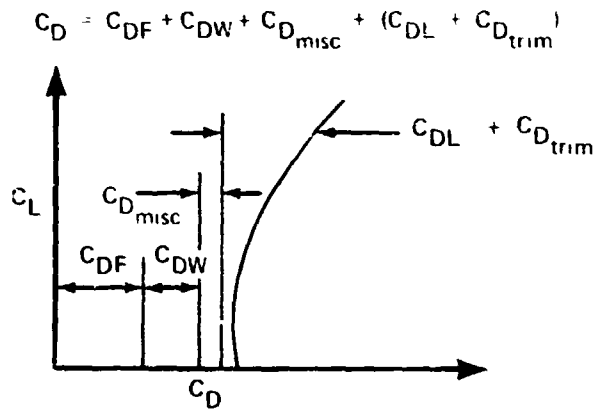


FIGURE 66.—MODEL 5-3 AERODYNAMIC DEFINITION

TABLE 15.—CRUISE DRAG ESTIMATION METHODS



Drag component	Method	Reference
C_{DF} friction drag	<ul style="list-style-type: none"> ● Sommer and Short T* method 	8
C_{DW} wave drag	<ul style="list-style-type: none"> ● Supersonic area rule ● Linear theory wing and body thickness pressures 	15
C_{DL} drag due to lift	<ul style="list-style-type: none"> ● Middleton-Carlson Mach box 	12, 14
$C_{D_{trim}}$ trim drag	<ul style="list-style-type: none"> ● Middleton-Carlson Mach box 	13
$C_{D_{misc}}$ miscellaneous drag <ul style="list-style-type: none"> ● Roughness drag ● Air conditioning ● Propulsion system ● Struts 	<ul style="list-style-type: none"> ● SST procedures ● Two-dimensional transonic similarity 	

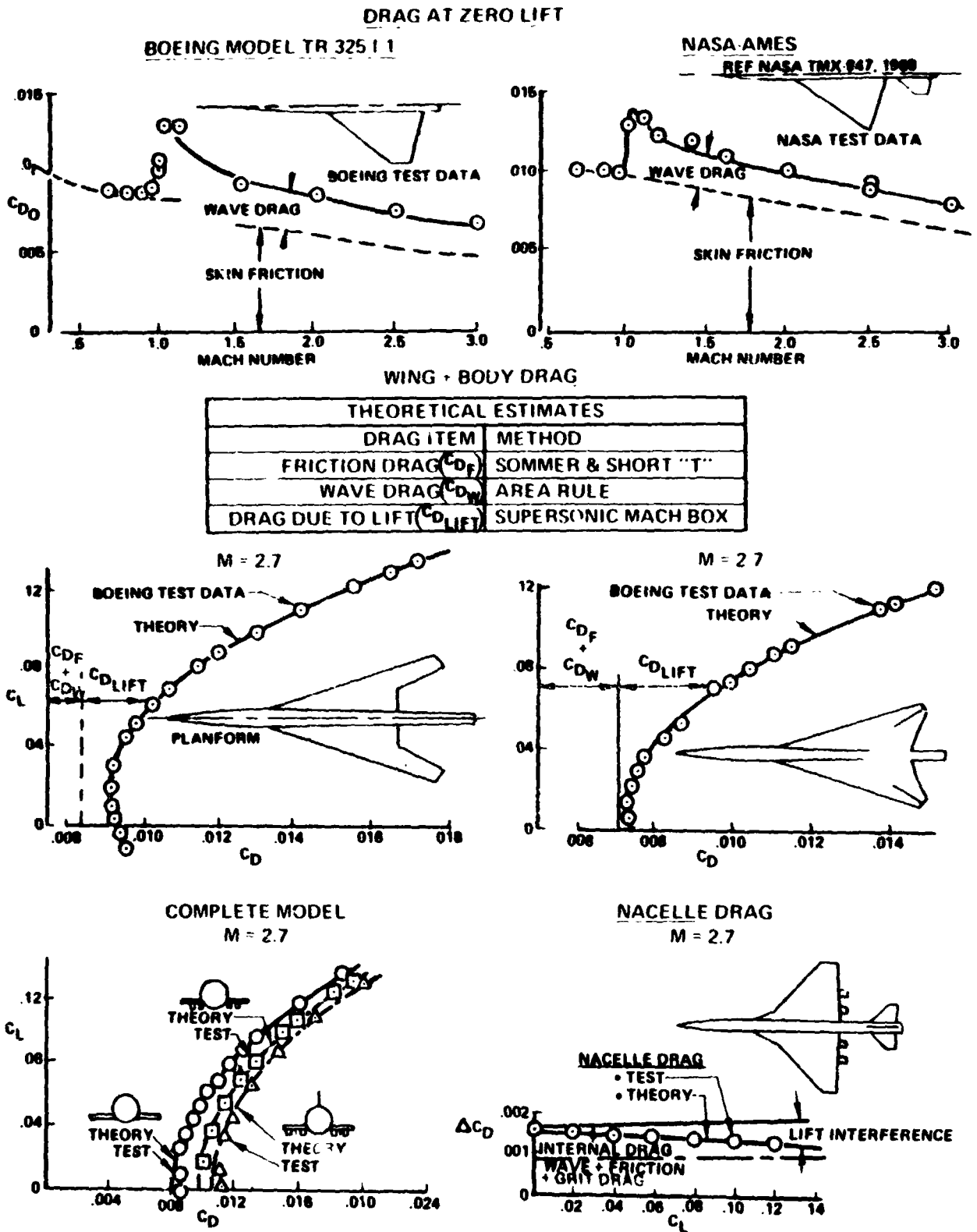


FIGURE 67.—TYPICAL TEST-THEORY COMPARISONS

$$\text{TRIM DRAG} = f^N (\delta H_{\text{TAIL}}, \epsilon, K_E, C_L, \text{ETC})$$

$$\delta H_{\text{TAIL}} = f^N (C_{M0}, \frac{\partial C_M}{\partial C_L}, \text{C.G.}, \text{ELASTICS}, \frac{\Delta C_{MH}}{\Delta \delta_H}, \text{ETC})$$

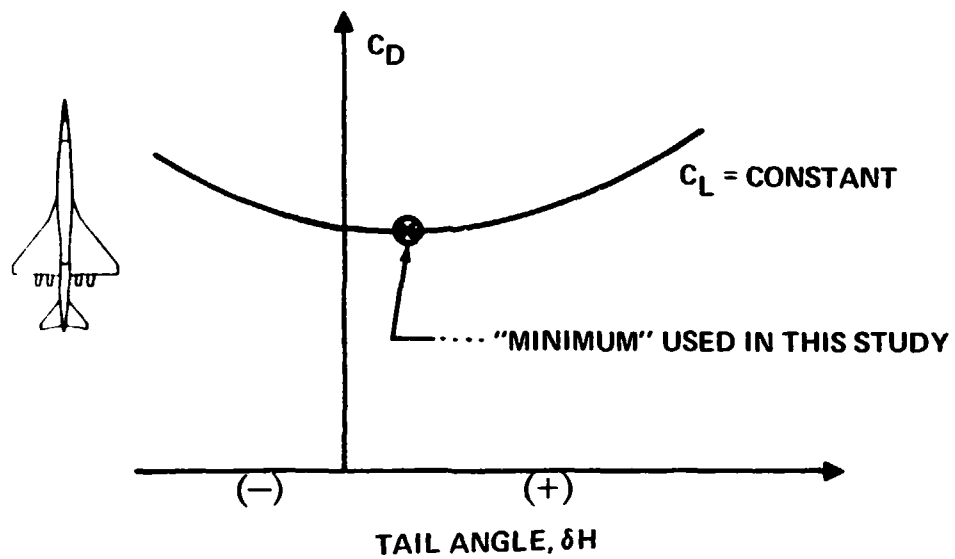
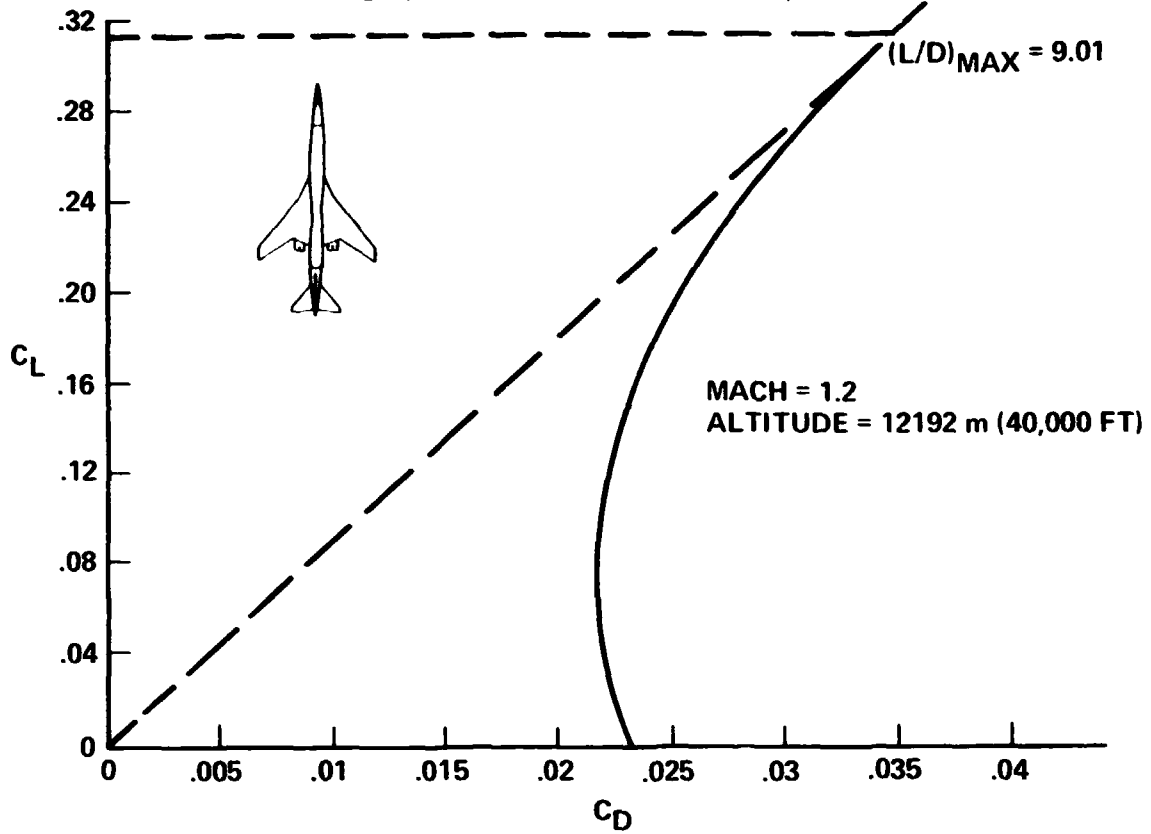


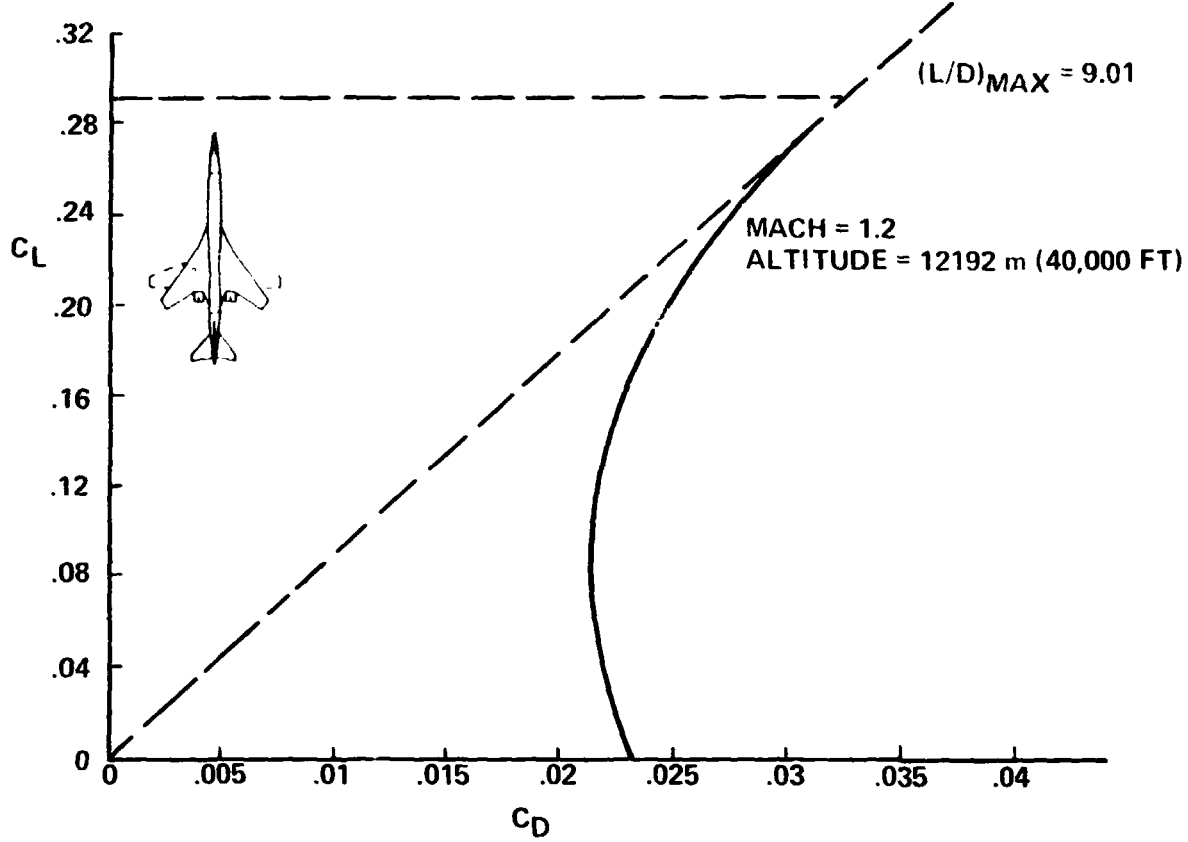
FIGURE 68.—TRIM DRAG

TABLE 16.—CRUISE DRAG SUMMARY, MODEL 1-2



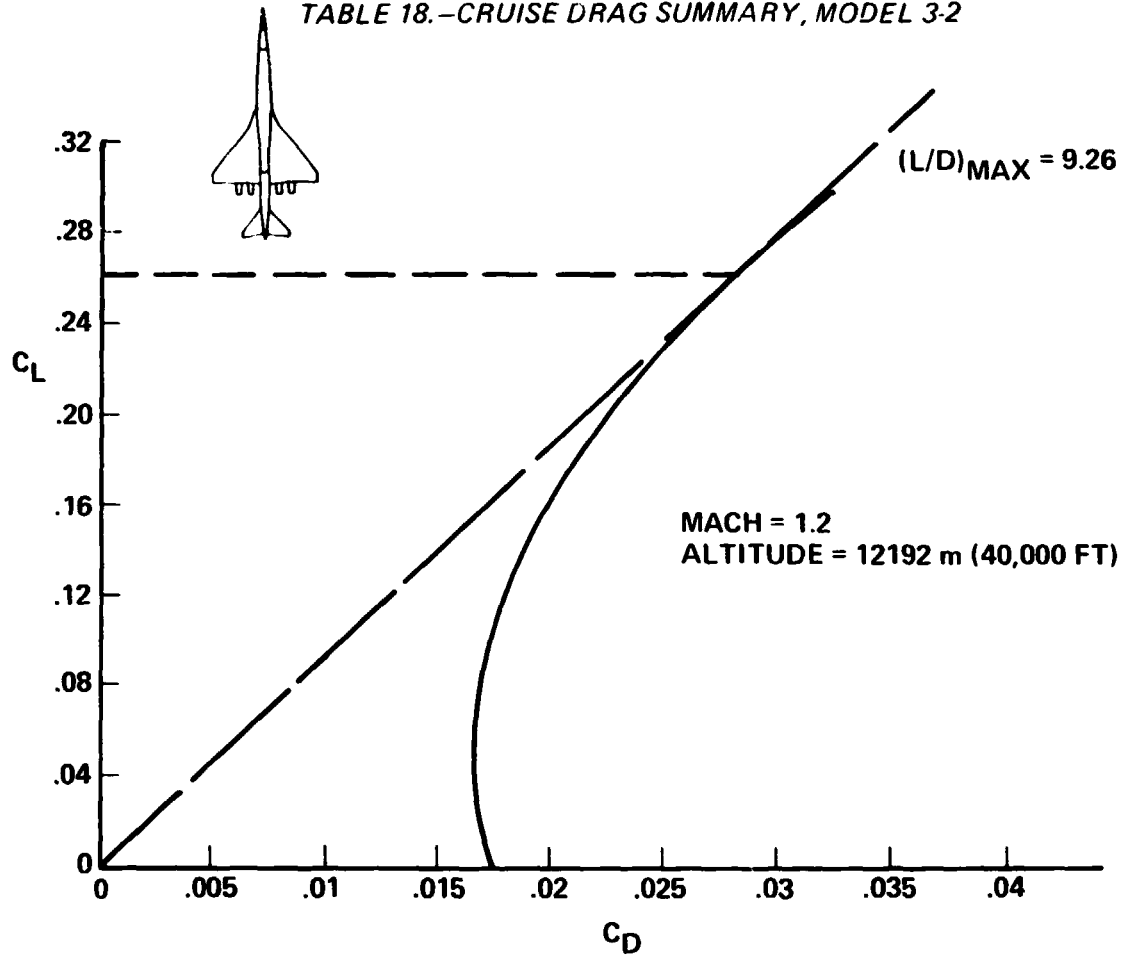
COMPONENT	$\frac{A_{WET}}{S}$	REF. LENGTH	C_{DF}	C_{DW}	COMMENT
		m (FT)			
BODY	1.681	78.49 (257.5)	.00244	.00386	
(W · B) INTERF.				.00520	
WING	1.634	11.73 (38.5)	.00308	.00670	$S_{REF} = 465.52 \text{ m}^2 (5000 \text{ FT}^2)$
NACELLES + INTERFERENCE	.376	11.43 (37.5)	.00071	.00502	THRUST · SLST = 206842 N (46,500 LB)/ENGINE
HORIZONTAL TAIL	.258	4.785 (15.7)	.00056	.00086	$S_H = 74.32 \text{ m}^2 (800 \text{ FT}^2)$
VERTICAL TAIL	.194	6.37 (20.9)	.00040	.00048	$S_V = 51.097 \text{ m}^2 (550 \text{ FT}^2)$
MISCELLANEOUS				.00107	
					NOMINAL UNSIZED AIRPLANE
TOTALS	4.143		.00719	.01279	

TABLE 17. - CRUISE DRAG SUMMARY, MODEL 2-2



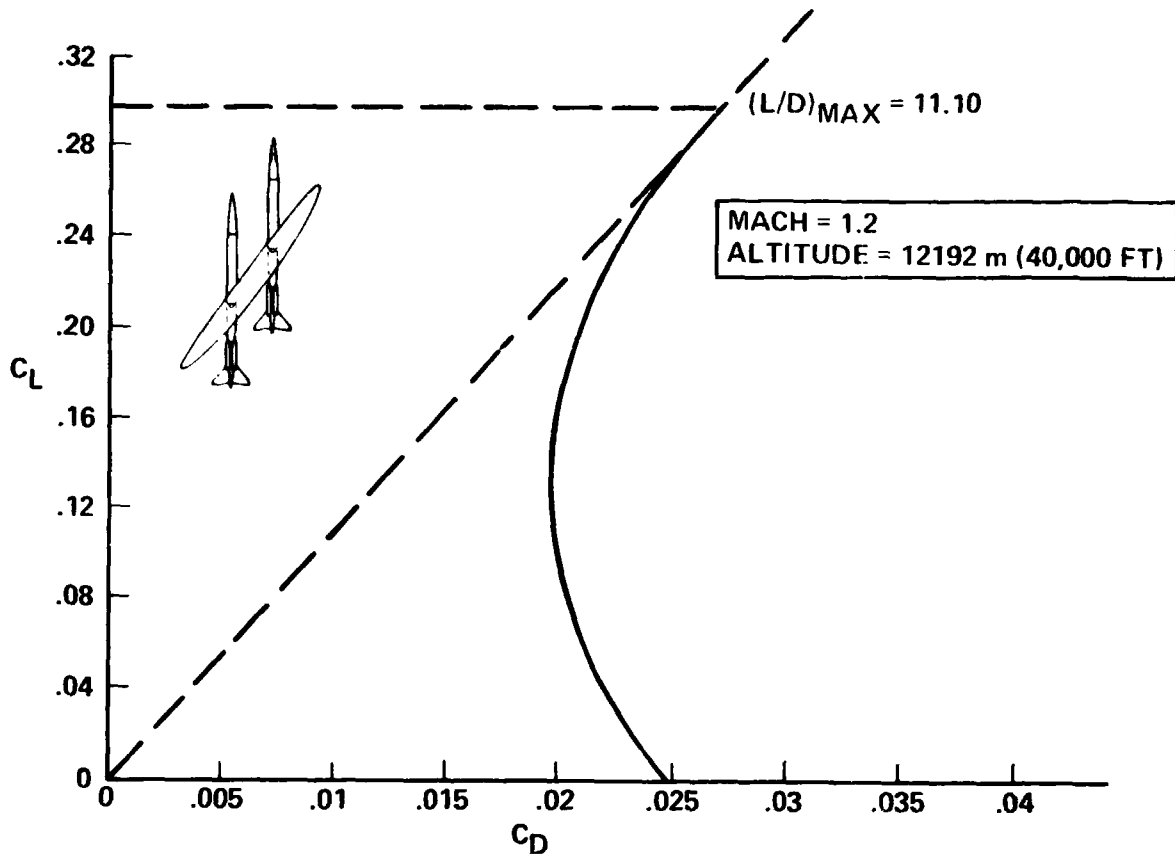
COMPONENT	A _{WET} /S	REF LENGTH		C _{DF}	C _{DW}	COMMENT
		m	(FT)			
BODY	1 666	78.49	(257.5)	00241	00302	
(W B) INTERF					00362	
WING	1 609	12.80	(42.0)	00299	00430	S _{REF} 465.5 m ² (5000 FT ²)
NACELLES + INTERFERENCE	376	11.43	(37.5)	00074	00526	THRUST SLST 206842 N (46500 LBI)/ENGINE
HORIZONTAL TAIL	302	5.18	(17.0)	00064	00102	S _H 74.32 m ² (800 FT ²)
VERTICAL TAIL	177	6.096	(20.0)	00037	00046	S _V 51.097 m ² (550 FT ²)
MISCELLANEOUS					00110	ROUGHNESS AND PROTUBERANCES
						NOMINAL UNSIZED AIRPLANE
TOTALS	4 130			00715	01154	

TABLE 18.—CRUISE DRAG SUMMARY, MODEL 3-2



COMPONENT	A _{WETS}	REF LENGTH		C _{DF}	C _{DW}	COMMENT
		m	(FT)			
BODY	1597	78.49	(257.5)	00231	00248	
(W. B.) INTERF.					00258	
WING	1698	13.56	(44.5)	00312	00359	S _{REF} = 506.3 m ² (5450 FT ²)
NACELLES + INTERFERENCE	450	11.06	(36.27)	00085	00233	THRUST SLST = 240204 N (54 000 LB) ENGINE
HORIZONTAL TAIL	176	4.133	(13.56)	00039	00057	S _H = 74.32 m ² (800 FT ²)
VERTICAL TAIL	187	6.56	(21.51)	00038	00047	S _V = 51.097 m ² (550 FT ²)
MISCELLANEOUS					00104	ROUGHNESS AND PROTUBERANCES
						NOMINAL UNIZED AIRPLANE
TOTALS				00705	00790	

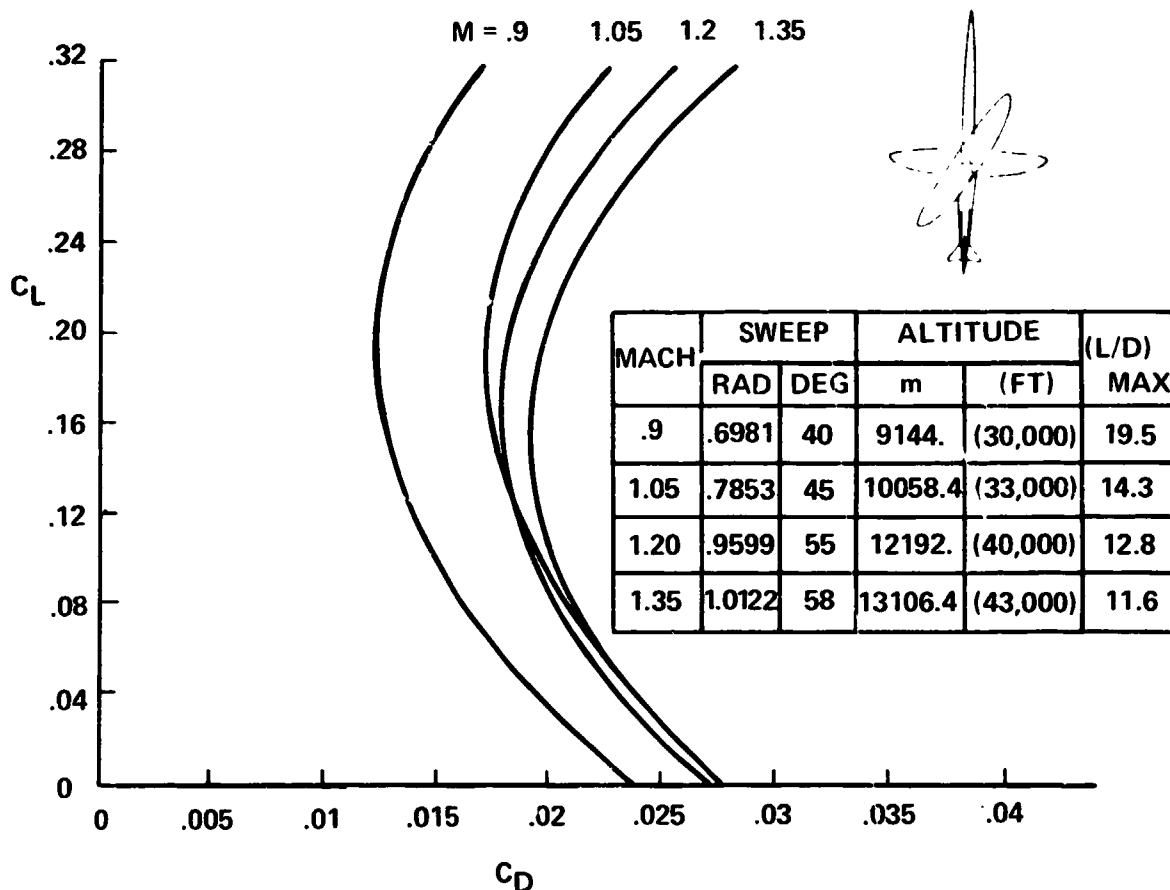
TABLE 19.- CRUISE DRAG SUMMARY, MODEL 4-2



M = 1.2
 ALTITUDE = 12192.0 m (40,000 FT)

COMPONENT	$\frac{A_{WET}}{S}$	REF. LENGTH		C_{DF}	C_{DW}	COMMENT
		m	(FT)			
BODY	2.288	65.78	(215.8)	.00341	.00220	
(W · B) _{INTERF.}					0.0	
WING	1.927	10.21	(33.5)	.00369	.00082	$S_{REF} = 464.5 \text{ m}^2 (5000 \text{ FT}^2)$
NACELLES + INTERFERENCE	.395	9.78	(32.1)	.00077	.00144	WITH NO INTERFERENCE
HORIZONTAL TAIL	.307	3.69	(12.1)	.00068	.00109	$S_H = 46.45 \text{ m}^2 (500 \text{ FT}^2)/\text{BODY}$
VERTICAL TAIL	.317	6.22	(20.4)	.00065	.00101	$S_V = 51.097 \text{ m}^2 (550 \text{ FT}^2)/\text{BODY}$
MISCELLANEOUS					.00125	ROUGHNESS AND PROTUBERANCES
						THRUST: SLST = 106825 N (42,000 LB)/ENGINE
						NOMINAL UNSIZED AIRPLANE
TOTALS	5.234			.00920	.00781	

TABLE 20.—CRUISE DRAG SUMMARY, MODEL 5-3



M = 1.2
 ALTITUDE = 12192.0 m (40,000 FT)

COMPONENT	A _{WET} /S	REF. LENGTH		C _{Df}	C _{Dw}	COMMENT
		m	(FT)			
BODY	2.100	87.78	(288.0)	.00309	.00129	"NO ENGINE" BODY
(W · B) INTERF.					.00005	"NO ENGINE" WING + BODY
WING	1.946	10.36	(34.0)	.00379	.00163	S _{REF} = 371.6 m ² (4000 FT ²)
NACELLES + INTERFERENCE	0.271	87.78	(288.0)	.00040	.00012	ALL WAVE DRAG RELATIVE TO "NO ENGINE" A/P
HORIZONTAL TAIL	0.185	3.642	(11.95)	.00041	.00054	S _H = 34.56 m ² (372 FT ²)
VERTICAL TAIL	0.177	5.407	(17.74)	.00037	.00040	S _V = 32.24 m ² (347 FT ²)
MISCELLANEOUS					.00070	ROUGHNESS AND PROTUBERANCES
						THRUST: SLST = 180136 N (36,000 LB)/ENGINE
						NOMINAL UNSIZED AIRPLANE
TOTALS	4.679			.00806	.00439	

MACH = 1.2 ALTITUDE = 12192 m (40 000 FT) $C_L = .26$

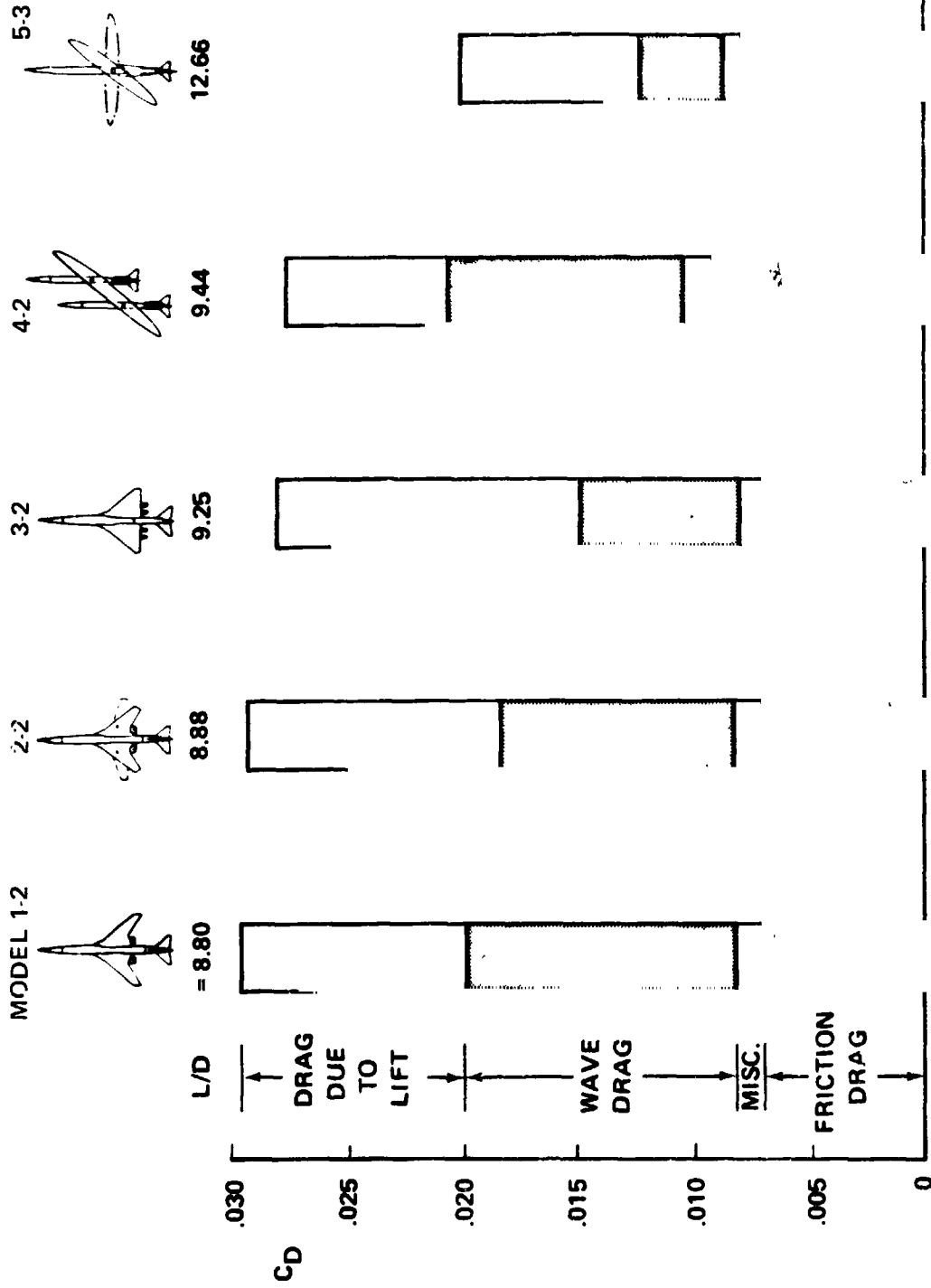


FIGURE 69.--UNCYCLED BASELINE CONFIGURATION CRUISE DRAG COMPARISON

The isolated and integrated wave drag buildup for each of the unsized configurations is shown in figure 70. The conventional airplanes and the single-fuselage yawed-wing configuration all have a net favorable interference. The double pod installed drag on the fixed wing and on the variable sweep is significantly higher than the single pod installation on the delta-wing concept. This is the result of the large size of the nacelles.

The integrated drag of the double-body yawed-wing concept is significantly higher than the sum of the isolated drags. This is primarily due to the unfavorable interference on the tail-mounted nacelle installation.

It should be possible to integrate the nacelles for no more than isolated nacelle wave drag. This drag level with zero nacelle interference has been used to identify the "drag potential" for the double fuselage yawed wing configuration. To achieve this reduced drag level, the nacelles would have to be separated. This can be achieved by moving the nacelles forward on the fuselage.

Low-Speed Capability and High Lift Systems

Estimation Methods and Procedures

The low-speed aerodynamic characteristics of the study configurations were estimated by methods used by the contractor for preliminary design configurations on which no wind tunnel data exists. In general, the procedures were based on theoretical considerations but were tempered by flight test and wind tunnel data wherever applicable. For rapid evaluation of low-speed characteristics, the procedures described briefly below have been programmed for processing by the CDC 6600 computer.

The basic flaps up lift curve was constructed from a zero angle of attack intercept and a lift curve slope which is a function of aspect ratio, thickness ratio, and quarter-chord sweep angle. The slope was adjusted for the effect of the body and for the addition to wing planform area effected by the extension of leading and trailing-edge flaps. The maximum lift coefficient of the basic, flaps-up wing was determined according to aspect ratio and quarter-chord sweep angle.

Leading edge devices reduce the lift coefficient in the linear lift range and this effect was computed using a theoretical value for flap effectiveness and part span effects. The lift increments due to trailing-edge flaps were determined from empirical section flap effectiveness data. Adjustments were made to account for three-dimensional effects and the geometry of the flap system.

The maximum lift increments due to leading edge and trailing edge flaps were determined from empirical data that has been correlated in terms of the ratio of leading edge device area to wing area, ratio of trailing edge device area to wing area, and ratio of wing area subtended by flaps to total wing area.

Drag polars were constructed by estimating the minimum parasite drag of the flaps-up configuration at typical takeoff and landing Reynolds numbers at sea level. Increments to

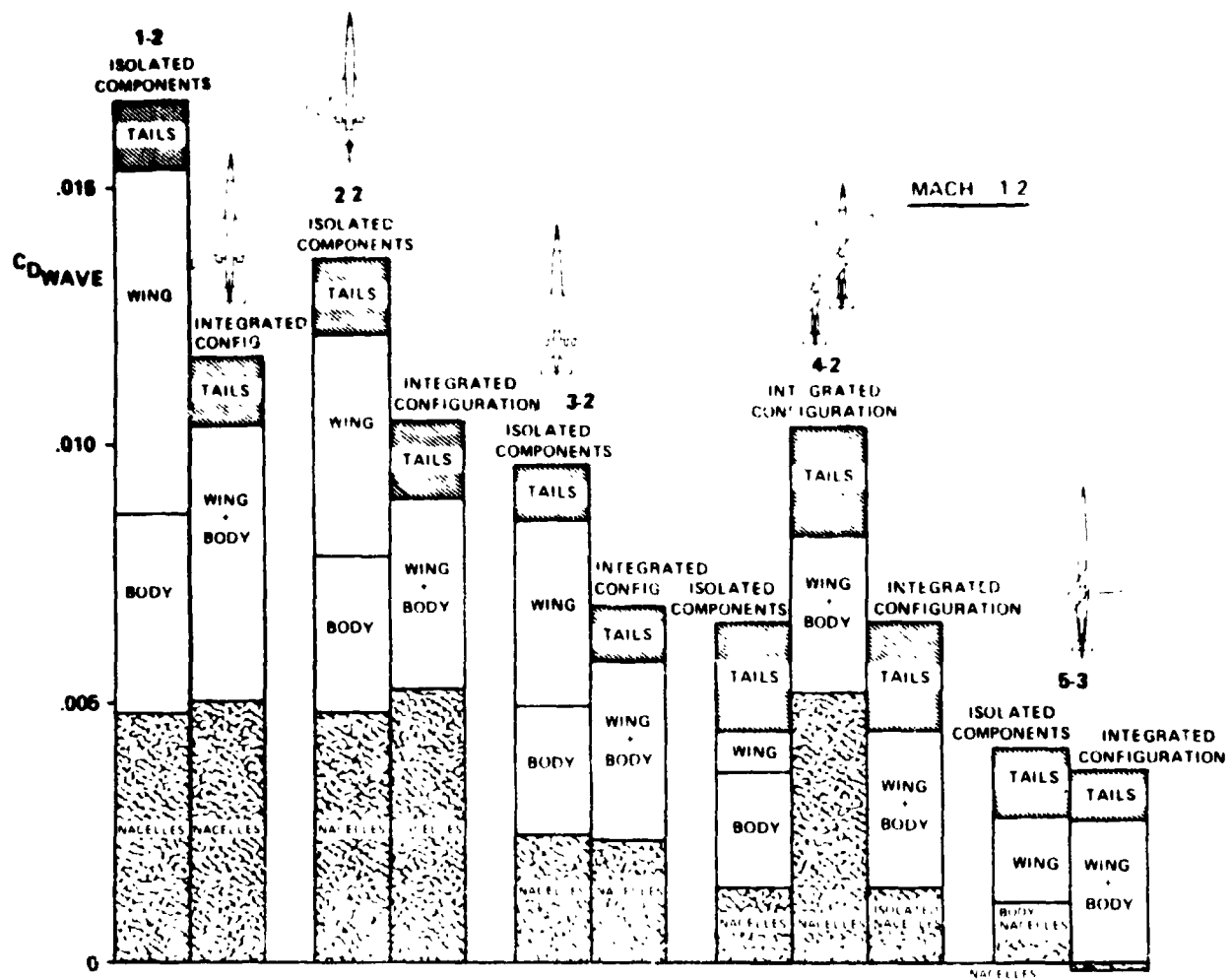


FIGURE 70.—UNCYCLED CONFIGURATION CRUISE WAVE DRAG COMPARISON

minimum parasite drag for leading and trailing edge devices were added from test data correlated on the basis of flap to wing area ratios, flap chord ratios, type of flap and flap deflection. Slotted, trailing edge flap parameters were evaluated in terms of the extended flap chord ratios.

Drag due to lift was added as $C_L^2/\pi AR$ then modified by additional drag terms. Additional parasite drag, ΔC_{Dp} , was applied as a function of $C_L - C_{Lp}$, necessitating the determination of an increment to C_{Lp} for leading and trailing edge devices. Again, this was evaluated from empirical data as a function of planform area to wing area for the leading edge flap and as a function of lift increment for the trailing edge flap. An additional drag due to lift, ΔC_{DiTE} , term was added to account for the discontinuous span loading due to the part span flaps. This term was evaluated using constants obtained from Royal Aeronautical Society data sheets.

Pitching moments were evaluated by first estimating the zero lift pitching moment, C_{M_0} and aerodynamic center of the basic flaps up configuration then adding the increment produced by the flap lift acting at its estimated center of lift position.

The incremental buildup of the above process is sketched in figure 71.

Ground effects were estimated from relationships derived from the computation of the effects of a vortex image upon a simple horseshoe vortex. The predominant effects are the reduction in downwash allowing a given lift to be produced at a lower angle of attack and the reduction of freestream velocity resulting in reduction of all coefficients at a given angle of attack. This procedure has shown reasonably good agreement with test data.

Low Speed Characteristics Summary

A summary of the low speed aerodynamic data for the study configurations in terms of second segment lift/drag ratios (L/D_{V_2}) versus lift coefficient ($C_{L_{V_2}}$) and operating attitudes for takeoff and landing is shown in figure 72. The 5-3 configuration summary curve is shown both with and without leading edge devices to show the large lift/drag increment associated with the leading edge flaps, particularly at low values of trailing edge deflection. The "without leading edge" curve also provides a better comparison with other yawed wing study configuration 4-2. The reduction of second segment lift/drag ratio of 5-3 from 4-2 is attributed to the lower aspect ratio and the large effective flap chord of the 5-3. Low speed performance of the 5-3 was based on the data with leading edges extended.

High Lift System Definition

Wing planform and flap system geometry are shown in table 21. All of the low speed analyses were performed using a nominal wing area of 465 m^2 , (5000 ft^2).

Rotating vs Non-Rotating Configurations

The nonrotating takeoff and landing procedures for the single fuselage yawed wing configuration, 5-3, are unorthodox for transport category airplanes but should present no

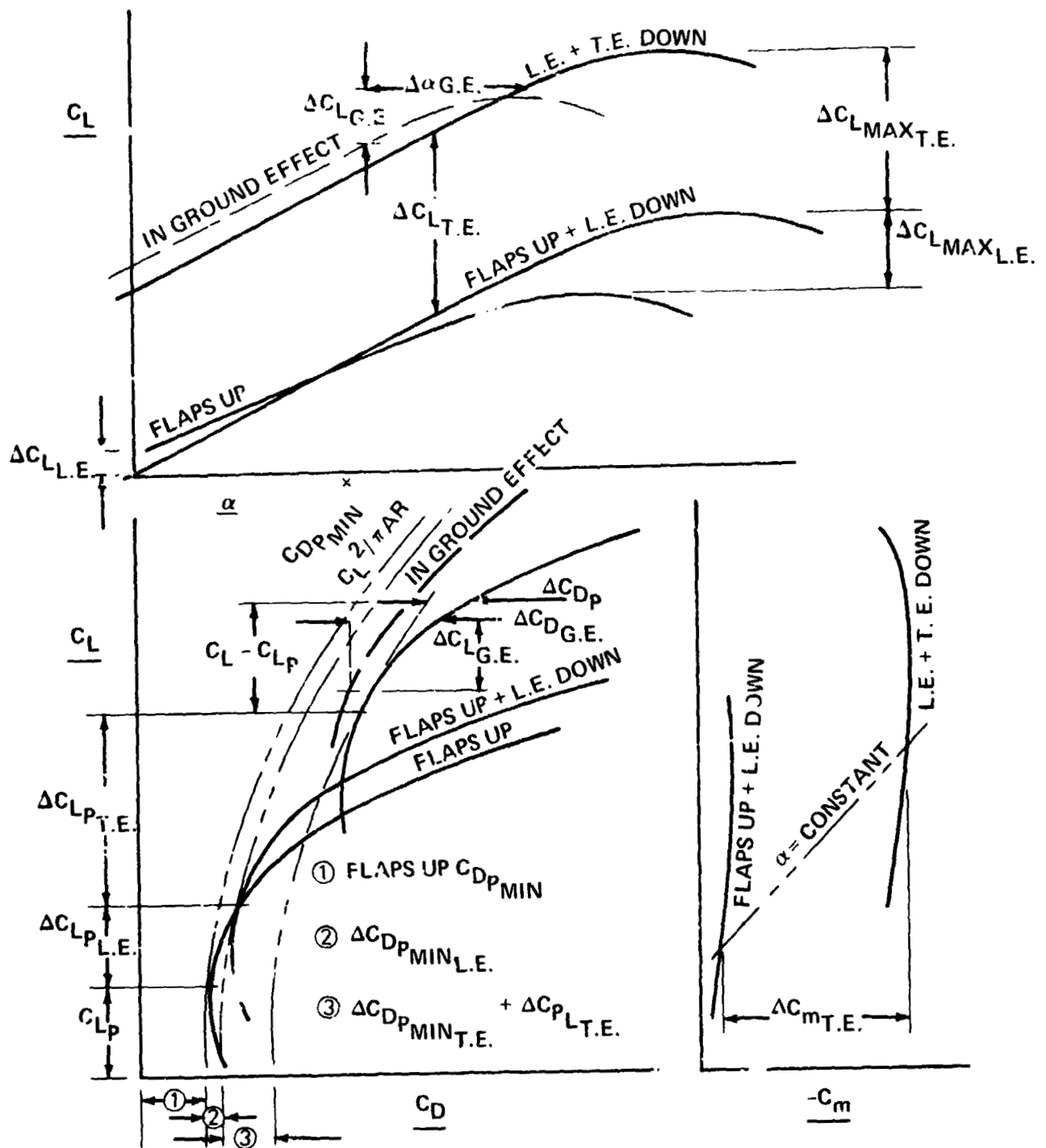


FIGURE 71. -LOW-SPEED AERODYNAMIC DATA GENERATION

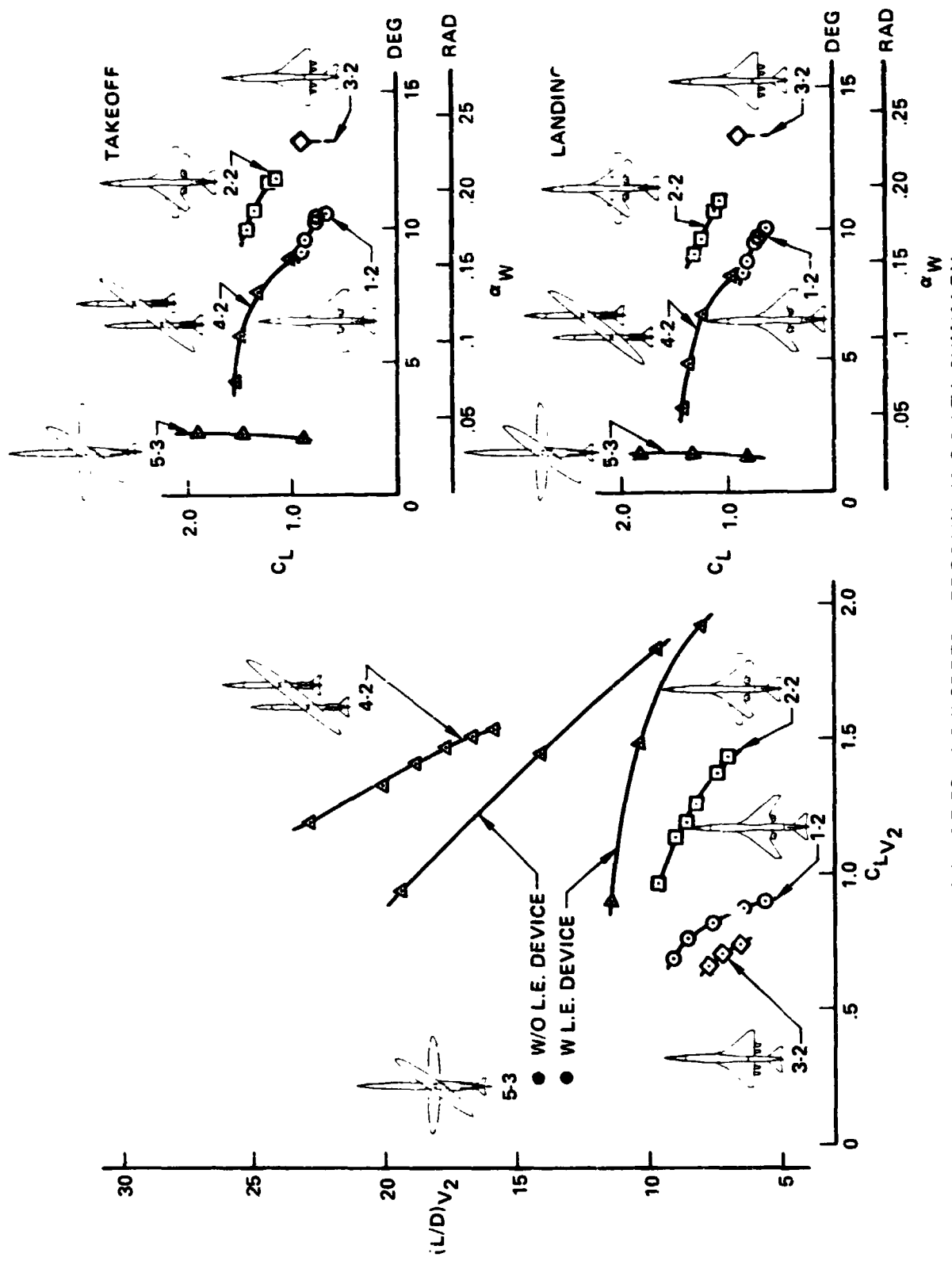


FIGURE 72. - LOW-SPEED AERODYNAMIC DATA SUMMARY

TABLE 21.—WING PLANFORM AND FLAP SYSTEM PARAMETERS

CONFIGURATION	NOMINAL PLANFORM	FLAP SYSTEM
1-2 (ARROW WING)	$S_{REF.}$ 465.5 m ² (5000 FT ²) $S_{TRAP.}$ 391.1 m ² (4210 FT ²) C/4, .803 RAD (46 DEG) AR 3.97 λ 0.30 b, 39.41 m (129.3 FT)	CURVED L.E. FLAP, $C_{L.E.}/C = 0.10$ DOUBLE-SLOTTED T.E. FLAP, $C_f/C = 0.30$ $C_A/C_f = 0.40$ $C'/C = 1.25$ $b_f/b = 0.35$
2-2 (VARIABLE SWEEP WING)	$S_{REF.}$ 465.5 m ² (5000 FT ²) $S_{TRAP.}$ 359.5 m ² (3870 FT ²) C/4, .262 RAD (15 DEG) AR (UNYAWED) 5.55 λ 0.31 b, 44.65 m (146.5 FT)	CURVED L.E. FLAP, $C_{L.E.}/C = 0.10$ DOUBLE-SLOTTED T.E. FLAP, $C_f/C = 0.30$ $C_A/C_f = 0.90$ $C'/C = 1.25$ $b_f/b = 0.48$
3-2 (DELTA WING)	$S_{REF.}$ 506.3 m ² (5450 FT ²) $S_{TRAP.}$ 506.3 m ² (5450 FT ²) C/4, .733 RAD (42 DEG) AR 2.56 λ 0.13 b, 36.06 m (118.3 FT)	DROOPED L.E. FLAP, SAME AS 2707-300 PLAIN T.E. FLAP, SAME AS 2707-300 $b_f/b = 0.59$
4-2 (ELLIPTICAL WING)	$S_{REF.}$ 465.5 m ² (5000 FT ²) C/4, 0. RAD (0 DEG) AR (UNYAWED) 12.75 10:1 λ ELLIPSE b, 76.93 m (252.4 FT)	NO L.E. FLAP PLAIN T.E. FLAP, $C_f/C = 0.25$ $C'/C = 1.0$ $b_f/b = 0.68$
5-3 (ELLIPTICAL WING)	$S_{REF.}$ 465.5 m ² (5000 FT ²) C/4, 0 RAD (0 DEG) AR (UNSWEPT) 10.2 8:1 λ ELLIPSE b, 68.88 m (226 FT)	CURVED L.E. FLAP, $C_{L.E.}/C = 0.15$ DOUBLE-SLOTTED T.E. FLAP, $C_f/C = 0.25$ $C_A/C_f = 0.40$ $C'/C = 1.2$ $b_f/b = 0.74$

operational problems since the concept has long since been proven on such airplanes as the B-47 and B-52. Discussions with B-47 and B-52 pilots verified the operational simplicity of a nonrotating configuration. At a speed slightly below scheduled liftoff speed a small amount of back pressure is applied to develop a definite upward acceleration to prevent the airplane from skipping along the runway when lift and weight are nearly equal. The flare out of the landing approach requires very little change in airplane attitude to achieve a "two point" touchdown. Both gears touching simultaneously or rear gear first is the preferred touchdown procedure as nose gear first tends to make the airplane porpoise.

Although a nonrotating configuration could be certified under current Federal Air Regulations a reexamination of FAR 25 would be recommended, particularly with regard to the section relating rotation speed, liftoff speed and minimum unstick speed.

Since the ground roll attitude is, in effect, the geometry limit, normal takeoffs would be performed at essentially minimum unstick speed. As shown in figure 73 these liftoff speeds provide adequate safety margins and requiring the airplane to lift off at speeds higher than minimum unstick would unnecessarily penalize takeoff performance.

The low speed aerodynamic characteristics which were calculated for model 5-3 as a rotating and as a nonrotating configuration are compared in figures 73 and 74. The performance calculations of the nonrotatable 5-3 were based on an angle of attack of .026 rad., (1.5 deg), equal to the wing incidence angle.

The second segment operating point was assumed to be at the same lift coefficient as liftoff. Landing approach was assumed at .026 rad., (1.5 deg), angle of attack, thus the landing flare would require an attitude change of only glide slope angle minus .026 rad (1.5 deg). Figure 73 indicates the differences in attitude and lift coefficient for a rotating versus a nonrotating configuration. At the maximum flap deflection investigated, .785 rad (45 deg), the nonrotating liftoff speed is 6.18 m/sec (12 knots) higher than that of the rotating airplane. Approach speed is higher by 2.06 m/sec, (4 knots).

Figure 74 shows similar lift/drag ratios for the two configurations when operated at the same flap setting, but a lower L/D for the nonrotating configuration when operating at the same speed. Elimination of the leading edge device would provide a substantial improvement in low speed performance, particularly at low flap angles. Elimination appears feasible for the 5-3 since the operating speeds would still be higher than the current $1.2 V_S$ and $1.3 V_S$ requirements of FAR 25 for all but the highest flap deflection.

The large difference between nonrotating operating speeds and $1.2 V_S$ leads to a possible operational concept to reduce sideline noise. The configuration performance section (fig. 25a) indicated how quickly takeoff noise rather than sideline noise becomes critical as thrust is reduced. If field length were not critical, takeoff thrust could be reduced to minimize sideline noise. After liftoff the airplane could continue to rotate to the attitude for $1.2 V_S$, thus trading excess velocity for altitude.

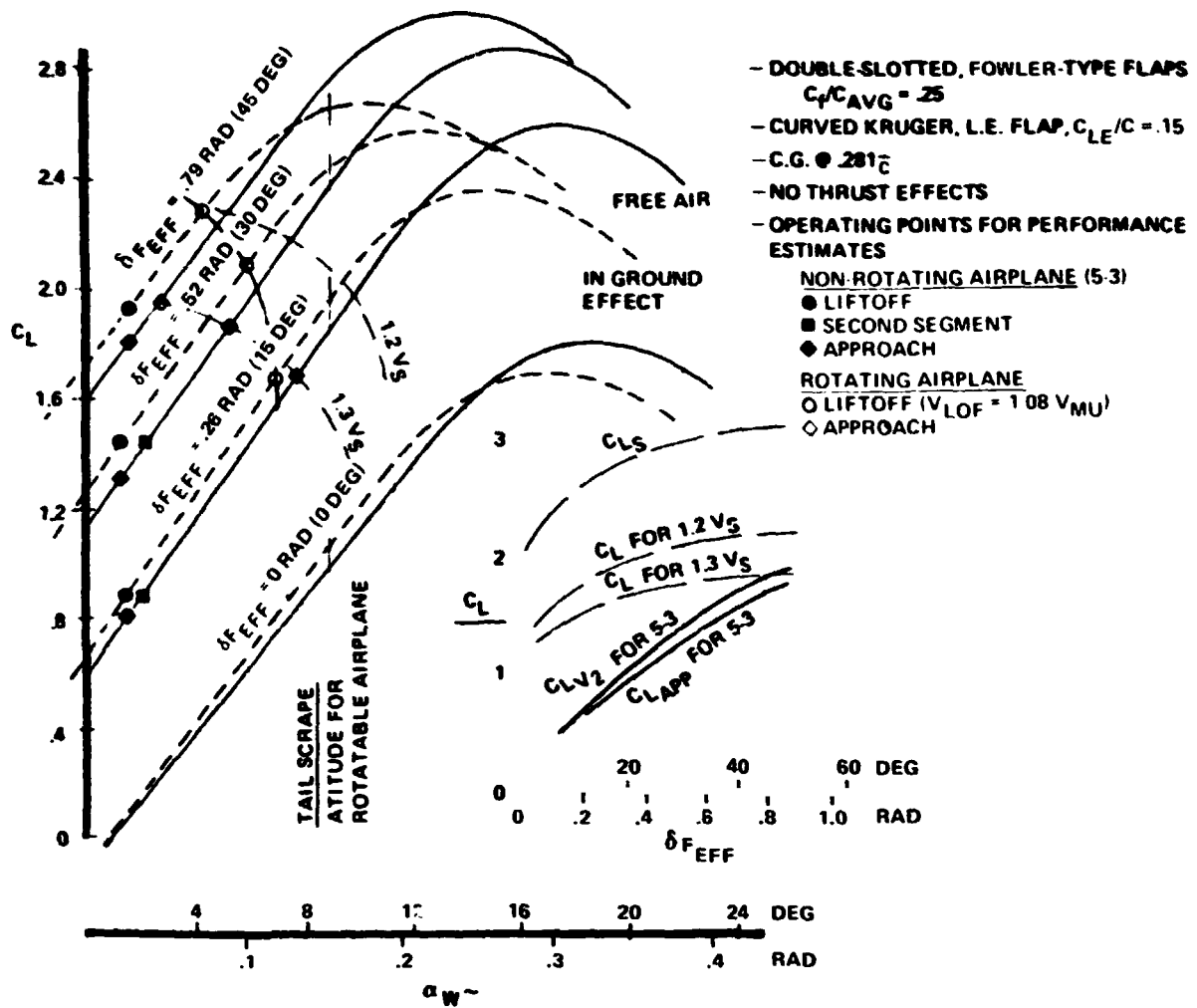


FIGURE 73.-LOW-SPEED LIFT CHARACTERISTICS, MODEL 5-3

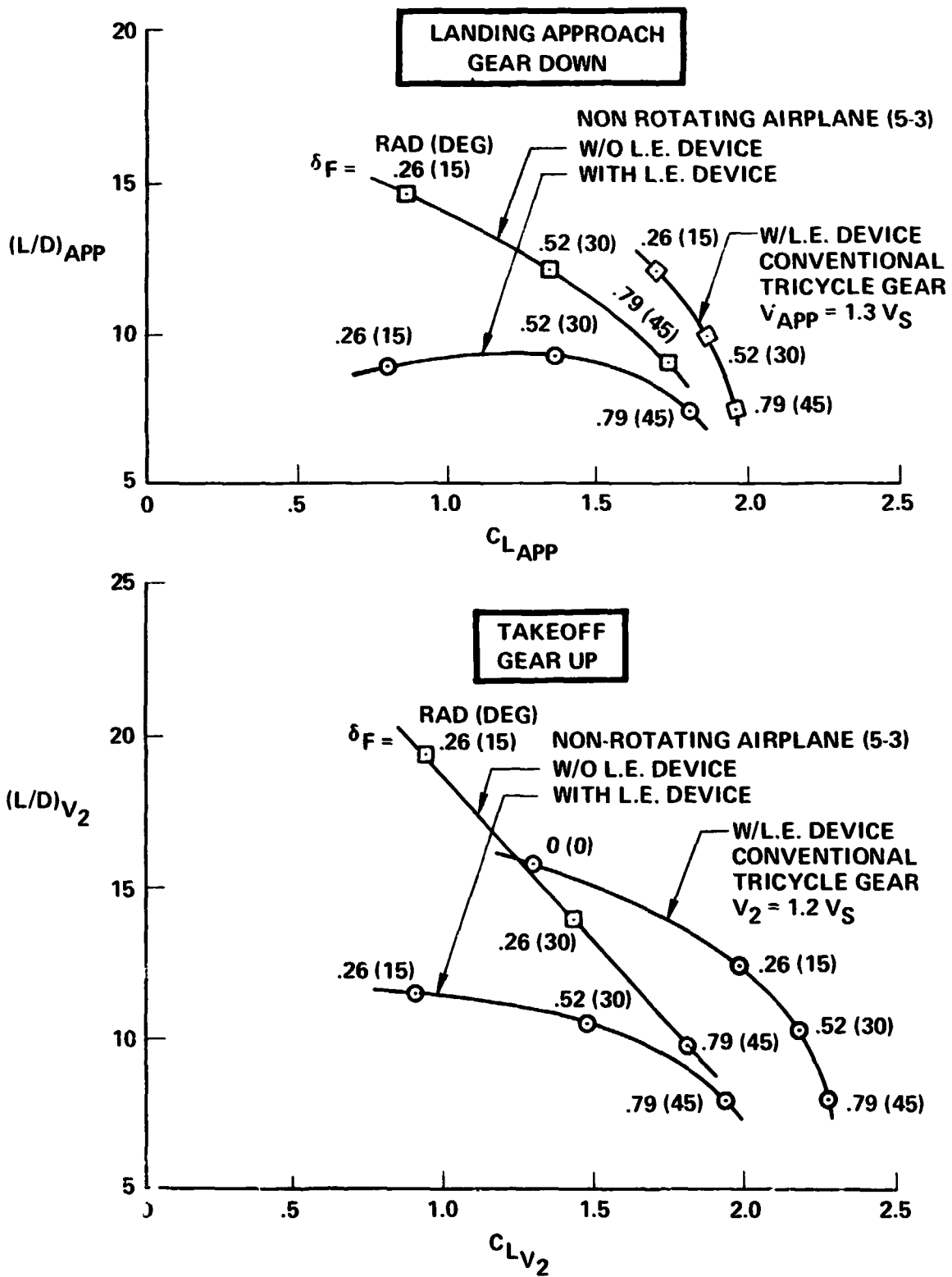


FIGURE 74.—LOW-SPEED DRAG CHARACTERISTICS, MODEL 5-3

Planform Study

The low speed characteristics of the yawed wing, nonrotating configuration were calculated for two planforms. The basic nonrotating configuration, 5-3, had an 8:1 ellipse planform with an aspect ratio of 10.2. Configuration 5-3-1, had a 6:1 ellipse planform with an aspect ratio of 7.65. Characteristics of the 5-3-1 are shown in figures 75 and 76.

Although operating speeds for the 5-3-1 would only be a few meters/sec faster than for 5-3, lift drag ratios would be reduced by several units. This would be detrimental to the landing and takeoff performance and community noise.

Nacelle-Airplane Integration Studies

Transonic or supersonic nacelle installed drag is critically dependent upon the aircraft configuration arrangement. A number of studies were undertaken to provide a better understanding of the nacelle interference drag at transonic speeds. These studies investigated:

- Nacelle separation and stagger effects
- Engine arrangement effects on nacelle installed drag.
- Engine size effects on wing-mounted, body-mounted and buried engine arrangement:..

Nacelle Drag Factors

The factors that contribute to nacelle drag on a conventional wing installation such as on the fixed-swept wing, variable-sweep wing and delta-wing arrangements are summarized in figure 77.

The major wave drag interference components on wing installations include the wing-nacelle buoyancy drag, the mutual interference between adjacent nacelles and the reflection drag of the nacelle pressures glancing off the wing back on to the nacelle.

The major interference drag components for a body mount engine installation include the mutual interference between adjacent nacelles plus the body-nacelle buoyancy drag. The mutual body buoyancy drag and the reflection drag of the body pressures bouncing off an adjacent planar surface on to itself, as shown in figure 78, are quite similar.

When two mutual bodies are close to each other the drag on each is nearly doubled. As the bodies are separated, the positive compression from the front of the bodies pushes from the back of the adjacent. This creates favorable interference and can produce a sizable reduction in drag. Staggering two adjacent bodies can produce a similar effect. In this case the nose compression pressures from trailing body push on the aft end of the forward body. The aft expansion pressures of the forward body pull on the nose of the trailing body. The combination of these two effects can produce favorable interference.

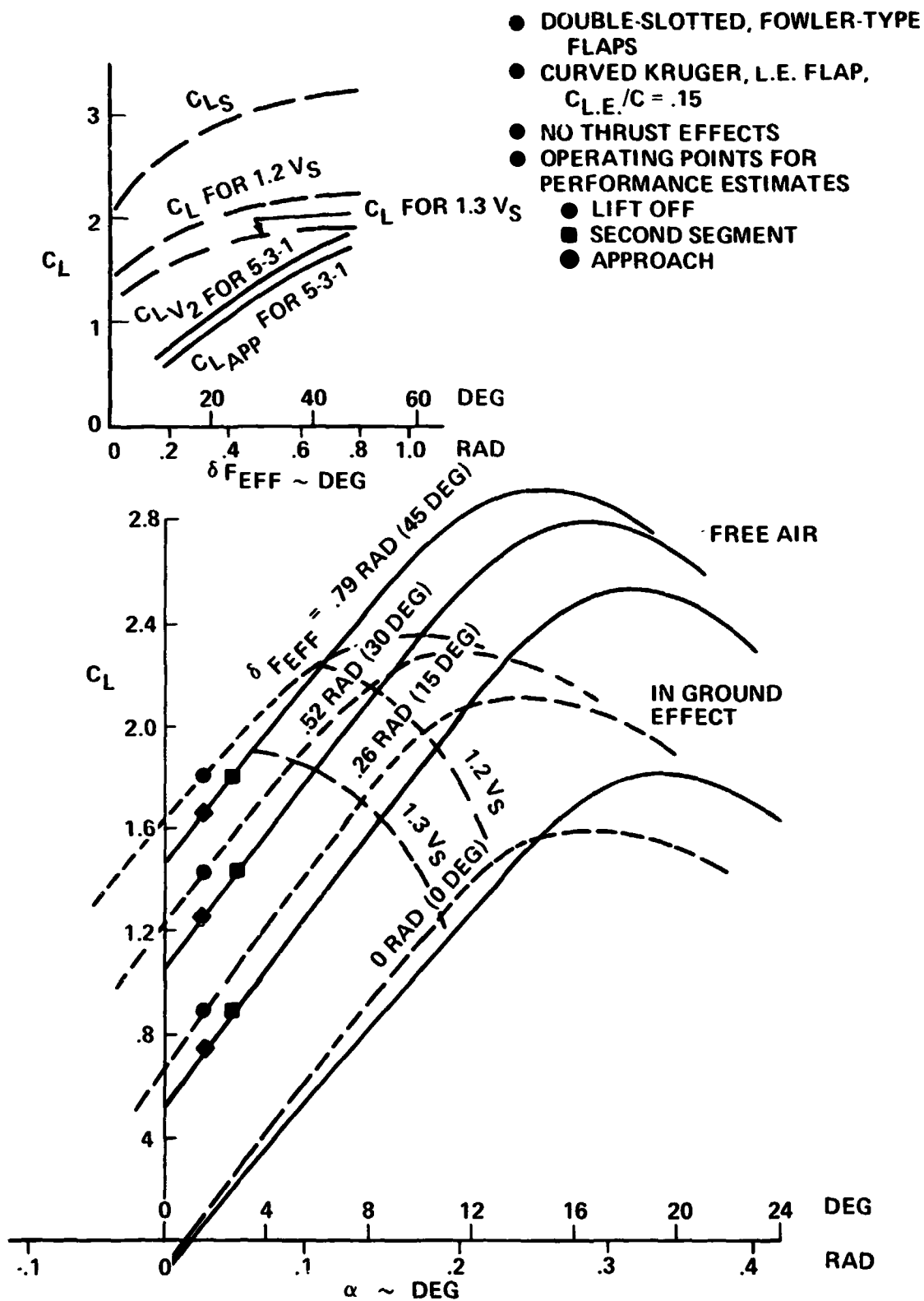


FIGURE 75.—LOW-SPEED LIFT CHARACTERISTICS, MODEL 5-3-1

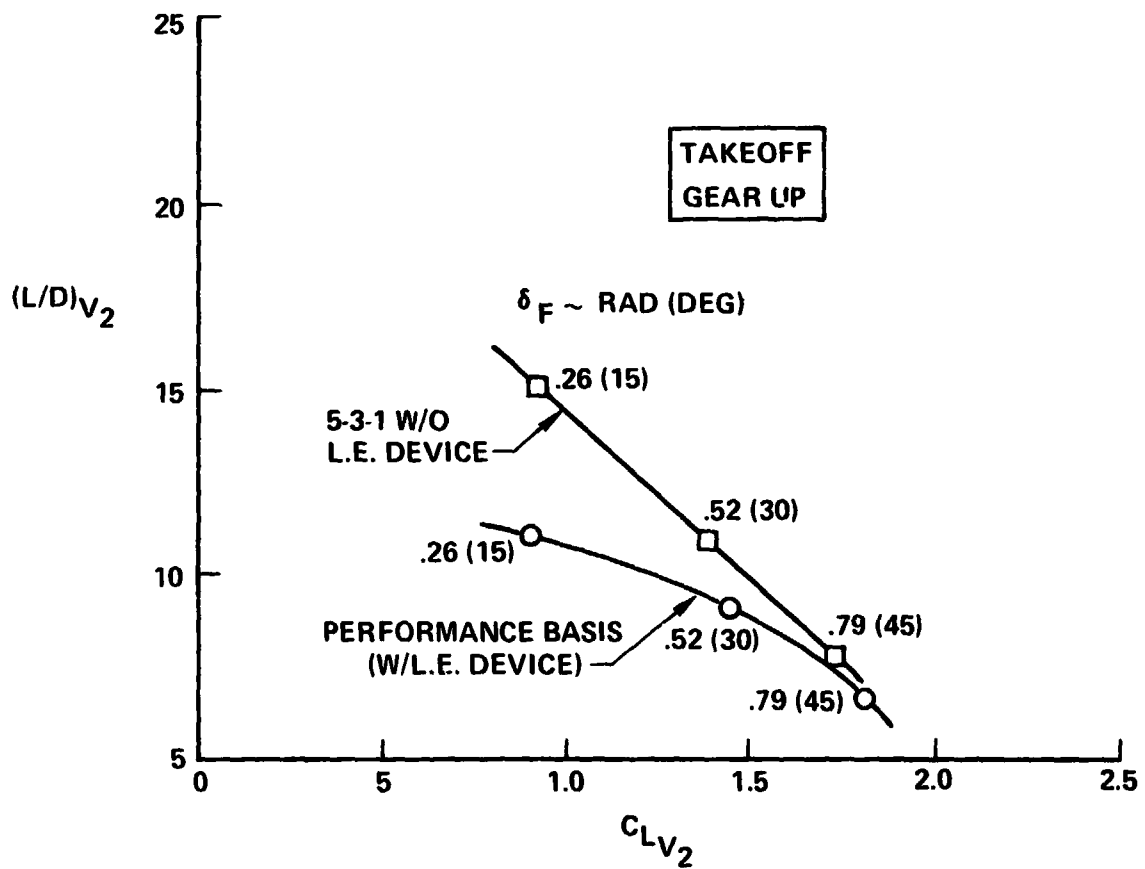
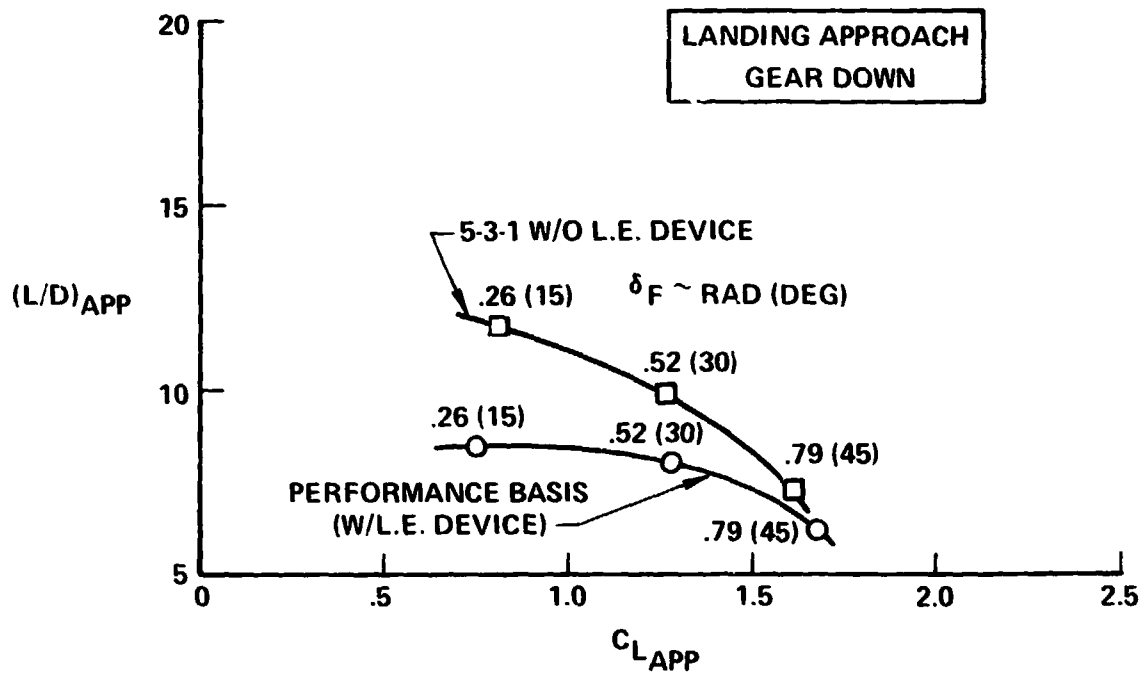


FIGURE 76.—LOW-SPEED DRAG CHARACTERISTICS, MODEL 5-3-1

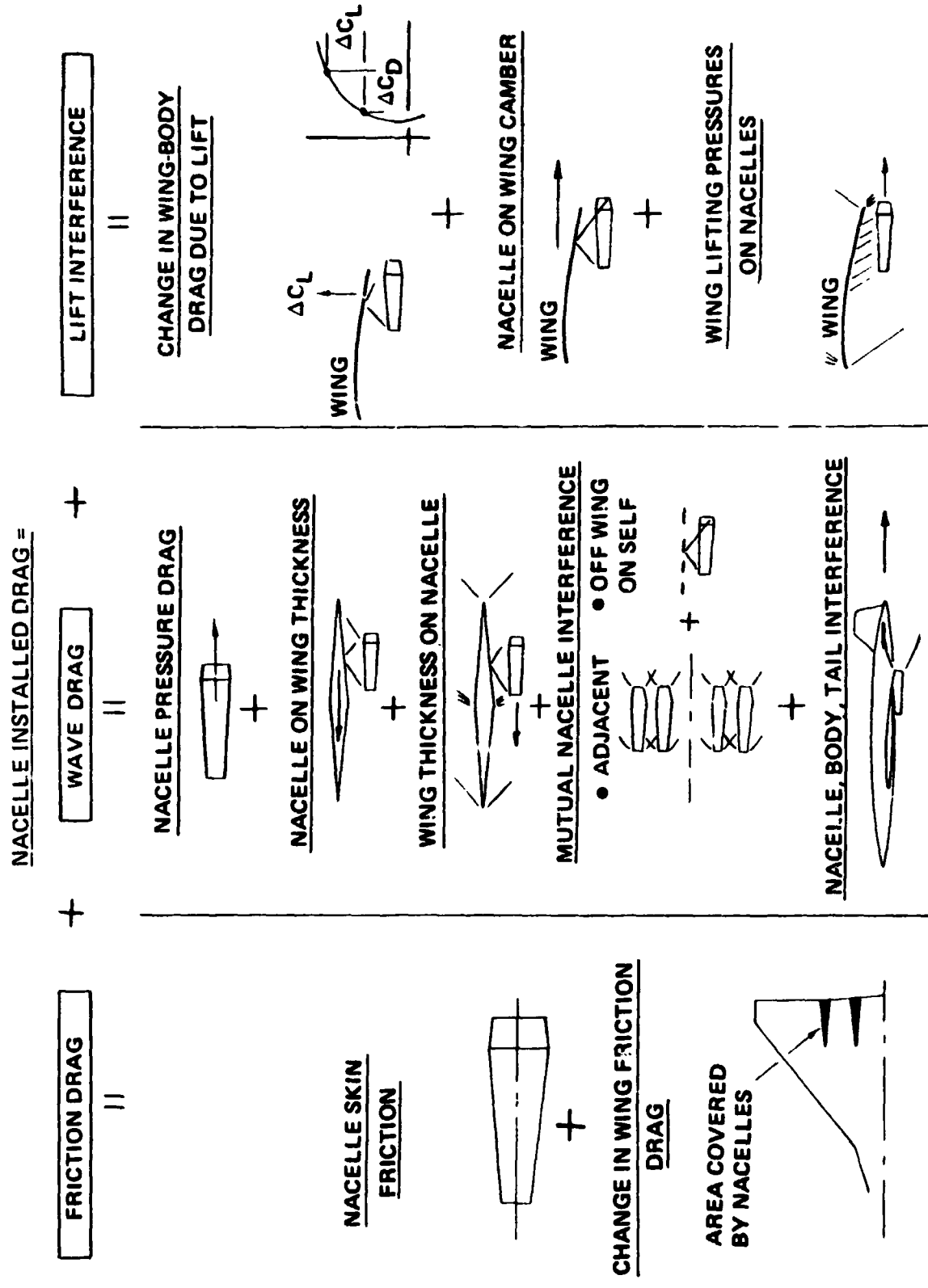


FIGURE 77.—NACELLE INSTALLED DRAG

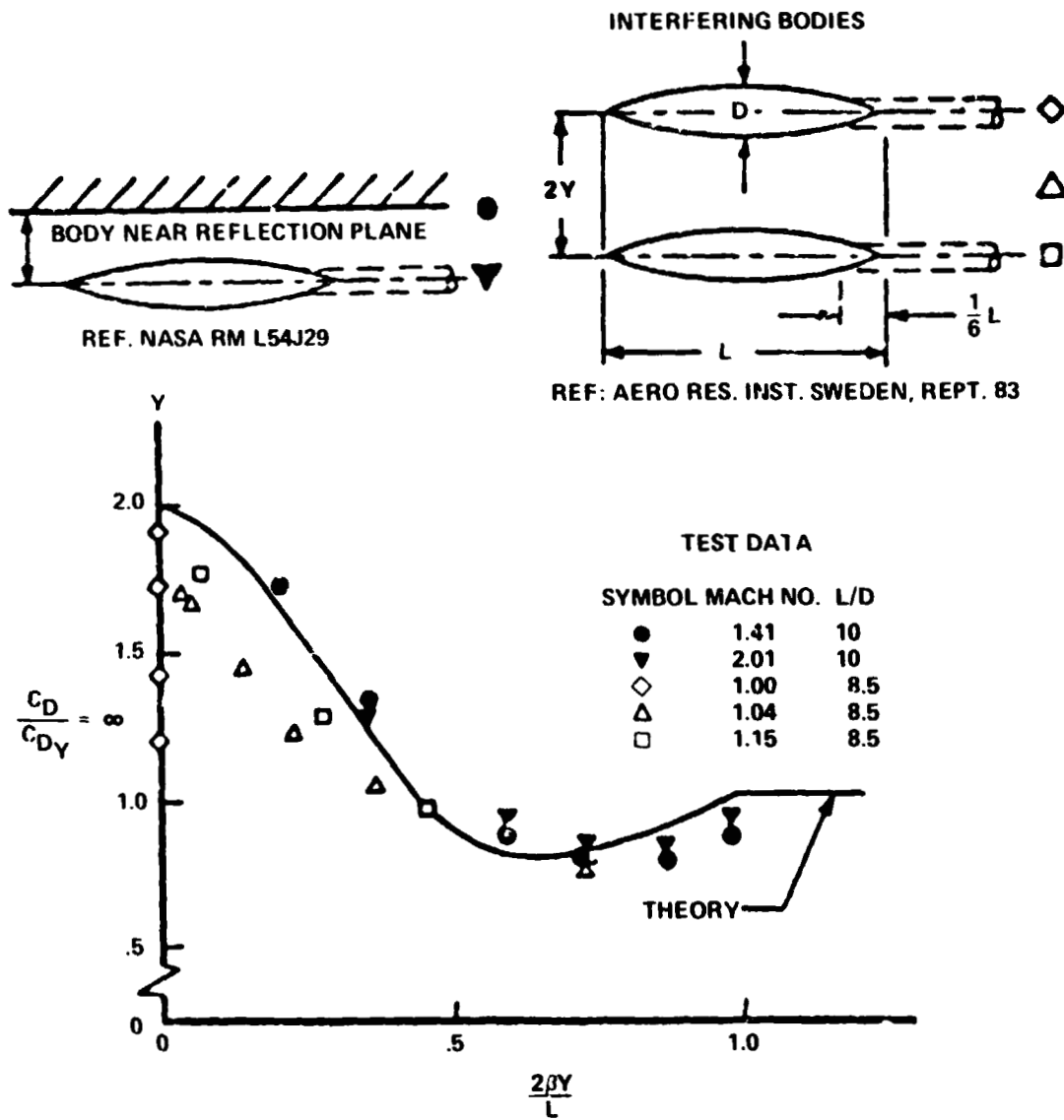


FIGURE 78.—INTERFERENCE BETWEEN BODIES OF REVOLUTION

Nacelle Stagger and Separation

A theoretical study of the combined effects of nacelle separation and stagger for a body mounted nacelle installation was conducted to provide aerodynamic design guidance for the yawed wing configurations. The body mounted nacelle installation on the early single fuselage yawed wing configuration 5-2-4 was selected as the base configuration for the study. Wave drag calculations were made at various separation distance between the nacelles, and for various amounts of stagger at the difference separation distances. In all cases the nacelles were staggered equally fore and aft to maintain the same center of gravity location as on model 5-2-4. For each nacelle location the fuselage was area ruled to minimize Mach = 1.2 wave drag. The mutual nacelle interference drag, and the body-nacelle interference drag were calculated for each location. In addition, the change in body wave drag associated with the required body area ruling (body shape drag) was also determined.

The results of this study as shown in figure 79 indicate that the lowest wave drag installation occurs when the nacelles are mounted close to the body without stagger. The mutual nacelle interference is high but the body area ruling produces a strong favorable pressure field that results in a net reduction in drag. The body shape drag partly cancels this effect.

Staggering the nacelles located close to the body (separation distance = 2.4 nacelle diameters), reduces the mutual interference and body shape drag. However, the corresponding loss in body-nacelle interference makes nacelle stagger undesirable. The effects of nacelle stagger for a separation distance equivalent to that on 5-2-4 (4.75 diameters) are quite similar.

The effect of nacelle shape, and further aft nominal nacelle locations and other Mach numbers were not investigated.

Engine Arrangement

A number of various engine installations were considered during the development of the single-fuselage yawed wing configuration. A comparison of the nacelle installed cruise drag for some of these arrangements is shown in figure 80.

The high installed drag of the 4-engine arrangement was primarily due to the unfavorable interference drag of the pair of tail mounted engines which is effectively a double pod installation.

The tail mounted nacelles were replaced by a center engine with an "S duct" and the engines were increased in size to provide the same thrust as the 4-engine arrangement. The nacelle friction drag was essentially unchanged but a net favorable interference drag was achieved.

In order to identify the drag associated with the integrated nacelle installation a comparable airplane configuration without engines was aerodynamically designed and analyzed. The changes in total skin friction drag relative to the "no engine" body friction

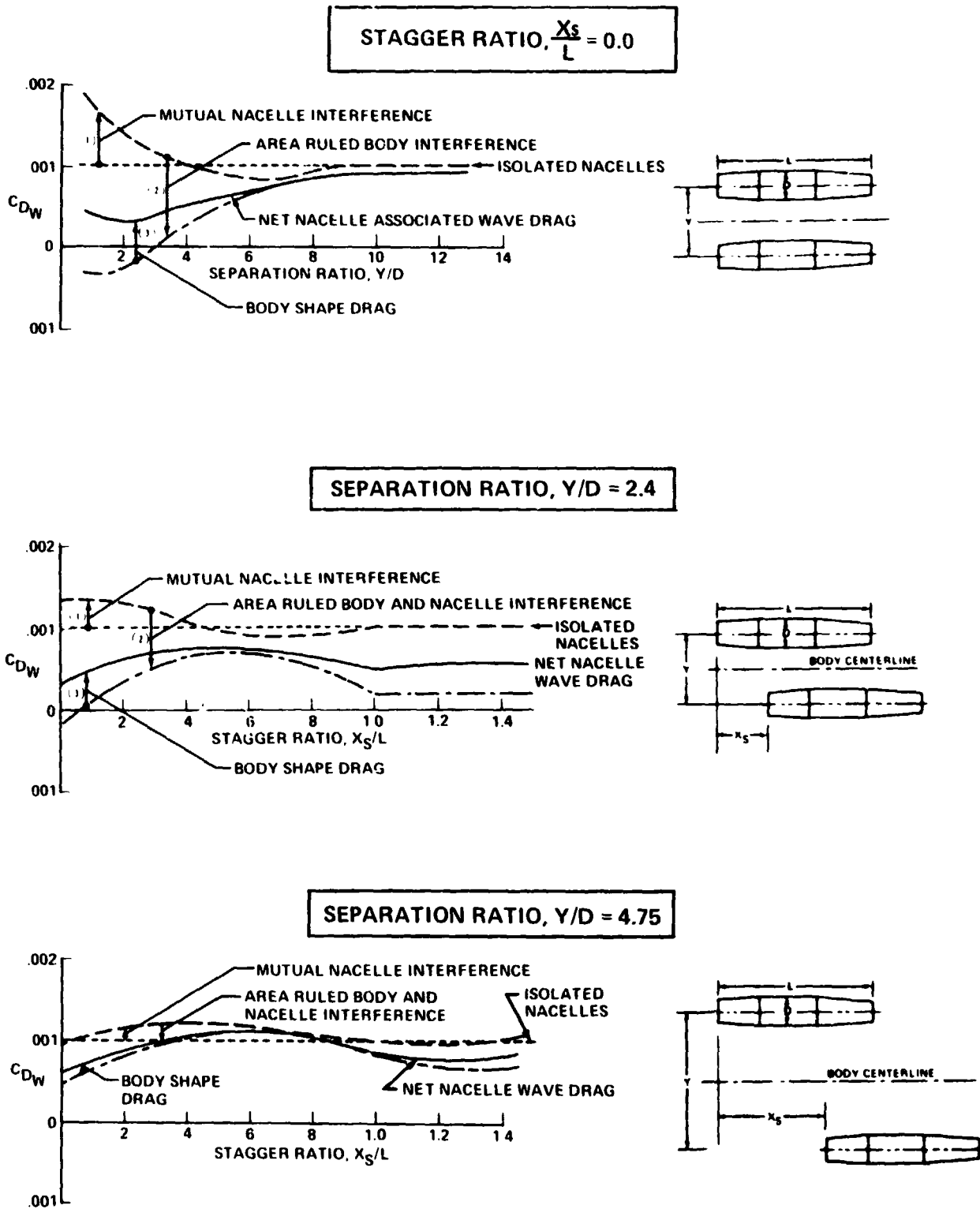


FIGURE 79.—EFFECT OF SEPARATION AND STAGGER ON BODY-MOUNTED NACELLE WAVE DRAG

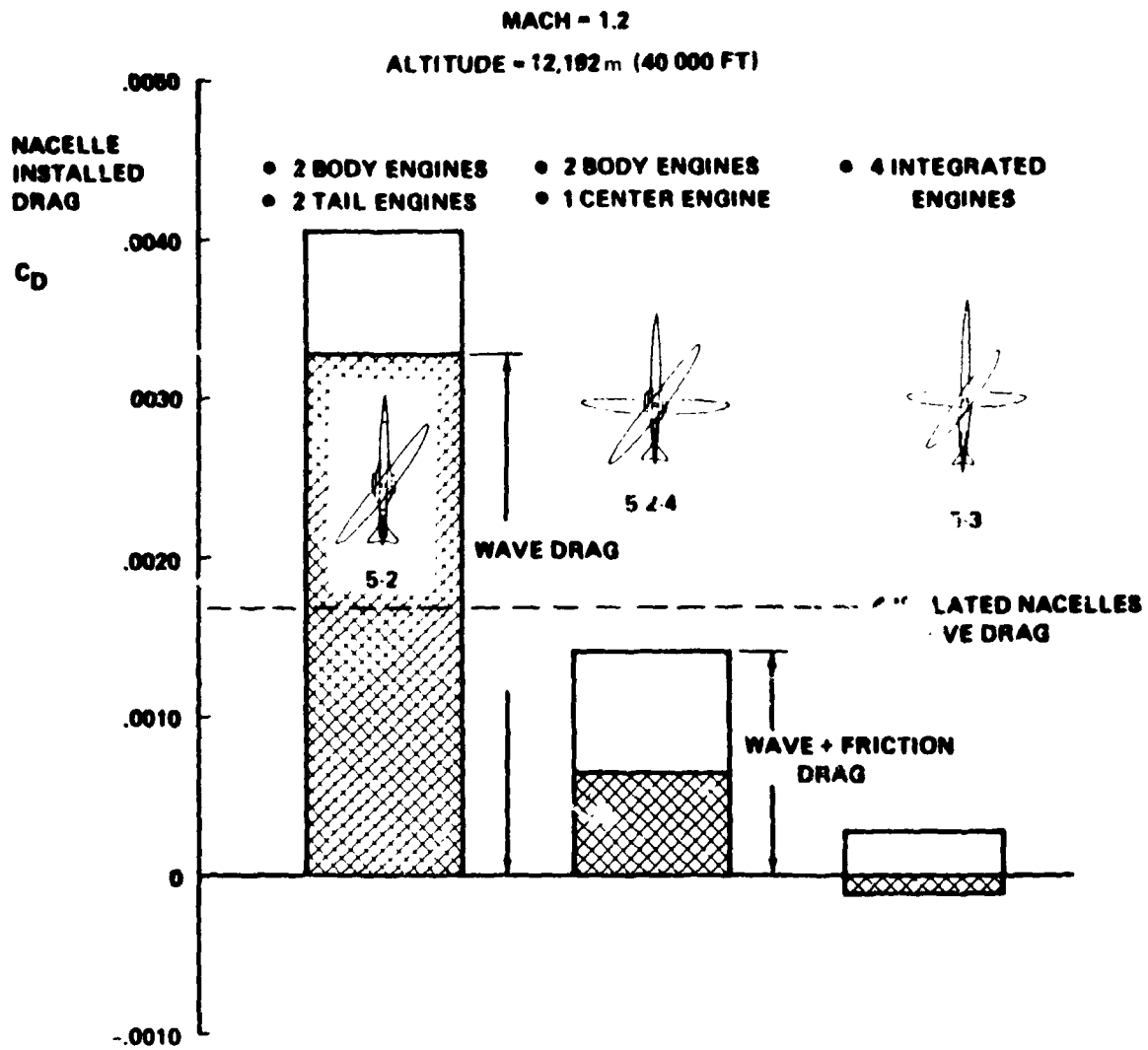


FIGURE 80.—ENGINE ARRANGEMENT EFFECT ON NACELLE INSTALLED DRAG

drag was called "nacelle friction drag." The "nacelle wave drag" included all of the wave drag differences between the integrated engine configuration and "no-engine" configuration.

The integrated nacelle arrangement on model 5-3 achieved a negative installed wave drag. In addition, the friction drag was reduced since the body wetted area was increased by a relatively small amount to contain the engines.

Engine Size Effects

It was necessary to determine the nacelle installed drag variation with engine size as part of the drag scaling input data for the airplane sizing studies.

The effect of engine size on nacelle installed drag for wing-mounted nacelle installation of the delta wing configuration 3-2 is shown in figure 81a. This also represents the effect of engine bypass ratio since the higher bypass ratio engines "look like" large low-bypass ratio engines.

The variation of nacelle installed drag with engine size for a three engine single fuselage yawed wing configuration is shown in figure 81b. The effect of engine size on the integrated nacelle design of model 5-3 is shown in figure 81c.

The installed nacelle drags for these configurations are compared with each other in figure 82. The results shown in these figures indicate that:

- The unfavorable effect of engine size on transonic nacelle drag is most severe for wing mounted installations
- The integrated engine arrangement has very low installed drag for low bypass ratio engines.
- The body mounted nacelle installation is the lowest drag arrangement for large bypass ratio engines.

Quasi-Elliptical Planform Study

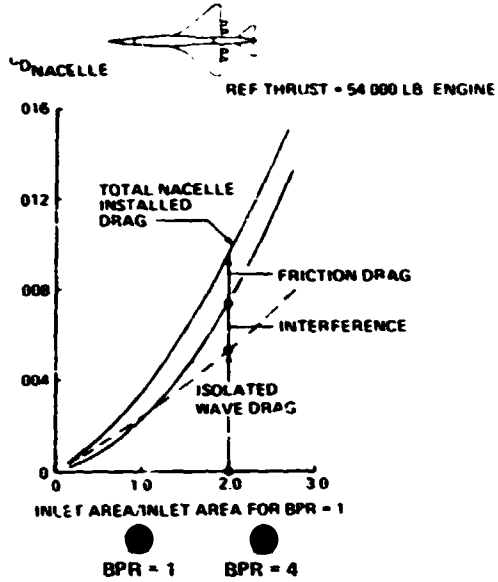
The yawed-wing and body wing tunnel models tested recently at the NASA Ames Research Center, (ref. 5) had quasi-elliptic planforms with a straight 25% chord line. A study has been made to identify the favorable or unfavorable characteristics of such a planform.

Equivalent elliptic axes ratio 8:1 wings ($AR = 10.2$), with the 1/4 chord line straight, and with the planform reversed so that the 3/4 chord line was straight were considered, (fig. 83). The straight 3/4 chord line tends to produce a nearly straight trailing edge. The straight 1/4 chord line produces a more curved trailing edge and a nearly straight leading edge.

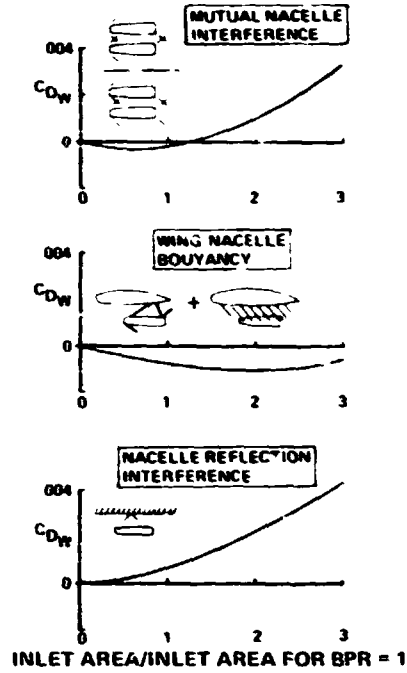
Cruise drag calculations and qualitative structural, and flap design assessments were made for each planform. The results are shown in figure 83.

WING-MOUNTED NACELLES

M = 1.2, ALTITUDE = 12,192 m (40,000 FT)

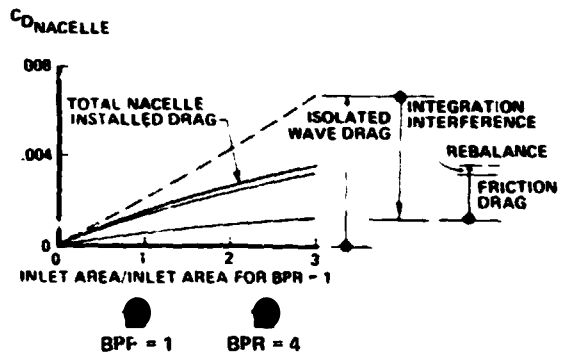


INTERFERENCE COMPONENTS



BODY-MOUNTED NACELLES

MACH = 1.2
ALTITUDE = 12192 m (40 000 FT)



INTEGRATED NACELLES

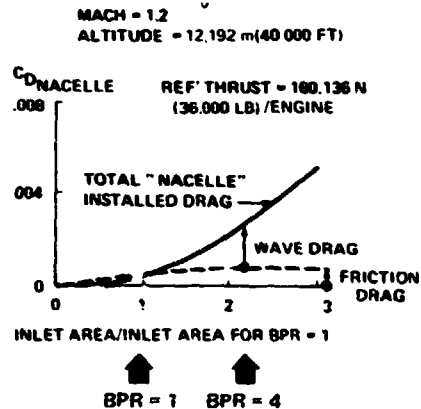


FIGURE 81.—ENGINE SIZE EFFECT ON NACELLE INSTALLED DRAG

M = 1.2 ALTITUDE = 12,192 m (40,000 FT)

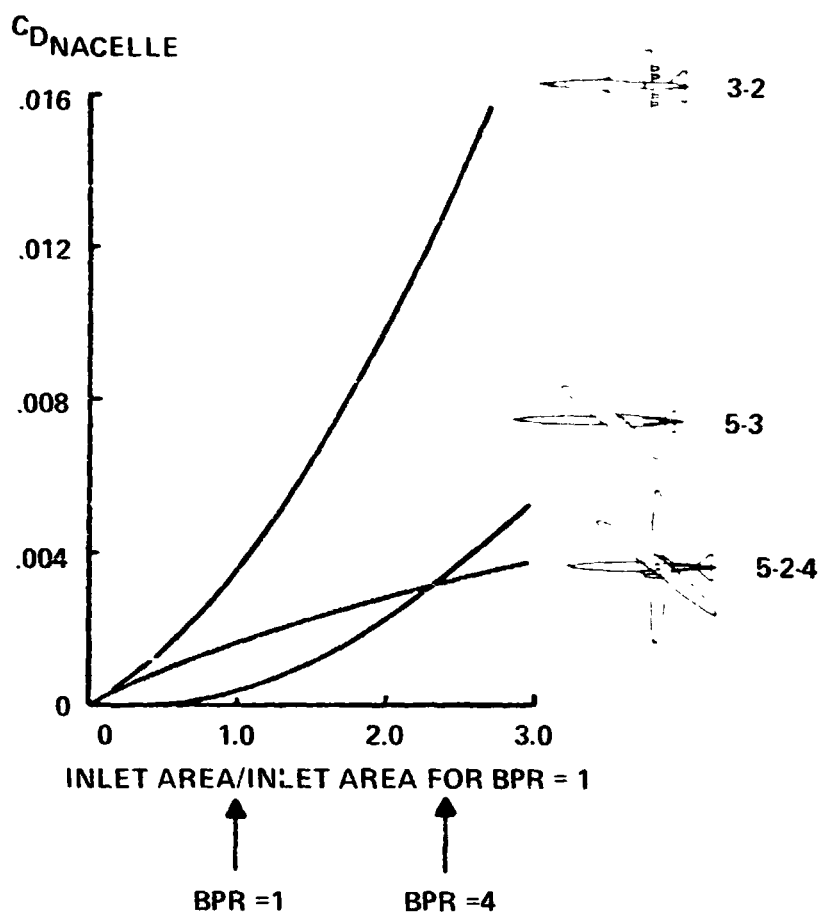
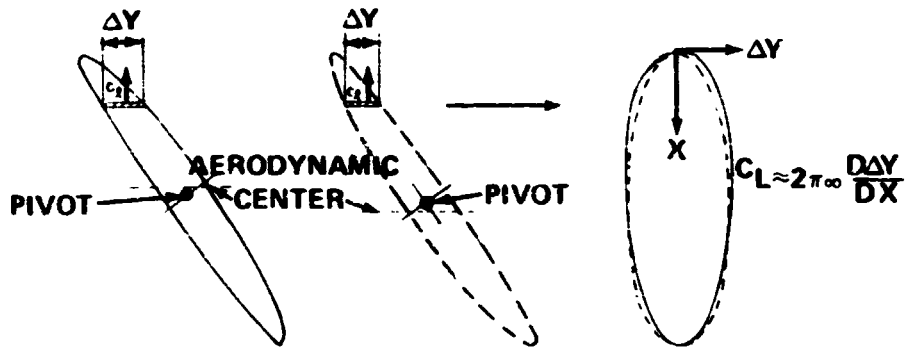
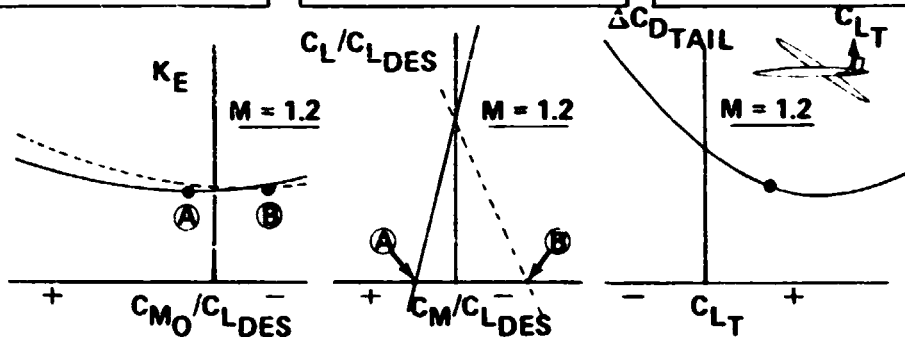


FIGURE 82.- NACELLE INSTALLED DRAG COMPARISON

STRAIGHT 3/4 CHORD PLANFORM **STRAIGHT 1/4 CHORD PLANFORM** **SPANWISE SECTIONAL LIFT**



DRAG DUE TO LIFT FACTOR **WING PITCHING MOMENT** **TAIL DRAG**



CONSIDERATIONS	STRAIGHT 3/4 CHORD	STRAIGHT 1/4 CHORD
TRAILING EDGE FLAP SYSTEM	FAVORED	—
STRUCTURES (ELASTIC AXES SWEEP)		—
CRUISE WAVE DRAG ($M = 1.2$)	$\Delta C_D = .00015$	0.0, (REFERENCE)
CRUISE TRIM DRAG ($M = 1.2$)	—	BEST

FIGURE 83.—QUASI-ELLIPTICAL PLANFORM STUDY

The straight trailing edge arrangement would allow a slightly better trailing flap system. In addition, the straight trailing would tend to sweep the wing elastic axes slightly aft. Neither of these considerations were identified as significant.

The cruise wave drag for the straight 3/4 chord planform is 1.5 drag counts more, ($\Delta C_D = .00015$), than the wave drag of the straight 1/4 chord planform. The minimum drag due to lift potential for each planform were calculated to be about equal. The minimum drag design for the planform with the 1/4 chord line straight produces positive zero lift pitching moment (C_{M_0}). This is generally desirable for trimming the airplane with a horizontal tail developing positive lift.

The pitching moment characteristics for the two 8:1 planforms indicate that at the design lift, ($C_L/C_{L_{des}} = 1.0$), the minimum drag wings produce equal but opposite pitching moments that are very nearly zero.

The aerodynamic center for the straight 3/4 chord planform lies forward of the aerodynamic center location for the straight 1/4 chord line planform. It is this difference in the aerodynamic center locations that accounts for the variations in the pitching moment at zero lift. For equal stability margins, the straight 3/4 chord planform would require a more forward center of gravity location and a tail down load to trim.

The differences in the relative aerodynamic center locations can be visualized by comparison of the equivalent low aspect ratio wing planforms whose local wing span corresponds to width of yawed planforms cut by parallel planes perpendicular to the streamwise direction.

According to slender wing theory, the local spanwise lift coefficient depends on the local rate of change of the span width. The equivalent slender wing for the straight 3/4 chord planform is "fuller" near the leading edge, hence, more lift is produced on the front wing panel. This accounts for the more forward aerodynamic center location for this planform.

The planform with the straight 1/4 chord was selected for the yawed wing configuration because of the wave drag and trim drag considerations.

Model 5-3 Drag Variation With Mach Number

The range variation with cruise speed was calculated for the single-fuselage yawed wing configuration 5-3. This required that:

- The variation of the optimum sweep angle with Mach number be determined.
- Off design cruise drag be calculated at the optimum sweep angles.

Detailed drag calculations were made for each Mach number with the design sweep position of .96 rad (55 deg). The variations of drag due to lift, wing wave drag and wing friction were then calculated by the analytic yawed wing optimization program previously described.

The results of the sweep selection study are shown in figure 84. The optimum sweep for model 5-3 differs very slightly from sweep angle for maximum isolation wing maximum lift/drag ratio. The corresponding normal Mach number is approximately constant and equal to 0.73.

The variation of the cruise drag of model 5-3 with Mach number is shown in figure 85. Maximum lift/drag ratios are shown for the baseline configuration as represented by the design layout in figure 8 and for the configuration sized to achieve the design mission. The maximum lift/drag ratio for the mission sized configuration varies from 20.4 at Mach 0.7 to 11.3 at Mach 1.35.

These maximum lift/drag ratios, $(L/D)_{MAX}$, significantly exceed the L/D ratios for the other configuration concepts in this study. To achieve these theoretical low levels of drag the elliptic wings develop lift near the trailing edges. The possibility of trailing edge separation induced by the pressure gradients near the trailing edge is an area of concern that requires wind tunnel guidance.

FLIGHT CONTROLS

The Flight Controls tasks have included the following:

- Empennage sizing and center of gravity limits—Estimation of horizontal and vertical tail sizes and center of gravity limits that satisfy critical stability and control criteria.
- Flight characteristics analysis—Estimation of static and dynamic stability for selected critical flight conditions.
- Synthesis of a flight control system—Examined briefly a stability augmentation concept for the yawed wing airplane configuration.
- Single fuselage yawed wing configuration development—Assessed the various configurations in terms of the flight controls design criteria.

Design Ground Rules

The study ground rules assumed 1985 state-of-the-art flight controls hardware capability, including fly-by-wire control systems. An all flying stabilizer/geared elevator longitudinal control system was employed to provide adequate control power for the high speed dive recovery maneuver. Longitudinal and lateral-directional stability augmentation systems (SAS) were assumed to be critical for safety of flight, such that the aerodynamic performance of each configuration would not be compromised in order to provide inherent stability. An alpha limiting control system was further assumed to avoid any undesirable high alpha pitch-up or lock-in stall characteristics. The use of an alpha limiter implies that an adequate useable angle of attack range is attainable throughout the flight envelope. This can

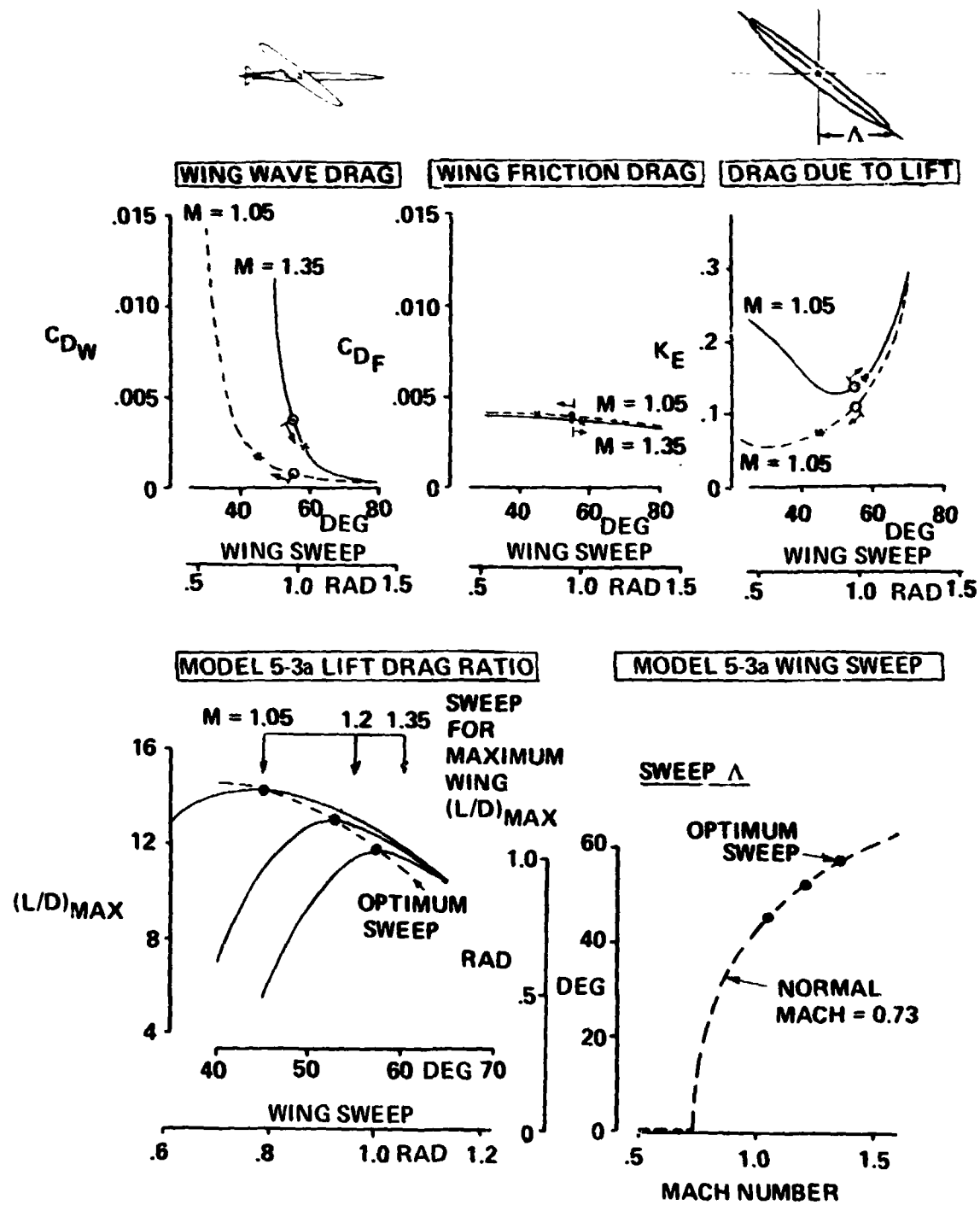


FIGURE 84.—SPEED-SWEEP SELECTION, MODEL 5-3a

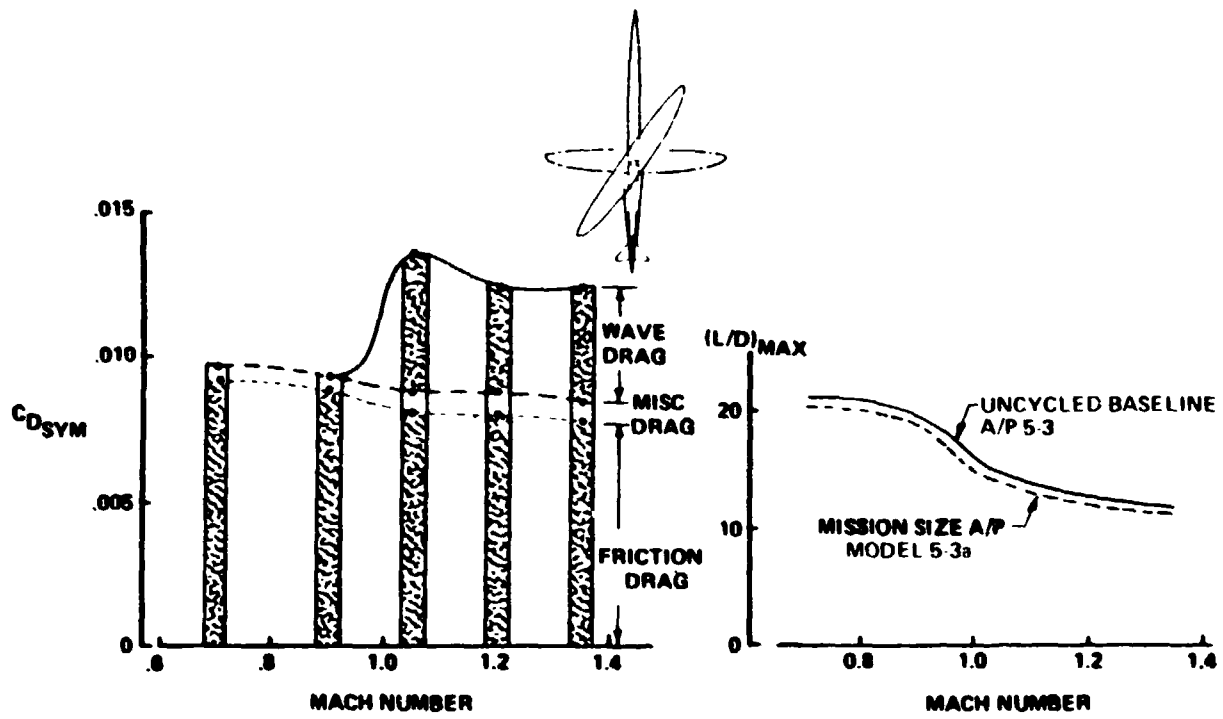


FIGURE 85.—CRUISE DRAG VERSUS MACH NUMBER, MODEL 5-3

be verified only with appropriate complete configuration wind tunnel testing. All the study philosophy ground rules, which involve research and development hardware design items, need to be developed to provide operational systems of high reliability.

Airplane Balance and Empennage Sizing

Design Criteria

In the design of each study configuration, the horizontal and vertical stabilizing and control surfaces were chosen to provide adequate trim and maneuvering capability throughout the flight envelope. The horizontal and vertical tails were sized to provide adequate augmented dynamic stability, takeoff rotation, engine-out control, landing trim and flare capability in addition to sufficient airplane nose down control power to avoid high alpha locked-in stall. A flight critical SAS, comparable to the B2707-300 design, was assumed to assure that the resulting augmented longitudinal and lateral-directional static and dynamic stability characteristics would be acceptable for the airplanes as balanced. The estimation of the stability characteristics necessitated an appraisal of the critical flight condition based on assumed rigid aerodynamic characteristics and aeroelastic properties of each configuration. The study design philosophy (flight critical SAS) resulted in airplanes having inherent aerodynamic characteristics that were statically unstable subsonically but stable for supersonic cruising flight conditions. Engine-out control capability was checked for each study configuration based on the specified takeoff field length and normal operation rotation schedules. Adequate ground steering capability was obtained on those configurations that rotate during takeoff by locating the main gear behind the aft center-of-gravity location so as to maintain three percent of the minimum takeoff weight on the nosewheel.

Longitudinal Analysis

A minimum size horizontal tail, compatible with the required center-of-gravity range and the allowable limits for stability and control, was chosen for each configuration. With a loading range established by weight and balance, adequate trim and control capability at the forward center-of-gravity location was then obtained by the sizing of the stabilizer/elevator system. The Flight Controls aft center-of-gravity stability limit was determined by locating the center-of-gravity aft of the most forward elastic airplane maneuver point encountered in the flight envelope. A preselected margin of -6.6 percent M.A.C. between the aft center-of-gravity and the critical most forward maneuver point was obtained from extensive contractor simulation analyses conducted on the SST. The B2707-300 employed a full-time stability augmentation system judged to be very acceptable by the pilots in stabilizing the minimum operational descent and landing flight conditions at heavy weight, where the aft center-of-gravity location was behind the airplanes unaugmented maneuver point.

The critical most forward elastic maneuver point on configurations 2-2, 3-2, 4-2 and 5-3 was encountered during the low speed approach. At higher Mach numbers, the variable sweep and delta planform rigid wing-body aerodynamic centers moved aft compensating for the increased aeroelastic losses that tend to move the elastic airplane maneuver point forward. The critical elastic maneuver point for the fixed wing configuration 1-2 occurs at a

high subsonic speed where the rigid wing-body aerodynamic center location has not moved aft but where the wing-body and tail aeroelastic losses have moved the airplane elastic maneuver point forward of its low speed location.

The forward center of gravity limit on all configurations was set by trim and flare requirements during the landing approach, flaps down. The horizontal tail planform was selected as a compromise between aerodynamic effectiveness and aeroelastic losses.

Directional Analysis

The vertical tail sizes were chosen to insure acceptable augmented levels of lateral-directional dutch roll dynamic stability during the minimum operational speed flight conditions. In addition, the vertical tail rudder control system was designed to provide adequate engine out control capability during takeoff. From B2707-300 augmentation studies, an unaugmented dutch roll undamped natural frequency ω_n of 2.3 rad/sec was selected as the dynamic stability design requirement. Vertical tail effectiveness, wing body directional instability, sidewash characteristics and inertial properties were then estimated and vertical tail sizes selected for each configuration. Engine-out control capability did not become a vertical tail size designing criteria for any configuration with the engines located relatively close to the fuselage centerline. The vertical tail planforms were selected as a compromise between aerodynamic effectiveness and aeroelastic losses. The airplane balance and empennage sizing criteria are summarized in table 22.






Single Fuselage Yawed Wing Configuration Dynamic Stability and Control Characteristics

The yawed wing airplane introduces unique stability and control characteristics as a result of the bilateral unsymmetric configuration. Because of the inertial and aerodynamic cross-coupling in the airplanes six degrees-of-freedom equations-of-motion, conventional methods of predicting an airplane's dynamic stability characteristics are not applicable to the analysis of the yawed wing airplane.

For airplanes having bilateral symmetry, the six degree-of-freedom equations-of-motion can be conveniently separated into two three degrees-of-freedom sets describing separately the longitudinal and lateral-directional dynamic stability characteristics. The yawed wing introduces inertial and aerodynamic cross-coupling between the equations-of-motion sets. A complete six degrees-of-freedom large disturbance solution of the equations of motion was required to predict the dynamic stability characteristics. These equations included all of the classical non-linear inertial coupling as well as the aerodynamic coupling of the yawed wing.

Aerodynamic strip theory was used to estimate the cross-coupling aerodynamic stability derivatives. In order to present meaningful dynamic response characteristics without defining a specific S_{ref} arrangement, a longitudinal statically stable airplane with a 10% static margin was assumed. The stability and control response characteristics were investigated for the rigid airplane at a subsonic flight condition. The analysis of the rigid yawed wing airplane dynamic stability and control characteristics concentrated on those flight characteristics peculiar to a single fuselage yawed wing configuration. The dynamic

TABLE 22.—AIRPLANE BALANCE AND EMPENNAGE SIZING

CONFIGURATION					
HORIZONTAL TAIL AFT C.G. LIMIT <hr/> FWD C.G. LIMIT	CRITICAL MANEUVER MARGIN AND HIGH ALPHA LOCK-IN AVOIDANCE	CRITICAL MANEUVER MARGIN	CRITICAL MANEUVER MARGIN	CRITICAL MANEUVER MARGIN	
	TAKEOFF ROTATION AND LANDING FLARE IN GROUND EFFECT				
VERTICAL TAIL	LATERAL-DIRECTIONAL DYNAMIC STABILITY CHARACTERISTICS				

stability analysis was conducted to understand the impact of the cross-coupling inertial and aerodynamic forces and moments uniquely associated with a yawed wing configuration.

Aerodynamic Cross-Coupling

The longitudinal/lateral aerodynamic coupling for a yawed wing airplane with the left wing forward, right wing aft, in a positive airplane nose-up pitch maneuver is shown in figure 86. In addition to the aerodynamic rolling moment resulting from sideslip, aileron and rudder deflections, roll rate and yaw rate, the bilaterally unsymmetric yawed wing airplane will also experience an aerodynamic rolling moment resulting from pitch rate. As a result of the positive pitch rate about the y-axis, the trailing wing pitching down sees an incremental increase in angle of attack and lift. The leading wing pitching up experiences an opposite incremental decrease in lift. A negative aerodynamic couple about the rolling x-axis, is therefore produced as shown.

The yawed wing airplane will experience an incremental pitching moment due to roll rate, yaw rate and aileron deflection in addition to the applied aerodynamic pitching moment which results from angle of attack, time rate-of-change of angle-of-attack and pitch rate. As shown in figure 87, in a positive roll maneuver (right wing down) about the x-axis, the trailing down going wing sees an incremental increase in lift while the forward up going wing sees an incremental decrease in lift producing an aerodynamic coupling about the y-axis. Furthermore, an incremental pitching moment is produced when the airplane is yawed about the z-axis. This pitching moment is a result of the increase in the normal velocity component on the left forward moving wing and decreases in the normal velocity component on the trailing rearward moving wing. This phenomenon is more commonly associated with the rolling moment which results from a yaw rate on conventional symmetric airplanes. A positive antisymmetrical deflection of the aileron controls will also produce a significant negative nose down pitching moment on the yawed wing airplane. An opposite (negative) aileron deflection will produce a positive nose up pitching moment. Consequently, rolling the airplane right or left results in an opposite transient coupled response with the yawed wing airplane. However, when a steady state roll rate is obtained, the pitching moment produced by the ailerons is effectively cancelled by the opposing pitching moment produced by the roll rate.

When a conventional swept wing airplane is sideslipping positively, the normal component of velocity on the leading wing is increased while the trailing wing normal component of velocity is decreased. The associated increase in leading wing lift and decrease in trailing wing lift produces a rolling moment (dihedral effect), with no change in the resultant total wing lift. However, the yawed wing in positive sideslip experiences a net increase in total wing lift with no resulting rolling moment because now both the leading and trailing wing panels see the same increase in the normal component of velocity. Conversely, negative sideslipping produces a net decrease in wing lift with the left wing forward as shown in figure 88.

Prediction of NASA Ames Yawed Wing Model Airplane Maneuvers

A radio controlled model of a single fuselage yawed wing design has been flown at the NASA Ames Research Center. A simulation was made of the elevator loop and aileron roll

ROLLING MOMENT

$$\frac{L}{\bar{q}_0 S b} = C_{l\beta} + C_{l\delta_a} \delta_a + C_{l\delta_R} + C_{l\hat{p}} \hat{p} + C_{l\hat{r}} \hat{r} + \boxed{C_{l\hat{q}}} \hat{q}$$

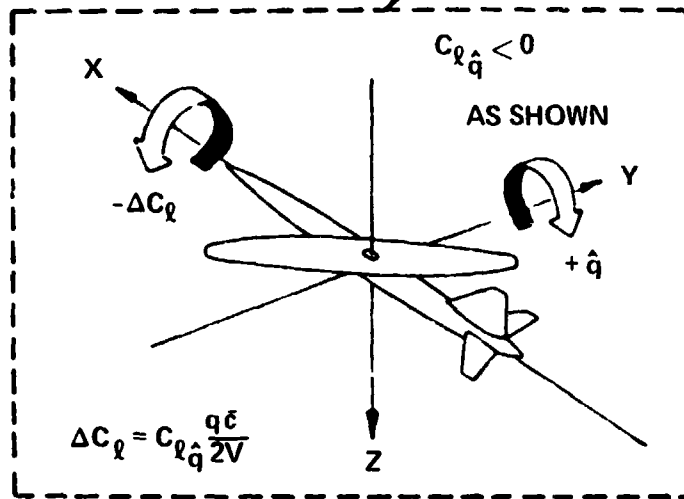


FIGURE 86.—YAWED WING AERODYNAMIC ROLLING MOMENT CROSS-COUPLED STABILITY DERIVATIVE

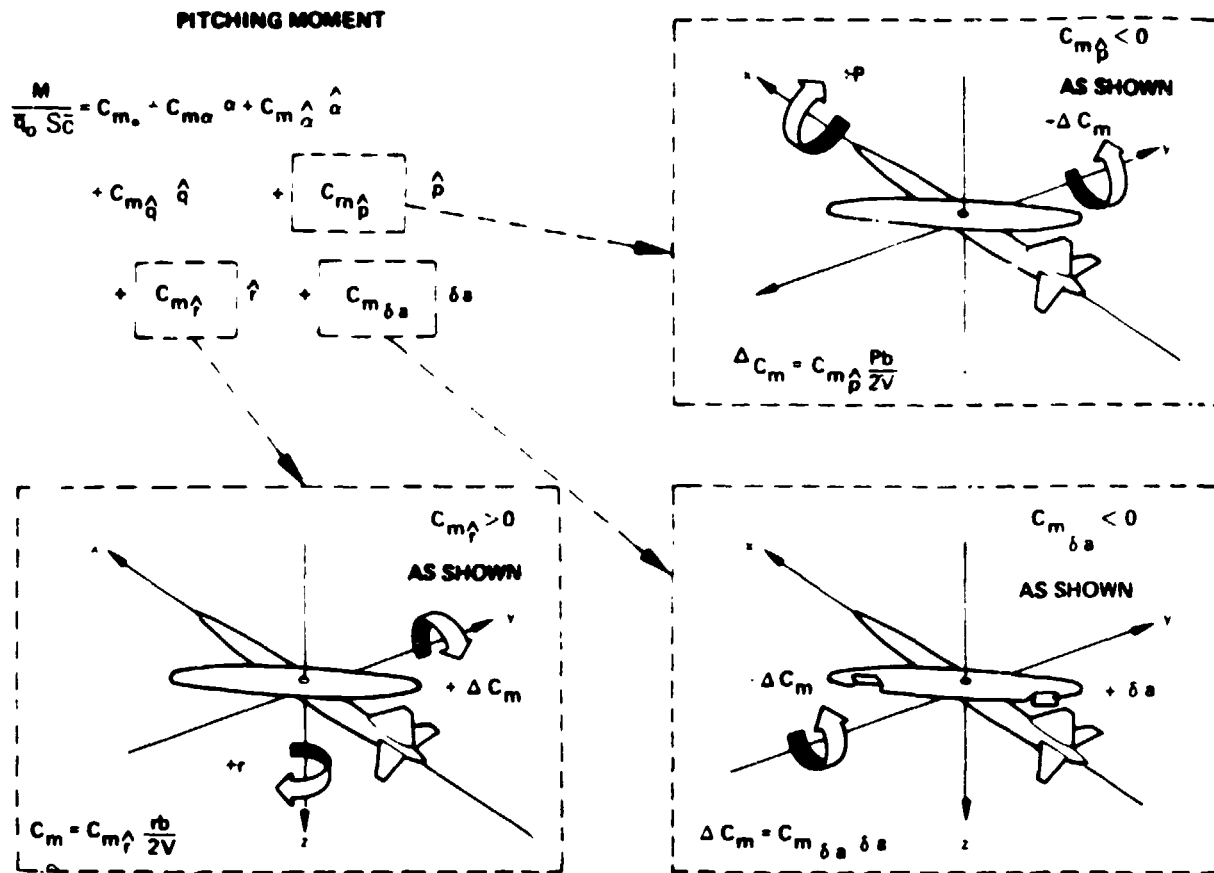


FIGURE 87.—YAWED WING AERODYNAMIC PITCHING MOMENT CROSS-COUPLING STABILITY DERIVATIVES

LIFT FORCE

$$\frac{F_Z}{q_0 S} = C_{Z_0} + C_{Z_\alpha} \alpha + C_{Z_\beta} \beta + C_{Z_{\dot{\beta}}} \dot{\beta} + C_{Z_{\delta_e}} \delta_e + C_{Z_q} \dot{q} + \boxed{C_{Z_\beta} \beta}$$

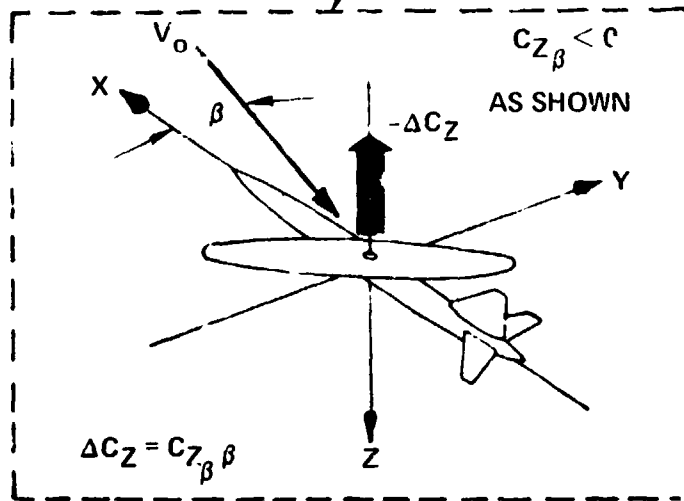


FIGURE 88.—YAWED WING AERODYNAMIC LIFT FORCE CROSS COUPLING

large disturbance maneuvers performed by NASA's airplane as a preliminary step in determining the dynamic stability characteristics of the yawed wing configuration. This simulation included the complete nonlinear equations of motion including aerodynamic and inertia cross-coupling terms. A transport type aircraft, however, would never be required to perform these maneuvers. These maneuvers are presented to illustrate the impact of the cross-coupling aerodynamic forces and moments.

With sufficient thrust available, the more conventional bilaterally symmetric airplane's response to a step elevator command is a loop in the x-z plane (fig. 89). The yawed wing airplane's response to an elevator step input is a "helical loop," a steady state pitching/rolling maneuver in which the airplane pulls up, rolls left and translates sideways in the x-y plane following a flight path about a cylinder whose axis is aligned with the yawed wing sweep angle (fig. 90). During the "helical loop," the airplane essentially rotates about its swept wing axis at a rate equal to the vector sum of the steady state pitch and roll rates about the x and y axes, respectively. The roll rate participation involved and the corresponding orientation of the cylindrical flight path in the x-y plane are proportional to the pitch rate developed and the yawed wing sweep angle, (fig. 91). The aerodynamic cross-coupling between the roll and pitch axes is a direct result of the rolling moment produced by the wing as it is pitched, as discussed previously. The essence of the steady state helical loop maneuver lies in the balance obtained between the applied aerodynamic rolling moments which result from the elevator induced pitch rate and the resistance of roll rate. The small pitch and roll angular accelerations present in the time history display reflect the increasing tightness of the loop as the step elevator command was not removed and the airplane slows down.

Another large disturbance maneuver flown with the radio controlled yawed wing model was an aileron roll (fig. 92). The computer simulation illustrates, as does the flying model, that the yawed wing airplane rolls with very little pitch involvement. The aileron roll demonstrates how quickly the pitching moment developed by the wing in roll cancels the pitching moment initially produced by the antisymmetric deflection of the ailerons. A complete 360 degree roll maneuver to the left is accomplished in eleven seconds. The maximum steady state roll rate is attained within one second of full aileron control deflection. However, before the steady state roll rate can be obtained the positive aileron deflection produces a nose down pitch rate and an incremental load factor $\Delta N_z = .4g$'s. As the steady state roll rate is obtained the aileron pitching moment is effectively cancelled by the pitching moment induced by roll rate. Conversely, a roll to the right results in a positive incremental load factor $\Delta N_z = +.3g$'s. The difference in the airplane's response to right and left roll maneuvers will be important in the flight control system synthesis. The motion following the transient response includes all the inertial and aerodynamic cross coupling forces and moments contained in the classical equations of motion.

Dynamic Stability and Control Response Characteristics

The yawed wing longitudinal dynamic stability characteristics include lateral-directional motion participation due principally to the aerodynamic cross coupling forces and moments. The response to an elevator control pulse illustrates a high frequency well damped motion comparable to the 747, (fig. 93). However, due to the rolling moment induced by the pitch rate, the motion also exhibits a lateral response in phase with the

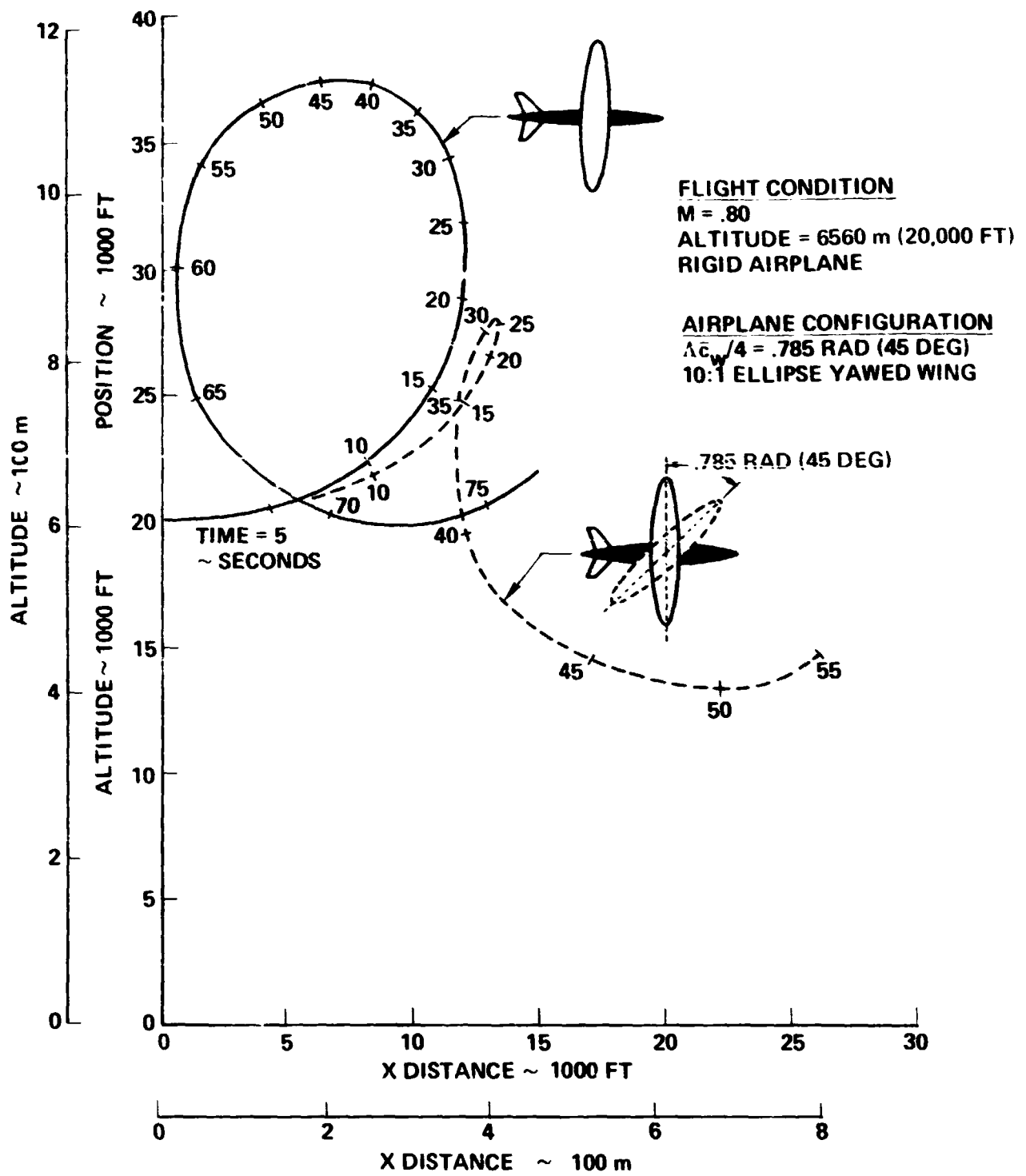


FIGURE 89.—YAWED WING AIRPLANE ELEVATOR LOOP MANEUVER—SIDE VIEW

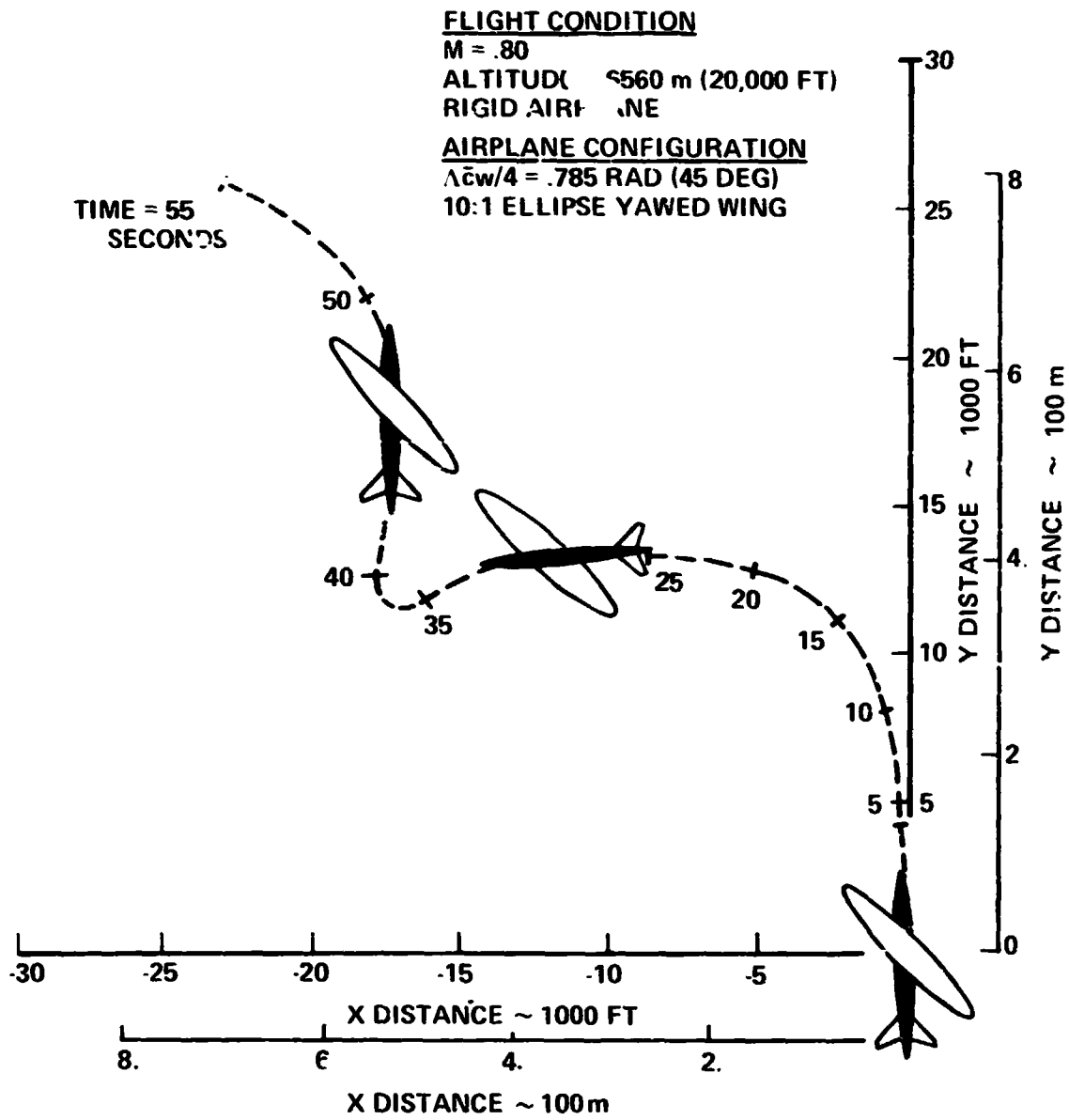


FIGURE 9C - YAWED WING AIRPLANE ELEVATOR LOOP MANEUVER - TOP VIEW

FLIGHT CONDITION

M = .80

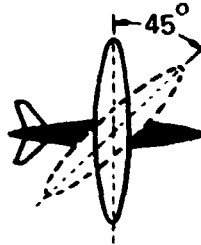
ALTITUDE = 6560 m (20,000 FT)

RIGID AIRPLANE

AIRPLANE CONFIGURATION

$\Delta w/4 = .785$ RAD (45 DEG)

10:1 ELLIPSE YAWED WING



— $\Delta W = 0^\circ$ RAD (0 DEG)
- - - $\Delta W = .785$ RAD (45 DEG)

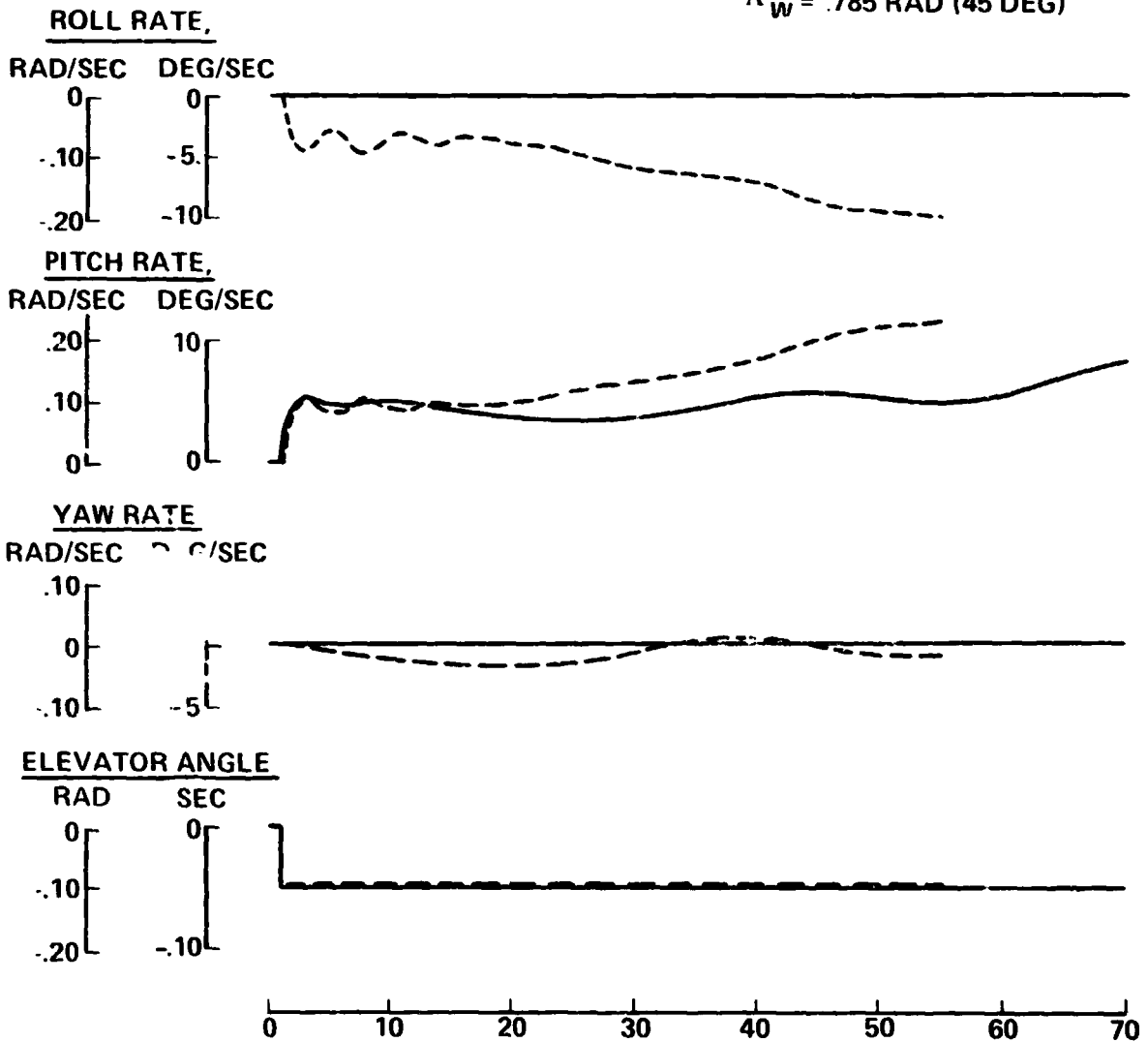


FIGURE 91. - YAWED WING AIRPLANE ELEVATOR LOOP MANEUVER-TIME HISTORY

FLIGHT CONDITION

$M = .80$
 ALTITUDE = 6560 m (20,000 FT)
 RIGID AIRPLANE

AIRPLANE CONFIGURATION

$\Lambda_{cw}/4 = .785 \text{ RAD (45 DEG)}$
 10:1 ELLIPSE YAWED WING

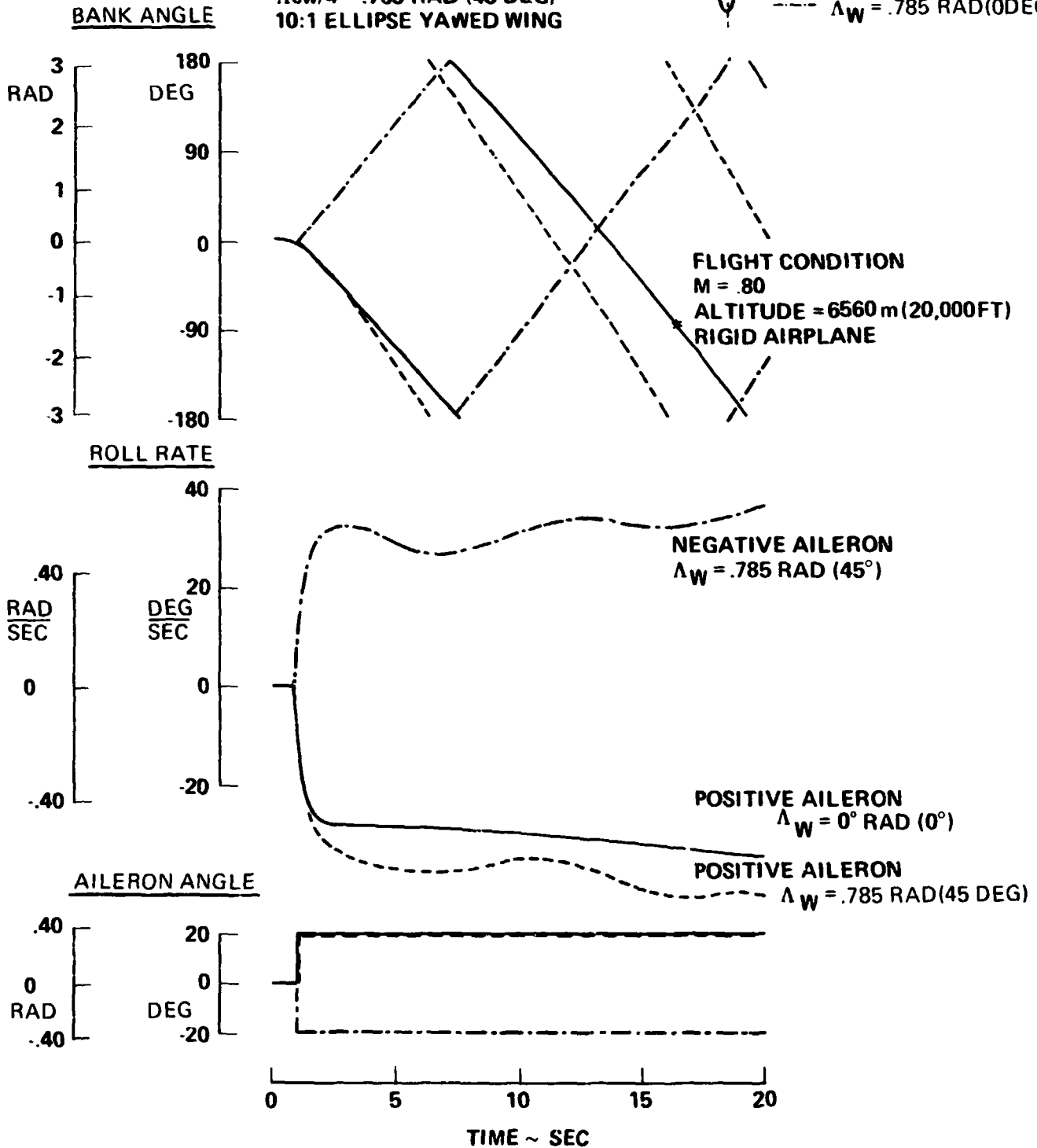
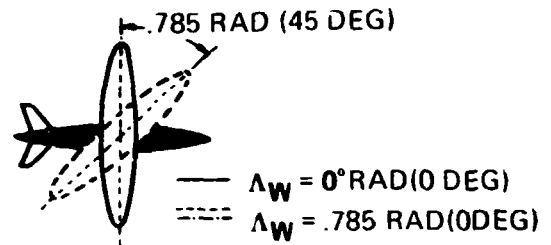
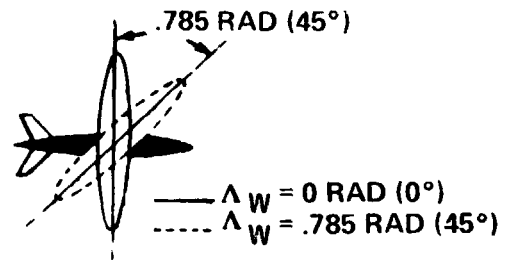


FIGURE 92.—YAWED WING AIRPLANE AILERON ROLL-TIME HISTORY

FLIGHT CONDITION

M = .60
 ALTITUDE = 4900 m (15 000 FT)
 RIGID AIRPLANE



AIRPLANE CONFIGURATION

$\Lambda_{CW/4} = .785 \text{ RAD } (45 \text{ DEG})$
 10:1 ELLIPSE YAWED WING

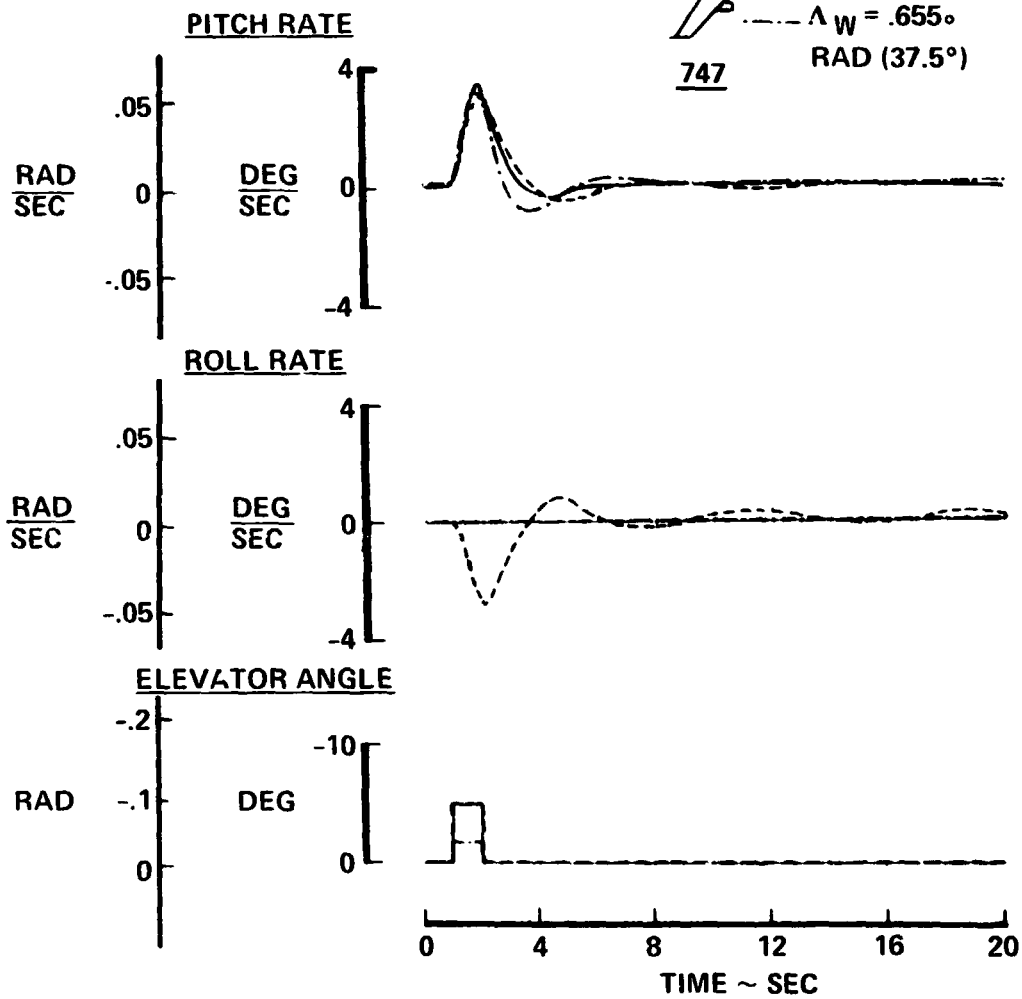
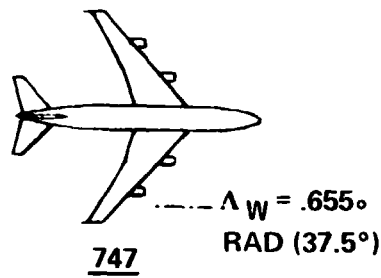


FIGURE 93.—YAWED WING AIRPLANE RESPONSE TO ELEVATOR CONTROL—SHORT PERIOD MOTION

longitudinal response. The induced roll rate produces a bank angle variation which results in an immediate heading change. The impact of the cross-coupling aerodynamic moments is apparent. The stability derivatives that were used for this simulation are shown in table 23. The flight control system of a yawed wing configuration must interconnect the longitudinal and lateral controls to maintain acceptable flying qualities. An example of the pitch/roll aerodynamic coupling is apparent in the low frequency lightly damped phugoid motion resulting from the elevator pulse, (fig. 94). As the pitch attitude changes, corresponding changes in bank and heading angles follow.

The lateral-directional dynamic stability and response characteristics (Dutch roll motion) of the straight wing configuration are very comparable to the 747 except for the lack of roll participation, (fig. 95). As was pointed out earlier, the yawed wing airplane does not develop a rolling moment when sideslipped due to wing sweep as do conventional airplanes. However, a small rolling moment due to sideslip does exist due to the upflow about the body in sideslip of this high wing configuration. As the yawed wing configuration increases its wing sweep, the aerodynamic resistance to rolling is decreased allowing more roll participation in the lateral-directional motion. However, as the roll participation (roll rate) increases with wing sweep, pitching moment induced from the roll rate is also increased. Consequently, in addition to the yawing and rolling accelerations felt by the passengers, a significant vertical acceleration would be apparent due to coupled pitch response, (fig. 96). Coupled axes motion response to control inputs may require a decoupling augmentation system for passenger comfort.

Conceptual Stability Augmentation Arrangement

As seen from the dynamic response characteristics of the yawed wing airplane, the yawed wing flight control system may be required to decouple the applied and induced cross-coupling aerodynamic forces and moments. The conceptual augmentation arrangement displays the conventional control system elements, figure 97. The longitudinal and lateral directional flight critical SAS feeds back forward velocity and pitch rate through the stabilizer, roll rate through the ailerons and side acceleration and yaw rate through the rudder. The feed forward control augmentation arrangement illustrates the interconnecting of the controls required to provide only pitch response to a stabilizer command and roll response to an aileron command. To ensure decoupled axes response, the decoupling stability augmentation system will feedback roll and yaw rate through the stabilizer with pitch and yaw rate feedback through the aileron. As with current Boeing airplanes, the flight control system would be designed such that normal operating maneuvers would not require rudder control coordination. The basic augmentation arrangement without the decoupling is essentially the B2707-300 design. The flight control system required for the yawed wing airplane would require additional design effort to synthesize the flight critical SAS, feed forward interconnecting control surfaces and the decoupling augmentation elements without saturating the control authority. This system would require more development than that necessary for a symmetrical airplane, but it is believed to be entirely feasible.

TABLE 23.—SINGLE FUSELAGE YAWED WING CONFIGURATION,
5-5 AERODYNAMIC DATA (RIGID)

PARAMETER	UNITS	$\Lambda_W = 0^\circ$	$\Lambda_W = 45^\circ$
C_{x_0}		- 0124	- 0121
C_{z_0}		044	044
C_{z_α}	1/DEG	- 114	- 076
C_{m_0}		.031	031
C_{m_α}	1/DEG	- 0114	- 0076
C_{y_β}	1/DEG	- 0061	- 0061
C_{n_β}	1/DEG	00074	00103
C_{l_β}	1/DEG	- 00063	- 00105
C_{z_α}	1/RAD	-0.83	-1.05
C_{m_α}	1/RAD	-3.35	-4.25
$C_{z_\dot{q}}$	1/RAD	-2.06	-2.06
$C_{m_\dot{q}}$	1/RAD	-8.3	-37.0
$C_{l_\dot{q}}$	1/RAD	0	-3.54
$C_{y_\dot{r}}$	1/RAD	.152	.215
$C_{n_\dot{r}}$	1/RAD	- .049	- .105
$C_{l_\dot{r}}$	1/RAD	.058	.070
$C_{m_\dot{r}}$	1/RAD	0	.383
$C_{y_\dot{p}}$	1/RAD	- .039	- .055
$C_{n_\dot{p}}$	1/RAD	.0115	.0230
$C_{l_\dot{p}}$	1/RAD	- .600	- .425
$C_{m_\dot{p}}$	1/RAD	0.	-3.54
$C_{n_{\delta_a}}$	1/DEG	0	0.
$C_{l_{\delta_a}}$	1/DEG	- .00224	- .00133
$C_{m_{\delta_a}}$	1/DEG	0.	- .0111
$C_{y_{\delta_r}}$	1/DEG	00256	00256
$C_{n_{\delta_r}}$	1/DEG	- .00077	- .00109
$C_{l_{\delta_r}}$	1/DEG	.00019	.00028
$C_{z_{\delta_e}}$	1/DEG	- .00222	- 00222
$C_{m_{\delta_e}}$	1/DEG	- .009	- .009

MACH = 6
 ALTITUDE = 4572 m (15,000 FT)
 $S_{REF} = 465 \text{ m}^2$ (5000 FT²)
 $\bar{c} = 6.5 \text{ m}$ (21.4 FT)
 $b_{REF \Lambda=0} = 76.8 \text{ m}$ (252 FT)
 $b_{REF \Lambda=45} = 54.3 \text{ m}$ (178 FT)
 LONGITUDINAL STABILITY BASED
 ON 10% STABILITY MARGIN
 $S_H = 51.6 \text{ m}^2$ (555 FT²)
 $S_V = 33.9 \text{ m}^2$ (365 FT²)
 $\bar{V}_H = .45$
 $\bar{V}_V = .034$ BASED ON $\bar{c}_W/4$ TO $\bar{c}_{TAIL}/4$

FLIGHT CONDITION

M = .60

ALTITUDE = 4572 m (15,000 FT)

RIGID AIRPLANE

AIRPLANE CONFIGURATION

$\Delta c_w/4 = .785 \text{ RAD (45 DEG)}$

10:1 ELLIPSE YAWED WING

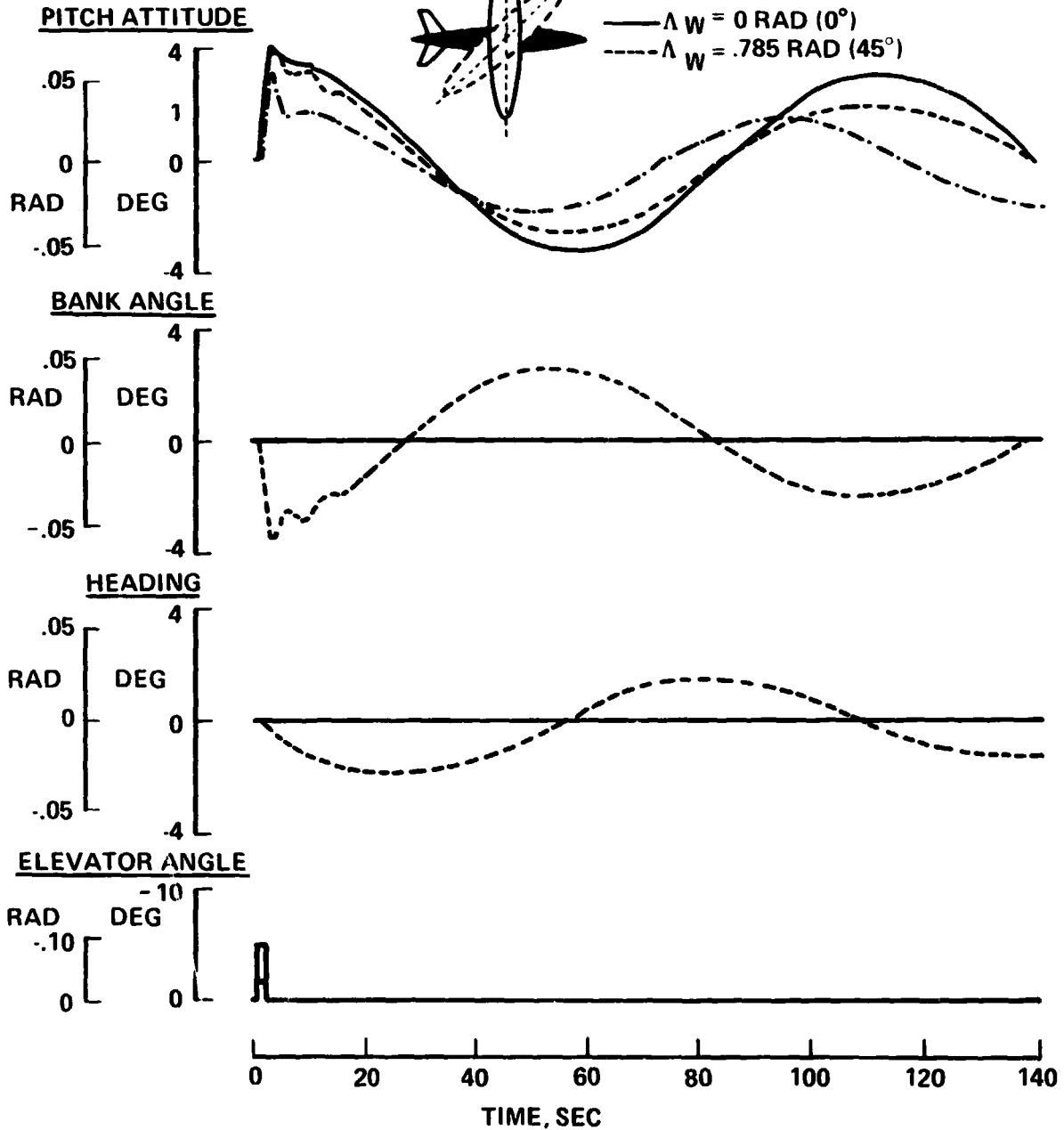
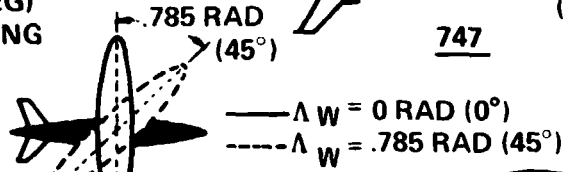
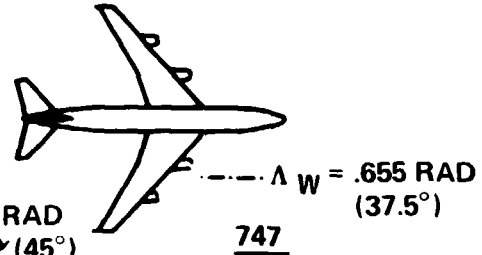


FIGURE 94.—YAWED WING AIRPLANE RESPONSE TO ELEVATOR CONTROL—PHUGOID MOTION

FLIGHT CONDITION

M = .60
 ALTITUDE = 4752 m (15 000 FT)
 RIGID AIRPLANE
AIRPLANE CONFIGURATION
 $\Delta CW/4 = .785 \text{ RAD (45 DEG)}$
 10:1 ELLIPSE YAWED WING

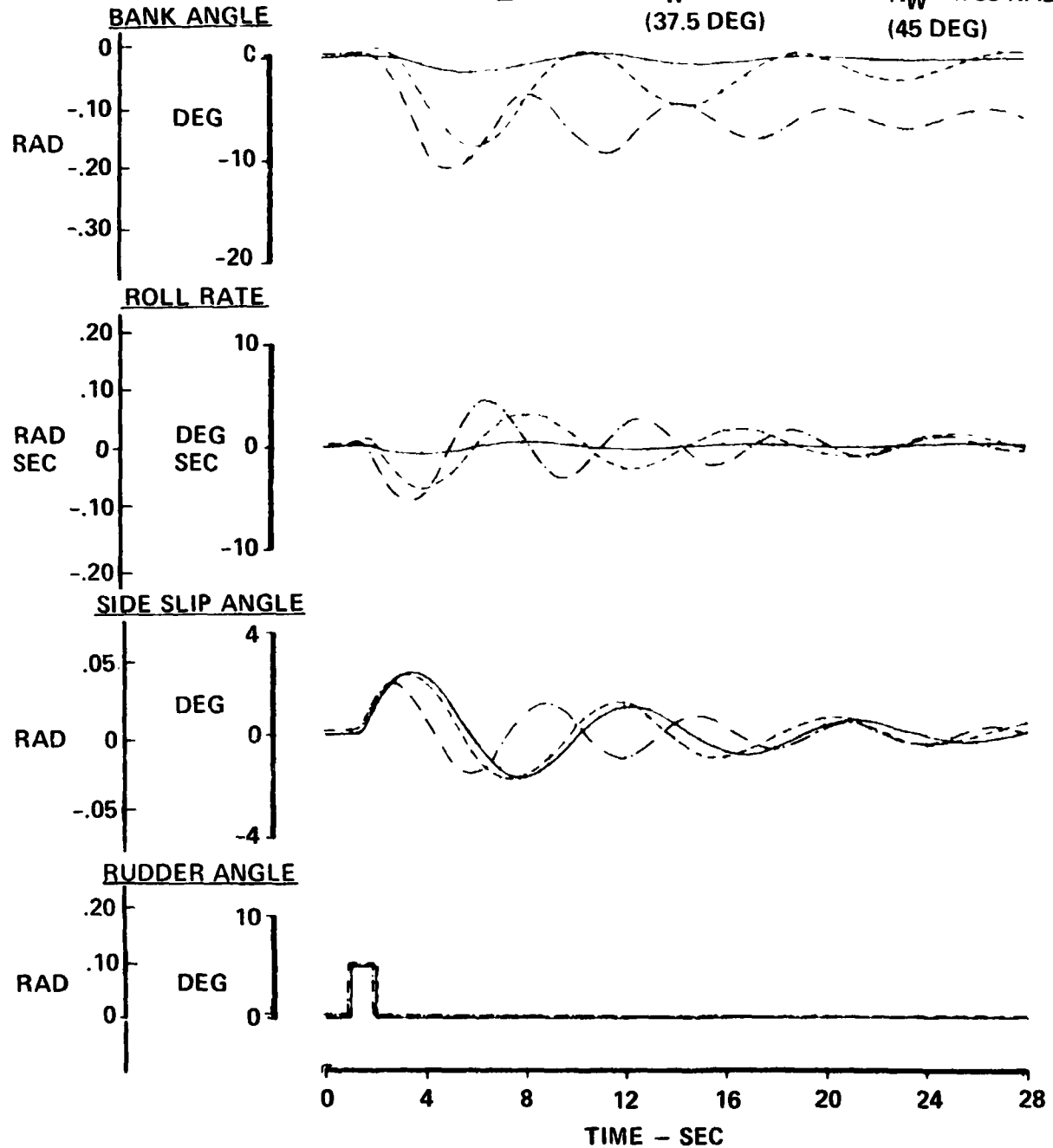
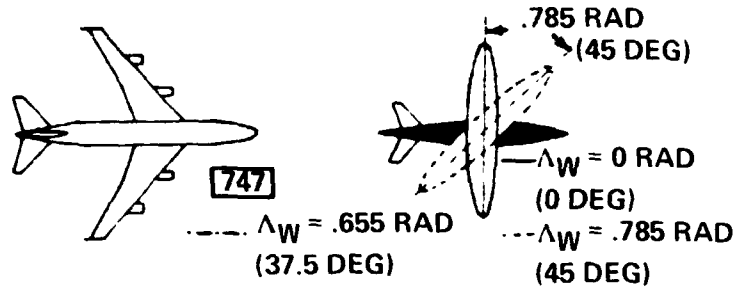


FIGURE 95. -YAWED WING AIRPLANE RESPONSE TO RUDDER CONTROL - DUTCH ROLL MOTION

FLIGHT CONDITION

M = .60

ALTITUDE = 4572 m (15,000 FT)

RIGID AIRPLANE

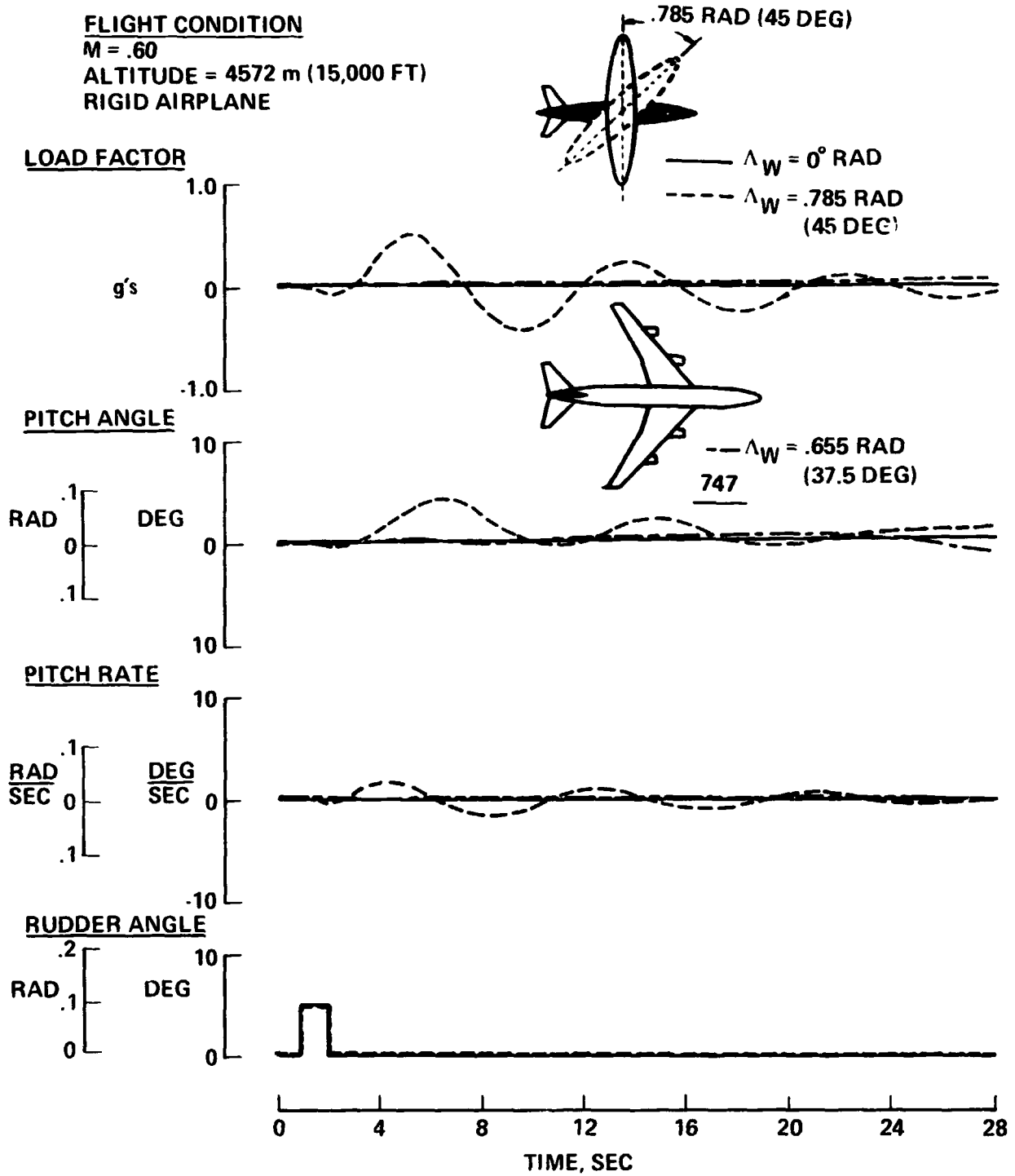


FIGURE 96.—RUDDER RESPONSE—DUTCH ROLL MOTION

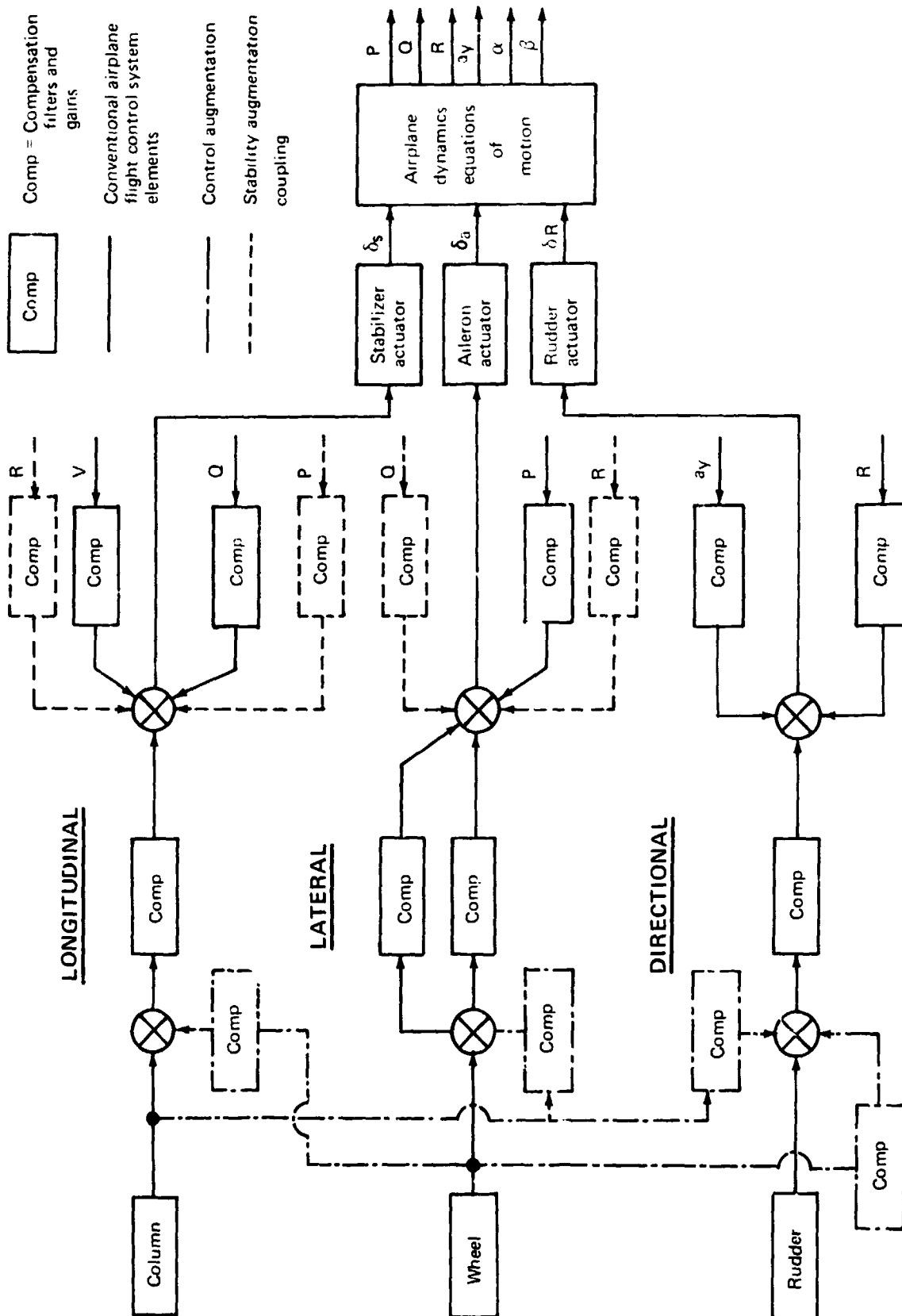


FIGURE 97.—CONCEPTUAL STABILITY AUGMENTATION AND CONTROL COORDINATION ARRANGEMENT FOR A YAWED WING AIRPLANE

POWER SYSTEMS AND ENVIRONMENTAL CONSIDERATIONS

The power systems and environmental considerations tasks included the following work:

- Propulsion system engine and installation data were developed to be consistent with advanced aircraft concepts suitable for use in the mid 1980 time period. These data were developed to a level sufficient to enable trade study evaluation of the impact of engine cycle, noise and installation effects on the overall performance of the aircraft concepts.
- An assessment was made of the current state of the art with respect to achievement of the desired environmental and propulsion performance requirements and an identification was made of technology areas requiring additional research and development.

Bare Engine Data

The engine performance, size and weight characteristics incorporated with the airplane studies were obtained from a computerized Advanced Transonic/Subsonic parametric engine family that was tailored to be representative of advanced technology engines designed for a specified time period. Each parametric engine is identified by using the thermodynamic cycle parameters of design cruise bypass ratio, maximum turbine inlet temperature, and design cruise overall compressor pressure ratio.

Figure 98 illustrates the basic engine weight characteristics of the ATT technology study engines. The base curve shows engine thrust to-weight plotted both against year into service and against engine bypass ratio. The data points on this curve illustrate engine trends for those engines typical of current airplanes. The thrust-to-weight values for two 1980 engines proposed by the engine manufacturers involved in the ATT Study are also shown along with projected engines which might be available for the 1985 time period.

Figure 99 shows a similar plot evaluating uninstalled cruise SFC. This illustrates the SFC trends for the "ATT-Technology" engines used in the current Mach 1.2 contract. The engines that have been used in the present study are seen to be consistent with those projected by the engine manufactureres under the ATT contract.

Propulsion System Candidates

Figure 100 shows 15 study engines which have been used in the NASA Mach 1.2 airplane studies. Five bypass ratios were considered. For each of these the other cycle parameters: overall pressure ratio and turbine entry temperature were fixed at values of 16 and 3000°R respectively as shown on the figure. The engine cycle and nacelles were configured to represent mixed-exhaust-system installations. Preliminary indications had shown potential benefits in the area of weight for the mixed-exhaust configurations as opposed to separate exhausts. The first five nacelles shown, designated as engine family A, had no noise constraint imposed on these installations. However, each of the nacelles shown

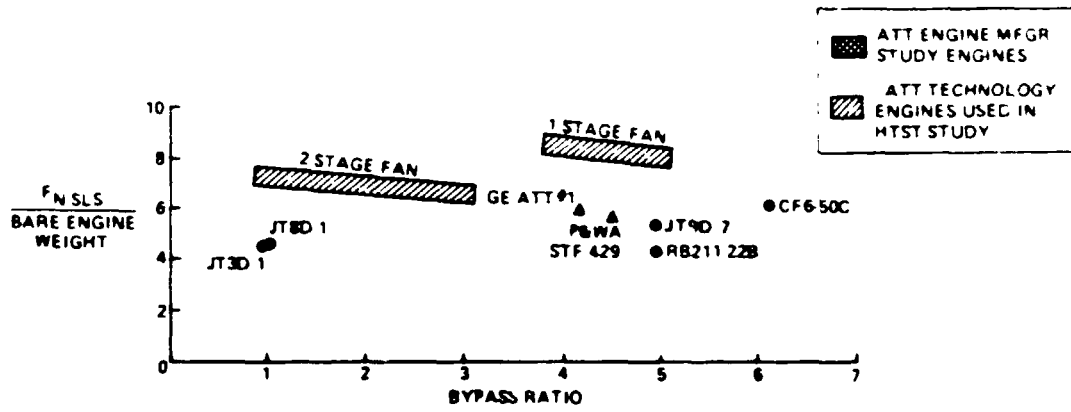
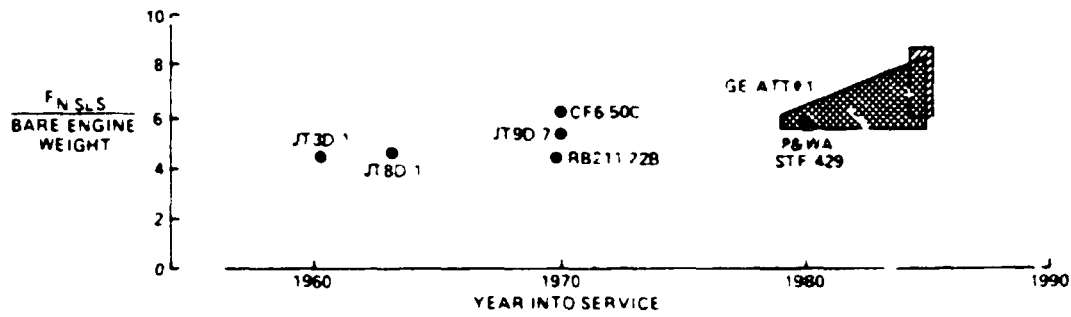


FIGURE 98.—ENGINE THRUST-TO-WEIGHT TRENDS

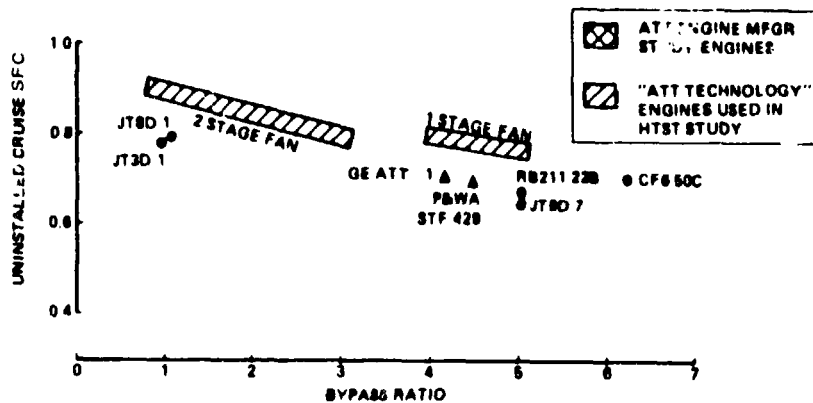
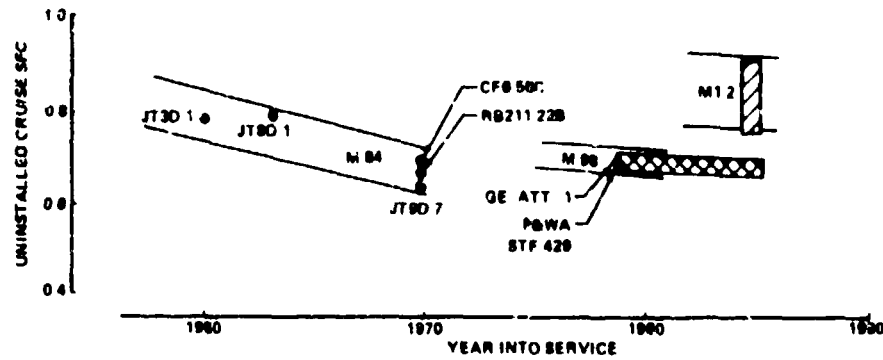


FIGURE 99.—ENGINE SFC TRENDS

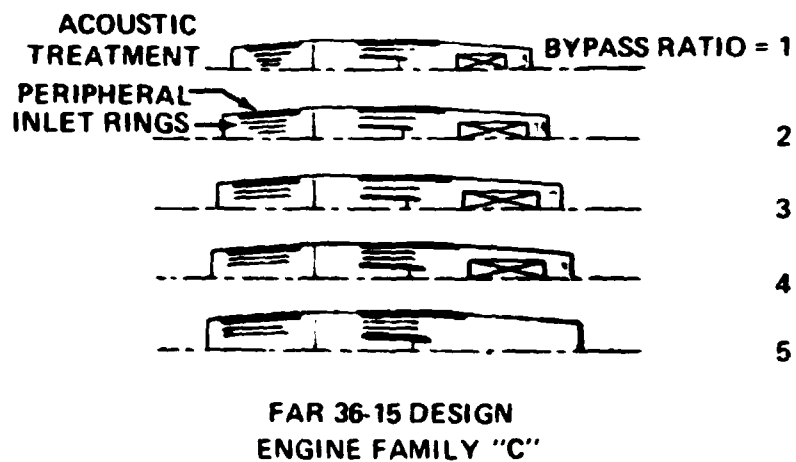
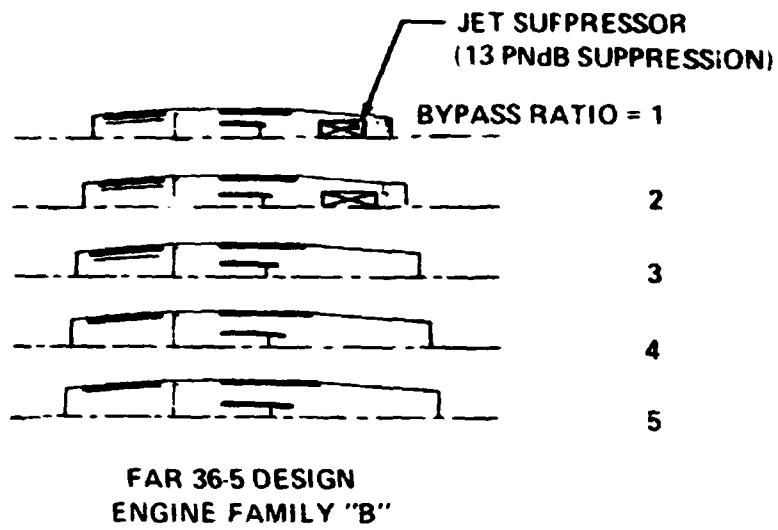
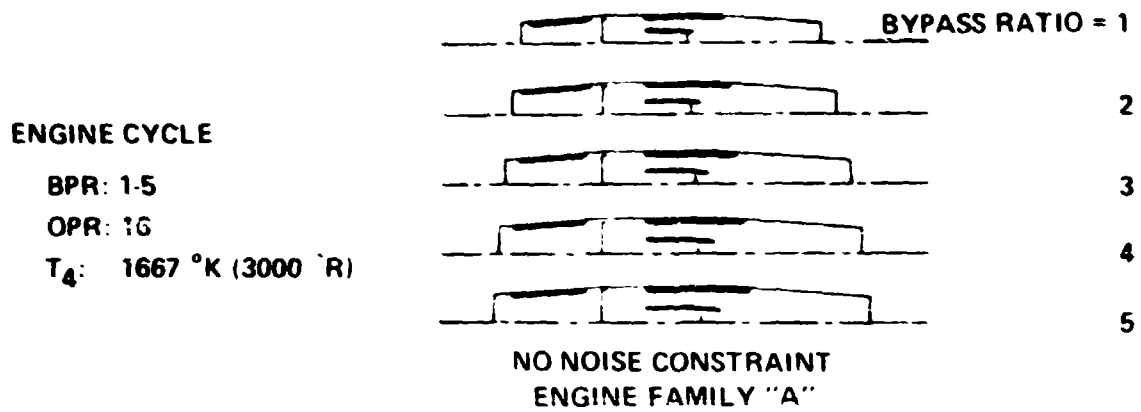


FIGURE 100.—"ATT TECHNOLOGY" M 1.2 STUDY ENGINES

was outfitted with acoustic peripheral treatment. A second engine family was designed to meet a nominal noise goal of FAR 36 minus 5 EPNdB and acoustic suppression was introduced as required. The number directly after the "X" symbol in the figure indicates the required number of PNdB of jet suppression.

The engine source noise estimates and the consequent noise suppression hardware were both developed based on "nominal" Mach 1.2 aircraft low speed aerodynamic and thrust characteristics.

Figure 100 also illustrates Engine Family C which was configured to meet a noise goal of FAR 36 minus 15 EPNdB. This noise goal required the introduction of considerable jet suppression and extensive acoustic treatment, both in the inlet and the fan duct, to reduce the turbomachinery noise. In some cases the levels of jet suppression shown, for example 23 PNdB for the bypass ratio 1 installation far exceed the levels of jet suppression which have currently been demonstrated by model or full scale data.

The nacelle shapes depicted in figure 100 were based on preliminary design definitions developed for this study. Previous contractor design studies indicated that a maximum nacelle diameter of 20 cm (8") larger than fan tip diameter is a reasonable value to allow for structural clearances and room for services, such as actuators for variable geometry, anti-icing ducts, etc. The nacelle length was established as a trade between wetted-area drag, wave drag, and nacelle length. These previous contractor transonic nacelle studies had established that an approximate optimum length for the inlet portion of the nacelle would be 1.5 times the nacelle maximum diameter. Similarly, the boattail portion of the nacelle was shown to have an optimum length approximately equal to twice the nacelle maximum diameter. These guidelines were used to establish the pod dimensions used in this study. Because of these fineness ratio constraints, it is seen in the figure that higher bypass ratio nacelles get to be considerably longer than the lower bypass ratios.

Figure 101 indicates the conventional installation penalties that have been accounted for in the current studies for the bypass ratio 1 and 4 installations.

Acoustic Considerations

The effect of bypass ratio and other cycle parameters on jet and fan noise have been calculated by the same methods used in the previous ATT study (ref. 1). The noise effectiveness of the acoustic treatment and performance of jet suppressors was based upon scale model and full-scale data. In calculating total airplane noise levels significantly below FAR 36, no account has been taken of nonpropulsive ("airframe") noise. Recent investigations show that this noise source may prevent achieving very low overall noise levels.

Additional assumptions have been made concerning the acoustics of the propulsion installation. The base curve of figure 102 shows the noise spectra for the bypass ratio 2 bare engine in terms of octave band number. The curve shown represents forward fan-radiated noise. The dashed curve indicates the noise attenuation associated with the heavily treated acoustic configuration for the Engine Family C installation. This curve was computed on the

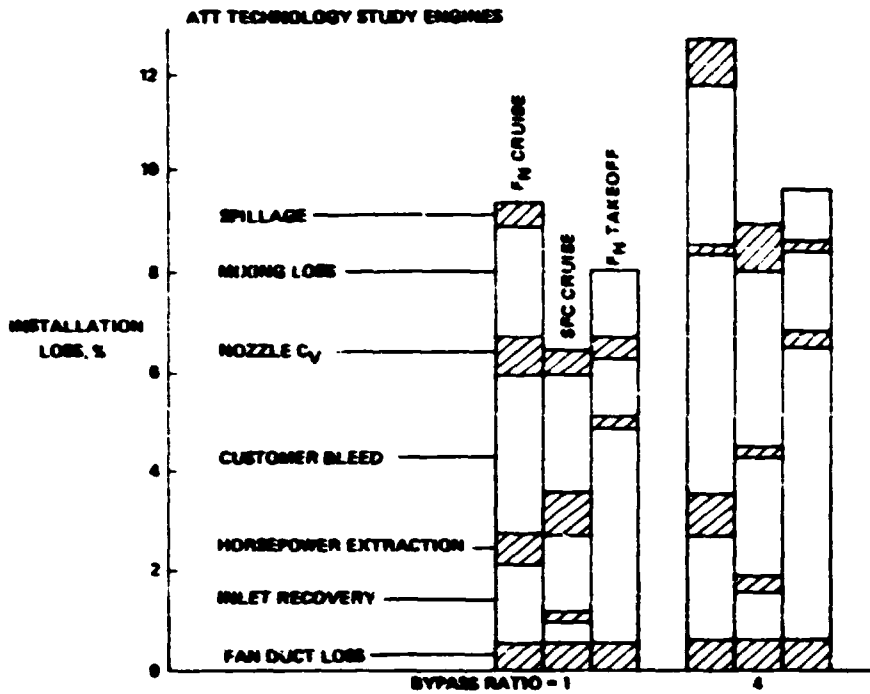


FIGURE 101.—INSTALLATION LOSSES CONSIDERED

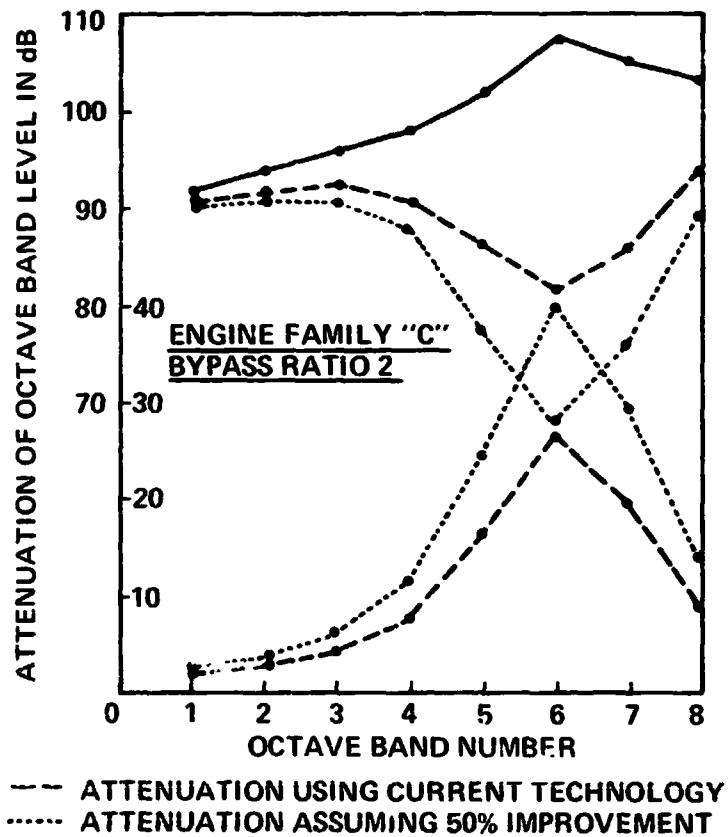


FIGURE 102.—EFFECT OF TECHNOLOGY ASSUMPTIONS ON INLET LINING TECHNOLOGY

basis of noise reduction achievable with current technology and is associated with the attenuation curve shown at the bottom. The dotted curve to figure 102 gives an indication of the acoustic attenuation improvements projected for an advanced "1985-Technology" acoustic installation. The 10 dB improvement at peak frequency using the projected advanced technology translates into about a 4 PNdB improvement in forward inlet radiated noise.

No penalty has been imposed to reduce engine "core" noise. The main reason for this is that engine core noise is currently not yet fully understood and calculations of the levels of core noise are still a matter of some dispute. In addition, the means for treating such noise is only now beginning to be explored and so assessments or penalties for reducing core noise are not readily available.

Figure 103 illustrates some of the technology extrapolations and assumptions that have been introduced. The figure shows incremental jet suppression plotted against engine bypass ratio. The upper curve indicates the jet suppression levels required for the "ATT-Technology" engines studied under this contract. To meet the noise goal of FAR 36 minus 15 EPNdB, the bypass ratio 1 engine will require on the order of 25 PNdB jet suppression. The bypass ratio 4 engine was estimated to need on the order of 3-4 PNdB. The lower shaded area in the figure indicates the levels of available suppression based upon current model and full scale test data. These estimates are based on data which have been analyzed in terms of the appropriate nozzle pressure and temperature properties associated with the study engines. In addition, a constraint has been placed upon jet suppressor area ratio in order to limit consideration of jet suppressors to those which might be reasonably configured within a conventional nacelle. Furthermore the assumption has been made that any jet suppressor introduced would be a variable-geometry design which would enable the jet suppressor to be removed from the internal airstream in order that the internal losses associated with jet suppression be minimized for the cruise condition.

Takeoff performance losses have been assessed at a 1% thrust loss for each 1.5 PNdB jet suppression. A 3.5% nozzle pressure drop has been assessed at cruise to account for the variable geometry jet suppressor interference with exhaust system internal lines. This penalty is consistent with experience gained in the contractor 727 Ejector/Suppressor program.

Engine Emission Levels

The emission requirements specified as ground rules for this study are compared with levels representative of current engines in table 24. Levels thought to be achievable by the engine manufacturers during the previous ATT studies for an advanced combustor design are also shown.

The study ground-rules emission goals for unburned hydrocarbons and carbon monoxide appear to be achievable with advanced combustor design. However, the goal for nitrogen oxide appears to be too stringent to be obtained simply by advanced combustor design and can only be met with the use of water injection. This approach, however, entails a great many operational disadvantages. The combustor design modifications were estimated

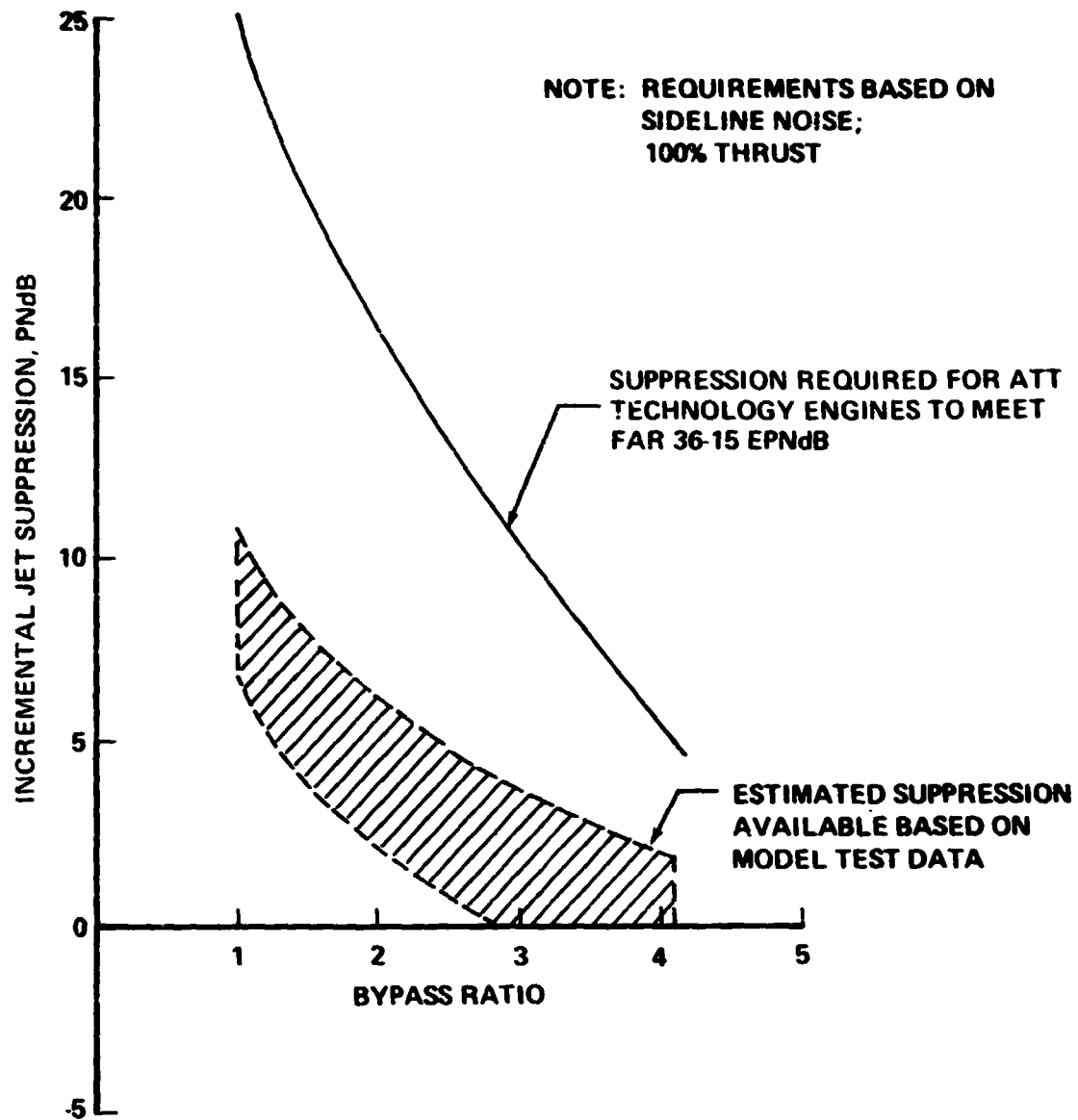


FIGURE 103.—JET SUPPRESSION REQUIREMENTS AND ESTIMATED AVAILABILITY

TABLE 24.—ENGINE EMISSION COMPARISON (G/KG FUEL)

SOURCE	CARBON MONOXIDE (IDLE)	UNBURNED HYDROCARBONS (IDLE)	NITROGEN OXIDE(S) (TAKEOFF POWER)
JT9D	58	15	42
ENGINE MANUFACTURER PROJECTIONS FOR 1985 WITH ADVANCED COMBUSTOR DESIGN	30-40	5-7	11-15
CONTRACT OBJECTIVES	40	8	3

to be achievable at negligible performance penalty. It should be noted that meaningful engine emission goals must be related to ambient air standards which have been developed to be consistent with a satisfactory air quality. It is not clear that the current contract goals can be justified on this basis.

Engine Cycle Selection

Initially, the effect of bypass ratio was studied utilizing "nominal" airplane characteristics. The objectives were to determine the penalty of reducing the jet noise by increasing engine bypass ratio as compared with that for the introduction of jet suppression for lower bypass ratio installations.

Additional studies were made specifically aimed at understanding the impact on noise of five study aircraft configurations as a result of considerable variations in their low speed performance.

"Nominal" Airplane Studies

Figure 104 summarizes the procedures used in the initial studies. The nominal aircraft characteristics are also defined.

The noise characteristics for each of the three FAR noise stations were computed at levels of takeoff and approach thrust equal for all engines. Figure 105 shows the results of the initial "nominal" aircraft/engine bypass ratio study. The results are shown relative to the bypass ratio 1 engine for the peripherally-treated family.

The bypass ratio 1 installation incurs a penalty of about 15%-20% range loss to meet FAR 36 minus 15 EPNdB. To meet this same noise level even without the jet suppressor, a bypass ratio 4 engine would incur an additional 12% range loss. On this basis the BPR 1 engine with the peripheral treatment was selected as the baseline engine for all of the airplane configurations. The FAR 36-5 design and the FAR 36-15 design BPR = 1 engines were used to investigate the impact of community noise on airplane gross weight. The results of these studies were discussed in the configuration performance section.

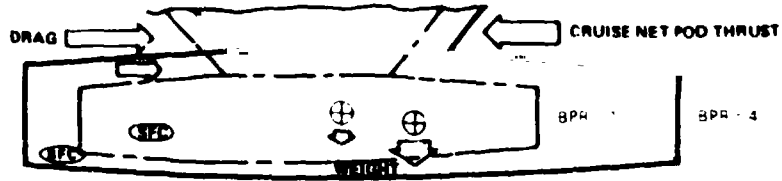
Figure 106 shows the engine source noise components for both the bypass ratio 1 at the top and bypass ratio 4 installations at the bottom. Noise levels are shown for both the peripherally treated case, Engine Family A, and the heavily treated case, Engine Family C for the approach, takeoff and sideline FAR noise stations. The figure shows the importance of the jet contribution to the overall noise for the bypass ratio 1 installation, particularly for the takeoff and sideline case. For the bypass ratio 4 installation the jet levels are well below levels of the other component noise sources.

Impact of Study Assumptions

Figure 107 gives an indication of how changes in certain of the assumptions could impact the calculated range loss. The figure shows again incremental range loss plotted against the installed pod drag divided by the isolated pod drag. When the parameter is equal

NOMINAL AIRCRAFT CHARACTERISTICS

- 272 185 KG. TOGW (600 000 LB)
- 8800 KM RANGE, 18 143 KG PAYLOAD (3000 NM 40 000 LB)
- M 1.2 CRUISE



BYPASS RATIO STUDY - - - - METHOD ANALYSIS

- ENGINES SIZED FOR CONSTANT NET POD THRUST
- INSTALLED PERFORMANCE COMPUTED FOR T/O & CRUISE
- WT/DRAG/SFC PENALTIES COMBINED BY SENSITIVITIES
- NOISE COMPUTED AT FIXED ABSOLUTE LEVEL OF TAKEOFF & APPROACH THRUST
- FIGURE OF MERIT INCREMENTAL RANGE CHANGE

FIGURE 104.-METHODS USED FOR ENGINE CYCLE SELECTION STUDY

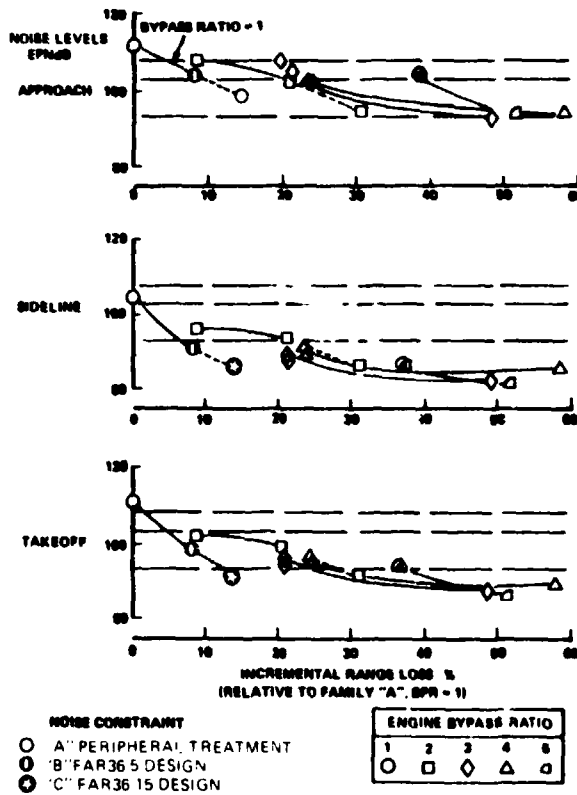


FIGURE 105.-NOISE/PERFORMANCE TRENDS OF "ATT TECHNOLOGY" ENGINES

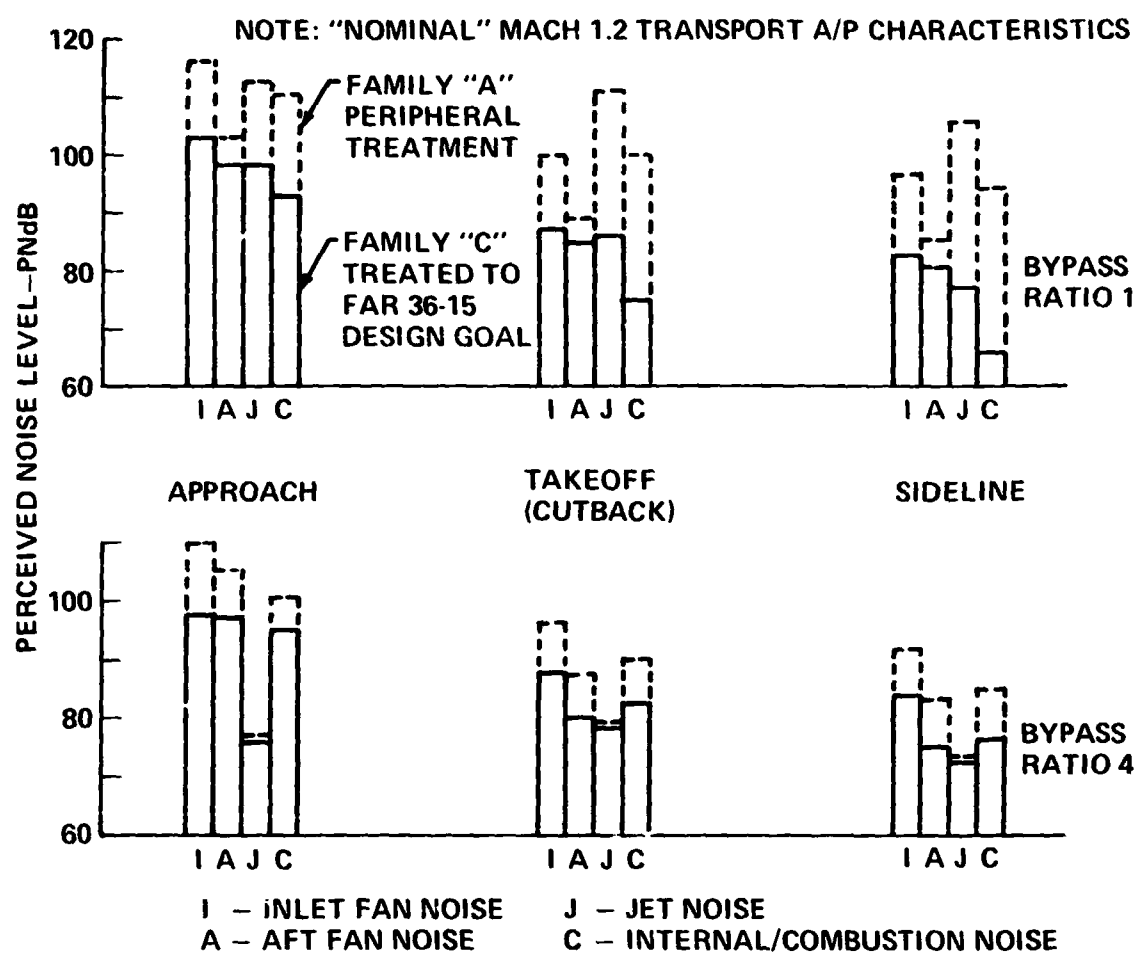


FIGURE 106.-COMPONENT NOISE LEVELS OF "ATT TECHNOLOGY" STUDY ENGINES

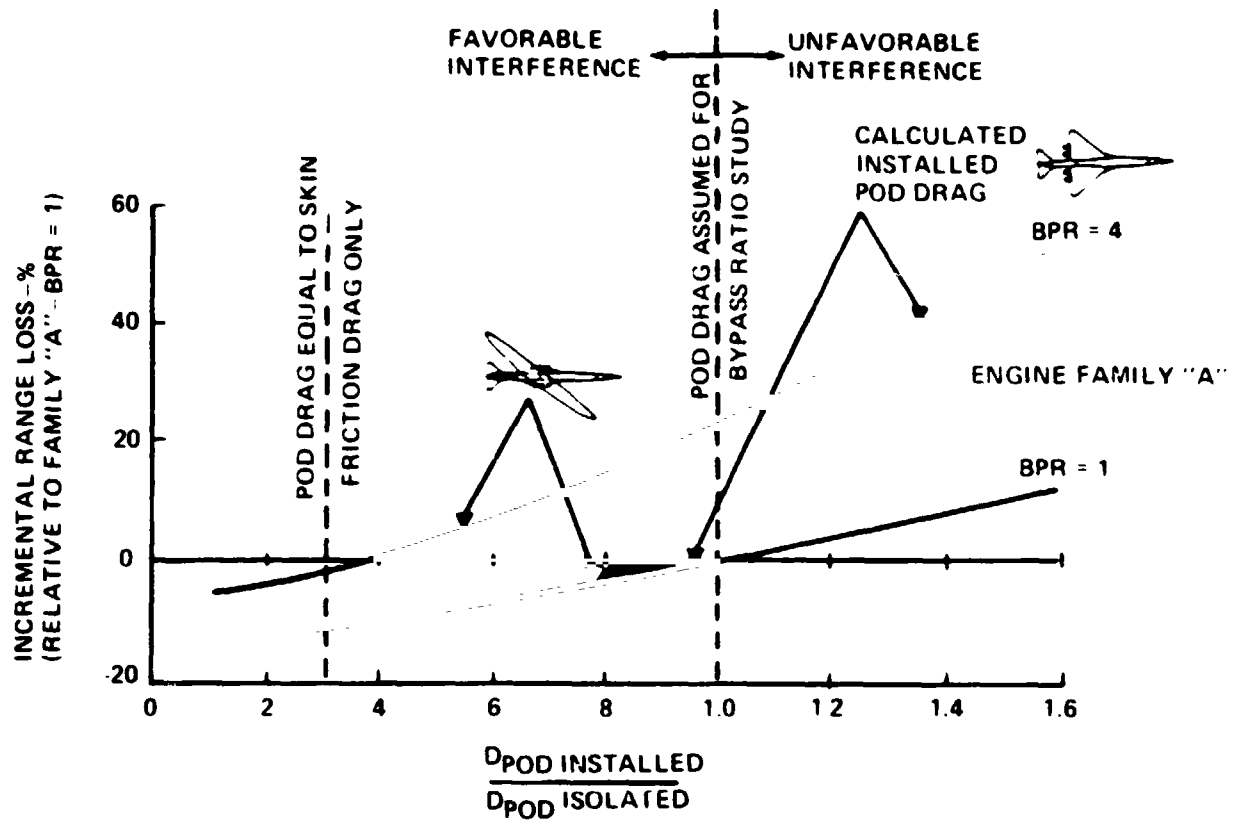


FIGURE 107.—EFFECT OF VARYING POD DRAG LEVEL ON RELATIVE AIRCRAFT RANGE

to 1.0, the pod drag is computed as the drag of an isolated pod. For values of $D_{pod\ inst.}/D_{pod\ isol.}$ greater than 1.0, which would involve unfavorable aerodynamic interference with the aircraft, it is seen that the range penalty increases considerably. Alternatively, for levels of $D_{pod\ inst.}/D_{pod\ isol.}$ less than 1.0, the situation of favorable aerodynamic interference, the levels of range penalty can be decreased significantly. The base curve shows trends for both the bypass ratio 1 and bypass ratio 4 installations.

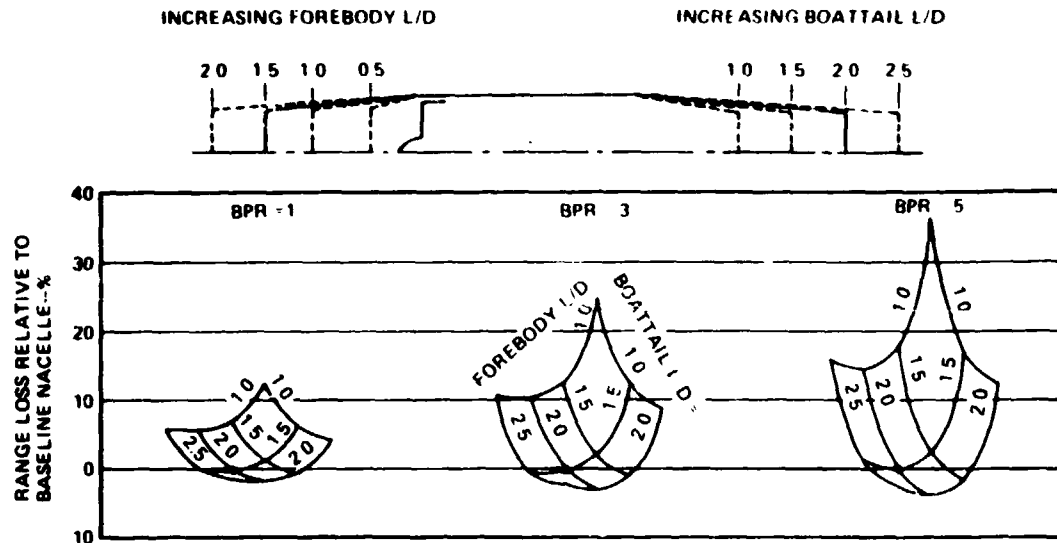
Also, shown in terms of a dash vertical line to the left of the plot is the level of pod drag associated with installing the pods for skin friction drag only. If such an installation were to be achieved it is seen that range savings on the order of 10% would be incurred for a bypass ratio 1.0 installation, whereas a range savings on the order of 20% would be realized for the bypass ratio 4 installation.

The figure also indicates the levels of installed drag which were determined for the delta wing airplane configuration 3-2. Also shown in figure 107 are the results of similar calculations for an early single fuselage yawed-wing arrangement. In this case, favorable interference between the pods and the aircraft fuselage was achieved and the figure shows the significant savings in aircraft range.

Figure 108 illustrates the range sensitivity to variations in pod fineness ratio where the L/D of the inlet and boattail were parametrically varied about the levels used in the preliminary design studies. These levels as noted were L/D equal to 1.5 for the forebody and $L/D = 2.0$ for the boattail. Variations of either the inlet or boattail fineness ratio result in trades between wave drag, skin friction drag, and nacelle weight. The results of these trades, shown in terms of range loss, are given for the bypass ratios 1, 3 and 5 installations. The results indicate that boattail L/D of 2.0, as used in the study, is approximately optimum. The inlet L/D could be somewhat increased with the resulting range savings. The figure indicates that a forebody $L/D = 2.0$ for the bypass ratio 1 installation, would result in an additional range savings of about 2%. A similar increase in fineness ratio for the bypass ratio 5 installation could result in a range improvement on the order of 5%. The relative range loss shown in the main carpet plot has been referenced to the absolute range loss. The insert indicates the large absolute range penalties associated with the increased bypass ratio as opposed to the incremental range gain for higher bypass ratio by optimizing the pod fineness ratio.

Impact of Aircraft Configurations

Figure 109 shows the impact of the 5 early version of the study aircraft configurations on approach, sideline and takeoff noise. The data refer to the peripherally treated bypass ratio 1 installation. For sideline noise, there is very little difference associated with different engine sizes. There is a large (on the order of 15 EPNdB) spread in takeoff noise between the five aircraft configurations. This large spread directly reflects the aircraft low speed aerodynamic capabilities and indicates the inherent noise reduction features of the yawed wing airplanes which for low speed operation employed a high aspect ratio unswept wing with exceedingly good lift to drag capability. The approach noise level data show less spread than might have been supposed. There are two reasons for this: (1) the three conventional platform aircraft shown here employed an unflapped landing configuration in order to reduce the approach thrust, and thus noise levels. As a result, the landing speed for these



- NOTES:
1. BASELINE NACELLE GEOMETRY IS
FOREBODY L/D = 1.5
BOATTAIL L/D = 2.0
 2. ATT TECHNOLOGY STUDY ENGINES
FAMILY "B"
"NOMINAL" AIRCRAFT CHARACTERISTICS

FIGURE 108.—EFFECT OF NACELLE FINENESS RATIO

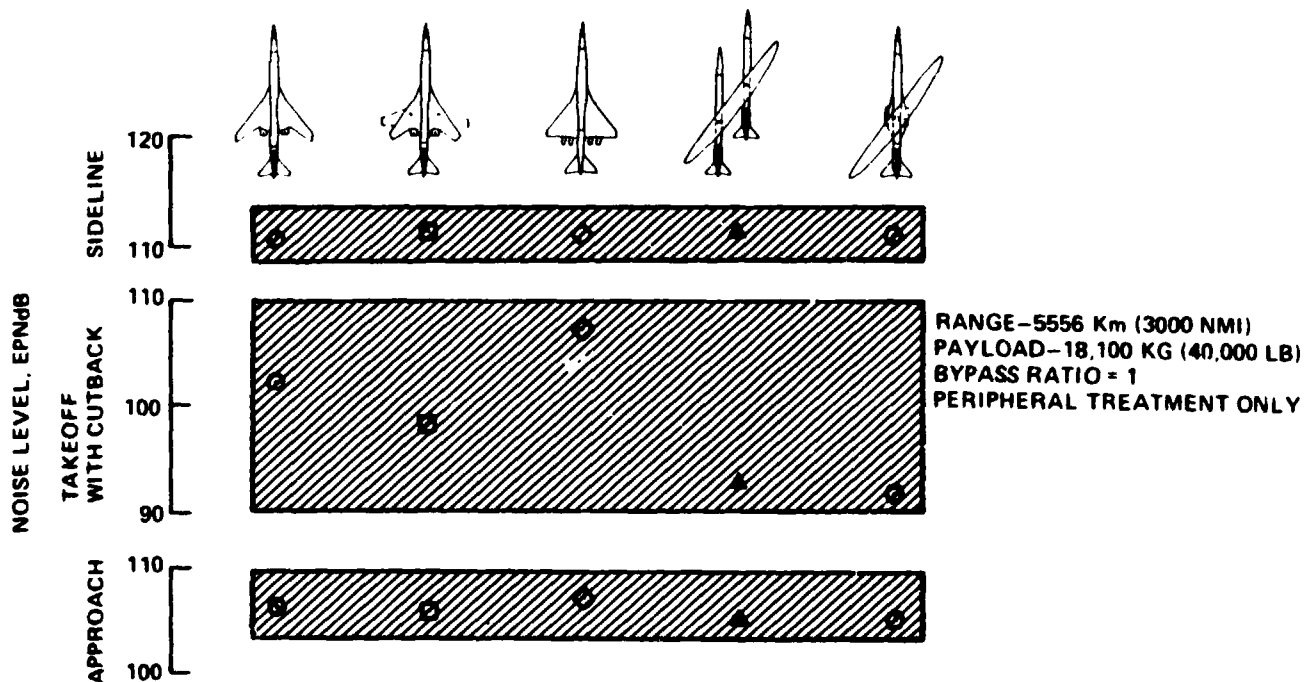


FIGURE 109.—EFFECT OF AIRCRAFT CONFIGURATION ON FLYOVER NOISE LEVELS

aircraft is on the order of 92.6 m/s (180 kts), compared with about 66.9 m/s (130 kts) for the yawed wing configurations: (2) in contrast, the excellent lift-to-drag capabilities of the yawed wing aircraft were not able to be fully utilized due to a flight idle limit of 12% of available thrust. The lower aspect ratio wing selected the Model 5-3 provides a better match of the noise characteristics as shown in the configuration analysis section.

STRUCTURES AND MATERIALS

The objectives of the Structures effort in this study were to:

- Assure structural feasibility of each configuration by providing the required space for the major structural elements, joints and mechanisms
- Define the structural system and materials representative of an advanced technology airplane.
- Provide a reliable base for weight prediction of the yawed wing configuration by sizing the structural elements.
- Assure a divergence-free configuration with a minimum weight increment over the strength design requirements.

General structural evaluations were made for all of the concept configurations. The selection, use and benefits of advanced structural materials were identified.

The nature of the divergence of a yawed wing was investigated. The results of this analysis helped to define the structural sizing criteria for the yawed wing.

Structural analyses of the yawed wing were made to aid in the selection of the wing planform and to define the structural material requirements for the weight estimates.

Configuration Evaluation

The structural feasibility was evaluated for configurations representative of each of the concepts studied. Constraints such as the requirement for area ruling, ground clearance, landing gear arrangement and engine location were considered. Estimates of load transfer were made to assure sufficient space for structure, pivots and mechanisms and to check for reasonable load paths. Primary structure layouts and wing pivot details are shown in the Configuration Description section.

Figure 110 represents the flight speed placard relating airplane equivalent airspeed, Mach number and altitude. Based on experience a maximum cruise speed of 180 m/s (350 kts) was selected to provide a low cruise dynamic pressure and allow cruise at an altitude for best performance. This choice of maximum cruise airspeed limited Mach 1.2 cruise to altitudes above 11890 m (39,000 ft). Adding a standard upset, and a flutter and divergence margin to the maximum cruise speed gave a maximum structural design speed of 216 m/s (420 kts) and a minimum flutter and divergence clearance speed of 260 m/s (505 kts).

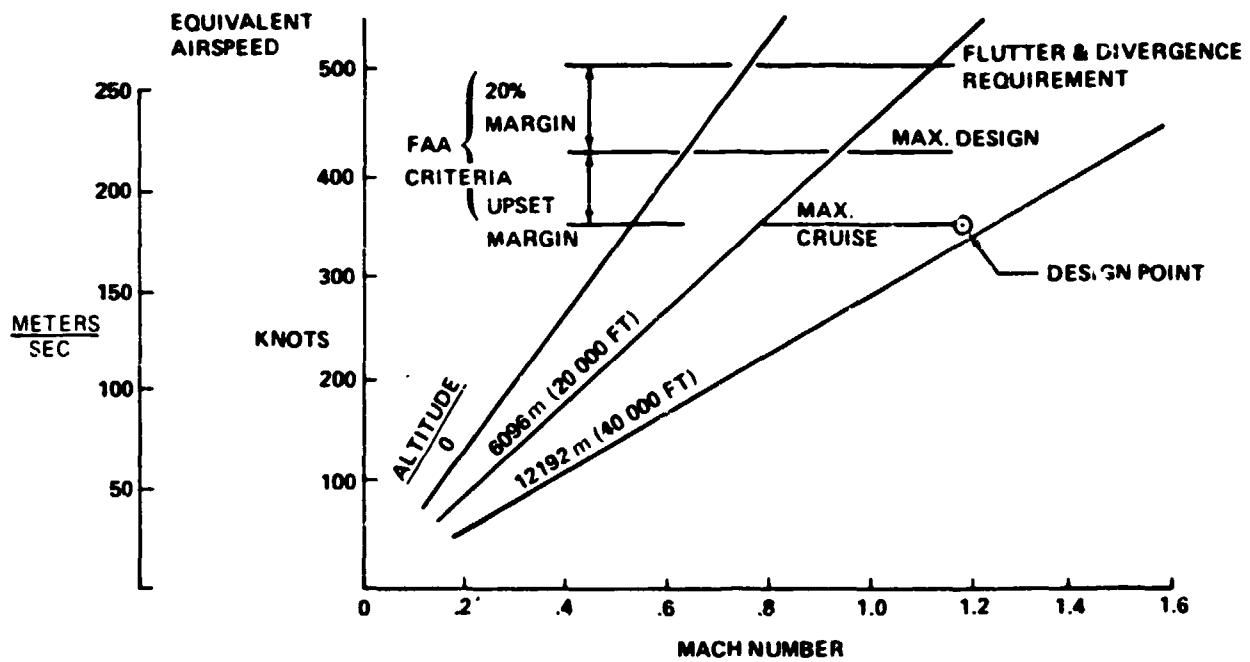


FIGURE 110.—STRUCTURAL DESIGN SPEEDS

Materials Selection

Advanced structural materials for all configurations were derived from the Advanced Transport Technology (ATT) study results (ref. 1). The level of advanced technology assumed is that corresponding to an airplane availability date of 1985. This availability date is contingent on the completion of the research program recommended as part of the ATT program, (ref. 16).

Structural materials selection analyses were directed at defining:

- The areas for each of the airplane concepts best suited for the application of the advanced composite materials.
- The types of structural materials to be considered.
- The percent weight savings of the advanced structural materials over conventional aluminum skin stringer construction.

The results of these analyses are shown for each configuration concept in figures 111 through 115.

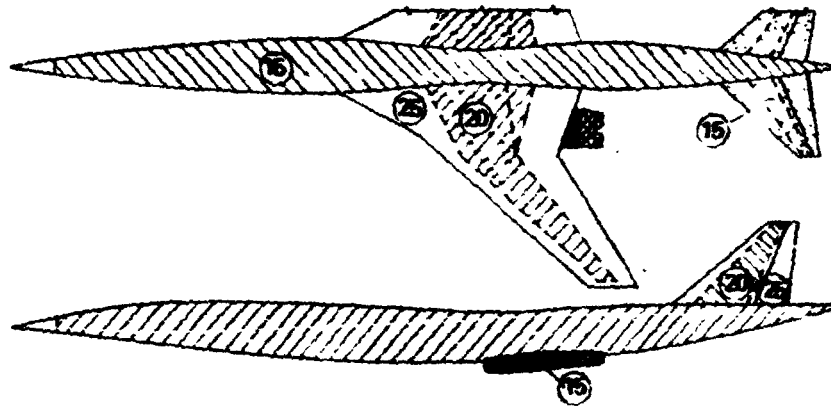
Graphite-epoxy honeycomb was selected for the wing, fuselage and vertical tail primary structure for all configurations. For all concepts, except the delta planform, inboard sections of the wing were stiffened due to high panel end loads. The weight savings was estimated to be 25% where wing box stiffness was critical. The weight savings was estimated as 20% for other highly loaded areas. The weight savings with graphite-epoxy on the fuselage was estimated to be 15%. Titanium was selected for the wing pivots and pivot support structures.

A high temperature matrix composite honeycomb was selected for the horizontal tails on all configurations. This selection was made because the horizontal tails were relatively close to the engine exhaust. Use of this material resulted in an estimated weight saving of 15% over aluminum skin/stringer construction designed for strength.

Honeycomb with face sheets composed of DuPont PRD-49 was selected for the wing and fin leading and trailing edge structures. The weight saving of this construction over aluminum construction was estimated to be 25%.

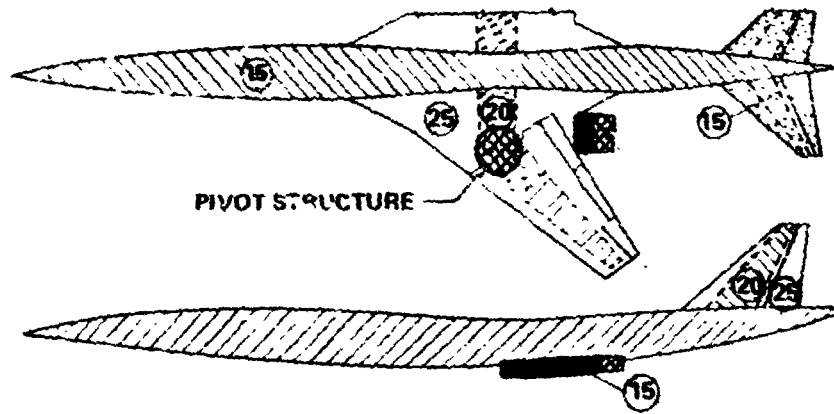
Graphite-epoxy has been used for the nontemperature critical area of the nacelles with the acoustic treatment integrated into the structure. This type of design would yield a 15% weight saving over a conventionally treated nacelle. Conventional construction was used for the temperature critical areas of the nacelle.

Weight estimates for all of the configurations were obtained by applying advanced technology weight adjustments to the calculated weights based on conventional aluminum skin stringer construction. The unique nature of the yawed wing configuration, however, made it necessary to base the weight estimates for the yawed wing on structural analysis rather than statistical weight data.



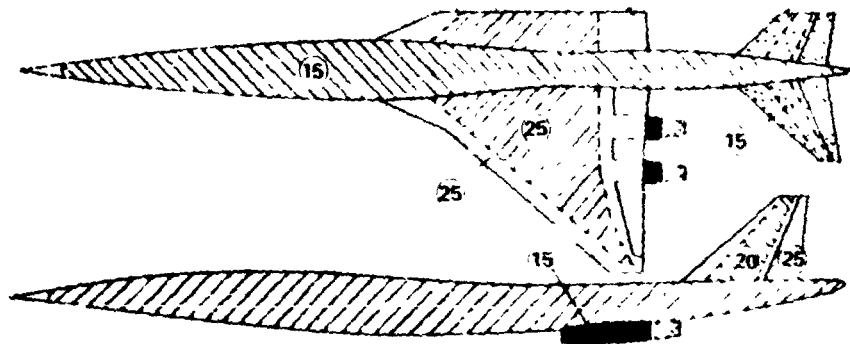
- ⊗ PERCENT WEIGHT SAVING RELATIVE TO 747/DC-10 TECHNOLOGY
- ▨ GRAPHITE-EPOXY HONEYCOMB
- GRAPHITE-EPOXY INTEGRATED ACOUSTIC STRUCTURE
- ▤ HIGH TEMPERATURE MATRIX COMPOSITE HONEYCOMB
- ▭ PRD-49 HONEYCOMB
- ⊗ CONVENTIONAL DESIGN
- ▧ STIFFENED GRAPHITE-EPOXY HONEYCOMB

FIGURE 111.—MATERIALS SELECTION—FIXED SWEEP WING AIRCRAFT



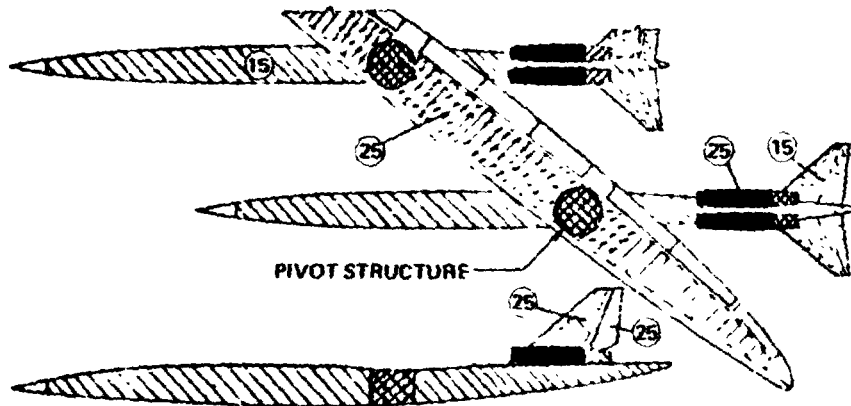
- ⊗ PERCENT WEIGHT SAVING RELATIVE TO 747/DC10 TECHNOLOGY
- ▨ GRAPHITE-EPOXY HONEYCOMB
- GRAPHITE-EPOXY INTEGRATED ACOUSTIC STRUCTURE
- ▤ HIGH TEMPERATURE MATRIX COMPOSITE HONEYCOMB
- ▭ PRD-49 HONEYCOMB
- ⊗ CONVENTIONAL DESIGN
- ▧ STIFFENED GRAPHITE-EPOXY HONEYCOMB

FIGURE 112.—MATERIALS SELECTION—VARIABLE SWEEP WING AIRCRAFT



- ⊗ PERCENT WEIGHT SAVING RELATIVE TO 747/DC-10 TECHNOLOGY
- ▨ GRAPHITE-EPOXY HONEYCOMB
- GRAPHITE-EPOXY INTEGRATED ACOUSTIC STRUCTURE
- ▤ HIGH TEMPERATURE MATRIX COMPOSITE HONEYCOMB
- ▭ PRD-49 HONEYCOMB
- ⊘ CONVENTIONAL DESIGN
- ▩ STIFFENED GRAPHITE-EPOXY HONEYCOMB

FIGURE 113.—MATERIALS SELECTION—DELTA-PLANFORM AIRCRAFT



- ⊗ PERCENT WEIGHT SAVING RELATIVE TO 747/DC-10 TECHNOLOGY
- ▨ GRAPHITE-EPOXY HONEYCOMB
- GRAPHITE-EPOXY INTEGRATED ACOUSTIC STRUCTURE
- ▤ HIGH TEMPERATURE MATRIX COMPOSITE HONEYCOMB
- ▭ PRD-49 HONEYCOMB
- ⊘ CONVENTIONAL DESIGN
- ▩ STIFFENED GRAPHITE-EPOXY HONEYCOMB

FIGURE 114.—MATERIALS SELECTION—TWIN FUSELAGE YAWED-WING AIRCRAFT

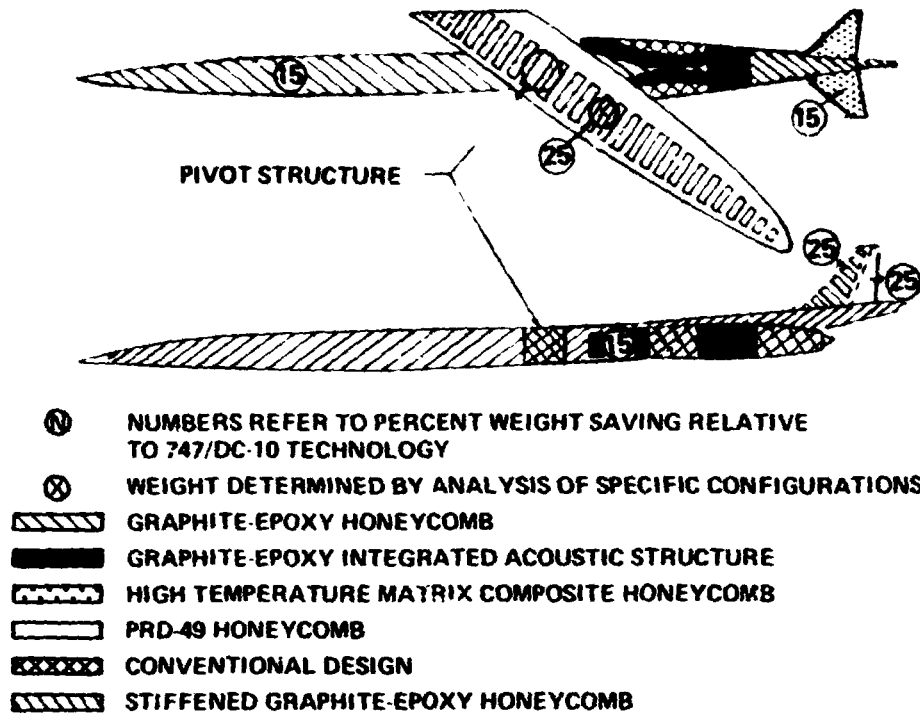


FIGURE 115.—MATERIALS SELECTION, MODEL 5-3

Initially structural analyses were conducted to establish critical strength design conditions and to determine the nature of aeroelastic divergence of a yawed wing airplane.

Yawed Wing Divergence

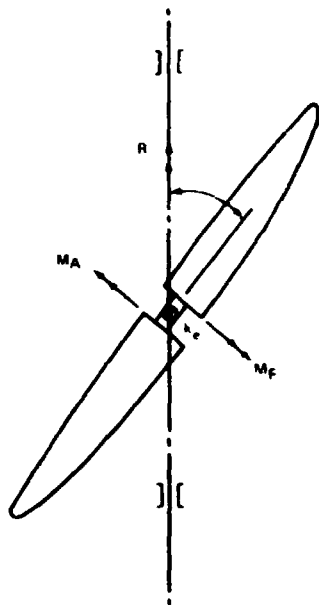
The nature of divergence of an unrestrained yawed wing airplane was first investigated, with a very simple elastic model. This model had rigid wings attached to the center pivot with a spring to simulate bending without twist (fig. 116). The aft wing and forward wing bending moment, M_A and M_F , applied to the springs and the rolling moment, R , were examined. The bending moment due to the forward wing shows the typical divergence characteristic for the case of the fuselage restrained in roll.

When the aerodynamic stiffness, K_a , which increases with dynamic pressure, equals the structural stiffness, K_e , the denominator of the expression for the forward wing bending moment, M_F , will vanish. This condition defines the cantilever divergence speed. The expression for the rolling moment, R of the unrestrained airplane has a denominator that will also vanish when K_a equals K_e . This will lead to a form of divergence unless the numerator of the rolling moment expression can also be made to vanish. A very specialized stability augmentation system would be required to either make the numerator vanish or to reduce the value of K_a .

The next step in determining the nature of divergence of a yawed wing airplane was to examine the dynamic stability with the airplane free to roll. The structural dynamics model simulating the wing is shown in figure 117. The wing mass was represented by a series of point masses. The aerodynamic lift distribution was represented by a section lift coefficient for each of the six wing panels on each wing. Wing flexibility was represented by beam bending and beam torsion, although it was found in the analysis that torsional stiffness had little effect on the divergence speed. Wing torsion flexibility was neglected. This same model, restrained in roll, was used to obtain the cantilever stability of each wing. The equations of motion included inertia, aerodynamic and elastic forces and moments. The aerodynamic forces provide both stiffness and damping, whereas the elastic forces provide only stiffness. Each wing panel was considered as a separate degree of freedom. Airplane roll was also treated as a separate degree of freedom, however, there were no stiffness forces or moments resulting from airplane roll. The equations that represent this dynamic system are shown in figure 117.

The results of the dynamic stability analysis are presented in figure 118 in terms of airplane speed versus damping ratio, which is the ratio of the airplane's damping to its critical damping. At zero airspeed, the structural response frequency for each wing treated as cantilevers and for the unrestrained airplane are all the same, 10 Hz. As speed is increased initially, the damping ratio increases in all three cases, however:

- the frequency decreases for the leading wing cantilevered and also for the unrestrained airplane
- the frequency increases for the trailing wing cantilevered



$$M_F = \frac{m_\alpha \alpha - \Delta M}{1 - \frac{k_a}{k_e}}$$

$$M_A = \frac{m_\alpha \alpha + \Delta M}{1 + \frac{k_a}{k_e}}$$

$$R = \frac{-2 (m_\alpha \alpha \frac{k_e}{k_a} - \Delta M) \cos \Lambda}{1 - \left(\frac{k_a}{k_e}\right)^2}$$

WHERE:

M_F = BENDING MOMENT ON SPRING SUPPORTING FORWARD WING

M_A = BENDING MOMENT ON SPRING SUPPORTING AFT WING

R = ROLLING MOMENT

ΔM = BENDING MOMENT RESULTING FROM ROLL RATE AND AILERON DEFLECTION

Λ = WING YAW ANGLE

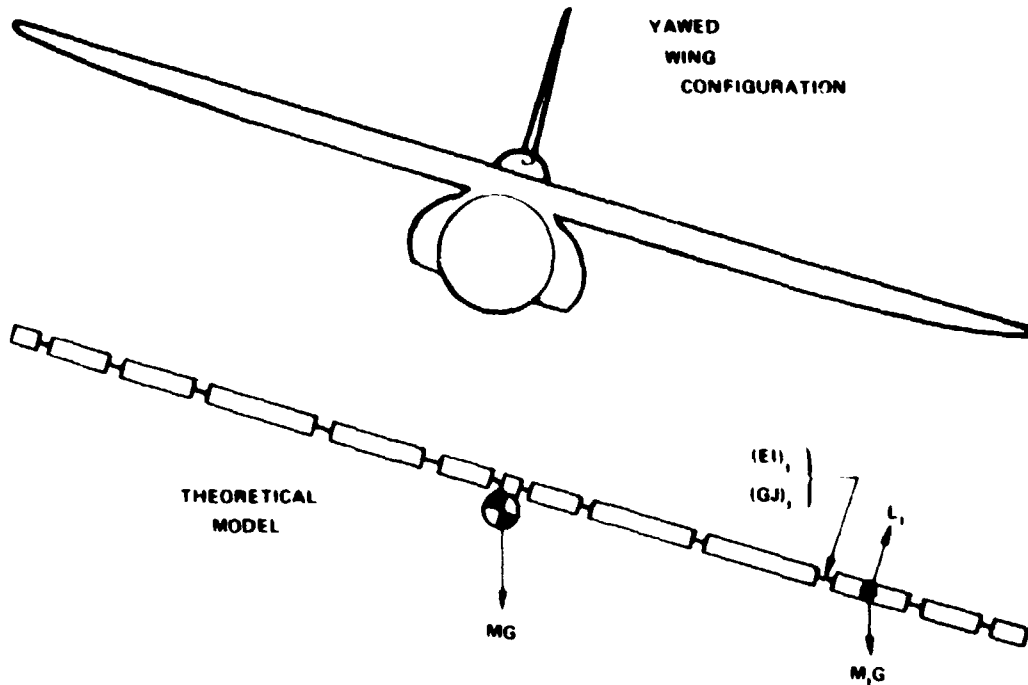
α = WING ANGLE OF ATTACK

m_α = BENDING MOMENT DUE TO A UNIT ANGLE OF ATTACK

k_e = SPRING STIFFNESS CONSTANT

k_a = $m_\alpha \sin \Lambda$ - AERODYNAMIC STIFFNESS

FIGURE 116.—SIMPLIFIED UNRESTRAINED YAWED-WING DIVERGENCE



	AIRPLANE ROLL	WING BENDING	WING TORSION
AIRPLANE ROLLING MOMENTS	<ul style="list-style-type: none"> ● INERTIA ● AERODYNAMIC DAMPING 	<ul style="list-style-type: none"> ● INERTIA ● AERODYNAMIC DAMPING ● AERODYNAMIC STIFFNESS 	<ul style="list-style-type: none"> ● INERTIA ● AERODYNAMIC DAMPING ● AERODYNAMIC STIFFNESS
WING PANEL FORCES (6 PER SIDE)	<ul style="list-style-type: none"> ● INERTIA ● AERODYNAMIC DAMPING 	<ul style="list-style-type: none"> ● INERTIA ● AERODYNAMIC DAMPING ● AERODYNAMIC STIFFNESS ● STRUCTURAL STIFFNESS 	<ul style="list-style-type: none"> ● INERTIA ● AERODYNAMIC DAMPING ● AERODYNAMIC STIFFNESS ● STRUCTURAL STIFFNESS

AIRPLANE ROLL $I\ddot{\phi} + \sum m_i y_i (z_i + a_i \theta_i) = -L\ddot{\phi} - \sum \frac{r_{10} y_i}{V} (z_i + a_i \theta_i) + \sum r_{10} y_i (\gamma_i \sin \Lambda + \theta_i \cos \Lambda)$

WING BENDING $m_i (y_i \ddot{\phi} + z_i + a_i \theta_i) = -\frac{r_{10}}{V} (y_i \ddot{\phi} + z_i + a_i \theta_i) + r_{10} (\gamma_i \sin \Lambda + \theta_i \cos \Lambda) - \sum k_{Bij} z_j$

WING TORSION $m_i (a_i y_i \ddot{\phi} + a_i z_i + a_i^2 \theta_i) = -\frac{r_{10} a_i}{V} (y_i \ddot{\phi} + z_i + a_i \theta_i) + r_{10} a_i (\gamma_i \sin \Lambda + \theta_i \cos \Lambda) - \sum k_{Tij} \theta_j$

INERTIA
AERODYNAMIC DAMPING
AERODYNAMIC STIFFNESS
STRUCTURAL STIFFNESS

FIGURE 117.—STABILITY ANALYSIS MODEL

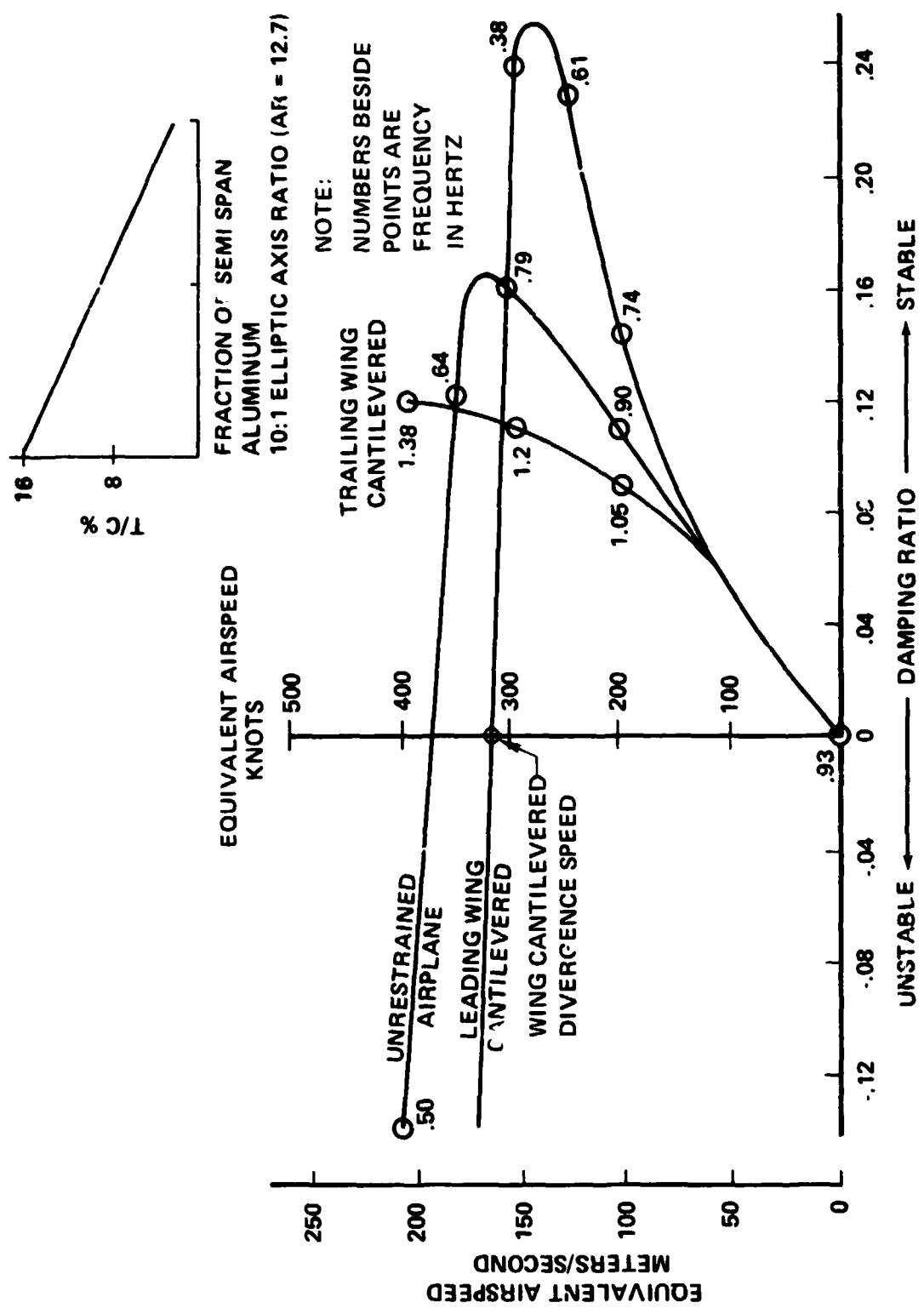


FIGURE 118.—UNRESTRAINED YAWED WING AIRPLANE STABILITY

The leading wing bending deflection for the unrestrained airplane increases relative to the trailing wing deflection. This starts an airplane roll oscillation.

At higher airspeeds, the damping ratio of the cantilevered leading wing starts to decrease. This trend continues until the leading wing cantilevered divergence speed is reached. At this speed the frequency becomes zero and the wing becomes unstable. This provides a source of energy to the unrestrained airplane. This energy is fed through the wing bending causing an increase in airplane roll and a decrease in its frequency until a low frequency, oscillating instability occurs. This instability is a combination of wing bending with a large amount of airplane roll. If the speed is increased slightly, the frequency goes to zero and elastic divergence takes place.

In addition to the speed-damping characteristics shown on figure 118, there is an unrestrained airplane mode with zero frequency and damping for all airspeeds. At low speeds, this mode is basically airplane roll. However, as the leading wing cantilevered divergence speed is approached (as the aerodynamic stiffness approaches the structural stiffness), the amount of leading wing bending relative to roll rate in this mode increases. At the leading wing cantilevered divergence speed, the ratio of leading wing bending to roll rate becomes infinite.

The results of these analyses and some preliminary strength analyses indicated that a reasonable approximation to the structural weight of the wing would result from sizing the structure to the more stringent of:

- Gust and maneuver loads at zero yaw angle, and
- Can .neuver divergence of the forward wing.

Yawed Wing Analyses

Graphite-epoxy advanced filamentary composite structure was applied to the yawed wing. The graphite-epoxy was evaluated by comparison with a conventional aluminum structure. Sizing criteria used were strength at zero yaw and divergence avoidance at 45° yaw. For the case using aluminum structure, the divergence avoidance criterion required considerably more material than the strength criterion. For the case using graphite-epoxy both divergence and strength required nearly equal amounts of material.

The aluminum construction was a skin-stringer assembly. The graphite-epoxy material requirements were based on the following assumptions:

- A ply arrangement was selected considering external load distributions and the bending stiffness required for divergence.
- Isotropic structural parameters such as yield strength and stiffness modulus were established to simulate the anisotropic ply arrangement.
- A compression buckling curve was estimated for built up panels.

Allowables and stiffnesses were determined from material data in the Air Force Advanced Composites Design Guide (ref. 17). High modulus graphite was used. Fibre orientations were selected to enhance wing bending direction strength and stiffness, while retaining some reasonable strength in other directions. Ply orientation in the graphite-epoxy face sheets, selected on the basis of experience, was 60% (0°), 30% (45°), and 10% (90°). In addition to material failure considerations the compression allowable calculation includes checks on panel compression stability, shear crimping, core shear strength and core crushing. The shear allowable calculation includes checks for panel shear stability and intracell buckling. The honeycomb ribbon direction is parallel to the spars, which helps prevent shear crimping. The allowables and stiffnesses used for the composite are compared to those for aluminum in Figure 119. The graphite-epoxy honeycomb has a density of 1605 kg/m³ (.058 lb/in.³). This includes face sheets, core and adhesive. The density of aluminum is 2800 kg/m³ (.101 lb/in.³). An allowance of 15% for aluminum and 25% for graphite-epoxy was added to the wing primary structural weight to account for fittings, fasteners, and joints.

The material requirements based on strength considerations were determined using a computerized wing structural synthesis program (ORACLE). ORACLE combines an aeroelastic loads analysis based on beam theory and lifting line aerodynamics as described in NACA TN 3030 (ref. 18), a simplified box beam stress analysis and a weight analysis of the wing box. The box beam stress analysis includes the effect of combined shear and tension. A flow chart for ORACLE is shown in figure 120.

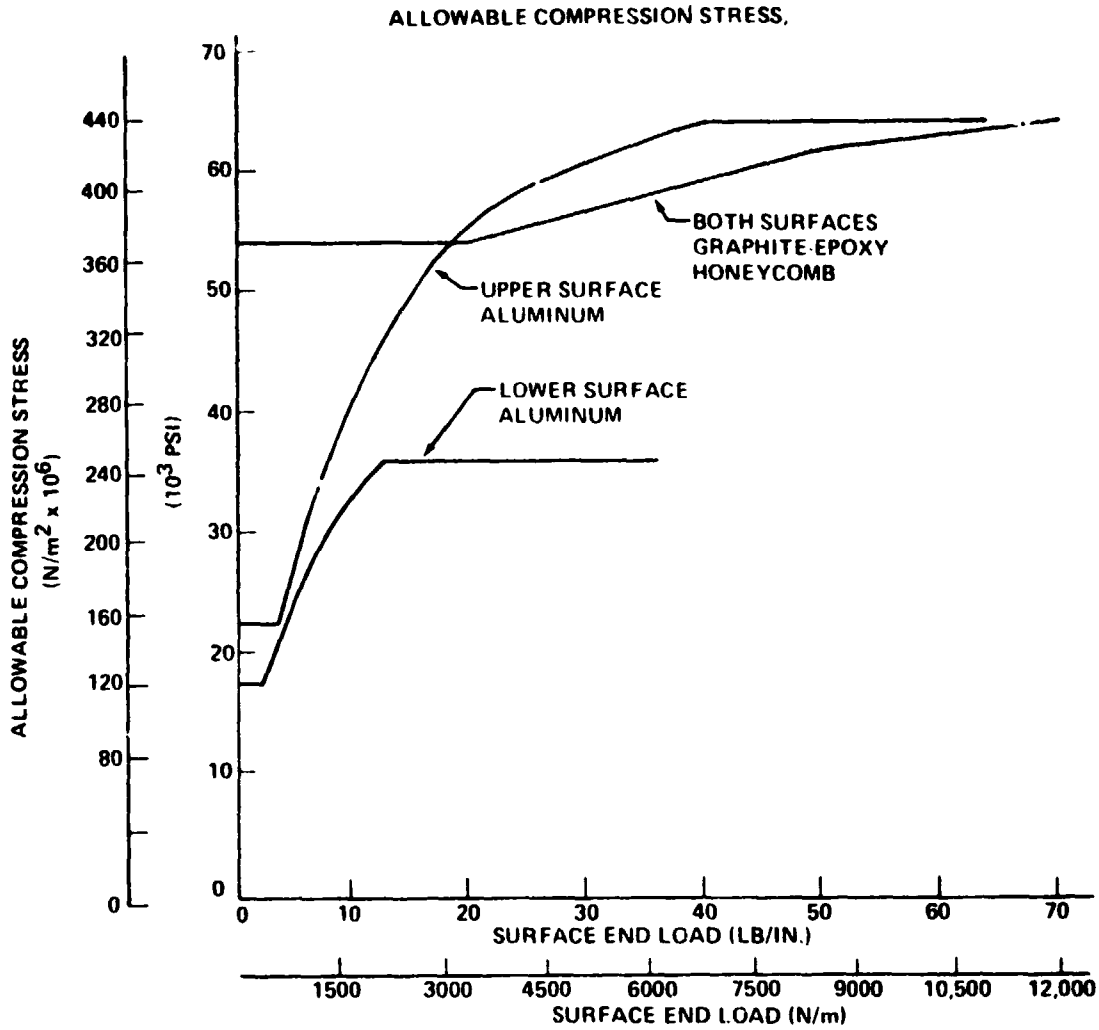
The strength design load conditions were a 15.24 m/s (50 ft/sec) gust at $V_e = 180$ m/s (350 keas), at an altitude of 6096 m (20,000 ft) with a gross weight of 163,300 kg (360,000 lb), and a 2.5 g symmetrical maneuver at $V_e = 216$ m/s (420 keas), at an altitude of 4877 m (16,000 ft) with a gross weight of 272,200 kg (600,000 lb). The loads that correspond to these conditions are plotted in figure 121. The material cross-section area necessary to support this level of loading is shown in Figure 122 and the wing section properties in the form of bending and torsional stiffness for both aluminum and graphite-epoxy construction are shown in figure 123.

The graphite-epoxy wing box was considerably lighter than the aluminum structure. Although the strength sized composite wing required more material than the aluminum wing, it was lighter because the density of the graphite-epoxy is less than aluminum. When sized to divergence avoidance the higher stiffness-weight ratio of the composite gives this material an even greater advantage over aluminum.

Yawed Wing Trade Studies

A series of wing structural analyses were conducted to aid in the development of a yawed wing planform. Aeroelastic structural sizing was performed to determine the weight sensitivity of the wing with respect to wing elliptic axis ratio thickness ratio, wing area and airplane weight.

Elliptic axis ratios of 10:1, 8:1 and 6:1 were analysed varying the maximum t/c (thickness to chord ratio). These correspond to unswept aspect ratios of 12.7, 10.2 and 7.6, respectively. The results of these analyses are shown on Figure 124 in terms of aluminum



ADDITIONAL PROPERTIES

COMPOSITE:	ALUMINUM:
$E = 115.1 \times 10^9 \text{ N/m}^2$ ($16.7 \times 10^6 \text{ PSI}$)	$E = 71.7 \times 10^9 \text{ N/m}^2$ ($10.4 \times 10^6 \text{ PSI}$)
$G = 16.5 \times 10^9 \text{ N/m}^2$ ($2.4 \times 10^6 \text{ PSI}$)	$G = 26.9 \times 10^9 \text{ N/m}^2$ ($3.9 \times 10^6 \text{ PSI}$)
$\rho = 1.605 \times 10^3 \text{ KG/m}^3$ (.058 LB/IN.^3)	$\rho = 2.796 \times 10^3 \text{ KG/m}^3$ (.101 LB/IN.^3)
ALLOWABLE TENSION STRESS = $.482 \times 10^9 \text{ N/m}^2$ (70,000 PSI)	ALLOWABLE TENSION STRESS:
MINIMUM GAGE = .00254 m (.1 IN.)	UPPER SURFACE = $.434 \times 10^9 \text{ N/m}^2$ (63,000 PSI)
	LOWER SURFACE = $.365 \times 10^9 \text{ N/m}^2$ (53,000 PSI)
	MINIMUM GAGE = .002032 m (.08 IN.)

FIGURE 119.—STRUCTURAL MATERIAL PROPERTIES

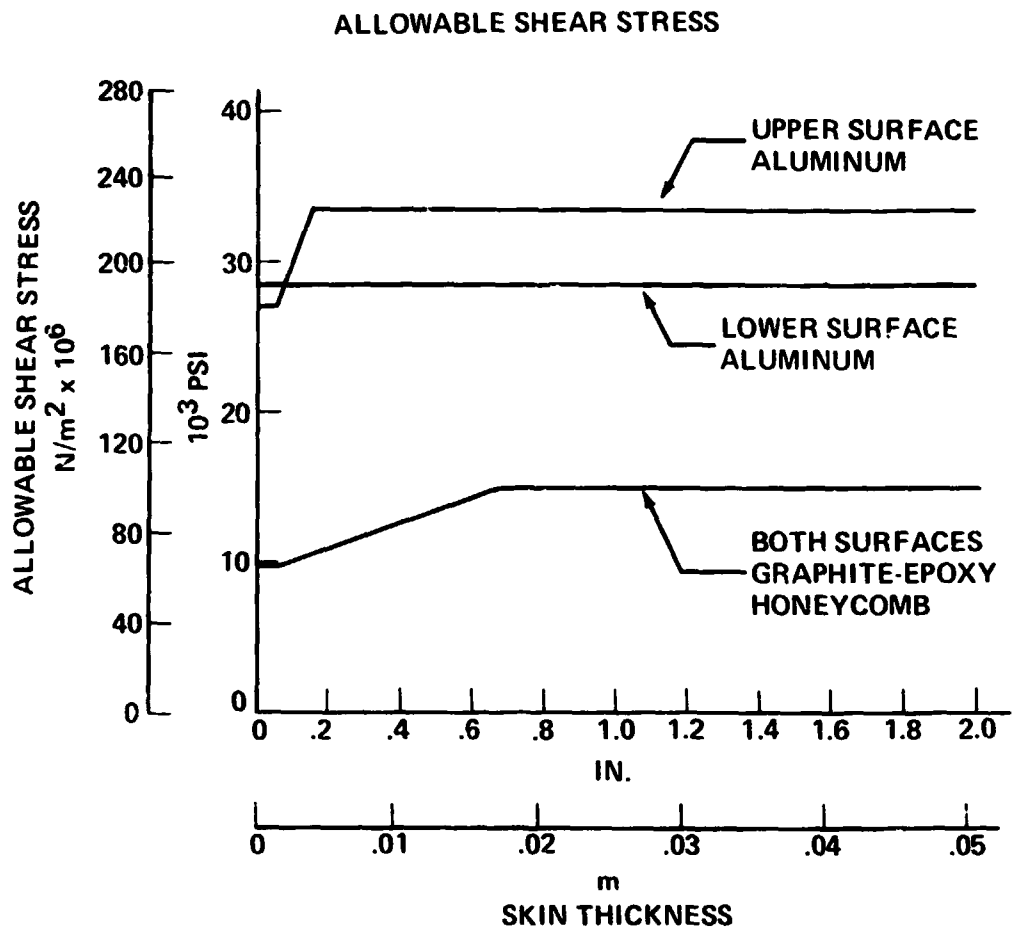


FIGURE 119.—STRUCTURAL MATERIAL PROPERTIES—CONCLUDED

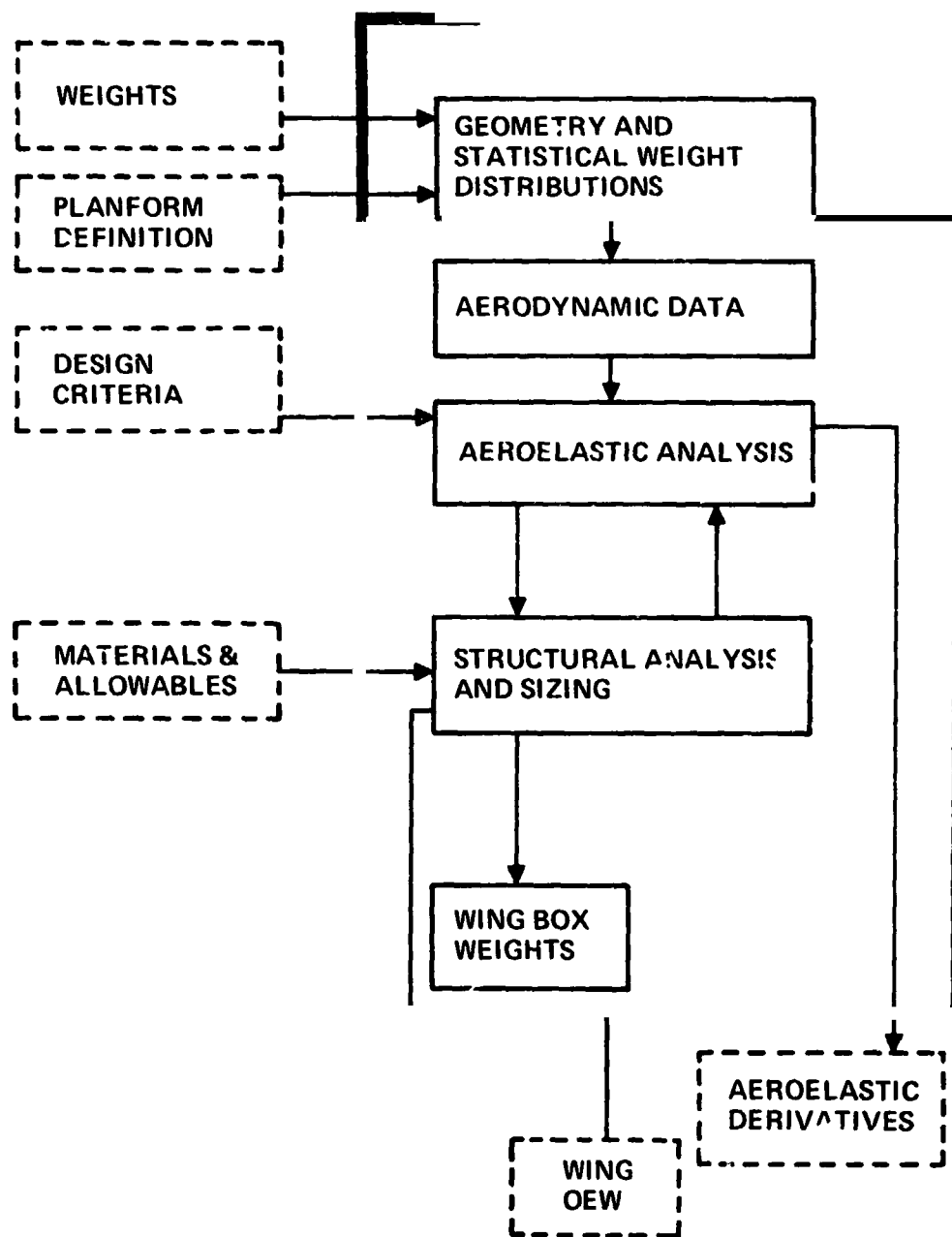


FIGURE 120.—ORACLE—STRUCTURAL SYNTHESIS PROGRAM

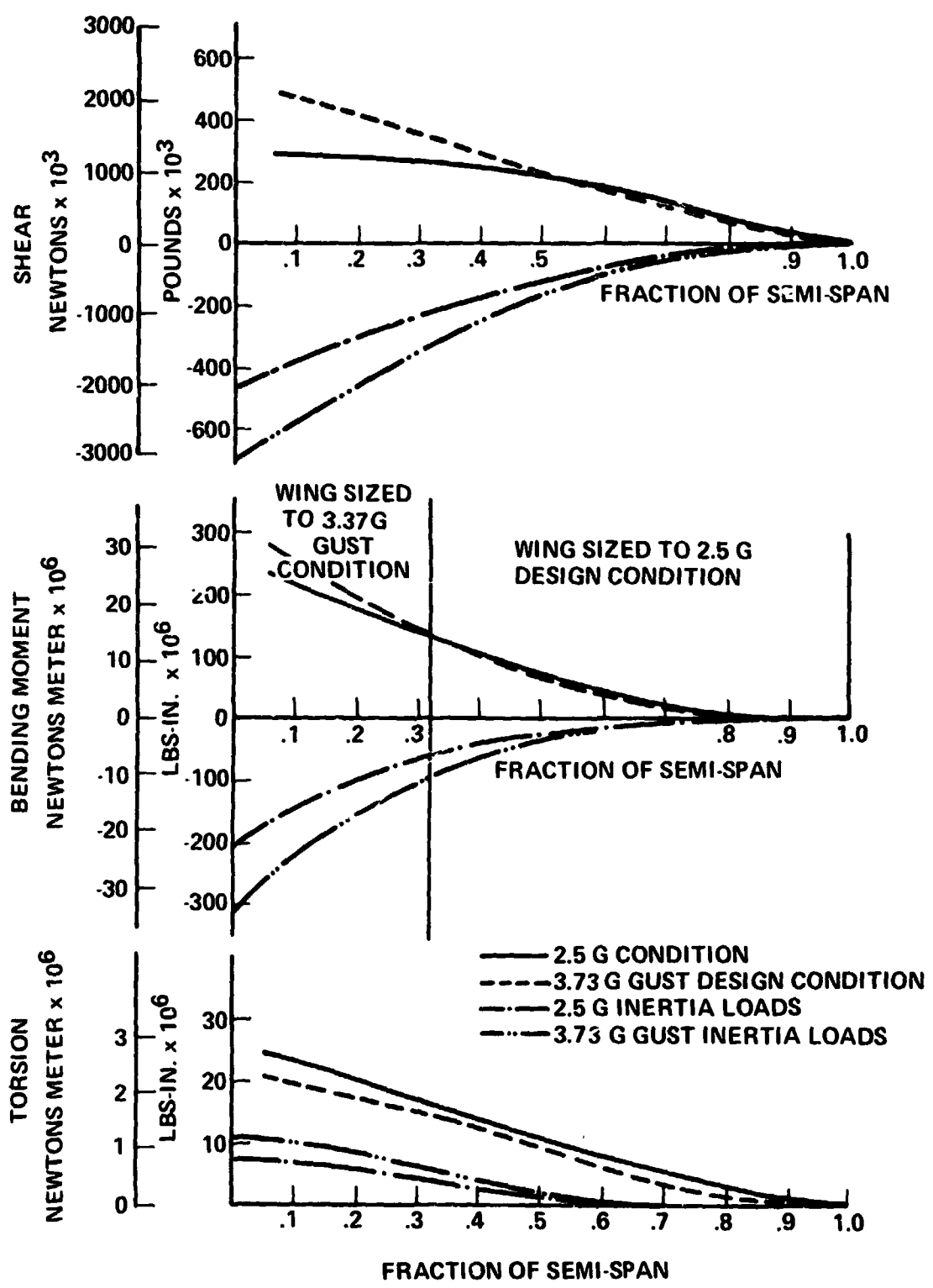


FIGURE 121.—WING ULTIMATE DESIGN LOADS

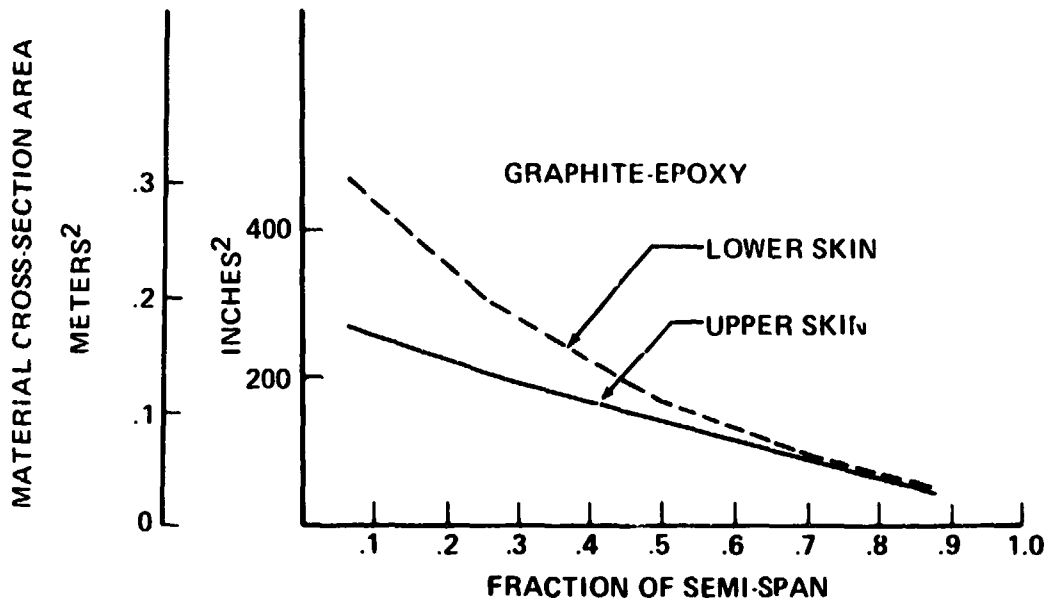


FIGURE 122.—WING SKIN THICKNESSES

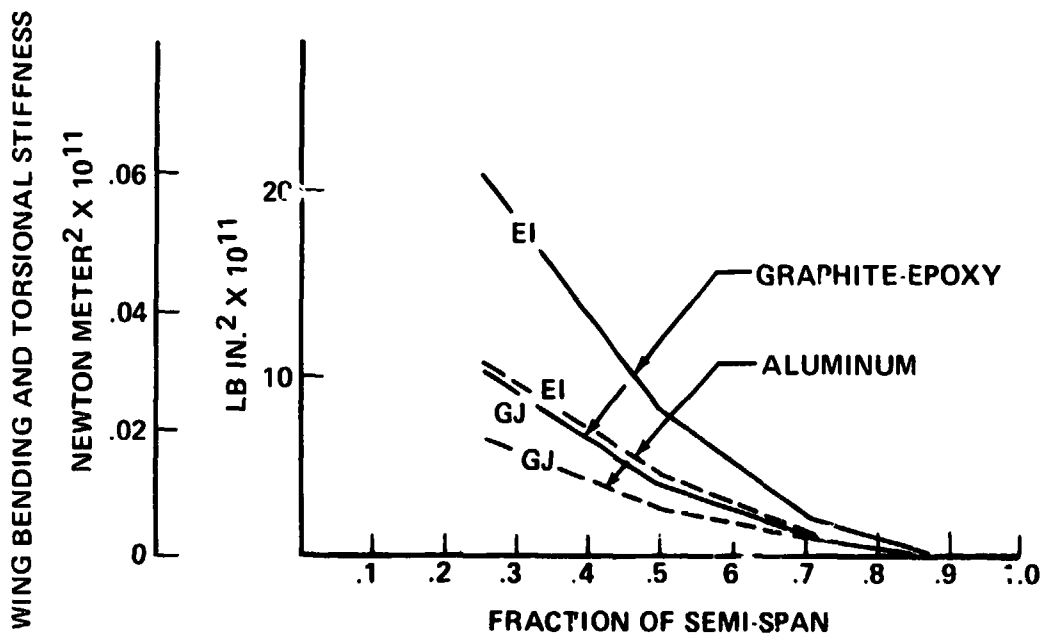


FIGURE 123.—WING SECTION PROPERTIES

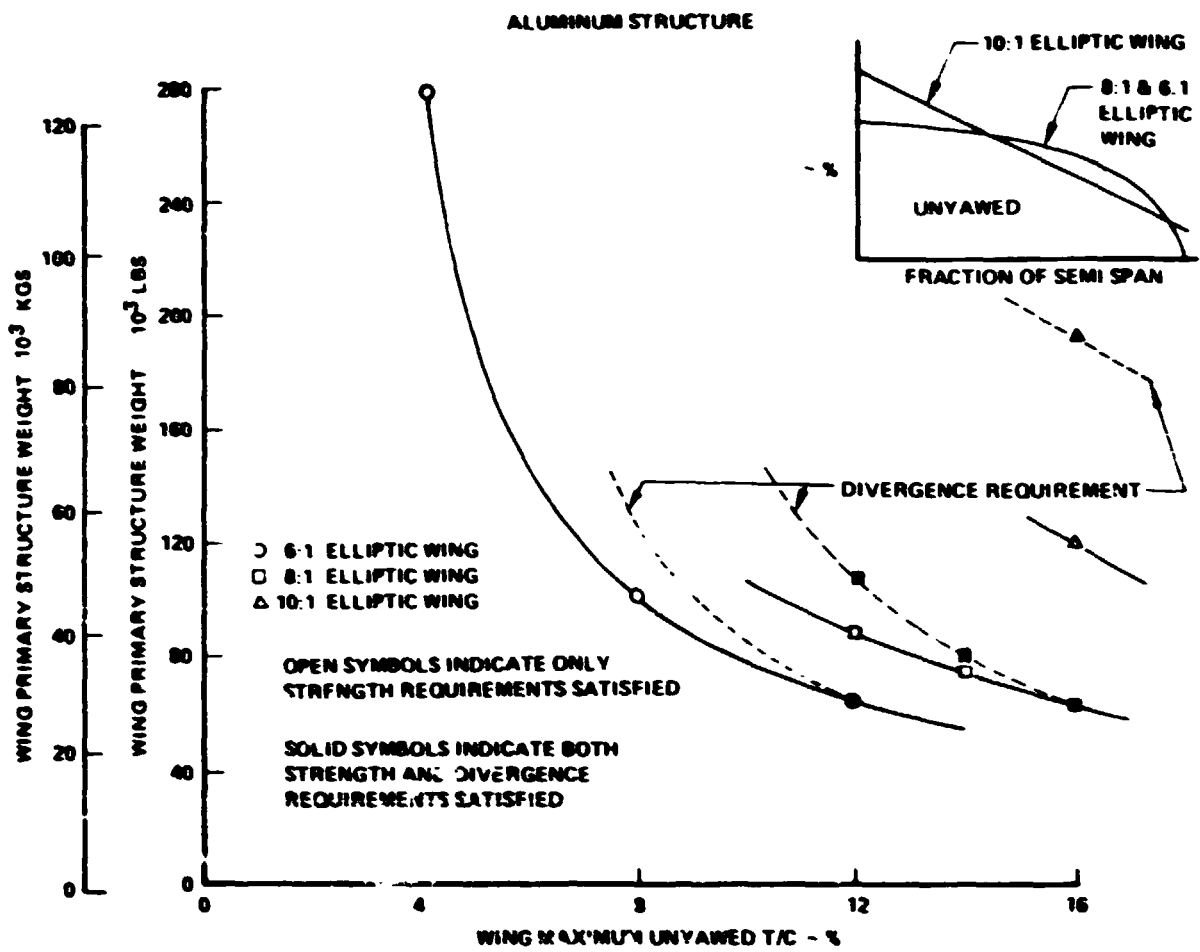


FIGURE 124.—YAWED WING VARIATIONS

wing primary structure weight. The t/c distribution was linear for the 10:1 wing and was elliptic for the 8:1 and 6:1 wings. The material requirements for the 10:1 wing were excessive, even with a maximum t/c of 16%, because of the stiffness needed to avoid divergence. At a maximum t/c of 14%, the 8:1 wing is nearly equally critical for strength and divergence.

The effect of applying graphite-epoxy to wings with a maximum t/c of 12% and an elliptic t/c distribution is shown on Figure 125. The increment in primary structure weight for strength designed graphite-epoxy wings was about 7711 kg (17,000 lb). The advantage of graphite-epoxy is even greater when the material requirements were dictated by divergence.

Wing bending material weight as a function of wing area and airplane gross weight is shown for aluminum structure on Figure 126 and for graphite-epoxy structure on Figure 27. The wing used for these variations had an 8:1 elliptic axis ratio and an elliptic t/c distribution with a maximum t/c of 12%. At high gross weights the aluminum wings are designed by maneuver loads. As gross weight is reduced at constant wing area, the designing criterion changes to gust loads, and then divergence avoidance.

The segment of the curves defined by the divergence requirements is independent of gross weight. The gross weight at which the design requirements change from gust and maneuver loads to divergence avoidance is strongly dependent on wing area. In the range studied, the graphite-epoxy wings were always designed by gust and maneuver loads rather than by divergence requirements.

WEIGHT AND BALANCE

The objectives of the weight studies were:

- Perform configuration weight and balance analyses
- Develop weight trade and sensitivity studies
- Conduct configuration parametric weight sizing analyses
- Undertake yawed wing weight studies based on structural analyses

Weight analysis and parametric weight studies were performed on the five airplane concepts during this study.

Weight trade and sensitivity studies supported engine cycle/sound suppression studies for the selection of engine bypass ratio and noise suppression treatment.

Weight studies were performed to support the single fuselage yawed wing configuration development trade and sensitivity studies.

Inertias and products of inertias were determined for the 10:1 elliptic axes ratio yawed wing configuration for the dynamic stability analysis.

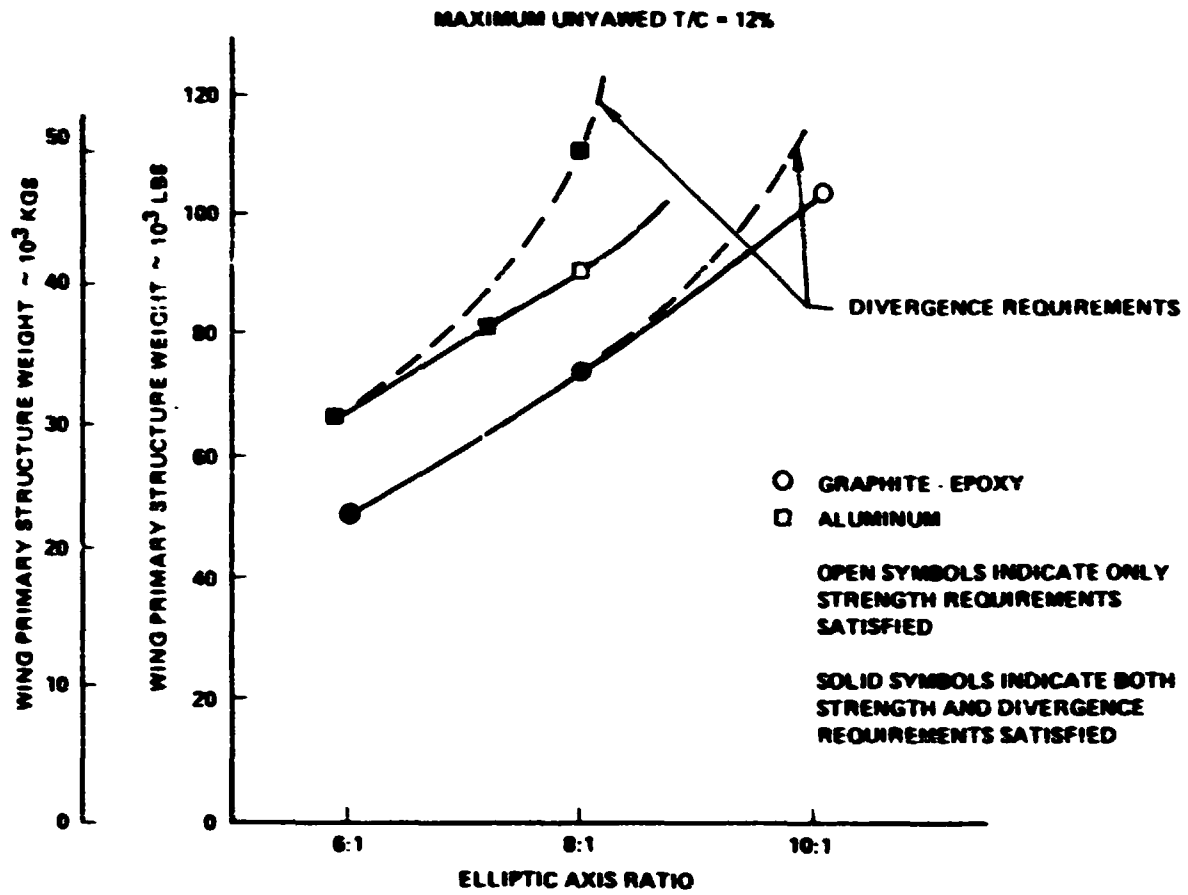


FIGURE 125.—ALUMINUM VERSUS GRAPHITE-EPOXY COMPARISON

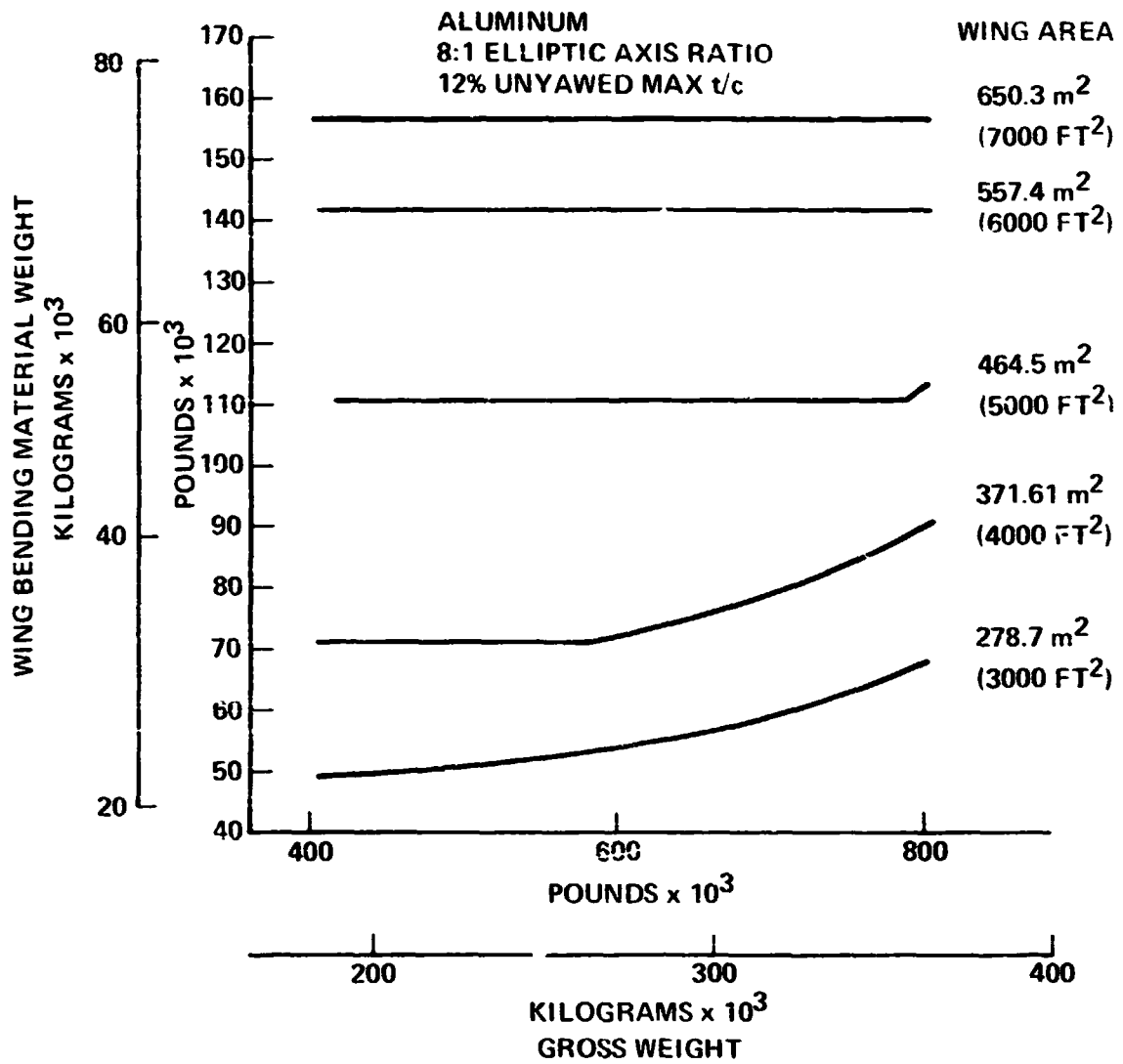


FIGURE 126.--YAWED WING SIZE SENSITIVITY--ALUMINUM

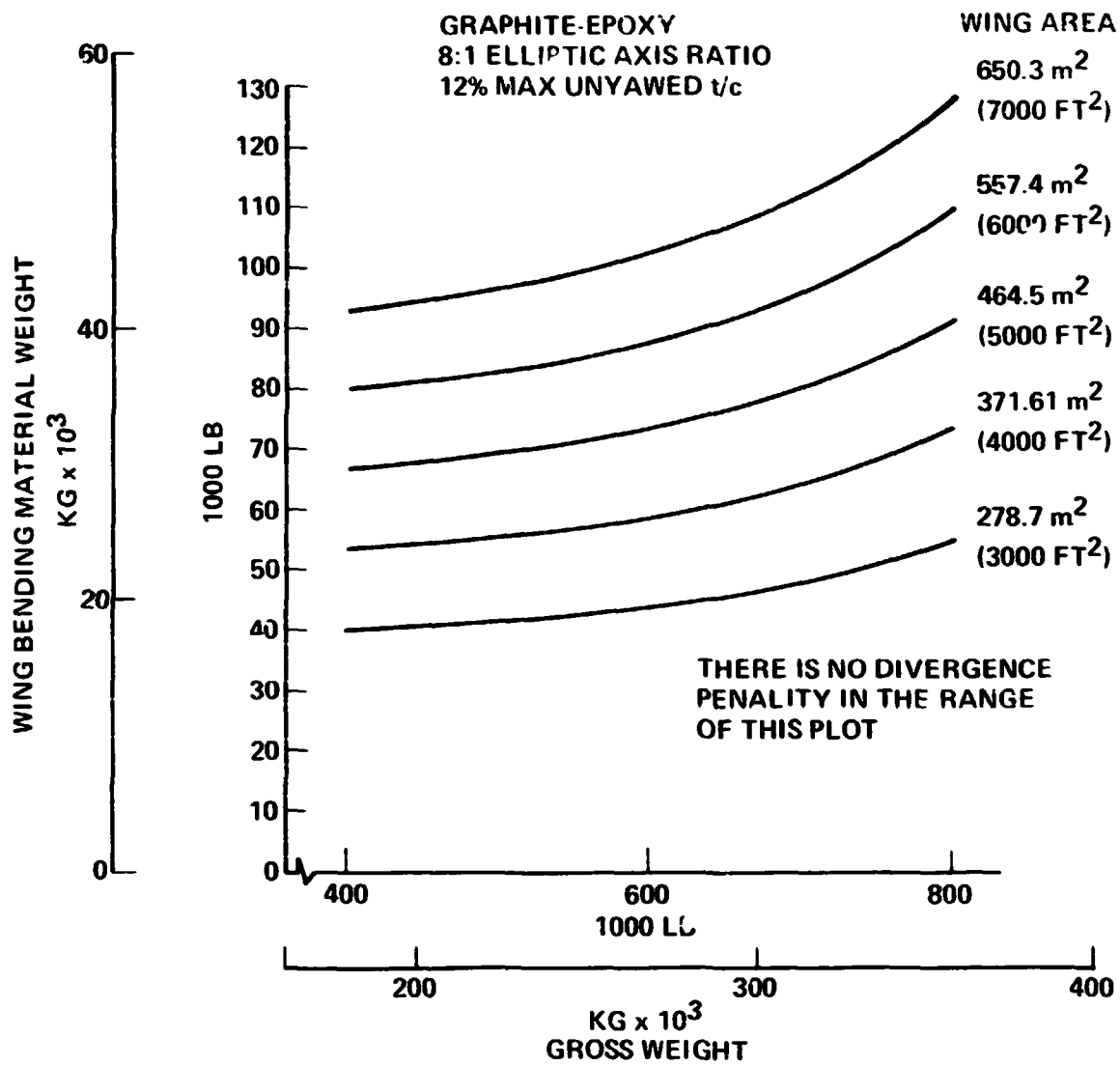


FIGURE 127.- YAWED WING SIZE SENSITIVITY-GRAPHITE-EPOXY

Weight Analysis Approach

The Model 2707-300 from the SST prototype program was selected as a base point to develop the weight for the structure and equipment systems. Weight adjustments were determined for changes in geometry, structural loading, and temperature effects on material selection for Mach 1.2. The weight analyses for the yawed wing configurations were based on wing structural analyses. Table 25 summarizes the weight analysis approach. Advanced technology weight adjustments were applied to the structure, propulsion, equipment and payload systems.

The use of the previously discussed advanced technology structural materials produced weight improvements consistent with the Level III results of the Advanced Technology Transport Program (ref. 1, page 78). The application of these structural improvements provide weight savings ranging up to 25% in the areas of application and produced an overall reduction of approximately 15% in total structural weight. Table 26 compares the applicable structural technology and level of weight used in the aircraft sizing analysis of the Advanced Technology Transport Program and the High Transonic Speed Transport Study.

Configuration Weight Analysis

Weight analyses were performed on five airplane concepts during the initial phase of this study. To form a basis for comparison the analysis was conducted on each concept at 272,155 kg (600,000 lb) maximum takeoff weight. The single-fuselage yawed-wing concept underwent a longer period of development. Improvements in the wing weight and aerodynamic performance were sufficient eventually to warrant a reduction in maximum takeoff weight of the base configuration to 226,800 kg (500,000 lb).

Table 27 contains a comparison of the uncycled baseline configurations fractional weight distributions. The yawed wing configurations have larger weight fractions for the wing and body, and lower weight fractions for the propulsion items. These reflect the influence of the higher wing aspect ratios, higher body fineness ratios, and lower thrust/weight ratios for the yawed wing concepts.

Weight calculations completed during the course of the study helped to identify the impact of bypass ratio, noise suppression and planform geometry on the gross weight of the sized airplanes.

The variations of wing weight with elliptic axis ratio (aspect ratio) and thickness ratio are shown in Figures 128 and 129. These figures indicate the powerful effects of wing thickness and aspect ratio on wing weights.

The weight increments calculated for the payload trade study are presented in Table 28. The impact of payload on operating empty weight is primarily due to body fineness ratio changes.

TABLE 25.-WEIGHT ANALYSIS APPROACH

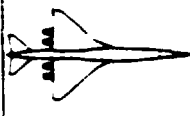


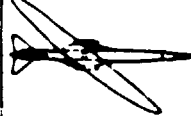
CONFIGURATION WEIGHT ELEMENT					CONFIGURATION TECHNOLOGY
WING		PRELIM. DESIGN ANALYSIS (STATISTICAL)	INCREMENT FOR PIVOT	STRUCTURAL DESIGN ANALYSIS	ADJUST FOR 1980 TIME PERIOD CONCEPTS (CONSISTENT WITH ATT PROGRAM) *1985 SERVICE ASSUMING 1972 PROGRAM GO AHEAD
BODY	BASELINE SST STATUS, 3/21/71 WITH ADJUSTMENTS TO ACCOUNT FOR GEOMETRICAL, STRUCTURAL LOADING & TEMP CHARACTERISTICS (MATERIALS) OF MACH 1.2 STUDY CONFIGURATIONS				
EMPENNAGE					
LANDING GEAR					
MISSION EQUIP & PAYLOAD SYS.					
PROPULSION	PRELIMINARY DESIGN EVALUATION OF MACH 1.2 PROPULSION CYCLES				

TABLE 26.-ADVANCED TECHNOLOGY COMPARISON

ITEM	PROGRAM	ATT BASE	HTSTAS BASE
STUDY SCOPE DELIVERY DATA		1975-1985 OPERATION 1981	1980-1980 OPERATION 1985 (SAME AS FINAL ATTP)
ADVANCED TECHNOLOGY, PRIMARY STRUCTURE		MULTI-DIRECTIONAL REINFORCEMENT, GRAPHITE/ BORON EPOXY.	COMPOSITE GRAPHITE EPOXY & HIGH TEMP. MATRIX COMPOSITE H/C
SECONDARY STRUCTURE		PRD 49 FIBER	PRD 49 FIBER
PREDICTED AIRPLANE STRUCTURAL WEIGHT REDUCTION		10-15%	15-25%
PERFORMANCE ANALYSIS BASE		10%	15%

TABLE 27.—UNCYCLED BASELINE CONFIGURATIONS WEIGHT DISTRIBUTIONS
(ADVANCED TECHNOLOGY)

CONFIGURATION	1-2	2-2	3-2	4-2	5-3
		KILOGRAMS x 10 ⁻³ (POUNDS x 10 ⁻³)			
OPERATIONAL EMPTY WEIGHT	120.15 (264.9)	129.68 (285.9)	120.91 (266.6)	144.7 (319.0)	123.8 (273.0)
MAX DESIGN TAKEOFF WEIGHT	272.15 (600.0)	272.15 (600.0)	272.15 (600.0)	272.15 (600.0)	226.8 (500.0)
	WEIGHT FRACTIONS, % OEW				
	1-2	2-2	3-2	4-2	5-3
WING	23.8	25.7	22.2	30.4	29.0
EMPENNAGE	3.1	3.1	2.6	3.3	2.0
BODY	15.7	14.7	15.0	21.5	21.0
LANDING GEAR	8.7	9.8	9.1	6.5	7.3
NACELLE AND STRUT	9.9	10.0	10.6	6.9	9.1
ENGINE	10.2	9.4	12.2	7.4	7.2
POWER PACK	3.0	2.8	3.2	2.6	2.5
EQUIP., PAINT AND OPTIONS	21.3	20.5	20.8	17.8	17.8
STANDARD AND OPERATING ITEMS	4.3	4.0	4.3	3.6	4.1

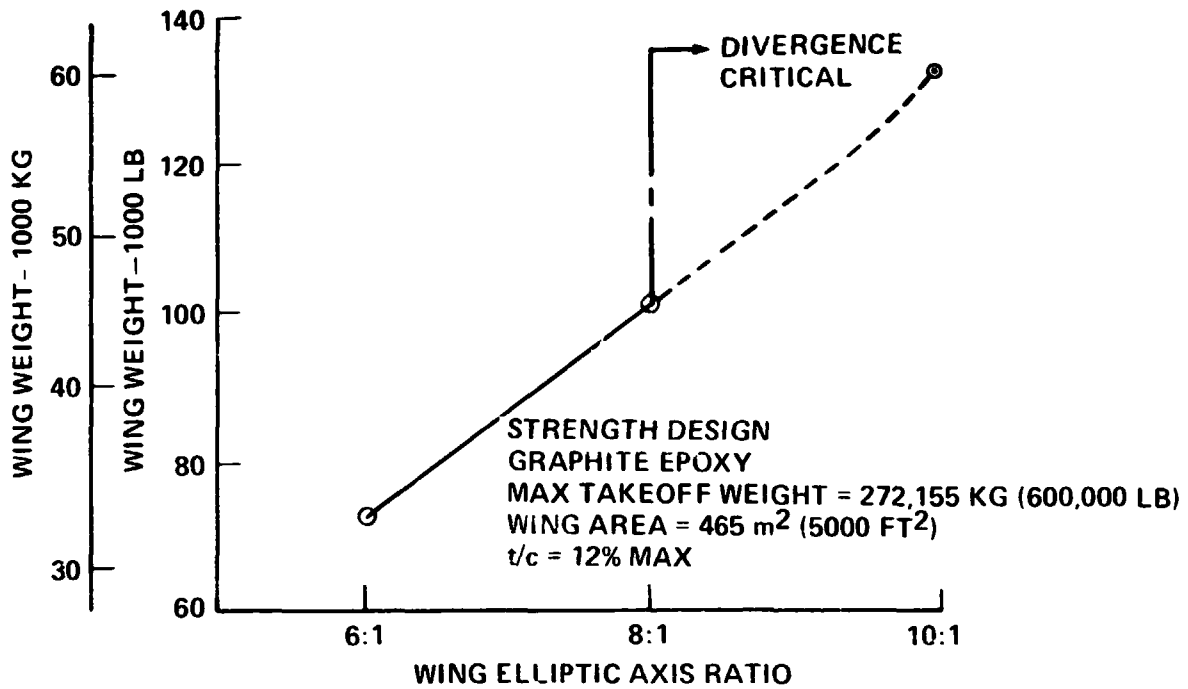


FIGURE 128.—WING WEIGHT VERSUS ELLIPTIC AXIS RATIO

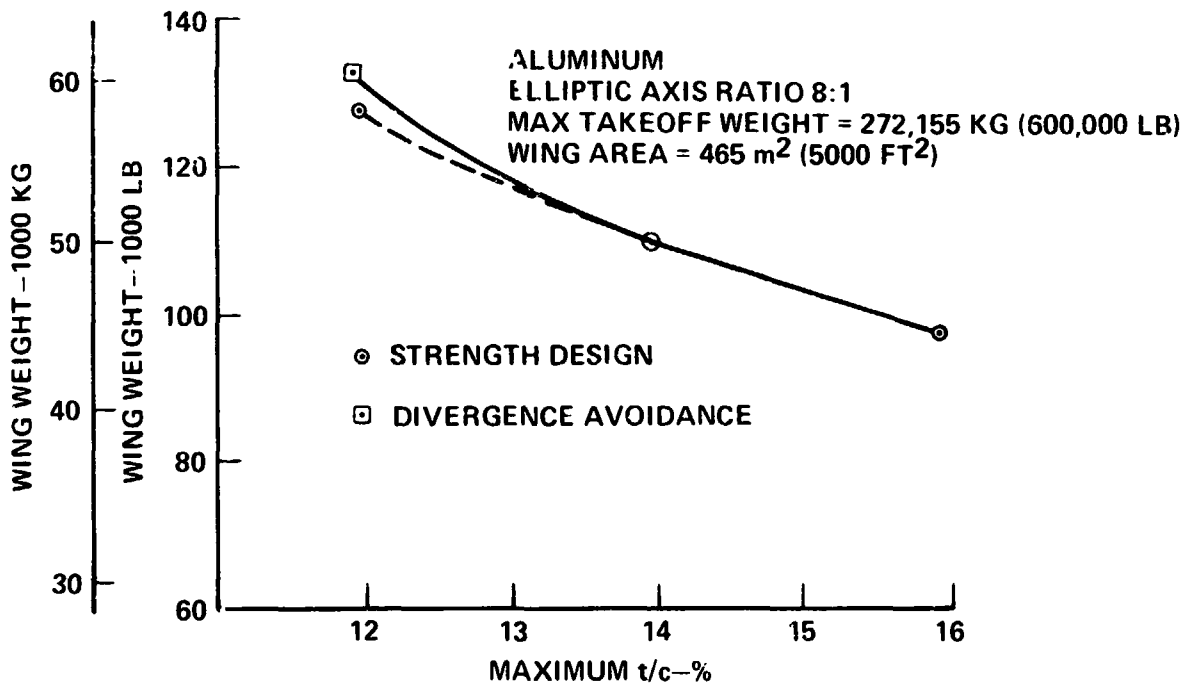


FIGURE 129.—WING WEIGHT VERSUS THICKNESS RATIO

TABLE 28.--PAYLOAD TRADE STUDY

	BASELINE CONFIGURATION: MODEL 5-3		
	226,796 (500,000)	226,796 (500,000)	226,796 (500,000)
MAXIMUM TAKEOFF WT--KG/(LB)	140	190	240
NO. OF PASSENGERS	78.94 (259.0)	87.63 (287.5)	96.31 (316.0)
BODY LENGTH--m/(FT)	3.53 (11.67)	3.53 (11.67)	3.535 (11.67)
BODY DIA AT PIVOT--m/(FT)	22.2	24.6	27.1
BODY FINENESS RATIO BASED ON DIA AT THE PIVOT			
WEIGHT CHANGES--KG/(LB)			
FUSELAGE	-3401 (-7500)	BASE	+4128 (+9100)
EMPENNAGE, (V CONSTANT)	-249 (-550)		+250 (+550)
ELECTRICAL & HYDRAULICS	-272 (-600)		+272 (+600)
CARGO HANDLING	-113 (-250)		+113 (+250)
PASSENGER ACCOMMODATION	-1587 (-3500)		+1588 (+3500)
EMERGENCY EQUIPMENT	-91 (-200)		+91 (+200)
AIR CONDITIONING	-204 (-450)		+204 (+450)
INSULATION	-158 (-350)		+159 (+350)
STANDARD AND OPERATIONAL ITEMS	-1134 (-2500)	BASE	+1134 (+2500)
△ OPERATING EMPTY WT	-7212 (-15900)	BASE	+7938 (+17500)
△ OEW, KG/PASS (LB/PASS)	-144 (-318)		+159 (+350)

Balance and Loading

Table 29 compares the balance and loading criteria that have been used for each of the study configurations with the loading criteria for subsonic and supersonic configuration arrangements with aft engine locations.

The weight and balance data for the uncycled baseline configuration 5-3 are presented in Table 30. The corresponding loading diagram for this configuration is shown in Figure 130. The weight distribution data for the uncycled baseline configuration 5-3 is compared with the corresponding weight data for the mission sized configuration in the configuration performance section, (Table 6).

The results of the balance and loading analysis for the uncycled single body yawed wing configuration 5-3 indicate that:

- forward ballast is required for low payloads and empty conditions (no payload).
- selective fuel management with an aft body fuel tank provides the capability to minimize cruise trim drag.
- A center of gravity range of 25% MAC is required for loading of passengers and baggage. This center of gravity range is within the limits provided by the stability and control system.

Forward balance requirements and fuel management are provided as on the National SST Program configuration (B2707-300), by a forward water tank for the low payload conditions and the inclusion of a center of gravity indication and control system.

Parametric Analysis

The sensitivity of structure, propulsion and equipment weight to wing area, maximum takeoff weight, thrust level and sound suppression treatment was determined in the configuration parametric sizing analyses for each design concept. The sensitivity of wing weight to area and maximum takeoff weight for the yawed wing configurations was evaluated from the results of wing structural analyses while statistical data were used for the other configurations. Figure 131 depicts the parametric nature of the weight scaling data that include the effects of maintaining a balanced airplane.

The structural weight estimates have been based in part on statistical data and also on detailed structural analyses. The unique nature of the single body yawed wing configuration warrants further detailed design and analysis investigations to validate fully the weight estimates of advanced technology materials. The details of the structural arrangement and methods of construction of the yawed wing and body need further investigations that include:

- Determining the transmittal of loads from the wing through the pivot and body structure to provide a complete understanding of the interaction of wing and body loads.

TABLE 29. -BALANCE AND LOADING CRITERIA (TYPICAL AFT ENGINE ARRANGEMENT)

ITEM	TYPE		
	SUBSONIC (TYPICAL)	TRANSONIC	SUPERSONIC
LOADING CRITERIA	UNRESTRICTED SEATING DISPATCH WITHOUT BALLAST AT ALL PASSENGER LOAD FACTORS	UNRESTRICTED SEATING DISPATCH WITHOUT BALLAST AT PASSENGER LOAD FACTORS GREATER THAN 45% (80% PROBABILITY)	UNRESTRICTED SEATING DISPATCH WITHOUT BALLAST FOR SPACE LIMITED PAYLOAD, FULL PASSENGER PAYLOAD WITH BAGGAGE OR 50% PAYLOAD WITH ZONE LOADING OF PASSENGERS
APPROX LOW SPEED OPERATIONAL C G RANGE	2.032 m (80 IN)	1.52 m (60 IN)	635 m (25 IN)
CONFIGURATION EFFECTS-CHANGE IN CENTER OF PRESSURE DUE TO MACH NO	NONE	TRIM TANK FUEL BALLAST AT LOW PAYLOADS ONLY	TRIM TANK FUEL BALLAST FOR MOST PAYLOADS
C G INDICATION AND CONTROL	NOT REQUIRED	REQUIRED	REQUIRED

TABLE 30.—UNCYCLED CONFIGURATION 5-3 WEIGHT AND BALANCE BASELINE DATA

	MASS KG	CG BODY STATION m	WEIGHT LB	CG BODY STATION IN.
WING	35,830	58.67	79,000	2310
HORIZONTAL TAIL	1,640	88.90	3,620	3500
VERTICAL TAIL	860	88.65	1,900	3490
BODY	26,040	50.55	57,400	1990
MAIN LANDING GEAR	6,920	69.09	15,250	2720
NOSE LANDING GEAR	2,090	30.48	4,600	1200
NACELLE AND STRUT	11,310	73.91	24,930	2910
TOTAL STRUCTURE	84,690	59.26	186,700	2333
ENGINE	8,890	77.47	19,600	3050
ENGINE ACCESSORIES				
ENGINE CONTROLS	650	77.47	1,430	3050
STARTING SYSTEM				
FUEL SYSTEM	2,460	61.98	5,430	2440
THRUST REVERSER (IN NACELLE)				
TOTAL PROPULSION GROUP	12,000	74.29	26,460	2925
ACCESSORY DRIVE SYSTEM	490	77.47	1,080	3050
INSTRUMENTS	430	21.84	1,050	860
SURFACE CONTROLS	3,030	61.21	6,690	2410
HYDRAULICS	1,970	65.79	4,330	2590
PNEUMATICS	660	66.29	1,450	2610
ELECTRICAL	1,810	47.50	3,980	1870
ELECTRONICS	1,390	20.57	3,070	810
FLIGHT PROVISIONS	430	17.78	950	700
PASSENGER ACCOMODATIONS	5,570	44.45	12,280	1750
CARGO HANDLING	750	42.93	1,660	1690
EMERGENCY EQUIPMENT	340	44.45	740	1750
AIR CONDITIONING	1,810	50.55	4,000	1990
INSULATION	1,330	44.45	2,930	1750
AUXILIARY POWER UNIT	610	88.90	1,350	3500
WATER BALLAST SYSTEM	110	24.89	250	980
TOTAL FIXED EQUIPMENT	20,780	49.66	45,810	1955
EXTERIOR PAINT	90	51.69	200	2035
OPTIONS	1,140	44.45	2,500	1750
MANUFACTURER'S EMPTY WEIGHT	118,700	58.95	261,670	2321
STANDARD AND OPERATIONAL ITEMS	5,140	44.45	11,330	1750
OPERATIONAL EMPTY WEIGHT	123,840	58.34	273,000	2297
MAXIMUM TAKEOFF WEIGHT	226,796		500,000	

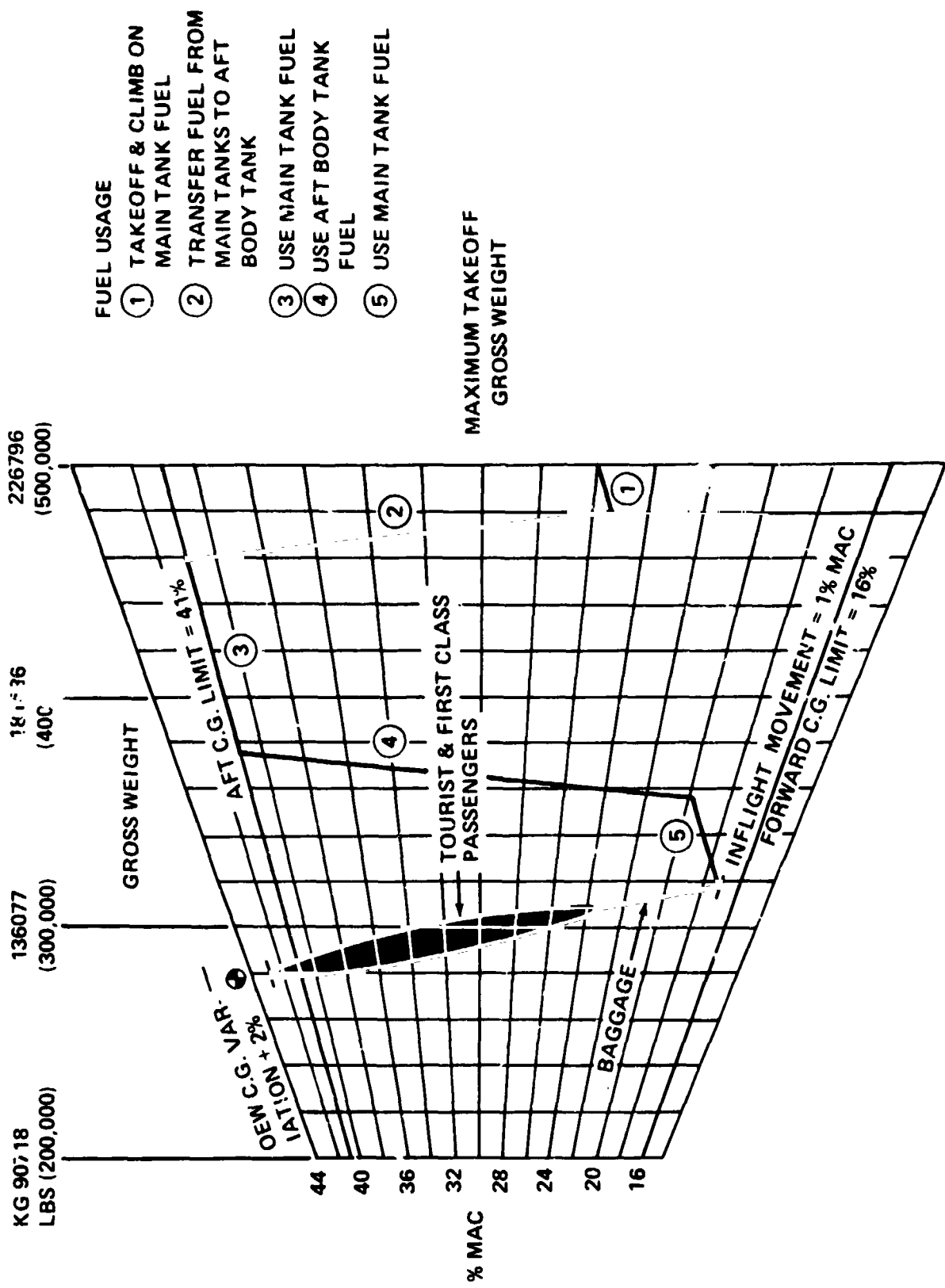


FIGURE 130. - LOADING DIAGRAM, MODEL 5-3

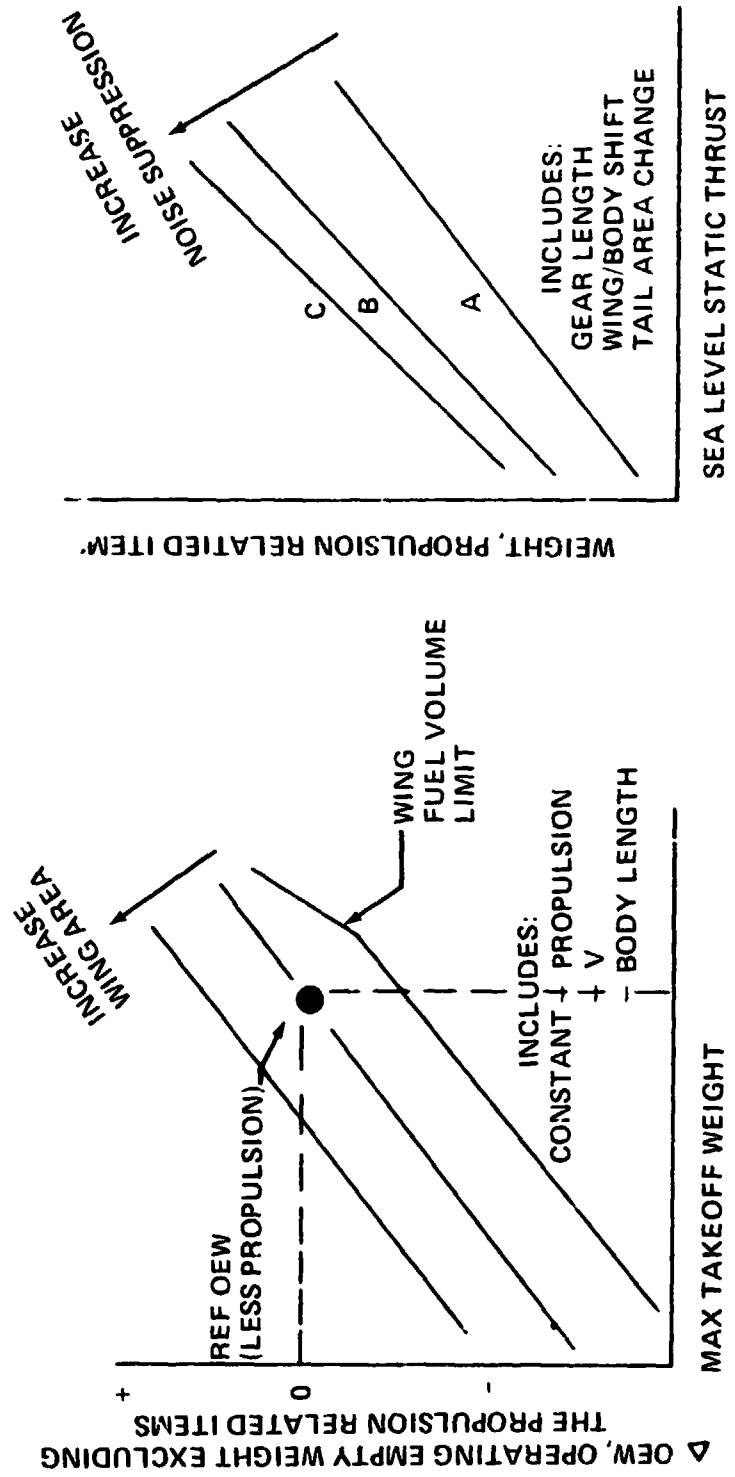


FIGURE 131.--PARAMETRIC REPRESENTATION OF THE WEIGHT SCALING DATA

C-3

- **Examining the impact of forward location of the payload and the aft location of the engine mass on the overall fuselage weight by a detailed design analysis.**

CONCLUSIONS

The most significant conclusions of this study are:

- The “boomless” supersonic mission requirements were met at FAR 36 noise levels by a delta configuration at 226,796 kg (500,000 lb) gross weight and by a single-body yawed-wing configuration at 211,828 kg (467,000 lb). The higher lift/drag ratio of the yawed-wing concept lead to its lower gross weight. Configurations based on the other concepts resulted in heavier airplanes.
- The noise goal of FAR 36 minus 15 EPNdB can be met with the single-body yawed-wing configuration at approximately 226,796 kg (500,000 lb) gross weight. This noise goal cannot be met reasonably by the other configurations. The yawed-wing configuration has a large advantage in takeoff and landing performance.
- A yawed wing configuration designed for Mach 1.2, can achieve the design range for all supersonic Mach numbers up to 1.2 and will have a 20% excess range capability at subsonic speeds.
- The selected structural design speed placard restricted the minimum Mach 1.2 cruise altitude to 11887 m (39,000 ft). This restriction constrained the size of all of the configurations and has probably resulted in performance losses.
- Although wing aeroelastic divergence is a primary design consideration for yawed-wing configurations, the graphite-epoxy wings of this study were designed by critical gust and maneuver loads rather than by divergence requirements.
- Advanced filamentary composite materials offer about a 20% structural weight saving over aluminum for a strength designed yawed wing.
- A variation in the yawed wing aspect ratio results in a trade between lift/drag ratio and wing due to divergence. The best planform was obtained with an elliptic axis ratio of 8:1 (unyawed aspect ratio 10.2) and an unyawed maximum t/c of 12%.
- The rigid dynamic stability and control characteristics of all five concepts are acceptable. However, aeroelastics may have a significant effect on the flying characteristics of the yawed-wing configurations.
- For high transonic speed applications low bypass ratio engines with suppression result in lower gross weight airplanes than configurations with high bypass ratio engines even at equal community noise levels.
- The total drag for any transonic configuration is very sensitive to the way in which the nacelles are installed. Double pod installations result in high wave drag. Engines integrated into the body result in low drag.

PRECEDING PAGE BLANK NOT FILMED

RECOMMENDATIONS

Because of the promising potential of the single-body yawed-wing concept it is recommended that a program be undertaken to verify and further develop this potential. A three phase program is recommended: Phase I consists of analytical studies which follow directly from this contract. Phase II is a combination of wind tunnel and lab test work with further theoretical studies. Phase III includes further development of Phase I and II work through detailed design followed by flight test of a demonstration vehicle.

PHASE I

- Determine the best structural design speed placard by studying the trade between airframe weight and aerodynamic performance.
- Develop a Mach 1.2 configuration alternate to configuration 5-3. The objective of this development should be to simplify the engine and landing gear installation while retaining the aerodynamic efficiency.
- Develop a low transonic speed yawed wing configuration to compare directly to the ATT configurations.
- Match the engine cycle, the amount of noise suppression required, the flap system and the takeoff and landing procedures to minimize the community noise for the synthesized basic and alternate yawed-wing configurations.
- Conduct an analysis of the stability and control characteristics of a flexible yawed-wing airplane to identify control system requirements.
- Conduct a theoretical and experimental wing development study to fully identify the maximum practical wing thickness/chord ratio and the minimum achievable drag due to lift.
- Analyze operational characteristics of a yawed-wing commercial transport in airline operation and estimate total operating costs. Compare these costs with wide-body and ATT operating costs for similar payload/range categories.

PHASE II

- Verify the performance of the best Mach 1.2 configuration developed in Phase I by a coordinated theoretical-experimental program covering both the low and high speed flight regimes.
- Conduct a market analysis to determine potential total airline fleet requirements.

- Based on the results of the Phase I stability and control study and available test data, develop a moving base simulation of the airplane in order to evaluate flight control systems.
- Perform an aeroelastic model wind tunnel test to confirm the wing divergence and flutter characteristics.
- Develop detailed plans including the design criteria for a yawed-wing flight test vehicle.

PHASE III

Design and fabricate a yawed-wing flight test airplane.

SUPPORTING TECHNOLOGY DEVELOPMENT

In addition to the development work described above for the yawed-wing configuration, the basic advanced technology programs recommended as part of the Advanced Transport Technology study (ref. 16) should be pursued since they apply nearly universally to this concept. This is particularly true in the structures, flight control and power systems areas that require the projected technology advances to achieve the potential identified in this study.

REFERENCES

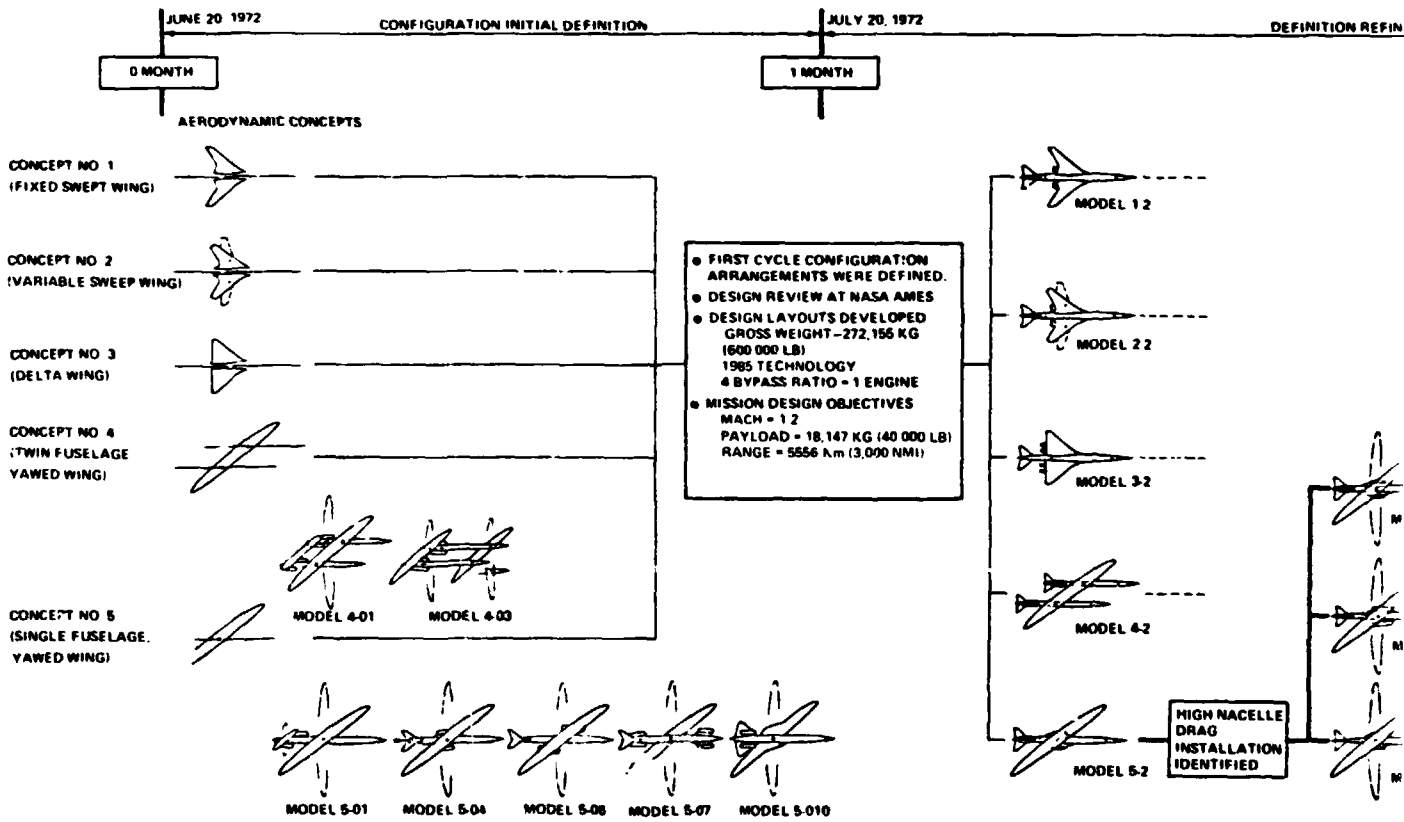
- 1 NASA Contracts NAS1-1071, NAS1-1073, NAS1-1073, "Study of the Application of Advanced Technologies to Long-Range Transport Aircraft."
- 2 Haglund, G. T.: A Preliminary Climatology of the Threshold Mach Number. Paper Presented at the Fourth Conference on Aerospace Meteorology, Am. Meteorol. Soc. and AIAA (Las Vegas, Nevada) May 1970, pp. 39-413.
- 3 Wallace, R. E.: "Parametric and Optimization Techniques for Airplane Design Syntheses." Paper No. 7, AGARD Lecture Series No. 56—Aircraft Performance—Prediction Method and Optimization Edited by J. Williams—April 24-28, 1972, VonKarman Institute, Belgium.
- 4 Wimpres, J. K., and Swihart, J.M.: "Influence of Aerodynamic Research on the Performance of Supersonic Airplanes." Journal of Aircraft, Vol. 1, No. 2, March-April 1964, pp. 71-76.
- 5 Graham, L. A., Jones, R. T., and Boltz, F. W.: "An Experimental Investigation of an oblique-Wing and Body Combination at Mach numbers between 0.6 and 1.40." NASA TMX-62.207, December 1972.
- 6 Smith, J. H. B.: "Lift/Drag Ratios on Optimized Slewled Elliptic Wings at Supersonic Speeds." The Aeronautical Quarterly, August 1961.
- 7 Jones, R. T.: "Theoretical Determination of the Minimum Drag of Airfoils at Supersonic Speeds." Jour. of Aero. Science, December 1952.
- 8 Sommer, S. G. and Short, B. J.: "Free-Flight Measurements of Turbulent boundary Layer Skin Friction in the Presence of Severe Aerodynamic Heating at Mach Numbers From 2.8 to 7.0." NACA TN 3391.
- 9 Sheppard, L. M.: "Methods for Determining the Wave Drag of Nonlifting Wing-Body Combinations." R.A.E. R&M No. 3077, April 1957.
- 10 Sheppard, L. M.: "The Wave Drag of Nonlifting Combinations of Thin Wings and Nonslender Bodies." R.A.E. R&M No. 3076, March 1957.
- 11 Carlson, Harry W. and Middleton, Wilber D.: "A Numerical Method for the Design of Camber Surfaces of Supersonic Wings With Arbitrary Planforms." NASA TN D-2341, 1964.
- 12 Middleton, W. D. and Carlson, H. W.: "A Numerical Method for Calculating the Flat-Plate Pressure Distributions on Supersonic Wings of Arbitrary Planform." NASA TN D-2570, 1965.

- 13 Shrouf, B. L.: "Extension of a Numerical Solution for the Aerodynamic Characteristics of a Wing to Include a Canard or Horizontal Tail." AGARD CP-71-71.
- 14 Mack, R. J.: "A Numerical Method for Evaluation and Utilization of Supersonic Nacelle-Wing Interference." NASA TN D-5057, March 1969.
- 15 Harris, Roy V.: "An Analysis and Correlation of Aircraft Wave Drag." NASA TM X-947, 1964.
- 16 NASA Report CR-112093, "Final Report-Study of the Application of Advanced Technologies to Long Range Transport Aircraft." Volume II Advanced Technology Program Recommendations, May 1972.
- 17 "Advanced Composites Design Guide." Advanced Composites Division Air Force Material Laboratory Air Force Systems Command, Wright-Patterson Air Force Base, Ohio, November 1971.
- 18 Gray, W. L. and Schenk, K.M.: "A Method for Calculating the Subsonic Steady-State Loading on an Airplane With a Wing of Arbitrary Planform and Stiffness." NACA TN 3030.

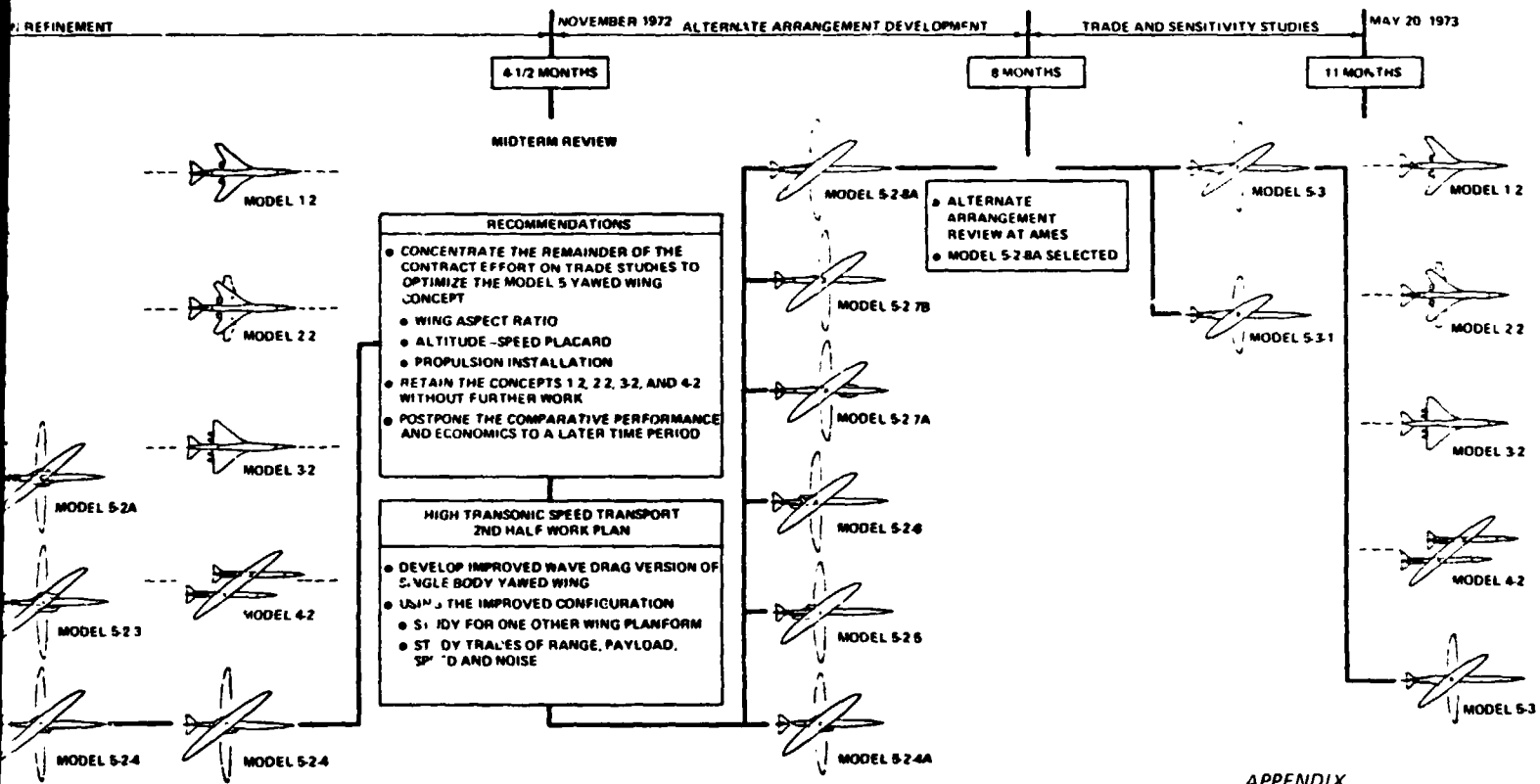
FOURDOUT FRAME

INITIAL PROGRAM OBJECTIVES

- SYNTHESIZE 5 BASIC HIGH TRANSONIC TRANSPORT CONFIGURATION CONCEPTS
 - CONSISTENT TECHNOLOGY
 - CONSISTENT PAYLOAD RANGE
- DEVELOP RESULTING PERFORMANCE AND ECONOMICS
- EVALUATE TECHNICAL FEASIBILITY OF BASIC CONCEPTS
- IDENTIFY HIGH RISK TECHNOLOGY AREAS



2



APPENDIX
CONFIGURATION EVOLUTION